

TECHNISCHE UNIVERSITÄT MÜNCHEN
Lehrstuhl für Molekulare Katalyse

**RHENIUM, MOLYBDENUM AND TUNGSTEN
ORGANOMETALLIC HOMOGENEOUS
CATALYSTS. SYNTHESIS,
CHARACTERISATION AND APPLICATION IN
OLEFIN EPOXIDATION**

Alejandro Capapé Miralles

Vollständiger Abdruck der von der Fakultät für Chemie der Technischen
Universität München zur Erlangung des akademischen Grades eines

Doktors der Naturwissenschaften

genehmigten Dissertation.

Vorsitzende: Univ. - Prof. Dr. S. Weinkauff
Prüfer der Dissertation: 1. Univ. - Prof. Dr. F. E. Kühn
2. Univ. - Prof. Dr. K. - O. Hinrichsen

Die Dissertation wurde am 17.06.2009 bei der Technischen Universität München
eingereicht und durch die Fakultät für Chemie am 29.07.2009 angenommen.

Als meus pares, el meu avi i el meu germà

No hi ha present: tots els camins són records o preguntes.
There is no present: all the roads are either memories or questions.

Miquel Martí i Pol (1929-2003), catalan poet

Die vorliegende Arbeit entstand in der Zeit von März 2006 bis Mai 2009 am
Anorganisch-chemischen Institute der Technischen Universität München

I would like to express my deep gratitude to my academic supervisor

Prof. Dr. Fritz E. Kühn

For his continuous supervision, encouragement and trust in my work.

Acknowledgements

I will begin by giving my most sincere thanks to the people who, in one way or another, made it possible for me to carry out a PhD in Germany. First of all, to Prof. Dr. F.E. Kühn, who accepted me into his group and since then has always encouraged me with my research. His trust, advice and most of all his patience have made this manuscript what it is. Second, to my parents, my brother and my grandfather, for their endless love and support from afar. Third, to my German family - my uncle, aunt, cousins, and the little Hannah - who, should a problem have arisen, were always available, and have made me feel at home. Last but not least, very special thanks go to Maria, without whom - I am most certain - these last years would have been much more difficult to endure.

The Molekulare Katalyse and the whole Lehrstuhl für Anorganische Chemie fully deserve to be mentioned here. With them I have had the chance to enjoy an incredibly positive and engaging work environment.

During the first and always difficult months I had the good fortune of getting the unconditional help of many co-workers. First, from the so-called "girl's lab" (originally composed of Claudia Linniger, Dina Tanase and Sandra Zinner) and then from the former dwellers of lab 37411 (Dr. Jin Zhao - my predecessor both in the workplace and research topics - Dr. Syukri, Dr. Akef Al-Hmaideen, Dr. Ahmed Hizaji and their neighbour Dr. Filipe Pedro). All of them are acknowledged not only for their helpful advice but also for the good moments both in the laboratory and out of it.

The Molekulare Katalyse group came into existence at that time, and has since then undergone considerable changes. The most noticeable was that it has ended up including Germans. It all started with Christian Fischer and Bernd Diebl, who are heartily acknowledged for their enduring friendship and the many good moments spent together either in the lab, in Italy or in my home town (and also for deciphering the mysterious language of the glass blowers). I am also equally grateful to the rest of the Bavarian bunch; Manuel Högerl, Serena Goh (not technically German, but in the process of becoming one) and Silvana Rach. Special thanks go to Alexander Raith, rightful heir to the *ansa* throne, whose collaboration in my research topic as well as a most enjoyable comradeship have helped transform a bunch of seemingly random reactions into the rather more structured work that is presented herein.

The international section of the group must also be mentioned. Ming-Dong Zhou is acknowledged – along with her Chinese colleagues – for her collaboration in the Re section of the present manuscript, as well as for her kindness, wonderful cooking skills and patience while having to share research topics and laboratory space with me. I am also grateful to Yang Li for the many interesting scientific conversations and a most enjoyable cultural exchange. Kavita Jain and Alev Günyar, who have also been part of the MK since its inception are also acknowledged, along with Nadezca Domanovic (and her husband Goran), Hitrisia Syska and the newer group members.

On the other hand, Philipp Altmann (now a PhD student in our group), Stefan Gigler, Christoph Edlinger (now a diploma student in our group) and Marlene Bruce are acknowledged for their invaluable help as assistants to my research.

I am also grateful to the new postdoctoral fellows – Dr. Hugh Chaffey-Millar (and his girlfriend Anthea) and Dr. Mónica Carril – which despite their higher rank have taken the effort of treating us PhD students as worthy beings. The new academic counsellor for the MK group, Dr. Mirza Cokoja, is also acknowledged for his valuable suggestions and corrections, which have been of critical importance in polishing the present manuscript.

The whole secretary staff – Frau Grötsch, Frau Hifinger, Frau Kauffmann and Frau Schubauer-Gerl – are acknowledged for their help in dealing with the tenuous bureaucratic aspects of my stay. Very special thanks go to Nora Boerschel, who overtook my former Auslandsbeauftragter duties, the fulfillment of which has since then significantly improved.

The technical staff are also acknowledged, especially Thomas Schröferl, who was always willing to help with the GC-MS experiments, and Georgeta Krutsch, who kindly performed many of the NMR experiments included in this work.

Dr. Draganco Veljanovski, who has intensely collaborated with our group, is acknowledged for his valuable lessons in life and science, along with Evangeline Tosh for her cheerfulness, hospitality and helpful suggestions (be it chemistry, improvement of my english skills or knitting issues). Agnes Bittermann, Oliver Hiltner (Chem.Eur.J. or Eur. J. Inorg. Chem, who cares!) and the other freelance Herrmann coworkers are acknowledged for their kindness during these years.

The whole Schneider and Eppinger groups are acknowledged for their help, especially when dealing with laboratory matters on weekends and holidays.

Dr. Eberhardt Herdtweck is acknowledged for his excellent work in the X-ray determination of the structures presented in this work. I am also grateful to Prof. Ahmad Al-Ajlouni for his mechanistic calculations.

Dr. Peter Härter, Dr. Gabrielle Raudaschl-Sieber, Prof. Klaus Köhler, Prof. Klaus Ruhland and Dr. Markus Drees (amongst many others) are acknowledged for their help and advice regarding many matters during this PhD.

I should also thank all the poor students who had to endure my terrible explanations and gruesome coaching during the Praktikum days in Weihenstephan.

Special thanks go to all the friends I have made during my stay in Munich. Most of them come from the ever friendly, ever noisy Spanisches Kolleg. Mentioning them all would make this section bulkier than the whole work, so I can only say thank you to all for letting me share with you this fantastic experience in Munich.

Finally, I would like to thank those that I have forgotten to mention in this section (hopefully not many). They, of course, are entitled to remind me of my mistake anytime.

My most sincere apologies!

Index

| | |
|--|-----------|
| I. INTRODUCTION | 1 |
| 1. OXIDATION CATALYSIS: AN OVERVIEW | 2 |
| 1.1 Scope of the Present Work | 2 |
| 2. THE EPOXIDATION REACTION. INDUSTRIAL SIGNIFICANCE | 4 |
| 2.1 Epoxides: A key industrial intermediate | 5 |
| 2.1.1 Significant epoxides in the industrial world | 7 |
| 2.2 Catalytic epoxidation | 9 |
| 2.2.1 The oxidant point of view. Introduction of catalytic processes in the epoxidation industry | 9 |
| 2.2.2 Current industrial advances in catalysis. Propylene oxide | 11 |
| 3. OLEFIN EPOXIDATION FROM A CATALYST POINT OF VIEW | 18 |
| 3.1 Homogeneous catalysis | 18 |
| 3.1.1 Homogeneous epoxidation catalysis. Transition metal oxides | 19 |
| 3.2 Asymmetric epoxidation | 23 |
| 3.2.1 Asymmetric homogeneous epoxidation catalysts | 24 |
| 4 OBJECTIVES OF THIS WORK | 27 |
| REFERENCES CITED IN THIS CHAPTER | 29 |
| | |
| II. SCHIFF BASE ADDUCTS OF METHYLTRIOXORHENIUM | 33 |
| 5. RHENIUM OXIDES AS EPOXIDATION CATALYSTS | 36 |
| 5.1 Alkyl- and aryl-trioxorhenium compounds | 36 |
| 5.2 Methyltrioxorhenium: an overview | 37 |
| 5.2.1 Properties | 37 |
| 5.2.2 Synthesis | 38 |
| 5.3 Catalytic applications of MTO | 39 |
| 5.3.1 Methyltrioxorhenium as a homogeneous oxidation catalyst | 40 |
| 5.3.2 Mechanistic implications in the epoxidation reaction | 41 |
| 5.3.3 Heterogeneous derivatives of MTO | 42 |
| 5.4 Base adducts of methyltrioxorhenium and their effect in epoxidation catalysis | 43 |
| 5.4.1 Nitrogen donor adducts | 44 |
| 5.4.2 Oxygen donor adducts. Chiral diols | 47 |

| | |
|--|----|
| 5.4.3 Schiff bases and its role in synthesis and catalysis | 47 |
| 6. SYNTHESIS AND CATALYTIC APPLICATIONS OF MTO SCHIFF BASE COMPLEXES | 49 |
| 6.1 Abstract | 50 |
| 6.2 Results and discussion | 50 |
| 6.2.1 Synthesis and spectroscopic characterisation | 50 |
| 6.2.2 Schiff base adducts of MTO: a comparative study of their stability | 56 |
| 6.2.3 X-ray structures of compounds 5-10 | 58 |
| 6.2.4 Application in epoxidation catalysis | 64 |
| 6.3 Conclusions | 66 |
| REFERENCES CITED IN THIS CHAPTER | 68 |

III. SYNTHESIS AND CATALYTIC APPLICATIONS OF CYCLOPENTADIENYL MOLYBDENUM AND TUNGSTEN ALKYL COMPOUNDS **73**

| | |
|--|----|
| 7. HIGH VALENT ORGANOMETALLIC OXIDES OF MOLYBDENUM AND TUNGSTEN AS EPOXIDATION CATALYSTS | 76 |
| 7.1 Dioxomolybdenum complexes | 77 |
| 7.1.1 Non-organometallic molybdenum dioxo compounds. Adducts with donor ligands | 77 |
| 7.1.2 Organometallic derivatives with M-C σ bonds | 78 |
| 7.1.3 Chiral derivatives | 79 |
| 7.1.4 Application in epoxidation catalysis | 80 |
| 7.1.5 Tungsten derivatives | 81 |
| 7.2 η^5 -Cyclopentadienyl compounds | 82 |
| 7.2.1 Cyclopentadienyl carbonyl metal derivatives | 83 |
| 7.2.2 Cyclopentadienyl oxo-metal derivatives | 84 |
| 7.2.3 Chiral derivatives | 85 |
| 7.2.4 Application in epoxidation catalysis | 86 |
| 7.2.5 Heterogenisation of cyclopentadienyl molybdenum compounds. Applications in ionic liquids | 87 |
| 7.3 Mechanistic implications in the epoxidation reaction. A comparative | 87 |
| 7.3.1 Mechanistic features of molybdenum dioxo species. The Mimoun and Sharpless mechanisms | 88 |
| 7.3.2 Cyclopentadienyl derivatives. Catalytic activity of dioxo and oxo-peroxo species | 90 |

| | |
|---|-----|
| 8. KINETIC STUDIES ON THE OXIDATION OF H ⁵ -CYCLOPENTADIENYL METHYL TRICARBONYL MOLYBDENUM(II) AND THE USE OF ITS OXIDATION PRODUCTS AS OLEFIN EPOXIDATION CATALYSTS | 92 |
| 8.1 Abstract | 92 |
| 8.2 Results and discussion | 93 |
| 8.2.1 Kinetic studies | 94 |
| 8.2.2 Catalytic epoxidation | 100 |
| 8.3 Conclusions | 107 |
| 9. ANSA COMPOUNDS | 108 |
| 9.1 Classification | 108 |
| 9.1.1 <i>ansa</i> bridged bent metallocenes | 109 |
| 9.1.2 Heteroatomic “half-sandwich” <i>ansa</i> compounds. Constrained geometry catalysts | 109 |
| 9.1.3 M-C <i>ansa</i> compounds | 110 |
| 9.2 <i>ansa</i> compounds of Mo and W as oxidation catalysts | 110 |
| 10. STABLE AND CATALYTICALLY ACTIVE ANSA COMPOUNDS WITH CYCLOALKYL MOIETIES AS BRIDGING UNITS | 112 |
| 10.1 Abstract | 113 |
| 10.2 Results and discussion | 113 |
| 10.2.1 Synthesis and characterisation of the spiroligands 1a-d | 113 |
| 10.2.2 Synthesis of the <i>ansa</i> compounds 2a-d | 114 |
| 10.2.3 Properties and characterisation | 117 |
| 10.2.4 X-ray structures of compounds 2a , 3a and 2b | 122 |
| 10.2.5 Application in epoxidation catalysis | 126 |
| 10.3 Conclusions | 130 |
| 11. CURRENT RESEARCH. NEW ANSA DERIVATIVES | 132 |
| 11.1 <i>ansa</i> -C ₄ Compounds. Dimer formation | 132 |
| 11.2 Synthesis and catalytic applications of highly enantioselective <i>ansa</i> compounds | 133 |
| 11.2.1 Revisiting the epoxidation catalysis of <i>ansa</i> compounds | 133 |
| 11.2.2 Use of the menthyl moiety as a chiral inducing agent | 135 |
| 11.2.3 Other alkyl <i>ansa</i> derivatives | 137 |
| 11.2.4 Heterogenisation of the cycloalkyl <i>ansa</i> compounds. Synthesis of 3,4-dihydroxypyrrolidines | 138 |
| 11.2.5 Mechanistic studies | 139 |
| REFERENCES CITED IN THIS CHAPTER | 140 |

| | |
|--|------------|
| IV. EXPERIMENTAL SECTION | 147 |
| 12. SYNTHESIS AND CATALYTIC APPLICATIONS OF MTO SCHIFF BASE COMPLEXES (CHAPTER 6) | 149 |
| 12.1 Materials and Methods | 149 |
| 12.2 Synthesis of the Schiff Base Adducts | 149 |
| 12.3 X-ray crystal determination of compounds 5-9 | 152 |
| 12.4 Catalytic reactions | 153 |
| 13. KINETIC STUDIES ON THE OXIDATION OF η^5 -CYCLOPENTADIENYL METHYL TRICARBONYL MOLYBDENUM(II) AND THE USE OF ITS OXIDATION PRODUCTS AS OLEFIN EPOXIDATION CATALYSTS (CHAPTER 8) | 154 |
| 13.1 Materials and methods | 154 |
| 13.2 Synthesis of $\text{CpMo}(\text{O}_2)\text{OCH}_3$ | 154 |
| 13.3 Kinetic studies | 155 |
| 13.4 Crystal data of compound 3 | 156 |
| 14. STABLE AND CATALYTICALLY ACTIVE ANSA COMPOUNDS WITH CYCLOALKYL MOIETIES AS BRIDGING UNITS (CHAPTER 10) | 158 |
| 14.1 Materials and methods | 158 |
| 14.2 Synthesis of the spiro ligands | 159 |
| 14.3 Synthesis of the Mo derivatives | 160 |
| 14.4 Synthesis of the W derivatives | 162 |
| 14.5 Application in epoxidation catalysis | 163 |
| 14.6 Crystal data of compound 2a | 164 |
| 14.6.1 Bond distances (in Å) | 164 |
| 14.6.2 Bond angles (in °) | 165 |
| 14.7 Crystal data of compound 2b | 166 |
| 14.7.1 Bond distances (in Å) | 166 |
| 14.7.2 Bond angles (in °) | 167 |
| 14.8 Crystal data of compound 3a | 168 |
| 14.8.1 Bond distances (in Å) | 168 |
| 14.8.2 Bond angles (in °) | 169 |
| 14.9 Preliminary crystal data of compounds 2e and 3b | 171 |
| REFERENCES CITED IN THIS CHAPTER | 172 |
| V. APPENDIX | 175 |
| APPENDIX A: SUPPLEMENTARY DATA FOR CHAPTER 8 | 177 |

| | |
|--|-----|
| A.1: Derivation of Equation 1 | 177 |
| A.2: Derivation of Equation 4 | 178 |
| APPENDIX B: NMR SPECTRA OF COMPOUNDS FROM CHAPTER 10 | 180 |
| B.1 Compounds 1a-1e | 180 |
| B.2 Compounds 2a-2f | 185 |
| B.3 Compounds 3a-3e | 193 |
| APPENDIX C: PUBLICATIONS RESULTED FROM THIS WORK | 198 |
| C.1: Publications as first author | 198 |
| C.2: Contributions to other publications | 198 |
| C.3: Communications | 199 |

Glossary

| | |
|----------------------------------|--|
| acac | <i>Acetylacetonate</i> |
| AIPO | <i>Aluminium Phosphate</i> |
| APB | <i>Acetylperoxyborate</i> |
| BHA | <i>tert-butyl hydroxyanisole</i> |
| BINOL | <i>1,1'-bi-2-naphthol</i> |
| BMIM | <i>1-n-butyl-3-methyl imidazolium</i> |
| CGC | <i>Constrained Geometry Catalysts</i> |
| C ₈ MIM | <i>1-n-octyl-3-methyl imidazolium</i> |
| CMHP | <i>Cumene hydroperoxide</i> |
| Cp | <i>cyclopentadiene/cyclopentadienyl</i> |
| Cp' | <i>Penta-substituted cyclopentadienyl (C₅R₅)</i> |
| Cp* | <i>1,2,3,4,5-Pentamethylcyclopentadienyl</i> |
| dbf | <i>dibenzofluorene</i> |
| dp _{ppm} O ₂ | <i>Methylenebis(diphenylphosphine oxide)</i> |
| EBHP | <i>Ethylenebenzene hydroperoxide</i> |
| EtO | <i>Ethylene Oxide</i> |
| IL | <i>(Room Temperature) Ionic Liquids</i> |
| ⁱ Pr | <i>isopropyl</i> |
| Kta | <i>Kilotonnes per annum</i> |
| m-CPBA | <i>meta-chloroperbenzoic acid</i> |
| MCM | <i>Mobile Crystalline Materials</i> |
| Me ₃ tach | <i>trimethyltriazacyclohexane</i> |
| Me ₃ tacn | <i>trimethyltriazacyclononane</i> |
| mes | <i>2,4,6-trimethylbenzyl</i> |
| MTO | <i>Methyltrioxorhenium (VII)</i> |
| NTf ₂ ⁻ | <i>bis(trifluoromethanesulfonyl)amide</i> |
| PAA | <i>Peroxyacetic acid</i> |
| PMTA | <i>Pentamethyldiethylenediamine</i> |
| PO | <i>Propylene Oxide</i> |
| POSS | <i>Polyhedral Oligomeric Silsequioxanes</i> |
| SBA | <i>Santa Barbara Amorphous Materials</i> |
| TBHP | <i>tert-butyl hydroperoxide</i> |

TOF

Turnover Frequency

TON

Turnover Number

UHP

Urea Hydroperoxide

I. INTRODUCTION

Introduction

For 80% of all compounds produced in chemical and pharmaceutical industries at least one *catalytic* step is essential during their synthesis.(1) Catalysisⁱ has been commonly divided in three main groups, based on the nature of the catalyst-substrate interactions. Hence, in homogeneous catalysis the catalyst is in the same phase as the reactants, whereas in heterogeneous catalysis they are in a different phase. The third group, biocatalysis or enzymatic catalysis, is based on substrate-active site interactions.(2) Although all three groups have typically been well separated,(3) new trends and needs both in the industrial and the academic world have blurred the line between them. Many examples of this fact, such as the heterogenisation of homogeneous catalysts or enzyme-inspired heterogeneous catalysts will be introduced in the work presented herein.

ⁱ From greek καταλειν, “to untie” or “to pick up”

1. Oxidation Catalysis: An Overview

One of the most important raw materials used in the industry are alkenes or olefins. These unsaturated molecules are susceptible of many key synthetic and industrial reactions, such as addition, polymerisation and oxidative processes.⁽⁴⁾ The latter, as its name implies, requires an *oxidation* step, which due to the relative stability of the olefinic double bond needs to be catalysed. Usually, this role is fulfilled by a transition metal compound. Consequently, *oxidation catalysis* is a major research field in chemistry, both in academia and in industry.⁽⁵⁻⁷⁾ Since in many catalytic oxidation processes metal-carbon bonds occur in one way or the other - for instance in key intermediates formed as part of the catalytic cycle - organometallic chemistry is one of the key research topics in the field, both in homogeneous and heterogeneous catalysis. As it will be introduced in the following chapters, organometallic oxides – in particular those of transition metals - constitute one of the main research topics in the abovementioned field.⁽⁸⁾

1.1 Scope of the present work

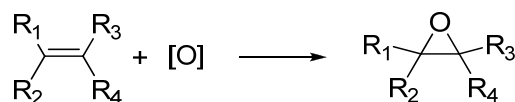
Recent reviews by F. E. Kühn, W. A. Herrmann *et al.* have outlined the promising results obtained for immobilised and homogeneous organorhenium, organomolybdenum and, to a lesser extent, organotungsten catalysts.^(5, 9-12) It has been demonstrated that the active species in the catalytic reaction are organometallic complexes based on Re(VII), Mo(VI) and W(VI) oxides. These complexes have been successfully applied in a broad range of oxidation reactions, and they have proven to be especially active in the catalytic epoxidation of olefins. Both concepts constitute the core of this work.

However, and before concentrating to the particular research topics that correspond to this manuscript, a little further insight in the industrial applications of the epoxidation reaction must be given, including a brief overview of the most common substrates, oxidants and processes. This not only responds to the need of giving a broader scope of this key reaction, but also to the fact that most of the work presented herein aims for

an industrial application. Furthermore, an overview of the current research in epoxidation catalysis will be included.

2. The Epoxidation Reaction. Industrial Significance

The catalytic epoxidation of olefins plays an important role in the industrial production of several commodity compounds, as well as in the synthesis of many intermediates, fine chemicals, and pharmaceuticals. The scale of production ranges from millions of tons per year (ethylene and propylene oxides) to a few grams per year.(13)



Scheme 1 General diagram for the epoxidation reaction.

The diversity of catalysts is large and encompasses all known categories of catalysts: heterogeneous, homogeneous, and biological. However, and as it happens with other fields of catalytic reactions, only the first is widely applied in the industry, accounting for more than the 80-85% of the total production.(14) This owes to many reasons, the most important being a much easier separation of the product from the fixed catalytic bed in heterogeneous systems, which usually is a critical step in every industrial procedure.

The huge advance in the field of catalysis during the second half of the 20th century has given rise to many reasonable alternatives to the already existing industrial procedures, either catalytic or non-catalytic. However, the implementation of these processes is a complicated matter, since the development of a new catalyst follows a “funnel-like” diagram in which most new proposals are dropped in favour of older (but more economic) procedures.(5) This is especially true in the case of homogeneous catalysts.

The increasing concern about the environmental impact of the industrial processes has supposed a turning point in the current panorama. Thus, many new processes have arisen during the last decades, most of them employing catalysts. This also applies to the epoxidation industry, whose primary production methods have experienced notorious changes during the last decades.

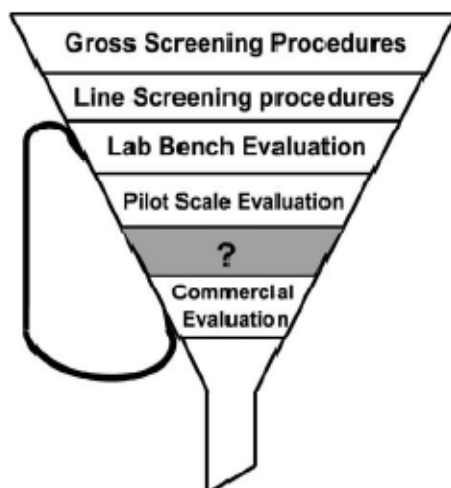


Figure 1 A “realistic development funnel”, as depicted by Cornils and Herrmann (From (5)).

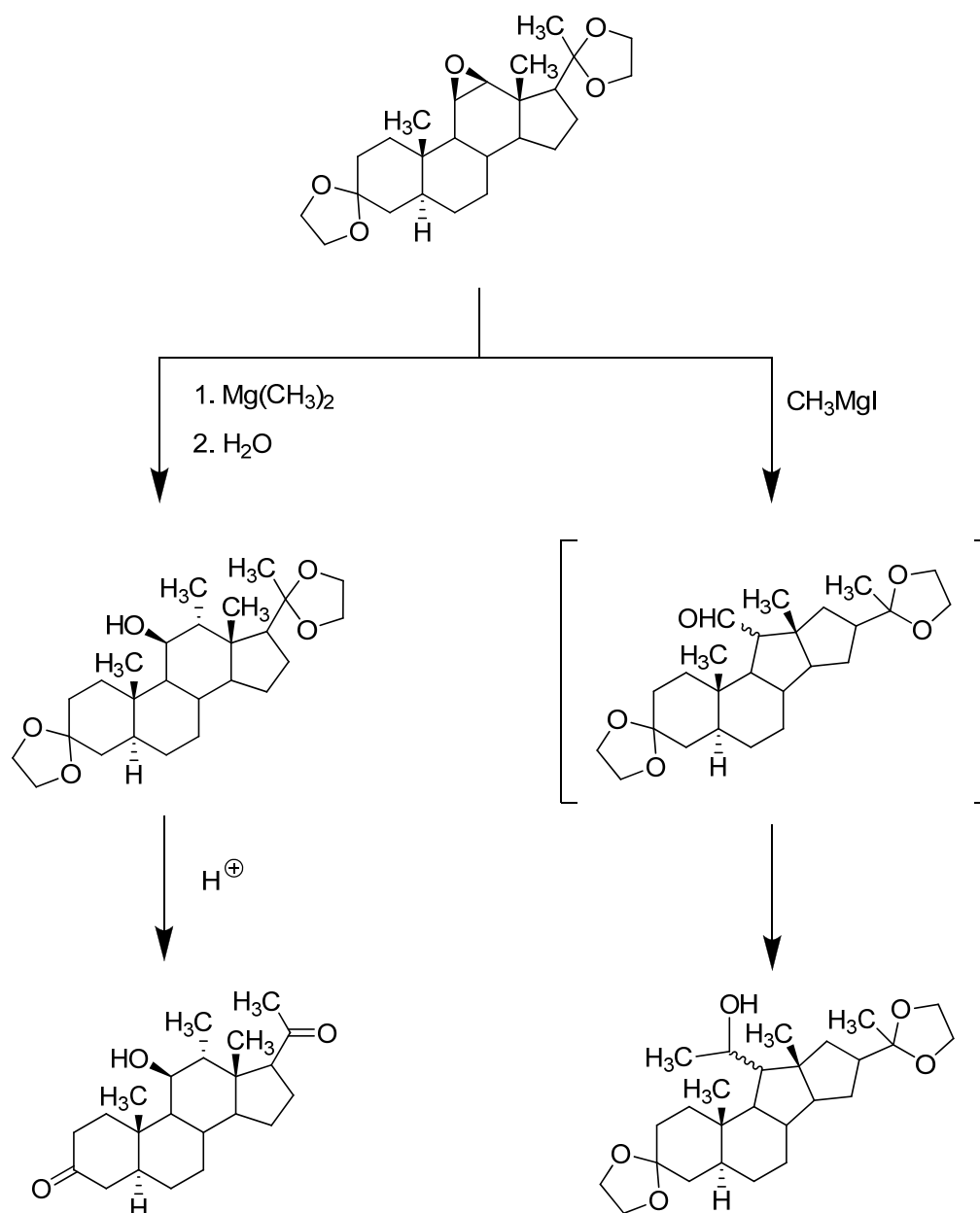
This chapter will summarise the evolution of this important field. Hence, the most relevant epoxides produced in the industry will be introduced, along with their primary production methods.

2.1 Epoxides: a key industrial intermediate

Epoxides are key raw materials for a wide variety of chemicals such as glycols, glycol ethers and alkanolamines, and they can be also be used as building blocks for polymers (e. g. polyesters and polyurethanes, amongst others).(14) The interest in epoxides, however, is not only limited to the commodity industry; their vast number of ring-opening possibilities makes them ideal intermediates in the functionalisation of more complex molecules. *Scheme 2* depicts one of these procedures, where a cholesterol epoxidised derivative is functionalised via two different nucleophiles, yielding two clearly differentiated derivatives.(15)

When dealing with significant epoxides, two main molecules must be cited first: ethylene and propylene oxide. Together, they account for the immense majority of the epoxide industrial production. Although the experimental part of the present work will not deal with these compounds, it is of great importance to stress their primary industrial roles, since they have been the motor around which the most important epoxidation procedures have been developed.

Some other molecules such as glycidol or styrene derivatives are also of special significance in the epoxidation industry. Due to their relevance in the present work, they will be also briefly introduced in this section.



Scheme 2 Nucleophile epoxide ring opening reactions, showing two of the many applications in organic synthesis using epoxides (From **(15)**).

2.1.1 Significant epoxides in the industrial world

Ethylene oxide (EtO)

The simplest olefin oxide, EtO is produced commercially by vapour-phase oxidation of ethylene with air or oxygen over a silver catalyst, promoted by alkali metals and supported on a non-porous form of β -alumina.⁽¹⁶⁾ This process was introduced by Union Carbide in 1937 and later by Shell in 1958 to replace the practice of ethylene oxide production via the obsolete, yet still widely used, chlorohydrin process.⁽¹⁷⁾ This silver catalysed process, however, can only be applied to olefins which do not possess C-H allylic bonds, such as ethylene, 1,3-butadiene and styrene. For all the other olefins, low yields of the desired product are obtained, due to the competing oxidation of allylic C-H bonds, which leads to numerous by-products.⁽¹⁸⁾

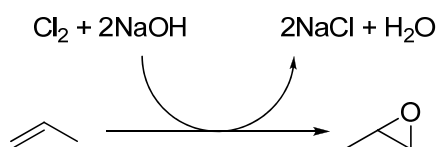
Amongst many applications, ethylene oxide is particularly known for its derivatives, such as ethylene, polyethylene glycols, glycol ethers and ethanolamine. They are employed in the plastics industry as precursors of polyester fibers, heat transfer liquids, lubricants, detergents, etc.⁽¹⁹⁾

Propylene oxide (PO)

The simplest and also industrially useful allylic olefin is propene, together with its epoxidised counterpart, propylene oxide or PO. The latter is a highly reactive oxide that has a plethora of potential applications. PO is used worldwide to produce many versatile products such as polyether polyols (polyglycol ethers), propylene glycols and propylene glycol ethers, which are found in many consumer applications. The former, which make up the largest share of propylene oxide usage (between 60% and 70% of the total volume), are one of the main components in polyurethane systems used in rigid foam insulation and flexible foam seat cushions. Moreover, PO finds many uses as a synthetic block, being applied in the fabrication of flame retardants, modified carbohydrates, synthetic lubricants, oil field drilling chemicals, textile surfactants, among others.⁽²⁰⁾

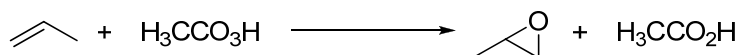
As it has been mentioned above, the allylic nature of propene rules out the silver-catalysed epoxidation process. Thus, many PO producers still employ the traditional chlorohydrin route, which comprises reacting propylene with hypochlorous acid to form propylene chlorohydrin and its subsequent dehydrochlorination to form propylene oxide (Scheme 3). This process, however, is currently outdated and is being gradually

substituted in favour of newer procedures due to the use of expensive, toxic and corrosive chlorine as reagent and the formation of highly toxic by-products.



Scheme 3 The chlorohydrin process and its use in propene epoxidation.

In light of the complexity and cost of the chlorohydrin route, the peracid routeⁱⁱ (Scheme 4) was developed.⁽²¹⁾ This route involves the formation of a peracid, such as peracetic acid, through the reaction of hydrogen peroxide with the organic acid and the subsequent epoxidation of an olefin with the peracid.



Scheme 4 The peracid route.

The disadvantages of the peracid route, however, are also sufficient to preclude significant commercialisation. The reagents are expensive, corrosive and nonregenerable, and the overall efficiency of the process is low. Notwithstanding, peracids have found many applications in more research oriented applications, and are widely used as epoxidation reagents in organic synthesis.^(22, 23)

Glycidol

Though ethylene and propylene oxides are by far the most common epoxides applied in the industry, many other olefinic substrates also find important applications. Thus, cyclic olefins such as cyclohexene and cyclooctene have aroused attentionⁱⁱⁱ, along with arylalkene derivatives such as styrene and stilbene (see Figure 2).

Amongst them, allyl alcohols have achieved great relevance in current academic and industrial research, mostly due to their potential applications in the expanding field of asymmetric epoxidation catalysis.

ⁱⁱ Also known as the Prilezhaev reaction.

ⁱⁱⁱ As it will be seen in chapters II and III, cyclohexene and cyclooctene are often used as model olefins in laboratory catalytic tests.

The simplest allyl alcohol epoxide, known generically as *glycidol*, contains two functional groups of alcohol and epoxide. It can form esters when reacted with ketenes, ethers when reacted with alcohols, and aminopropanediols when reacted with amines. Moreover, it is used as a stabiliser for natural oils and vinyl polymers, demulsifier and dye-levelling agent^{iv}. It is also used as an industrial intermediate in the synthesis of glycerol, glycidyl ethers, esters and amines. It is also applied in surface coatings, sanitary chemicals, in sterilising milk of magnesia and as a gelation agent in solid propellants.(24-26) Glycidol is used as intermediate in the synthesis of many fine chemicals, including pharmaceutical applications in protein synthesis inhibition or anticancer drugs. (27) It must be noted that, in the latter case, enantiomerically pure derivatives are needed, further increasing the current need for catalytic enantioselective procedures.

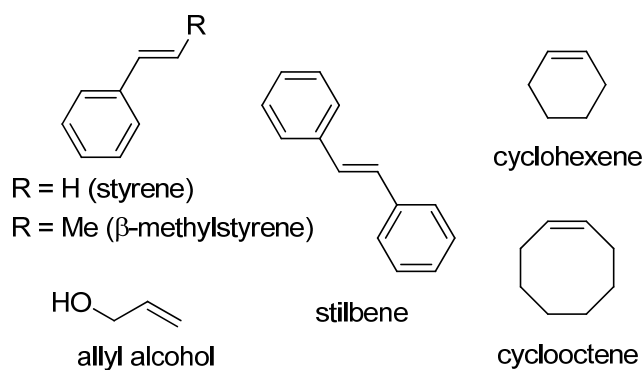


Figure 2 Some common olefinic substrates for catalytic olefin epoxidation.

2.2 Catalytic epoxidation

2.2.1 The oxidant point of view. Introduction of catalytic processes in the epoxidation industry

Despite the current widespread use of comparatively efficient catalysed methods, stoichiometric reactions such as the abovementioned peracid route are still commonly used for the oxidation of fine chemicals.(8, 28, 29) For example, the most widely used epoxidation reagent in research is meta-chloroperoxybenzoic acid (m-CPBA).(22, 23)

^{iv} Glycidol is suspected of being a cancerigen agent; the use of the epoxide without further modifications is therefore being questioned.

This, however, has not hampered the urgent need of developing new efficient methods which should involve *cleaner* oxygen sources such as water peroxide, O₂ or other newly developed reagents such as Oxone[®].(30) These oxidants demand in most cases the presence of a catalyst.

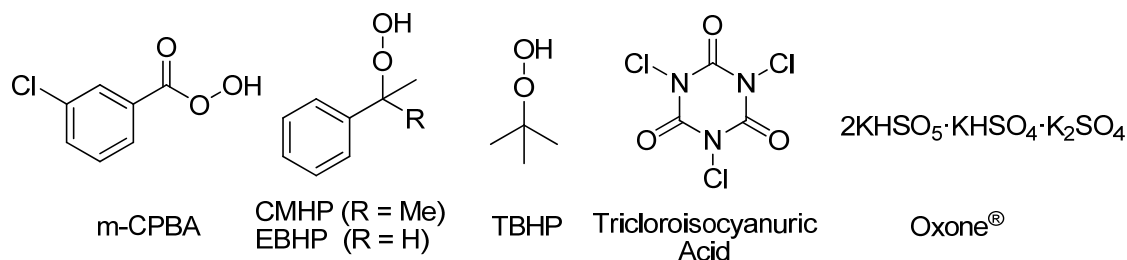


Figure 3 Some common oxidants. Most oxidation reactions carried out with these reagents must be triggered by a catalyst, with the exception of peracids such as m-CPBA.

During the 20th century, and in parallel with the exponential growth of the catalytic-based procedures, a number of olefin epoxidation systems were developed.(31) Amongst them, high valent transition metal oxides, which had been long regarded as powerful oxidation species^v became the backbone of these new catalytic systems, along with peroxides as oxygen-transfer agents. However, none of the reported systems was considered commercially feasible in comparison with the already known, non catalysed routes.

Significant examples include the work of Hawkins, who was the first to report a metal-catalysed epoxidation in the synthesis of cyclohexene oxide in 30% yield, using an alkyl hydroperoxide (cumene hydroperoxide) in combination with V₂O₅.(32)

Moreover, another well known alkyl peroxide, *tert*-butyl hydroperoxide or TBHP, was found to be an active oxidant of olefins in the presence of catalytic amounts of hydrocarbon soluble acetyl acetonates of molybdenum, vanadium and chromium.(33) On the other hand, molecular oxygen was directly considered the active oxidant species together with the hydroperoxide in certain Co and Ce systems.(34)

The Halcon-ARCO process

In 1967, a feasible catalytic epoxidation procedure based on alkyl hydroperoxide oxidants and high valent transition metal catalysts was finally found for an industrial application. Halcon and Atlantic Richfield (ARCO) independently developed processes

^v Some examples include Osmium tetroxide and Sodium permanganate, which are well known dihydroxylation agents.

for the production of epoxides using an alkyl hydroperoxide in the presence of homogeneous catalysts based on molybdenum, tungsten, titanium, niobium, tantalum, rhenium, selenium, chromium, zirconium, tellurium, uranium and vanadium. From all the referred metals, molybdenum, tungsten and titanium were found to be most efficient. The inventors suggested the utilisation of the molybdenum catalyst in the form of organic salts, oxides, chlorides, oxichlorides, fluorides, phosphates, sulfide and molybdic acid. Solubilisation through organometallic modifications was also mentioned.(35-38)

After the success of the two independently developed processes, ARCO and Halcon formed a joint venture, the Oxirane Corporation, to exploit the technology for the manufacture of propylene epoxide using a Mo (VI) catalyst and organic hydroperoxides. Molybdenum catalysts gave the highest rate and selectivity when used with TBHP or ethylbenzene hydroperoxide (obtained from molecular oxygen and ethylbenzene). On the other hand, *tert*-butanol and 1-phenyl ethanol, which are obtained as by-products of the epoxidation process, are finally converted into methyl *tert*-butyl ether (MTBE, which can be used as an octane booster in gasoline) and styrene, both of them being versatile bulk products.(39)

2.2.2 Current industrial advances in catalysis. Propylene oxide

The success of the Halcon-ARCO process has situated it amongst the primary epoxide production methods, especially propylene oxide. However, around 50% of the annual worldwide industrial production capacity (approximately 6500kta) is still carried out by the obsolete chlorohydrin process.(40) This situation, however, is rapidly changing in order to meet economical as well as ecological standards, and new alternatives continue to be developed.

Shortly after Halcon and ARCO, Shell Oil patented the heterogeneous SHELL process, in which TBHP is used in the presence of a Ti(IV)/SiO₂ catalyst for the epoxidation of propene.(41-43) This catalyst, being suitable for continuous fixed bed operation, surpassed the homogeneous systems in industrial standards, and was proven to be a potential candidate in utterly substituting the non-catalysed chlorohydrin process.

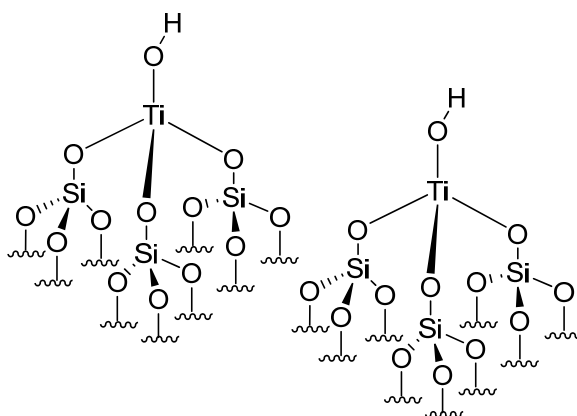


Figure 4 The surface molecular structure of the Ti(IV) Shell epoxidation catalyst.

Following Shell's abovementioned process, a modified version of the ethylbenzene hydroperoxide-based procedure developed by the Oxirane Corporation^{vi} - the Propylene Oxide / Styrene Monomer process - has rapidly found its way into the market, effectively becoming the second main PO production method in the industry.

In this case, cumene hydroperoxide (CMHP) is used instead of ethylbenzene peroxide, and the main by-product of the reaction is α -methylstyrene^{vii}. By the end of 2002, Shell and BASF joined industrial venture (Ellba) opened a PO/SM plant in Singapore with an average production of 550kta of styrene and 200kta of PO.⁽⁴⁴⁾ On the other hand, Lyondell Chemical Co. recently announced the construction of another similar plant in China with an estimated capacity of 227kta of PO and 602kta of styrene.⁽⁴⁵⁾

The main drawback of this process, which might make it not interesting for those companies aiming for a PO-only industrial method, is the olefinic by-product. Consequently, the Sumimoto process was developed.

The Sumimoto process

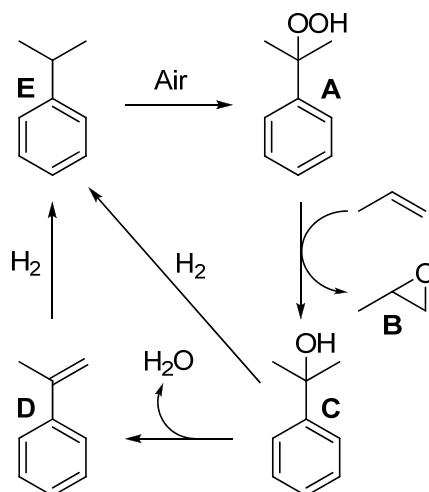
Closely related to both abovementioned processes, the Sumimoto process has gradually been implemented as an interesting alternative to the PO/SM method.⁽⁴⁶⁾ *Scheme 5* depicts this process, in which cumene hydroperoxide (A) is used as oxidant to yield PO (B). The main by-product, cumene alcohol (C) is dehydrated to yield styrene (D), which afterwards is hydrogenated to obtain cumene (E). Cumene alcohol can also

^{vi} These methods are nicknamed PO/TBA (propylene oxide/tert-butyl alcohol) and PO/SM, respectively.

^{vii} It is worth mentioning that cumene peroxide offers a significant improvement over ethylbenzene peroxide in terms of stability, allowing higher concentrations and temperatures.

be directly hydrogenated to cumene via a single hydrogenolysis step. Finally, cumene hydroperoxide is obtained by treatment of the the cumene residue.

Sumimoto, in cooperation with Nihon Oxirane Co., has an operative plant using this process in Chiba, Japan, with a capacity of ca. 200kta.(47)



Scheme 5 The Sumimoto process.

The Enichem process

The use of alkyl hydroperoxides, however, has been questioned during the last decades. The growth of the so-called “Green Chemistry”,(48) which encourages environmentally friendly processes with non-toxic, recyclable side products, has prompted the industrial development of processes that use *green* oxidants over those that use complex hydroperoxides or peracids.

Therefore, ecological concern has radically changed the perspectives for some known oxidants, especially hydrogen peroxide. Previously, this peroxide had not been considered a good oxidant due to its high price and the impossibility of selling or regenerating its by-product (water).(35, 38) However, current industrial standards have outweighed former scepticism and now regard H₂O₂ as an interesting choice, mainly due to the formation of the same side product that had at first discouraged its industrial application.

One of the first companies which successfully applied this new focus on oxidation catalysis was Enichem, which developed an integrated process for a variety of liquid phase oxidations in 1983.(49, 50) In this process, hydrogen peroxide is produced from water and methanol by the anthraquinone route and is used as oxidant with a titanium-substituted silicate (TS-I) catalyst without further separation. TS-I is obtained by

hydrothermal crystallisation of a gel obtained of a mixture of tetraethyl orthosilicate (TEOS) and tetraethyl orthotitanate (TEOT) in the presence of tert-propylammonium hydroxide. The material obtained has a zeolite-like structure, in which Ti atoms partially substitute Si in its lattice, affording a structure with a $x\text{TiO}_2(1-x)\text{SiO}_2$ composition ($0 < x < 0.04\text{M}$). One of the main advantages of this catalyst is its negligible deactivation in the aqueous phase, something unusual for early transition metals^{viii}. Moreover, this system benefits of a lack of Lewis acidic sites, which significantly reduces the possibility of ring opening reactions^{ix}. This process, however, has been commercialised for other reactions but not for the epoxidation of propylene.⁽¹⁸⁾

In the last years increasingly cost-effective, green processes for propylene epoxidation have been introduced. In order to summarise these progresses, a recent report from Nexant's ChemSystems PERP (Process Evaluation/Research Planning) Program has identified four main categories in the current modern industrial epoxidation processes involving catalytic procedures: (51)

- Cumene hydroperoxide-based propylene oxidation with cumene recycle (i.e. the abovementioned Sumimoto process)
- Hydrogen peroxide-based propylene oxidation (or HPPO)
- Direct propylene oxidation with oxygen
- Direct propylene hydro-oxidation with oxygen and hydrogen^x

Of all these alternatives, the second has aroused great attention, and is gradually gaining production quota over other alkylhydroperoxide-based methods.

The HPPO process

2006 possibly marked a turning point for industrial scale epoxidation, as BASF, Dow and Solvay formed a joint venture to build a Hydrogen Peroxide-Based Propylene Epoxide process plant based on the Enichem TS-I catalyst (*Figure 5*).⁽⁵²⁾ This plant has recently been put into service in Antwerp, Belgium and has a current capacity of 300kta. Further installations are planned in the US and the Far East^{xi}.

^{viii} Early transition metals are usually deactivated via hydroxylation processes.

^{ix} As it will be explained in the second part of this work, ring opening reactions due to high Lewis acidity are a relevant issue in Re and Mo systems.

^x This category can be inscribed within the second, since the oxidant formed in this process is hydrogen peroxide. Both processes, however, can be separated from an industrial point of view.

^{xi} Additional information is available on the websites of the respective companies.

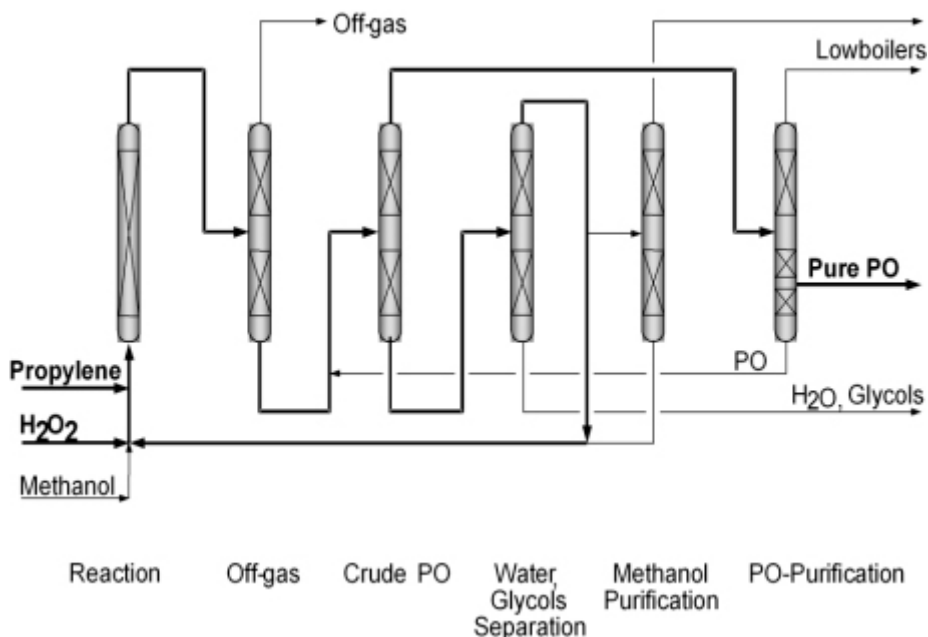


Figure 5 The BASF-Dow-HPPO process.

Moreover, similar HPPO technologies are being implemented by other companies. Degussa AG and Uhde GmbH developed a similar epoxidation procedure using a TS-I catalyst, and its license has been acquired by Korean-based SKC. A plant in Ulsan, South Korea is currently operative, with a capacity of 100kta. SKC is planning to build yet another plant in China with an increased capacity of 400kta, thus becoming one of the main PO producers in a zone with an ever increasing demand.(53)

O₂-based oxidation processes

In spite of the importance and success of the processes with transition metal catalysts and organic hydroperoxides, the direct epoxidation of either propene or other olefins with molecular oxygen is still an attractive goal.(54) This owes to the increasing concern over the use of harmful oxidants - a category in which even hydrogen peroxide is included - and mostly to economic reasons.(55)

Stoichiometric oxidants

$K_2Cr_2O_7$, CrO_3 (Jones Reagent), CrO_2Cl_2 , $KMnO_4$, $PhIO$, peracids (m-CPBA), percarbonates, perborates, H_2O_2 , H_2O_2 :urea, H_2O_2 :DABCO, alkyl hydroperoxides (TBHP, CMHP, EBHP), pyridinium chlorochromate, DMSO, H_2SO_5 , Oxone[®], BRSP, SeO_2 , NaOCl

Table 1 Some commonly used oxidants considered harmful or aggressive (From (55)).

Olin Corporation, for example, patented a process in which propylene is oxidised by O₂-enriched air.⁽⁵⁶⁾ In this process, the reactants (and some recycled by-products) are passed through a molten mixture of alkali metal nitrates, which function both as reaction medium and catalyst.⁽⁵⁴⁾ Also, Berndt et al. have recently presented a method in which an ozone-oxygen mixture and NO₂ epoxidises small alkenes at moderate temperature and pressure.⁽⁴⁰⁾ This method has shown promising industrial applications, since it might substitute both the well known Ag-catalysed ethylene epoxidation and the HPPO processes. However, and despite considerable effort the above-mentioned processes are still not economically viable.

Current perspectives: academic research

The application of the abovementioned procedures has radically changed the production structures in the epoxidation industry. As of 2003, less than 50% of the overall propylene oxide production is still being manufactured via the chlorhydrine process.⁽⁵⁷⁾ This percentage, however, has decreased in the last years due to the broader implementation of newer methods, such as the HPPO or the Sumimoto processes.

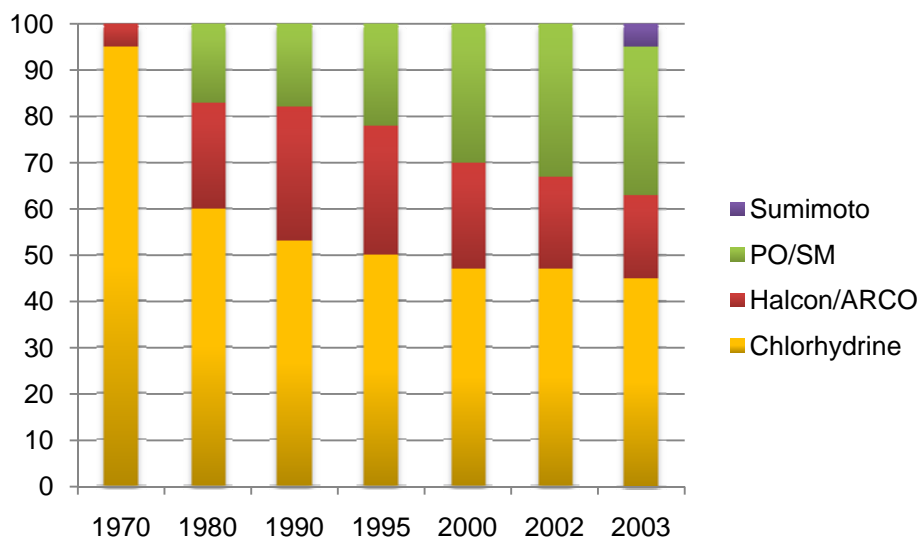


Figure 6 Percentage of PO capacity share by process (1970-2003).

Current academic research continues to develop new catalytic systems, either from a homogeneous or a heterogeneous perspective. The next chapter will change the focus from the olefinic substrate to the catalytic species itself, concentrating on the more recent developments in the field of organometallic chemistry. A specific section will be

devoted to asymmetric catalysis, which has rapidly become a critically important research topic in the last years.

3. Olefin Epoxidation from a Catalyst Point of View

Whereas epoxidation of simple substrates - such as the abovementioned PO - have been successfully applied in the industry, this does not apply to other equally interesting olefins, mainly prochiral substrates which could account for highly added value intermediates in the pharmaceutical industry.

Although the field of heterogeneous catalysis has found a far greater application in the industry, current academic research concentrates in the synthesis of both homogeneous and heterogeneous catalysts^{xii}. Enzymatic or biological catalysis, which is classically considered a third category, has also found little application in the industry. However, many systems from the first two categories are inspired on biological catalysts. Also, and as it will be commented in the next sections, enzymes can play a significant role in the obtention of highly enantiomerically pure epoxides.

This chapter will briefly describe the current laboratory advances in epoxidation catalysis, later concentrating on the field of asymmetric epoxidation. Special attention will be drawn to organometallic species based in transition metals.

3.1 Homogeneous catalysis

Heterogeneous catalysis has been one of the major fields of academic research during the last 50 years. It has become a skilful method to produce a large variety of products owing to the optimised behaviour of the catalytically active species in a homogeneous phase. Moreover, the much simpler catalyst-substrate interactions have proven helpful in elucidating the catalytic mechanism, thus facilitating the search of improved

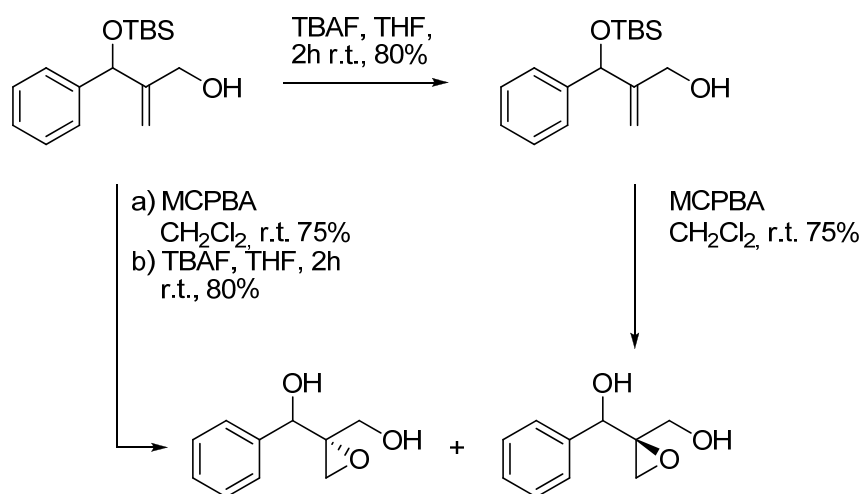
^{xii}, It is a common procedure to synthesise homogeneous catalysts and, in a further step, graft them into a surface, effectively heterogenising them. Many examples of this fact will be commented in upcoming sections.

catalysts. Typical homogeneously catalysed processes include hydroformylation, carbonylation, oxidation, hydrogenation, metathesis and hydrocyanation.(5, 58)

Though always overshadowed by the heterogeneous processes in the industrial field, homogeneous catalysis continues to evolve. In the last years, attention has been concentrated in improving the catalyst selectivity, achieving an unparalleled degree of versatility and specificity. Thus, the design of fine-tuned, tailor-made ligands has become one of the determining characteristics of an homogeneous catalyst. Other factors, such as the solvent, may decisively influence the outcome of the catalytic reaction.

3.1.1 Homogeneous epoxidation catalysis. Transition metal oxides

As it has been stated above, epoxidation reactions in a laboratory scale usually involve stoichiometric reagents such as peracids.(22, 23)



Scheme 6 Epoxidation reaction of unprotected allylic alcohols with the peracid *m*-CPBA (from **(23)**).

Regardless of this fact, the use of transition metal-based oxidising reagents is still quite common in research. Amongst them, high oxidation state species have been considered key molecules in the oxidation of organic substrate due to their enhanced Lewis acidity. Classical organic synthesis oxidation reagents such as OsO_4 ,(59) the Cr-based Jones reagent (60) or NaMnO_4 , for example, have been extensively used in hydroxylation reactions during the past century. The major drawback of these reagents

is their application as stoichiometric reactants, which in the case of osmium involves the formation of highly toxic by-products.

The more recent introduction of related high valent transition metal species as catalysts in oxidation reactions has opened new perspectives in both the industry and the academic research fields.

In his 1989's exhaustive review, Jørgensen summarised the most relevant catalytic epoxidation systems based on transition metals. The author chose to organise them from a group perspective. This section will follow a similar structure.(8)

Group IV: Ti, Zr, Hf

The most relevant metal in this group is titanium. Some of its oxides have been successfully applied in the industry, such as Ti(IV) alkyloxo derivatives (which, for example, are the core of Enichem's TS-I catalyst^{xiii}). Other examples include Ti cyclopentadienyl derivatives and the well known Ti-based Sharpless asymmetric epoxidation, which will be introduced in the following chapters.(61)

Zr and Hf have also been employed in epoxidation catalysis, though the catalytic systems are closely based in the previous Ti studies.(62)

In all cases, TBHP is the usual epoxidation agent; green oxidants such as O₂ have been introduced with average results at best.(54)

Group V: V, Nb, Ta

The application of vanadium (V) oxides as epoxidation catalysts was already reported during the first half of the 20th century.(32) These species show many similarities with certain Ti compounds.(63) Related Nb and compounds have shown similar properties, although their catalytic performance is significantly lower.(62)

Ta species, on the other hand, are a most promising candidate in mimetising alkyloxo Ti(IV) compounds in the heterogeneous phase due to their additional coordination site. This compounds will be described in the following chapters.(64)

Group VI: Cr, Mo, W

Although certain chromium species have been found to be active in epoxidation catalysis^{xiv}, they have been eclipsed by the huge success of Mo(VI) oxides, which are

^{xiii} See section 2.2.2

^{xiv} Amongst them, one of the first salen complexes used for olefin epoxidation (See section 3.3.1).

considered to be the best epoxidation catalysts with alkyl hydroperoxides.(10, 65-67) Part III of the present work will be entirely dedicated to organometallic Mo complexes and their application in epoxidation catalysis. Moreover, related W species, which show similar properties albeit with lower activities, will also be studied. It must be noted that, unlike molybdenum species, tungsten oxides have been shown to be suitable epoxidation catalysts with hydrogen peroxide.(31)

Group VII: Mn, Re^{xv}

Manganese compounds, in special Mn(III) oxides, have attracted a lot of interest due to the similarities with biologically relevant systems, such as manganese porphyrins.(68)

A special trait of manganese catalysed reactions is the use of the hypochlorite moiety as oxygen source. This applies to the abovementioned porphyrin systems, but specially to the later developed Mn(III) salen compounds, whose asymmetric epoxidation capabilities will be described in section 3.3. High oxidation Mn oxides such as the permanganate ion can also trigger epoxidation reactions; however, and apart from being a stoichiometric reagent, this species is often involved in further ring-opening reactions, leading even to the cleavage of the double bond.(69)

Still unknown by the time of Jørgensen's review, the application potential of Re oxides has bloomed during the last decades, especially in the case of methyltrioxorhenium.(9, 70-72) Part II of this work will deal with Re olefin epoxidation chemistry in detail.

Group VIII: Fe, Ru, Os

Iron complexes have an enormous importance in the field of organometallic chemistry, thus making their application as catalysts a primary concern amongst researchers.(73, 74) Although many important catalytic systems based in Fe have been reported, the number of references concerning iron epoxidation catalysis is relatively low. Among them, Fe porphyrin systems based on the biologically relevant cytochrome P-450 (75) have been approached and found to catalyse the epoxidation of sterically crowded olefins such as cyclooctene, norbornene and *cis*-stilbene, using iodobenzene as oxygen-transfer agent.(76) Related enantioselective systems will be discussed in Chapter 3.

Ruthenium oxo-complexes with N-donor ligands such as Schiff bases, bisamides, pybox complexes or the abovementioned porphyrins have been examined in

^{xv} Due to its radioactive nature, technetium is automatically discarded in most industrial applications.

epoxidation catalysis.⁽⁷⁷⁾ Due to their enantioselective properties, similar as those of similar Mn derivatives, they will be discussed in the next chapter.

On the other hand, osmium complexes show a comparatively low range of applications in epoxidation catalysis, and have therefore not been as studied as its neighbouring transition metals. The well known dihydroxylation reagent OsO₄ and other related strongly oxidising agents are not suitable for epoxidation reactions. Therefore, attempts have been made to synthesise less reactive Os (VI) species, using the structure of methyltrioxorhenium derivatives as template.⁽⁹⁾

Group IX: Co, Rh, Ir

Whereas Rh and Ir are particularly useful in the field of homogeneous hydrogenation, they find no significant applications in oxidation catalysis. On the other hand, and in parallel to manganese, cobalt (III) salen compounds have aroused attention in the field of asymmetric catalysis and chiral resolution; some examples will be introduced in Section 3.3.⁽⁷⁸⁾

Groups X and XI: Ni, Pd, Pt, Cu, Ag, Au

Unlike earlier transition metals, most elements in groups X and XI do not fare well in epoxidation catalysis, with the exception of silver and more recently, certain copper compounds. All tested applications find much better examples in other systems, and are therefore of no special relevance in the framework of the present manuscript.

As it has been discussed in the previous chapters, silver is of great importance in the epoxidation of ethylene and other non-allylic olefins via heterogeneous catalysis, being the active catalyst in the Union Carbide and Shell EtO production processes (see Section 2.1).

A recent review from Punniyamurthy *et al.* has highlighted the versatility of copper compounds as oxidation catalysts.⁽⁷⁹⁾ Amongst them, some copper (II) salts have been found to catalyse alkene epoxidation with molecular oxygen in the presence of aliphatic aldehydes as correductants. Other examples of aerobic epoxidations have been reported, but the epoxide yield is very low in comparison to other oxidation byproducts.

Homogeneous catalysts in the epoxidation industry

Despite the plethora of homogeneous epoxidation catalysts discovered throughout the last decades, only a minority have found their way through the “development funnel”

into an industrial successful application.⁽⁵⁾ Currently, even the most well established epoxidation methods, such as the Halcon/ARCO process, are losing ground in front of the heterogeneous HPPO process^{xvi}.

Despite this, new trends in homogeneous and heterogeneous catalysis plead for mutual collaboration. The last decades have seen the introduction of an ever growing number of techniques and procedures which belong neither to homogeneous nor heterogeneous catalysis, but lie somewhere in between. Surface organometallic chemistry and single site heterogeneous catalysis, to name two important examples, belong to this actively researched field.^(64, 80-82)

3.2 Asymmetric epoxidation

In parallel with the ever increasing applications of enantiomerically pure compounds, the industry has been forced to adopt new strategies in order to fulfil the current demand. Unfortunately, current large scale procedures still employ rather obsolete methods, the most important of them (<50% of enantioenriched drugs) still being *classical resolution*, which has the obvious disadvantage of having the whole wrong enantiomer as waste.⁽⁸³⁾ On the other hand, the *chiral pool* approach uses chiral building blocks originating from natural products. Since many natural products offer a high degree of enantiomerical purity, this approach is often chosen in the early development of drugs. A third common method is the *enantioselective synthesis*, in which a covalently bonded chiral auxiliary helps forming the target chiral product. An obvious complication is that the auxiliary part must be either discarded or recycled once the target molecule has been synthesised. *Enantioselective catalytic* reactions, based either on chemocatalysts or biocatalysts, offer many advantages over the abovementioned synthetic procedures, including greater atom economy and versatility. However, only a minority of methods based on asymmetric catalysis are applied in an industrial scale.⁽⁸⁴⁻⁸⁶⁾ As it has been stated above, this also applies to the epoxidation reaction. This chapter will briefly describe the enantioselective reactions in the olefin epoxidation field known to date, along with the current perspectives in the field.

^{xvi} See section 2.2

3.2.1 Asymmetric homogeneous epoxidation catalysts

Homogeneous catalysis has led the academic attempts in designing industry-suitable enantioselective procedures.⁽⁸⁷⁾ Asymmetric hydrogenation has proved to be one of the main research topics in the field. Thus, one of the first reported catalytic asymmetric reactions was 1968's Knowles' Rh-mediated catalytic hydrogenation of α -phenyl acrylic acid to hydratopic acid, obtaining a 15 % ee.⁽⁸⁸⁾ Knowles followed a similar approach in the following years, developing in 1974 the first industrial application of a catalytic asymmetric reaction.⁽⁸⁹⁾ The catalyst for this process, a Rh cationic complex with a chiral inducing diphosphine (R,R-Di-PAMP), successfully hydrogenised highly enantiomerically pure L-DOPA from prochiral amides.

Asymmetric hydrogenation is still the leading field in enantioselective catalysis, but it is closely followed by asymmetric oxidation.^(83, 90) Due to the many reasons stated in previous chapters, epoxidation constitutes a most important segment of this research field. Amongst other significant contributions, the work of Sharpless, Katsuki and Jacobsen has proven to be determining in expanding the field of asymmetric epoxidation. As it will be described below, their work has spawned two of the most significant catalytic systems in the field.

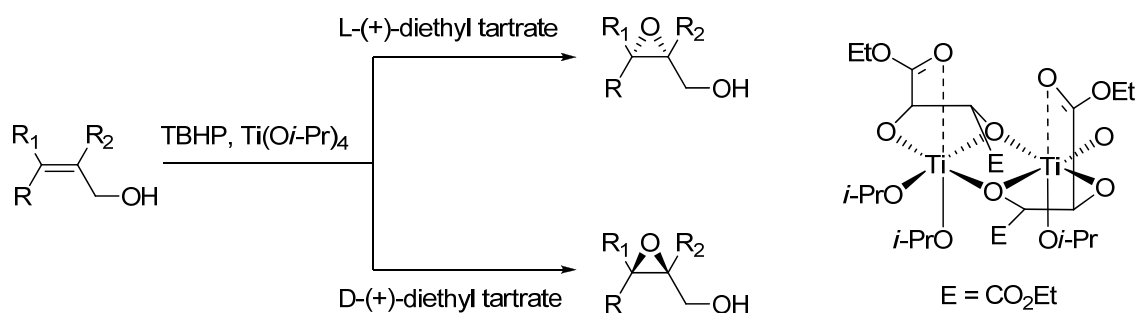
Sharpless epoxidation

The first and to date one of the most significant catalysed asymmetric epoxidation reactions is the Sharpless epoxidation^{xvii}, which consists of the enantioselective epoxidation of allylic alcohols using TBHP, Ti(OⁱPr)₄ and optically pure diethyl tartrate.^(91, 61) This system affords reasonable yields and very high ees (generally over 95%) and has found a plethora of applications in organic synthesis, including kinetic resolution procedures.^(84, 92, 93)

In spite of this method's significance, the Sharpless epoxidation is still only being applied in a laboratory scale, mainly due to its homogeneous nature and the use of alkyl hydroperoxides as oxidants.

This is not the case of the new generation of Salen-based oxidation catalysts - developed by Jacobsen and Katsuki - which, as it will be seen below, have found sound industrial applications.

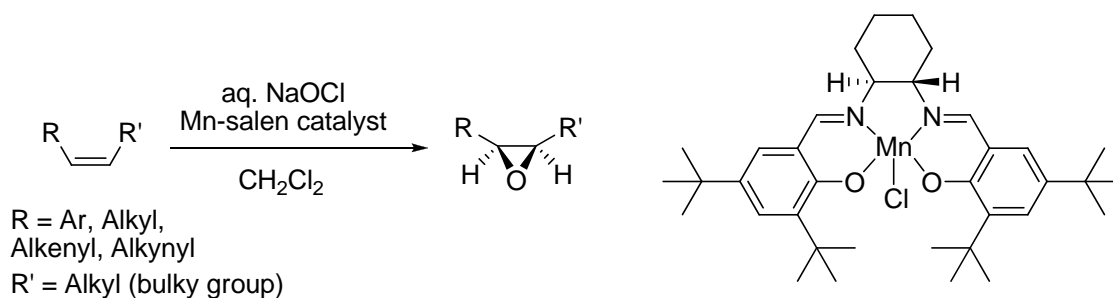
^{xvii}Also known as Katsuki-Sharpless epoxidation.



Scheme 7 The Sharpless asymmetric epoxidation process and the putative active catalyst (right).

Metal-salen catalysts. The Jacobsen-Katsuki epoxidation

The pioneering work of Sharpless and Katsuki significantly contributed to the development of similar enantioselective catalysis. Thus, two similar methods for asymmetric epoxidation were independently developed in 1990 by the groups of Jacobsen and Katsuki.⁽⁷⁷⁾ Based in the earlier work of Kochi et al, who reported the synthesis and characterisation of Cr(V) salen complexes,⁽⁹⁴⁾ this reaction uses cationic Mn(salen) complexes instead. The reaction proved to be extraordinarily effective in the asymmetric epoxidation of *cis*-olefins^{xviii} using NaOCl (bleach) as oxidant and affording very high enantioselectivities (>95% ee).



Scheme 8 The Jacobsen-Katsuki epoxidation, showing the active Mn-salen catalyst (right).

This system has already found an industrial application by ChiRex Inc. (now a joint venture with Rhodia) for the stereoselective HIV-protease-inhibitor Crixivan (Merck & Co).⁽⁹⁵⁾

The field of Mn(III) salen enantioselective catalysts continues to grow. Apart from Mn, other metals such as Ru or Co are being successfully applied as catalysts; also, ligand modification has broadened the range of applications, making certain unfunctionalised

^{xviii} *trans*-olefins, however, cannot be employed as substrates due to the Mn oxo transfer mechanism.

or *trans*-olefins feasible epoxidation candidates.(96, 97) Moreover, this reaction has been found to have promising applications in a plethora of topics, such as asymmetric benzylic oxidation, asymmetric hydroxylation, kinetic resolution of alkenes and allenes, etc.(77, 98) For example, a Co(salen) complex has been successfully applied in the hydrolytic kinetic resolution (HKR) of monosubstituted olefins. This process is currently being employed by Rhodia-ChiRex.(78)

Other systems

Following the results obtained with previously developed Fe-porphyrin systems, Grove and Myers have employed the π -interaction of the olefinic substrate and the aromatic substituent on the chiral Fe(III)-porphyrin complex to obtain optical inductions of ca. 51% with iodosylbenzol as oxidant.(99) However, the synthesis of the chiral porphyrin ligand is very expensive, making salen derivatives more suitable for similar reactions. On the other hand, it has been shown that chirally modified lithium and magnesium *tert*-butyl peroxide can be used for the epoxidation of electron deficient olefins, like chalcones, leading to yields of ca. 60 % and ees of 90%.(100)

4 Objectives of this Work

Following the work carried out in our group, the manuscript presented herein will concentrate on the synthesis, characterisation and catalytic applications of organometallic compounds, in particular high valent rhenium, molybdenum and tungsten and complexes. The objectives of this work can be divided in two main blocks:

I. Schiff base adducts of methyltrioxorhenium:

This block will be preceded by a short overview of MTO and its related donor adducts (Chapter 5).

- Synthesis and characterisation of Schiff base MTO adducts, and study of the adduct stability
- Application in epoxidation catalysis
- Conclusions and perspectives in the field

II. Synthesis and catalytic applications of η^5 -cyclopentadienyl molybdenum and tungsten alkyl compounds:

As above, this part will be introduced by an overview of the most relevant high valent molybdenum and tungsten catalytic systems (Chapter 7), paying special attention to the half-sandwich cyclopentadienyl derivatives. On the other hand, Chapter 9 will give some insight into *ansa* bridged complexes.

- Mechanistic studies of the olefin epoxidation reaction catalysed by $\text{CpMo}(\text{CO})_3\text{Me}$
- *ansa* compounds of Mo and W
 - *Synthesis of the spiro ligands*
 - *Synthesis and characterisation of new Mo and W carbonyl ansa derivatives with cycloalkyl moieties as bridging units*
 - *Application of the novel ansa compounds in olefin epoxidation*

- Perspectives in the field and current work
 - *Studies on the dimerisation of C₄-bridged ansa derivatives*
 - *Synthesis of chiral ansa derivatives The menthyl moiety.*
 - *Catalysis at low temperatures. Application in asymmetric catalysis.*
 - *Synthesis of novel alkyl bridging units*
 - *Heterogenisation via the ansa bridge*
 - *Mechanistic studies.*

References cited in this chapter

- (1) Meyer, F.; Limberg, C. *Organometallic Oxidation Catalysis*; Springer Berlin / Heidelberg; **2007**.
- (2) Cornils, B.; Herrmann, W. A.; Schlögl, R.; Wong, C. *Catalysis from A to Z: A Concise Encyclopedia*; 2nd ed.; Wiley-VCH Verlag GmbH & Co. KGaA, **2003**.
- (3) Sheldon, R. A. *Adv. Synth. Cat.* **2001**, 343, 377-378.
- (4) Wade, L.G.; *Organic Chemistry*, 6th ed.; Pearson Prentice Hall, **2006**, pp. 279.
- (5) Cornils, B.; Herrmann, W. A. *J. Catal.* **2003**, 216, 23-31.
- (6) Veljanovski, D. *PhD Thesis*, Technische Universität München, **2009**.
- (7) Herrmann, W. A.; in his speech "Technologies of the Future: Catalysis". *Technische Universität München*, **2000**.
- (8) Joergensen, K. A. *Chem. Rev.* **1989**, 89, 431-458.
- (9) Herrmann, W. A. *J. Organomet. Chem.* **1995**, 500, 149-174.
- (10) Kühn, F. E.; Santos, A. M.; Herrmann, W. A. *Dalton Trans.* **2005**, 2483-2491.
- (11) Kühn, F. E.; Jain, K. R.; Zhou, M. *Rare Metals* **2006**, 25, 411-421.
- (12) Jain, K. R.; Kühn, F. E. *J. Organomet. Chem.* **2007**, 692, 5532-5540.
- (13) Oyama, S. T.; *Mechanisms in Homogeneous and Heterogeneous Epoxidation Catalysis*; Elsevier, **2008**.
- (14) Weissermel, K.; Arpe, H. *Industrial Organic Chemistry*; Wiley-VCH: Weinheim, **2003**.
- (15) Gorzynski Smith, J. *Synthesis* **1984**, 629-656.
- (16) Kitty, P. A.; Sachtler, W. M. H. *Catal. Rev.* **1974**, 10, 1-16.
- (17) McClellan, P. P. *Ind. Eng. Chem.* **1950**, 42, 2402-2407.
- (18) Sheldon, R. A. In *Applied Homogenous Catalysis with Organometallic Compounds – A Comprehensive Handbook*; Cornils, B.; Herrmann, W. A., Eds.; Wiley-VCH, Weinheim: Germany, **2002**; Vol. 1, pp. 412-426.
- (19) Information available via the Dow Chemical Company website (URL: <http://www.dow.com/ethyleneoxide/applications/index.htm>).
- (20) Information available via the Dow Chemical Company website (URL: <http://www.dow.com/propyleneoxide/app/index.htm>).
- (21) Wurcz, A. *Ann. Chim.* **1859**, 55, 406.
- (22) Jana, N. K.; Verkade, J. G. *Org. Lett.* **2003**, 5, 3787-3790.

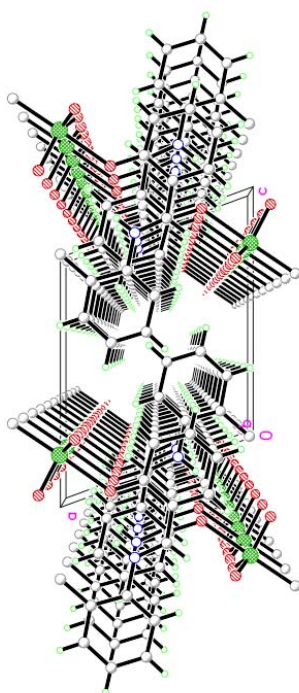
- (23) Porto, R. S.; Vasconcellos, M. L. A. A.; Ventura, E.; Coelho, F. *Synthesis* **2005**, 2297-2306.
- (24) National Toxicology Program; US Department of Health and Human Services *Report on Carcinogens. 11th Edition.*
- (25) *IARC Monographs* **2000**, 77, 469-486.
- (26) Heathcock, C. H.; McLaughlin, M.; Medina, J.; Hubbs, J. L.; Grier, A.; Wallace, R. S.; Claffey, M. M.; Hayes, C. J.; Ott, G. R. *J. Am. Chem. Soc.* **2003**, 125, 12844-12849.
- (27) Palomo, J. M.; Segura, R. L.; Mateo, C.; Terreni, M.; Guisan, J. M.; Fernández-Lafuente, R. *Tetrahedron: Asymmetry* **2005**, 16, 869-874.
- (28) Herrmann, W. A.; Cornils, B. *Angew. Chem. Int. Ed. Engl.* **1997**, 36, 1048-1067.
- (29) Cornils, B.; Herrmann, W. A.; Eckl, R. W. *J. Mol. Catal. A: Chem.* **1997**, 116, 27-33.
- (30) Travis, B. R.; Sivakumar, M.; Hollist, G. O.; Borhan, B. *Org. Lett.* **2003**, 5, 1031-1034.
- (31) Payne, G. B.; Smith, C. W. *J. Org. Chem.* **1957**, 22, 1682-1685.
- (32) Hawkins, E. G. E. *J. Chem. Soc.* **1937**, 59, 2342.
- (33) Sharpless, K. B.; Verhoeven, T. R. *Aldrichimica Acta* **1979**, 12, 63-74.
- (34) Brill, W. F. *J. Am. Chem. Soc.* **1963**, 85, 141-145.
- (35) Halcon Int.; DE 1.939.791, **1979**
- (36) Kollar, J.; US; 3.350.422, US 3.351.635, **1967**.
- (37) Sheng, M. N.; Zajacek, G. J. *ACS Adv. Chem. Ser.* **1968**, 76, 418.
- (38) Sheng, M. N.; Zajacek, G. J.; GB 1.136.923, **1968**
- (39) Hodnett, B. K. In *Heterogeneous Catalytic Oxidation: Fundamental and Technological Aspects of the Selective and Total Oxidation of Organic Compounds*; John Wiley and Sons: Chichester, **2000**; p. 160.
- (40) Berndt, T.; Böge, O.; Heintzenberg, J. *Ind. Eng. Chem. Res.* **2003**, 42, 2870-2873.
- (41) Shell Oil; US 3.829.392, **1974**
- (42) Wulff, H. P.; US 3.829.392, **1974**
- (43) Sheldon, R. A. *J. Mol. Catal.* **1980**, 7, 107.
- (44) Specifications: <http://www.chemicals-technology.com/projects/ellba/specs.html>.
- (45) White, L. *Urethanes Technology International*. February **2007**.
- (46) Yamamoto, J.; Junpei, T.; US 6.096.910, **1999**.
- (47) *Focus on Catalysts* **2002**, 5.
- (48) U.S. Environmental Protection Agency (<http://epa.gov/gcc/>).
- (49) Clerici, M. G.; Ingallina, P. *J. Catal.* **1993**, 140, 71-83.
- (50) Clerici, M. G.; Bellussi, G.; Romano, U. *J. Catal.* **1991**, 129, 159-167.

- (51) Nexant Chemsystems *Process Evaluation/Research Planning Program: Propylene Oxide*. **2007**.
- (52) Schindler, G.; Walsdorff, C.; Koerner, R.; Goebbel, H.; WO 2007000396, **2007**.
- (53) Alperowicz, N. *Urethanes Technology International*. July **2008**.
- (54) Monnier, J. R. *Appl. Catal. A: General* **2001**, *221*, 73-91.
- (55) Thomas, J. M.; Raja, R. *Catal. Today* **2006**, *117*, 22-31.
- (56) Meyer, J. M.; Pennington, B. T.; US 4992567, **1991**.
- (57) Nexant's Chemsystems *Process Evaluation/Research Planning Program: Propylene Oxide*. January **2004**,
- (58) Crabtree, R. H. *The Organometallic Chemistry of the Transition Metals*; 4th ed.; Wiley, **2005**; p. 538.
- (59) Ray, R.; Matteson, D. S. *Tetrahedron Letters* **1980**, *21*, 449-450.
- (60) Bowden, K.; Heilbron, I. M.; Jones, E. R. H.; Weedon, B. C. L. *J. Chem. Soc.* **1946**, 39-45.
- (61) Katsuki, T.; Sharpless, K. B. *J. Am. Chem. Soc.* **1980**, *102*, 5974-5976.
- (62) Sheldon, R. A.; Wallau, M.; Arends, I. W. C. E.; Schuchardt, U. *Acc. Chem. Res.* **1998**, *31*, 485-493.
- (63) Fischer, E. O.; Vigoureux, S. *Chem. Ber.* **1958**, *91*, 1342-1344.
- (64) Copéret, C.; Chabanas, M.; Petroff Saint-Arroman, R.; Basset, J. *Angew. Chem. Int. Ed.* **2003**, *42*, 156-181.
- (65) Freund, C.; Abrantes, M.; Kühn, F. E. *J. Organomet. Chem.* **2006**, *691*, 3718-3729.
- (66) Kühn, F. E.; Santos, A. M.; Abrantes, M. *Chem. Rev.* **2006**, *106*, 2455-2475.
- (67) Bottomley, F.; Boyle, P. D.; Chen, J. *Organometallics* **1994**, *13*, 370-373.
- (68) Haber, J.; Matachowski, L.; Pamin, K.; Poltowicz, J. *J. Mol. Catal. A: Chem.* **2000**, *162*, 105-109.
- (69) Dash, S.; Patel, S.; Mishra, B. K. *Tetrahedron* **2009**, *65*, 707-739.
- (70) Herrmann, W. A.; Fischer, R. W.; Scherer, W.; Rauch, M. U. *Angew. Chem. Int. Ed.* **1993**, *32*, 1157-1160.
- (71) Herrmann, W. A.; Fischer, R. W.; Rauch, M. U.; Scherer, W. *J. Mol. Catal.* **1994**, *86*, 243-266.
- (72) Al-Ajlouni, A. M.; Espenson, J. H. *J. Am. Chem. Soc.* **1995**, *117*, 9243-9250.
- (73) Fischer, E. O. *Angew. Chem.* **1955**, *67*, 475-482.
- (74) King, R. B.; Bisnette, M. B. *J. Organomet. Chem.* **1967**, *8*, 287-297.
- (75) White, R. E.; Coon, M. J. *Ann. Rev. Biochem.* **1980**, *49*, 315-356.
- (76) Groves, J. T.; Nemo, T. E. *J. Am. Chem. Soc.* **1983**, *105*, 5786-5791.

- (77) Katsuki, T. *Synlett* **2003**, 3, 281-297.
- (78) DiMare, M. *Innovations in Pharmaceutical Technology* **2002**, 116-121.
- (79) Punniyamurthy, T.; Rout, L. *Coord. Chem. Rev.* **2008**, 252, 134-154.
- (80) Raja, R.; Thomas, J. M.; Xu, M.; Harris, K. D. M.; Greenhill-Hooper, M.; Quill, K. *Chem. Commun.* **2006**, 4, 448-450.
- (81) Comas-Vives, A.; González-Arellano, C.; Corma, A.; Iglesias, M.; Sánchez, F.; Ujaque, G. *J. Am. Chem. Soc.* **2006**, 128, 4756-4765.
- (82) Thomas, J. M.; Raja, R. *Top. Catal.* **2006**, 40, 3-18.
- (83) Blaser, H.; Pugin, B.; Spindler, F. *J. Mol. Catal. A: Chem.* **2005**, 231, 1-20.
- (84) Keith, J. M.; Larrow, J. F.; Jacobsen, E. N. *Adv. Synth. Cat.* **2001**, 343, 5-26.
- (85) Straathof, A. J. J.; Panke, S.; Schmid, A. *Current Opinion in Biotechnology* **2002**, 13, 548-556.
- (86) Blaser, H.; Schmidt, E. In *Large Scale Asymmetric Catalysis*; Wiley-VCH: Weinheim, **2003**; p. 1.
- (87) Lohray, B. B. *Current Science* **2001**, 81, 1519-1525.
- (88) Knowles, W. S.; Sabacky, M. J. *Chem. Commun.* **1968**, 1445-1446.
- (89) Knowles, W. S. *Acc. Chem. Res.* **1983**, 13, 106.
- (90) Rouhi, A. M. *Chem. Eng. News* **2004**, 82, 47-62.
- (91) Li, J. J. In *Name Reactions*; Springer Berlin Heideberg, **2007**; p. 533.
- (92) Pfenniger, A. *Synthesis* **1986**, 89-116.
- (93) Katsuki, T.; Martín, V. *Org. React.* **1996**, 48, 1-299.
- (94) Siddall, T. L.; Miyaura, N.; Huffman, J. C.; Kochi, J. K. *Chem. Commun.* **1983**, 1185-1186.
- (95) Tempesti, E.; Giuffré, L.; Modica, G.; Montoneri, E.; EP-a0 159, 619, **1985**.
- (96) Schwenkreis, T.; Berkessel, A. *Tetrahedron Letters* **1993**, 34, 4785-4788.
- (97) Kureshy, R. I.; Khan, N. H.; Abdi, S. H. R.; Singh, S.; Ahmed, I.; Shukla, R. S.; Jasra, R. *V. J. Catal.* **2003**, 219, 1-7.
- (98) Adam, W.; Humpf, H. U.; Roschmann, K. J.; Saha-Möller, C. R. *J. Org. Chem.* **2001**, 66, 5796-5800.
- (99) Groves, J. T.; Myers, R. S. *J. Am. Chem. Soc.* **1983**, 105, 5791-5796.
- (100) Elston, C. L.; Jackson, R. F. W.; MacDonald, S. J. F.; Murray, P. J. *Angew. Chem. Int. Ed.* **1997**, 36, 410-412.

II. SCHIFF BASE ADDUCTS OF METHYLTRIOXORHENIUM

Schiff Base Adducts of Methyltrioxorhenium



Transition metal oxides have been established as important species in many catalytic transformations (1, 2). Amongst them, rhenium oxides have achieved great relevance, mainly due to the unprecedented success of one single species, methyltrioxorhenium (MTO). In the last two decades, the synthesis and modification of this and other Re alkyl oxides has become a field of research of critical importance in our laboratories. This chapter will first highlight the importance of Re alkyl oxides both in synthesis and in catalysis, concentrating on MTO and its derivatives, especially N-donor adducts. Recent attempts in either asymmetric catalysis or heterogenisation will also be presented, along with the current perspectives.

5. Rhenium Oxides as Epoxidation Catalysts

Being the last naturally occurring stable atom to be discovered, the application of rhenium and its derivatives in catalysis is relatively recent. Thus, the synthesis of organometallic compounds and specifically high oxidation Re compounds was first reported in the seventies, when Wilkinson *et al.* synthesised $(\text{CH}_3)_4\text{ReO}$.⁽³⁾ Soon after, Beattie and Jones reported the serendipitous synthesis of methyltrioxorhenium (VII) by oxidation of Wilkinson's tetramethyloxorhenium.⁽⁴⁾ Five years later, Herrmann *et al.* reported the synthesis of the unexpectedly stable $\eta^5\text{-Cp}^*\text{ReO}_3$ ($\text{Cp}^* = 1,2,3,4,5\text{-pentamethylcyclopentadienyl}$), one of the first aryl organorhenium (VII) complexes to be described.⁽⁵⁾

Re(VII) oxides display a d^0 electronic configuration, thus making them relatively stable and Lewis-acidic.⁽⁶⁾ Since similar oxides from neighboring atoms display catalytic activity in oxidation reactions, the use of rhenium species in epoxidation catalysis was considered as soon as they were available in sufficient quantities. Due to the scope of this work, only σ -bound Re-C compounds will be studied in detail.

5.1 Alkyl- and aryl-trioxorhenium compounds

Though classically considered much less stable than their arene counterpartsⁱ, σ -alkyl and aryl metallorganic compounds have attracted much attention during the last decades.⁽⁷⁾ This is particularly true in the case of organometallic rhenium oxides.

Herrmann *et al.* originally concentrated on the synthesis and applications of $\eta^5\text{-Cp}^*\text{ReO}_3$ compounds and derivatives, originally discovered in 1984 (8), but these studies were

ⁱ One of the alleged reasons is that arene compounds can apport more electrons than σ bound complexes; thus, stable $18e^-$ species can be formed in the former case, while the latter are traditionally electron-deficient. This, as it will be seen later, is the case of methyltrioxorhenium (VII), with a formal electron number of 14.

quickly overshadowed by methyltrioxorhenium (VII), which, unlike other related compounds, showed an improved stability both in air and moisture.⁽⁹⁾

The unprecedented success of MTO has not stopped the search for similar alkyl derivatives. Thus, in the last two decades a renewed interest for σ -aryl and alkyl rhenium oxides has arisen.^(8, 10) Some examples of these compounds are included in Figure 1.

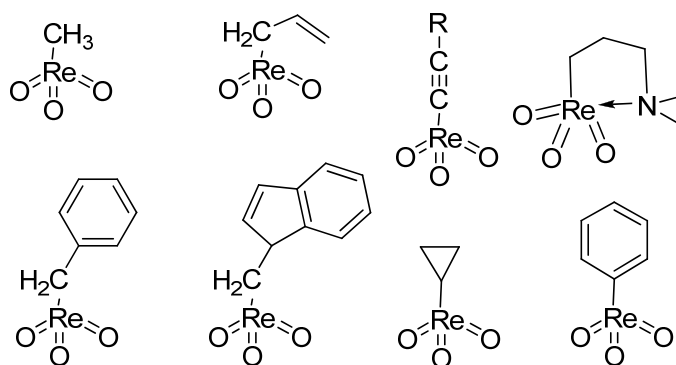


Figure 1 Some aryl and alkyltrioxorhenium complexes, including MTO (upper left corner).

These compounds, though extremely interesting in a synthetic point of view, have not yet surpassed the capabilities of MTO itself both in terms of synthesis, stability, and catalytic applications; therefore, the latter remains the state-of-the-art.

5.2 Methyltrioxorhenium: an overview

5.2.1 Properties

MTO presents unique properties amongst other Re alkyl derivatives. It can be easily melted and sublimed without noticeable decomposition; moreover it is soluble in most solvents, including water (see Table 1).

Moreover, MTO has certain characteristics that determine its catalytic capabilities. These are a remarkable steric accessibility (low coordination number, small ligands), a strong metal-carbon bond (with $\Delta H > \sim 237 \text{ kJ mol}^{-1}$), and a pronounced Lewis acidity at the metal due to its high oxidation state. In contrast, other derivatives such as the cyclopentadienyl and phenyl congeners suffer from either steric crowding or insufficient stability under catalytic conditions.

Experimental data for methyltrioxorhenium

 Colourless needles

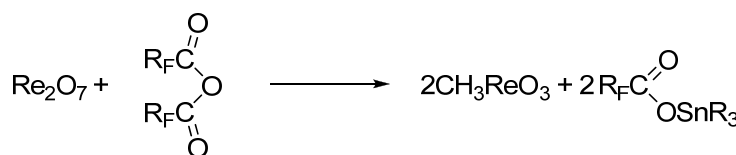
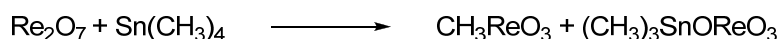
 Soluble in common organic solvents (especially polar solvents) and water
 Melting point: 111°C (without decomposition), Sublimable at 25°C/1mmHg
 No decomposition in the gas-phase < 300°C

 Density = 4.103g·cm⁻³

 IR(cm⁻¹): ν(ReO) 1001w, 965vs(CS₂); ν(CH) 2989m, 2986vw, 2900m (CH, str.)
 UV/Vis (diethylether): λ₁(max) = 260nm (ε₁ = 1400L·mol⁻¹·cm⁻¹), λ₂(max) = 232 (1900)
 NMR (CDCl₃, 25°C): δH = 2.61, δC = 19.03[²J(CH) = 138Hz], δO = 829 ppm
 NMR (solid state, 25°): δH = 2ppm (ext. H₂O), δC = 36 ppm (ext. adamantane)
 MS: m/z = 250 (M⁺, 187Re), 220 ([M-H₂CO]); 100%

Table 1**5.2.2 Synthesis**

Originally obtained as a long term oxidation subproduct of (CH₃)₄ReO₄, (4) MTO was only made easily available in reasonable yields in 1989, using Sn(CH₃)₄ along with Re₂O₇ as starting materials.(11)

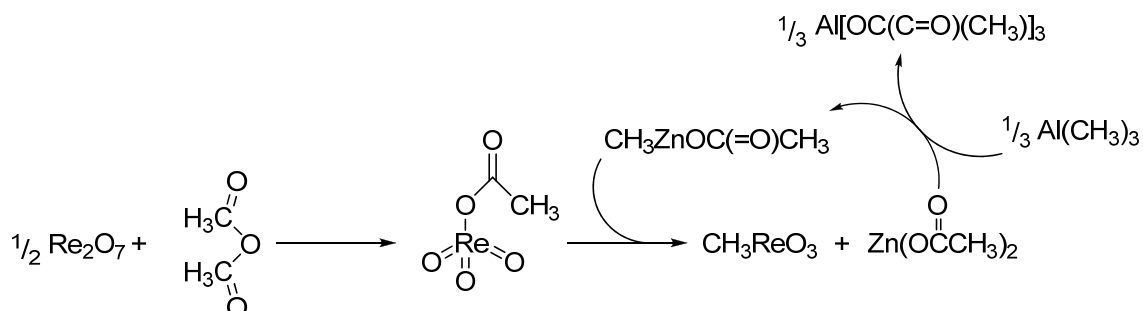


Scheme 1 The tetramethyltin approach (above) and the improved synthetic method developed by Herrmann, Kühn *et al.* (below).

This reaction, however, has a major drawback, since part of the dirhenium heptoxide forms a non reactive compound with the tin reactant (stannyl perrhenate), thus limiting the overall yield to a 50% at best with respect to the rhenium metal.

The work of Herrmann, Kühn *et al.* in 1992 found a convincing solution to this problem, using anhydrides of perfluorinated carboxylic acids and two molar equivalents of tetramethyltin.(12) This approach, which can also be applied to other alkyltrioxorhenium (VII) derivatives, has been improved over the years. Currently, MTO has been easily obtained using methyl zinc acetate and non-fluorinated perrhenylacetate, obtaining both high yields (ca. 85%) and an a rather easy purification of the product.(13, 14) It is also

worth mentioning that these new procedure drops the use of hazardous reagents such as tetramethyltin or perfluorinated compounds.

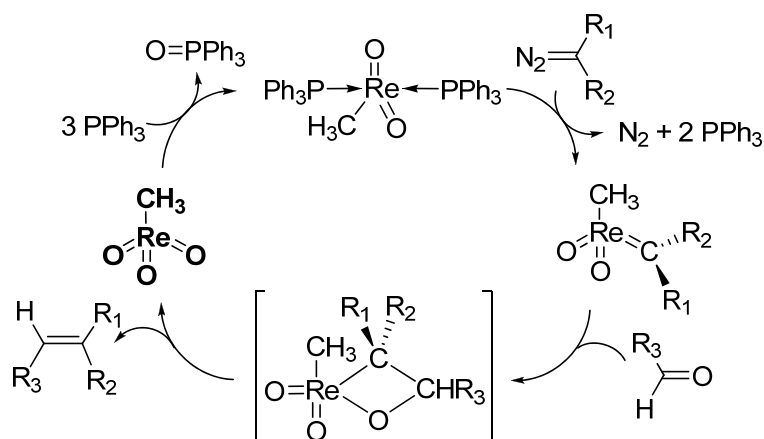


Scheme 2: The new, “green” synthesis of methyltrioxorhenium, as reported by Herrmann *et al.*

It must be noted that the carboxylato compound shown in Scheme 2 is a most valuable precursor in the synthesis of ReO_3 -based derivatives, together with the less stable ROReO_3 species. Due to this fact, the abovementioned methods have been adapted to synthesise similar alkyl and aryl derivatives.(10)

5.3 Catalytic applications of MTO

The unexpected high stability of methyltrioxorhenium prompted many studies concerning both its properties and reactivity.(11) Immediately after, research was focused on potential catalytic applications, due to the similarity of MTO with other high valent transition metal oxides.(15)



Scheme 3 Catalytic aldehyde olefination mechanism with MTO according to Herrmann *et al.* (From (16)).

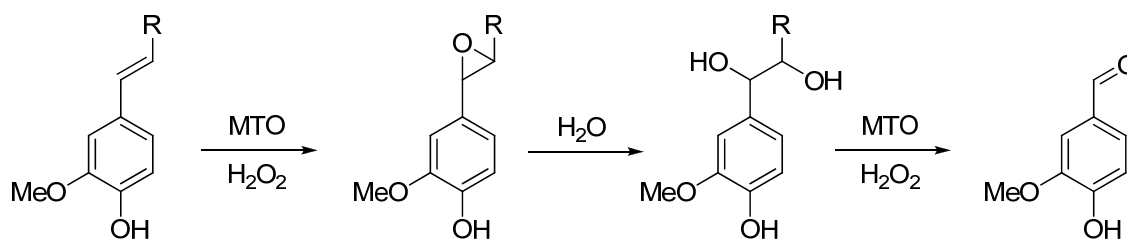
It turned out that the new Re species was an extremely versatile and powerful catalyst, with applications ranging from olefin oxidation to olefin metathesis, Diels-Alder cycloaddition and aldehyde olefination.(16, 17) The mechanism of the latter reaction is depicted in Scheme 3.

Despite the above-average results obtained in other fields, MTO is first and foremost considered an oxidation catalyst, and is particularly well known for its almost unparalleled epoxidation capabilities.

5.3.1 Methyltrioxorhenium as a homogeneous oxidation catalyst

As it has been mentioned above, MTO was applied in olefin oxidation soon after its synthesis was optimised. Thus, Herrmann *et al.* reported the successful application of MTO as an olefin epoxidation catalyst, using H_2O_2 as oxidant.(6) The subsequent dihydroxylation reactions have also been thoroughly studied.

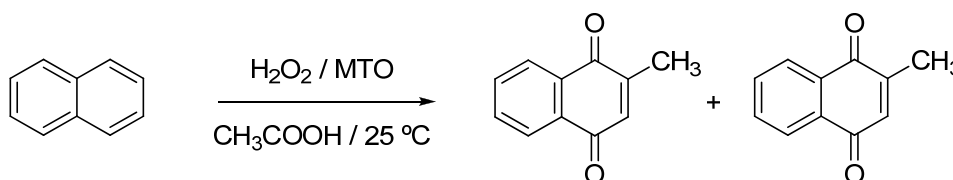
Moreover, and amongst many other applications, MTO proved extremely effective in other reactions such as the Baeyer-Villiger oxidation,(18) arene oxidation (Scheme 5),(19) C-C bond cleavage (via an epoxide intermediate, see Scheme 4),(20) secondary amine oxidation to nitrones(21) and terminal alcohol oxidation.(22)



R = CH_3 (Isoeugenol)

R = COOH (*trans*-ferulic acid)

Scheme 4 C-C MTO-catalysed cleavage of olefins via an epoxide intermediate.



Scheme 5 Arene oxidation reaction with MTO.

It is important to highlight that, unlike related transition metal oxidesⁱⁱ, H₂O₂ can be used as oxidant without noticeable decomposition of the catalyst.

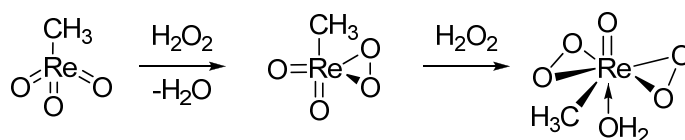
When looking through the recent literature, the olefin epoxidation reaction clearly stands out as the most significant application of MTO. This owes to certain key factors, such as the abovementioned use of water peroxide as the oxidant or the low catalyst concentration needed for the reaction to take place.

5.3.2 Mechanistic implications in the epoxidation reaction

The extraordinary versatility of methyltrioxorhenium soon aroused questions about the reaction mechanisms of MTO-catalysed processes, amongst them the most relevant oxidation reactions. Herrmann *et al.* soon reported mechanistic studies of the olefin epoxidation reaction.⁽²³⁾ Since then, this reaction has been extensively studied.⁽²⁴⁻²⁷⁾

Peroxo and bis-peroxo MTO derivatives

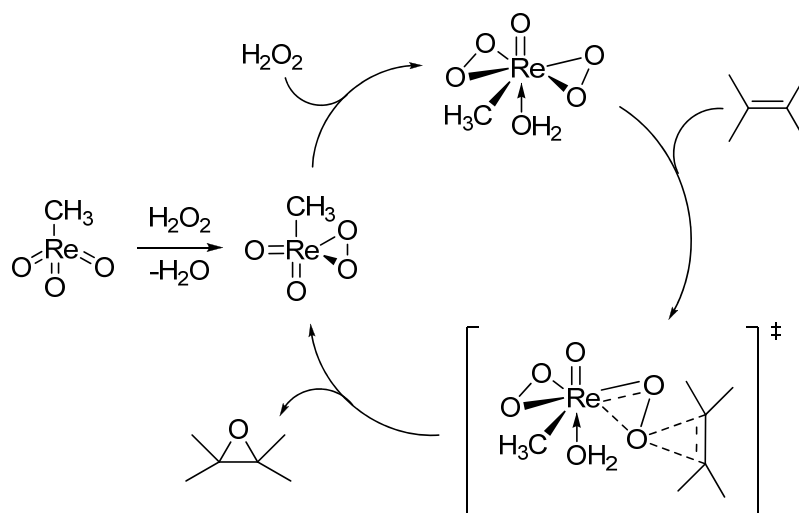
Methyltrioxorhenium (VII) shows a similar behaviour to other high valent d⁰ transition metal oxides, such as Mo(VI), V(V) and Ti(IV). Thus, the active species is an electron-deficient *peroxometal*, which is formed by heterolyzation of the oxidant via an *electrophilic* mechanism.⁽²⁷⁾



Scheme 6 Formation of the mono- and bis-peroxide derivatives of MTO.

In the case of MTO, both the mono- and the bis-peroxo complexes are comparably active.⁽²⁸⁾ However, the much higher oxidant concentration forms preferably the bis-peroxo species, which is normally a more active oxidation catalyst. The mechanistic features of the reaction are resumed in Scheme 7.

ⁱⁱ On the other hand, Mo oxides, which will be introduced in the following chapters, are preferably reacted with alkylhydroperoxides such as TBHP.



Scheme 7 The proposed mechanism for the MTO-catalysed epoxidation.

The formation of the active species involves a single oxygen transfer. Furthermore, the mechanism proceeds without the formation of radical species; as a result, the selectivity of the reaction is very high in most cases. Obviously, the use of this catalyst can avoid many undesired by-products, something uncommon for other species such as stoichiometric oxidising agents.

The properties of MTO have been thoroughly studied, including its deactivation mechanisms. In 1996, Espenson *et al.* reported an exhaustive study of MTO decomposition, studying all the species involved in the catalytic reaction and the possible pathways that deactivate the catalyst.⁽²⁹⁾ It has been shown that MTO and the monoperoxo complex (and the bisperoxo complex to a much lesser extent) decompose via a pH and $[H_2O_2]$ dependant mechanism.

However, due to the high Lewis acidity of methyltrioxorhenium which is a characteristic of high oxidation species, many epoxidised substrates undergo a further ring opening, yielding in the respective diols. While this can be useful in certain processes, it is mostly an undesired side reaction. In order to reduce the diol formation, several strategies involving donor bases were developedⁱⁱⁱ.

5.3.3 Heterogeneous derivatives of MTO

The hydrolysis of MTO in the absence of oxidant promotes the formation of the so-called “poly-MTO”.⁽¹⁶⁾ The structure of this metallorganic polymer has been found to be

ⁱⁱⁱ See Section 5.4

$\{H_{0.5}[(CH_3)_{0.92}ReO_3]\}^+$. Some of its most prominent properties including its inherent conductivity have been studied, but to the best of our knowledge no catalytic applications have been reported.(30) Similarly, using a solvent-free, auto-polymerisation procedure, ceramic MTO has been obtained. Amongst other properties, this compound has been found to promote certain amine oxidation reactions.(31)

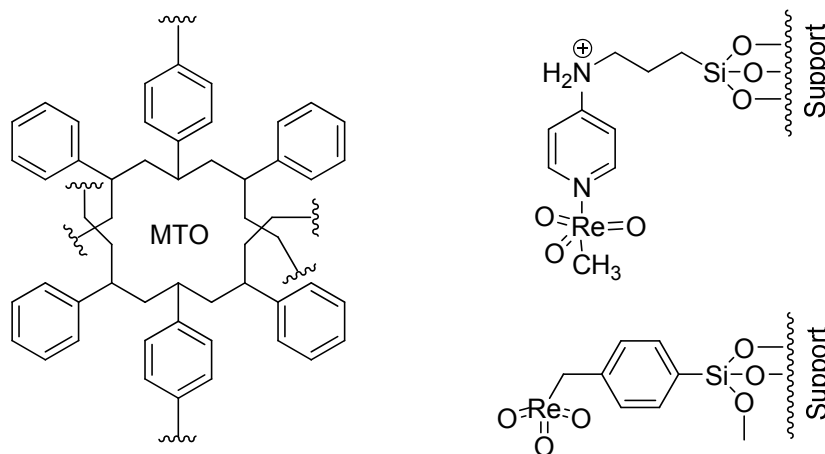


Figure 2 Examples of MTO-based heterogeneous catalysts.

On the other hand, many attempts to graft methyltrioxorhenium on solid supports have been reported. These include the inclusion of the MTO moiety within zeolites, or the use of Niobium-supported MTO (together with urea hydroperoxide (UHP) as oxidant) in olefin epoxidation. Various modified mesoporous materials have been reported to directly graft MTO moieties.(32-35)

Moreover, heterogeneous Lewis base-MTO adducts based on polystyrene (microencapsulated organometallic moieties) and poly(4-vinylpyridine) (bound to the pyridine fragments) have been synthesised and tested in glycol oxidation catalysis.(36-39) Lewis adducts of MTO will be introduced in the next section.

5.4 Base adducts of methyltrioxorhenium and their effect in epoxidation catalysis

The use of donor bases in high oxidation Re species has been common in the last years, as described in the comprehensive review by Romão, Kühn and Herrmann.(17)

The highly versatile Re_2O_7 was used to synthesise adducts based on the ReO_3^+ moiety, first stabilising it with donor species such as triazocycloalkyls and THF.(40) Albeit its

undeniable synthetic interest, these species have not found further relevant catalytic applications.

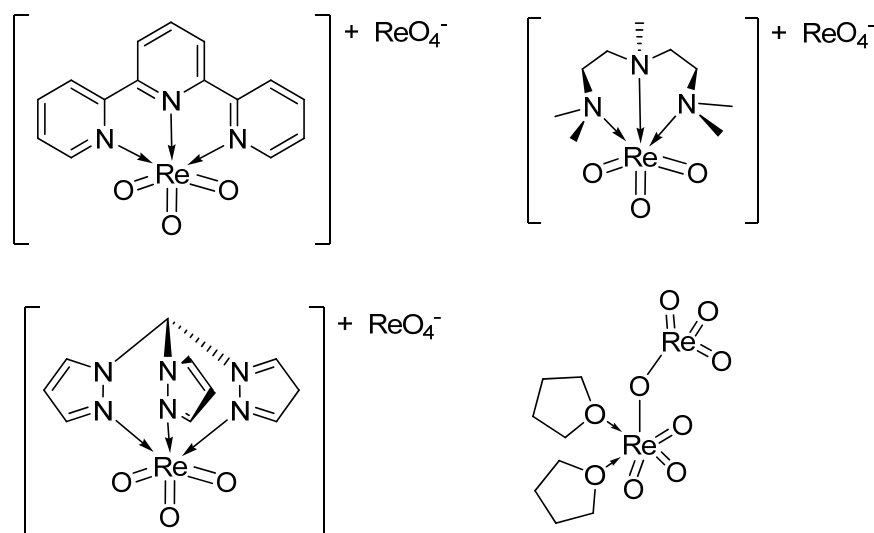


Figure 3 Some examples of Re oxides stabilised by donor adducts. In some cases, adducts with weakly donor ligands such as THF (lower right corner) are formed.

The use of donor adducts has afforded much more significant results when applied in alkyltrioxorhenium chemistry. As it has been introduced above, the production of water stemming from H_2O_2 combined with the pronounced Lewis acidity of MTO were identified as the main reasons for ring opening reactions of sensitive epoxides.⁽¹⁷⁾ Shortly after, it was found that Lewis-base adducts of MTO largely suppress this reaction.⁽¹¹⁾ Hence, a number of studies reporting MTO-donor adduct systems have been reported and its catalytic capabilities tested. In certain cases, they have been found to outperform the original catalyst in terms of activity and selectivity.

5.4.1 Nitrogen donor adducts

Herrmann *et al.* reacted N-donor ligands to form the first stable methyltrioxorhenium adducts, first out of mere synthetic interest and later to reduce the acidity of MTO.^(9, 11, 24, 41) In all cases, results shown that whereas the selectivity to epoxide was significantly increased, it was at the expense of a significant loss of catalytic activity.

In light of these results, Sharpless *et al.* reported the critical dependence of the catalyst lifetime on the amount of pyridine present in the reaction media.⁽⁴²⁾ Hence, the addition of 1 mol % or 12 mol % of pyridine under similar conditions lead to the decomposition of the catalyst or to a 95% conversion and the preservation of the catalyst, respectively.

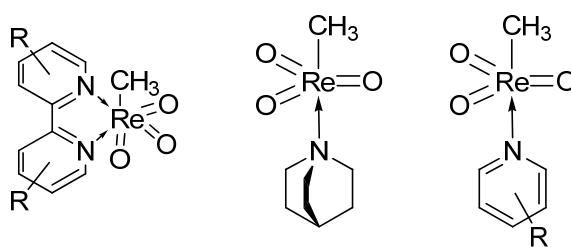


Figure 4 N-donor adducts of methyltrioxorhenium.

Moreover, the ring opening reactions were minimised, even for highly reactive epoxides such as β -methylstyrene and stilbene oxides. Further studies with meta-substituted cyanopyridine afforded high yields with terminal olefins.(43, 44)

The work of Sharpless *et al.* with pyridine derivatives prompted many similar investigations. Thus, a plethora of meta- and para-substituted pyridines were introduced, including 4,4'-bipyridine, along with their respective oxides and other heterocycles such as pyrazole.(28, 45, 46) The results show that pyridine derivatives give overall better results than pyrazole derivatives. However, the oxidation of the former ligands plays a major role during the catalytic reactions, and albeit similar or even greater bonding strength to MTO these oxides are far less efficient ligands. More recently, new substituted 4,4'-bipyridine adducts have been reported, showing interesting catalytic capabilities depending on the substituent.(47) This topic is currently being researched in our group.

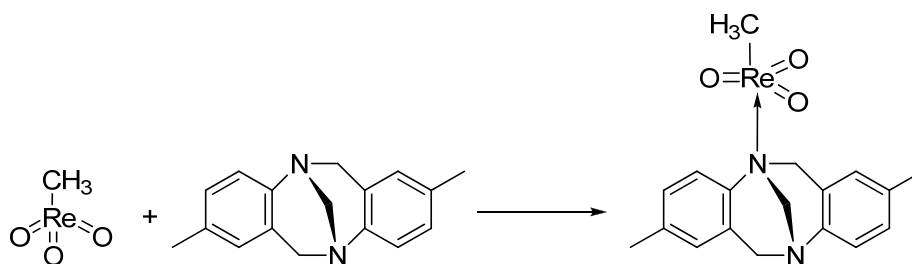
Many of these adducts have been isolated and characterised via X-ray crystallography. Moreover, some comprehensive studies have been made on the pyridine derivatives equilibrium binding constants and their influence in the catalytic activity of MTO.(28) Moreover, the affinity of MTO for donor ligands as well as the influence in its Lewis acidity has been studied via DFT calculations.(48)

Another relevant synthetic attempt involved the exclusion of water using the well known urea hydrogen peroxide adduct, which had been successfully applied in olefin epoxidation with Mn salen and porphyrin complexes.(49)

Chiral derivatives

The stability of the MTO adducts quickly aroused the possibility of employing chirality inducing Lewis bases. One significant example is the reaction of the Tröger's Base with MTO, forming a stable compound which has been characterised by X-ray crystallography.(50) The application of this adduct in enantioselective catalyst, however,

afforded no enantiomeric excesses, due to the rapid equilibria of MTO with the ligand in solution.



Scheme 8 Formation of the MTO-Tröger Base chiral adduct.

On the other hand, modified chiral pyrazoles have been also applied in asymmetric epoxidation catalysis, obtaining very low conversions and ees. The weak coordination of these ligands has been assumed to be the cause of this poor catalytic performance.(50)

Heterogenised Lewis-base adducts of MTO have been introduced in the previous sections. In the abovementioned polymeric species, MTO is stabilised either by a homogeneous donor ligand before encapsulation or by N-donor polymeric compounds such as PVP-2 or PVP-25.(39) Other attempts include the successful synthesis of a heterogenised 4-ferrocenylpyridine-MTO adduct over β -cyclodextrin; the catalytic performance of this system, however, is very poor.(51)

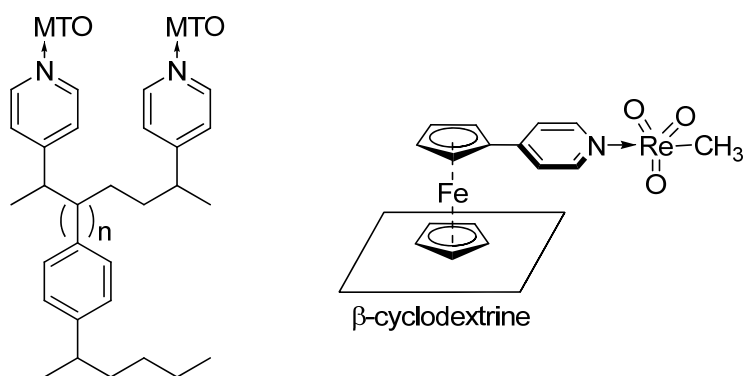


Figure 5 Heterogenised MTO-Lewis Base adducts.

As it will be introduced in the next section, Schiff bases are interesting candidates for the heterogenisation of methyltrioxorhenium.

5.4.2 Oxygen donor adducts. Chiral diols

As it has been previously introduced, certain O-donor compounds have been found to form adducts with MTO. Other ligands with both O and N donor atoms, such as 2-aminophenols, 8-hydroxyquinoline and catechol have been found to form stable adducts with MTO.(52, 53)

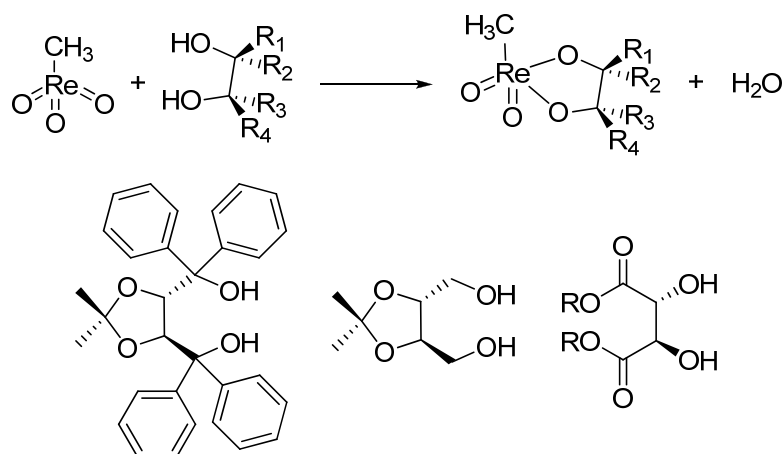


Figure 6 The reaction of MTO with a diol (above) and some examples of prochiral diols.

The previously reported reaction of MTO with diols - forming the respective glycolates - (54) has been used as template for the synthesis of prochiral MTO complexes.(55) They, however, yield ees of 41% at best, along extremely low conversions due to the temperatures applied.

5.4.3 Schiff bases and its role in synthesis and catalysis

Schiff bases, i.e. compounds that contain a carbon-nitrogen double bond with the N atom connected to an aryl or alkyl group- but not hydrogen, have become relevant ligands in coordination and organometallic chemistry. A notorious example of this class of compounds are the previously mentioned salen complexes, which have been found to induce high enantioselectivities in a number of olefin epoxidation reactions^{iv}.

There are few reported examples of the reaction of bidentate and tetradentate Schiff bases with Re (V) species.(56, 57) These compounds (specially those with bidentate ligands) are active in cyclooctene epoxidation using TBHP as oxidant, achieving moderate conversions.

^{iv} See Section 3.3 of the Introduction

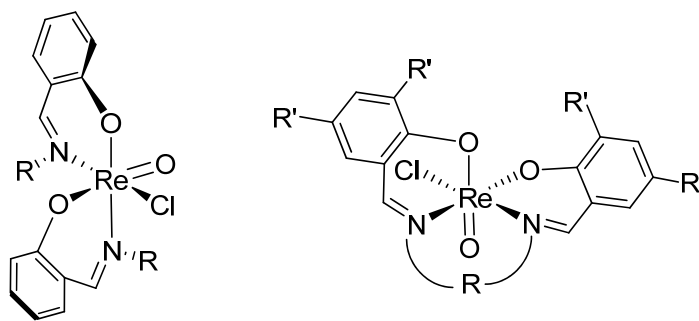


Figure 7 General structure of bidentate (left) and tetradentate (right) Re (V) Schiff base adducts.

Recently, MTO-Schiff base adducts based on salicylaldehyde and substituted anilines have been reported.⁽⁵⁸⁾ Though originally considered to be bound via both the O and the N atom in a similar fashion to the abovementioned Re(V) species, it has been found that they coordinate only through the oxygen atom. These adducts will be studied in detail in the next chapter.

Heterogenised Schiff bases

Several Schiff base Au(III) and Pd(II) adducts have been successfully grafted to mesoporous materials such as MCM-41 and applied in hydrogenation catalysis as well as in the Heck and Suzuki coupling reactions.⁽⁵⁹⁻⁶³⁾

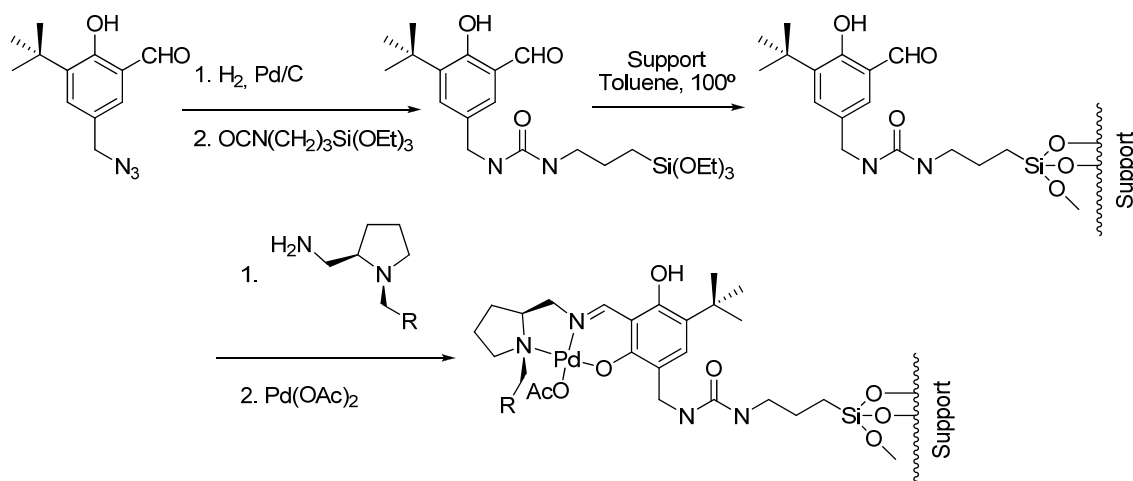


Figure 8 Synthesis of heterogenised Pd(II)-Schiff base complexes on a silica support.

The stability of the reported grafted complexes under catalytic conditions could lay the foundation of related, heterogenised MTO oxidation catalysts. Further studies on this matter are currently being carried out in our laboratories.

6. Synthesis and Catalytic Applications of MTO Schiff Base Complexes

The application of MTO donor adducts of Lewis bases and, more recently, Schiff bases shows very promising features and constitutes a main research topic in our group.(42, 45-47, 58, 64) As it has been mentioned in previous sections, decreasing the Lewis acidity of MTO reduces the tendency of epoxide ring opening to yield diols. Furthermore, the ligand-MTO ratio has been studied in detail to optimise the catalytic systems because in some cases addition of Lewis bases can lead to catalyst deactivation or decomposition while in other cases excess of these bases enhance both activity and selectivity.(47)

Recently, stable Schiff base adducts of MTO have been synthesised in our laboratories (Figure 9).(58)

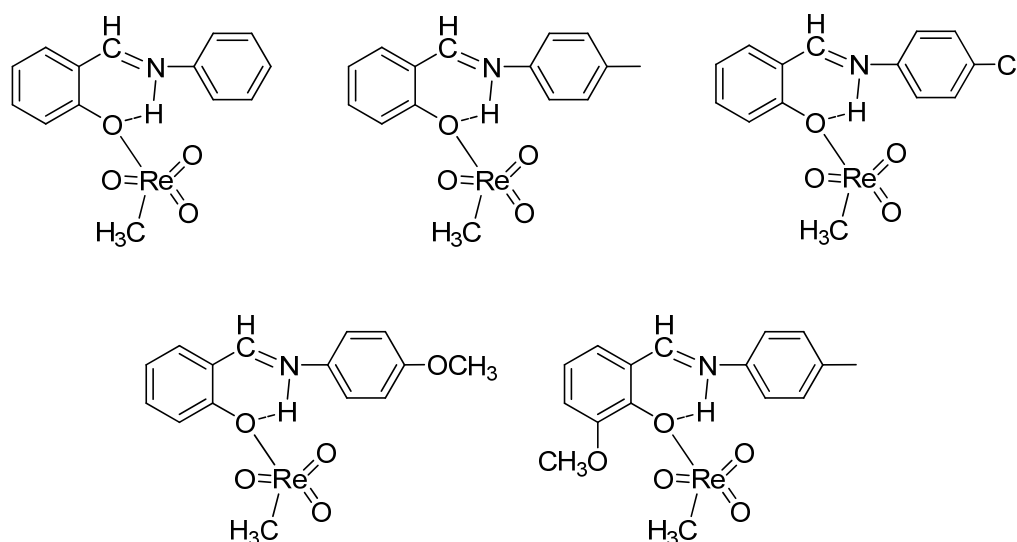


Figure 9 Schiff Base MTO adducts previously synthesised in our group (see reference (58)).

The majority of these adducts show good catalytic activities and above-average stability under catalytic conditions. Since an excess of ligand is not required for these

compounds to be used in catalysis, they might be promising candidates not only in homogeneous but also in heterogeneous catalysis, where catalyst leaching should be avoided.^(59, 60, 38, 36)

In this chapter, a follow-up of this work is presented. Hence, the synthesis of new catalytically active Schiff base adducts, based on either salicylidene or 2-hydroxynaphthalene moieties is described and their catalytic activity in olefin epoxidation is tested. Special insight in the coordination of MTO to the ligand is given, including variable temperature NMR experiments and structure determination of the adducts by X-ray single crystal diffraction. Furthermore, in a comparative study of the metal-ligand interaction of the synthesised complexes the stability of such adducts is discussed.

6.1 Abstract

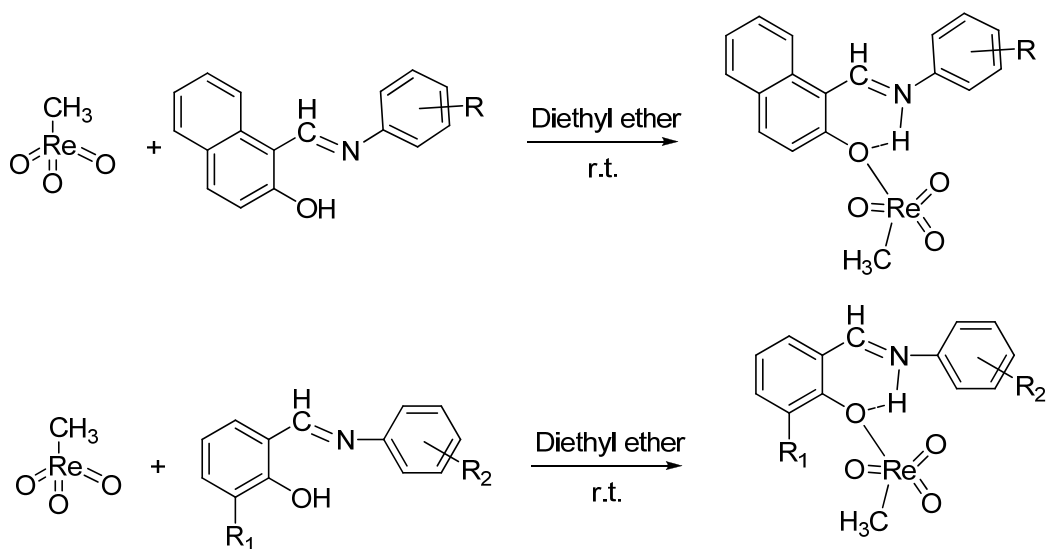
The equimolar reaction of derivatives of (salicylidene)aniline and ((2-hydroxynaphthalene-1-yl)methylene)aniline with MTO affords complexes with the ligand OH group coordinating to the Re atom. Crystallographic studies of these compounds show characteristic distorted trigonal-bipyramidal structures, with the methyl group oriented either in a *cis* or *trans* coordinated position to the Schiff base. Amongst a plethora of different bases, only certain ligands, which apply to some specific structural requirements may be used to form stable adducts with MTO. Such compounds have been tested as catalysts in olefin epoxidation, with a catalyst : substrate : oxidant ratio of 1 : 100 : 200. The Schiff base ligands modify the catalytic behaviour of the MTO moiety, ranging from very good conversions to catalyst decomposition.⁽⁶⁵⁾

6.2 Results and discussion

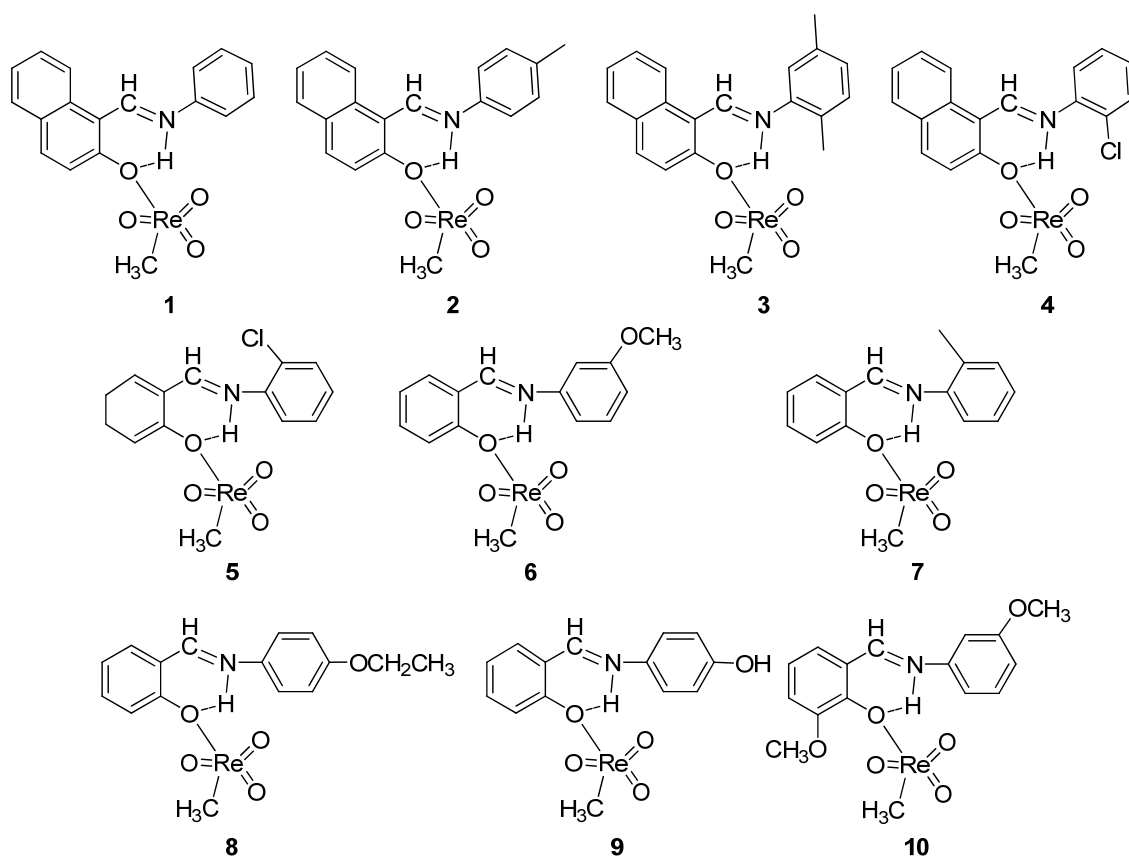
6.2.1 Synthesis and spectroscopic characterisation

In continuation of the previous work on Schiff base adducts of MTO,⁽⁵⁸⁾ carried out in our laboratories, compounds **1-10** were synthesised by reacting MTO with the respective ligands, at room temperature in diethyl ether. It has to be emphasised that below 0°C no reaction takes place. Yields of 80 – 90 %, however, are obtained in all

examined cases when the reaction is performed at 20 °C. All products were recrystallised from dichloromethane / *n*-hexane mixtures.



Scheme 9 General reaction pathway for the synthesis of Schiff bases with MTO.



Scheme 10: Synthesised Schiff base adducts.

All compounds are relatively stable and show no evident signs of decomposition under an air atmosphere, either in the solid state or in solution. However, it has been detected that compounds **4**, **6** and **10** are slightly moisture sensitive and need to be stored under dry hexane (**6**) or at low temperatures (**4**, **10**) in order to avoid decomposition.

IR spectroscopy

The IR spectra (in KBr) of the compounds show some common features. The stretching bands of the iminic bonds, located at ca. 1600 - 1650 cm^{-1} , are shifted to higher wave numbers when compared to the free ligands in the case of the adducts due to electron delocalisation. The geometry and coordination of the compounds can be inferred qualitatively when looking at the characteristic Re=O and Re-C stretching bands of the CH_3ReO_3 moiety (see Tables 2 and 3).

On account of the expected complex symmetry (C_{3v}), a splitting (ca. 15 cm^{-1}) of the asymmetric ReO_3 stretching band can be expected. This is seen in the case of compounds **3**, **5-7**, **9** and **10**, but for complexes **1**, **2**, **4** and **8**, only one broad peak is observed. As the separation between the peaks is only ca. 10 cm^{-1} in the case of compound **3**, it is likely that the splitting is too small in these compounds to be resolved properly. Due to the donor capability of the ligands - which reduce somewhat the Re=O bond order - and the moderate charge transfer from the ligand to the Lewis acidic MTO, average symmetric and asymmetric Re=O stretching vibrations are slightly red-shifted (20 - 30 cm^{-1}) in comparison to non-coordinated MTO. This difference is generally higher for salicydene(aniline) complexes than in the case of ((2-hydroxynaphthalen-1-yl)methylene)aniline derivatives. The same conclusion can be drawn from the observed blue shift changes of the iminic stretching vibrations. While the difference between the coordinated and non-coordinated ligands is only ca. 10 cm^{-1} in compounds **1** - **4**, it is significantly bigger (20 - 50 cm^{-1}) in complexes **5** - **10**. As pointed out in our previous work, (58) this displacement of the C=N stretching band could be explained in part by the formation of an intramolecular H bond between the N atom and the phenolic proton, which - according to the obtained IR data - seems to be quite weak in the case of adducts **1** - **4**. It must be noted that molecules of the type PhCH=NPh usually display a medium strength IR band at about 1650 cm^{-1} , arising from the C=N stretching mode, if undisturbed. For the ligand complexes **5-10**, these bands are found between 1601-1619 cm^{-1} (Table 3). This lowering of 40-50 cm^{-1} also strengthens the assumption of the existence of an intramolecular hydrogen bond between the phenolic hydrogen and

nitrogen atoms. After complexation, the proton is attached to the nitrogen atom, the C=N vibrations being observed at higher wave numbers ranging from 1620 to 1650 cm^{-1} .

| MTO | 1 | 2 | 3 | 4 | 5 | 6 | 7 | 8 | 9 | 10 | Assignment |
|------|------|------|------------|------|------------|------------|------------|------|------------|------------|------------------------------------|
| 1368 | 1355 | 1366 | 1355 | 1356 | 1369 | 1378 | 1375 | 1385 | 1363 | 1371 | CH ₃ , asym.def. |
| 1205 | 1215 | 1217 | 1219 | 1217 | 1247 | 1245 | 1252 | - | 1217 | 1266 | CH ₃ , sym.def. |
| 998 | 991 | 989 | 1006 | 992 | 999 | 1000 | 1001 | 1011 | 1005 | 1006 | ReO ₃ sym. str. |
| 965 | 930 | 926 | 940 931 | 925 | 930 913 | 931 918 | 930 918 | 918 | 926 913 | 931 917 | ReO ₃ asym. str. |
| 567 | 566 | 567 | 558 | 553 | 575 | 576 | 553 | 558 | 558 | 555 | ReC str. |
| 981 | 961 | 958 | 959 | 959 | 947 | 950 | 950 | 965 | 948 | 951 | ReO str. average |
| 33 | 61 | 63 | 71 | 67 | 77.5 | 76 | 76.5 | 93 | 83.5 | 82 | ($\nu_s-\nu_a$) ReO ₃ |

Table 2 Characteristic vibrations of the MTO fragments (cm^{-1}) in **1-10**.

| Compound | Imine group | Phenolic OH group and coupled ring vibrations | | | | |
|--|-------------------|---|------------------|------------------|------------------|----------|
| | $\nu(\text{C=N})$ | β | $\nu(\text{CX})$ | $\nu(\text{CX})$ | $\nu(\text{CX})$ | γ |
| C₁₇H₁₃NO 1 | 1621 1629 | 1331 | 1251 | 1138 | 821s | 750vs |
| C₁₈H₁₅NO 2 | 1620 1631 | 1327 | 1251 | 1083 | 815m | 742m |
| C₁₉H₁₇NO 3 | 1619 1632 | 1339 | 1257 | 1108 | 829m | 747m |
| C₁₉H₁₇NCIO 4 | 1622 1615 | 1324 | 1257 | 1092 | 821m | 752vs |
| C₁₇H₁₃NCIO 5 | 1615 1633s | 1367m,sh | 1281s | 1056m,sh | 818m | 750vs |
| C₁₄H₁₃NO₂ 6 | 1601s 1650s | 1368m | 1287s | 1045s | 834m | 752s |
| C₁₄H₁₃NO 7 | 1617vs 1643s | 1365m | 1280s | 1035m | 835s | 754vs |
| C₁₃H₁₅NO₂ 8 | 1617m 1634s | 1367m | 1258s | 1107m,sh | 838s | 754s |
| C₁₃H₁₁NO₂ 9 | 1619s 1645s | 1391m,sh | 1241vs | 1047s | 841m | 741s |
| C₁₅H₁₅NO₃ 10 | 1617s 1646s | 1359m | 1263s | 1036m | 850s | 680m |

Notation of vibrational modes: $\nu(\text{C=N})$, C=N stretching; $\beta(\text{OH})$, hydrogen bonded OH in-plane deformation; $\nu(\text{CX})$ substituent sensitive aromatic ring stretchings; $\gamma(\text{OH})$ phenolic out-of-plane vibrations.

Table 3 Selected IR data (cm^{-1}) for MTO and Schiff Bases **1-6**.

Moreover, the absence of OH stretching bands of the Schiff bases in the region around 3400 cm^{-1} further indicates the presence of a strong hydrogen bond with the nitrogen atom of the imine group to form a six-membered ring. The broad band with a specific fine structure in the range $2900\text{--}2400\text{ cm}^{-1}$ is most likely from the phenolic OH stretching feature characteristic of a strong hydrogen bond. There are other low-frequency bands, which are characteristic for a phenolic OH group in the spectra of the pure Schiff base ligands. These bands, together with the OH stretching vibrations, are also conspicuously absent in the spectra of the newly synthesised compounds **1**–**10** (see Table 3), thereby supporting our original ideas about the coordination of the Schiff base ligands to MTO.

The differences between the averaged symmetric and asymmetric stretching vibrations as given in the last row of Table 2 deserve some attention. In the previous work from our group, the differences between the values were mainly ascribed to the symmetry of the coordination around the Re atom.⁽⁵⁸⁾ However, the larger quantity of data available now leads to a somewhat different hypothesis as an explanation. The value obtained for compound **8** is the most prominently different from the value of compound **2** or the previously synthesised unsubstituted salicydene(aniline) adduct. Compound **8** has a donor ligand in the *para* position of the aniline moiety. The weaker donor in compound **9** lead to a considerably less pronounced enlargement of the value, while electron acceptor ligands (such as the *para*-Cl derivative of our previous work) or the *para*-methyl ligand of compound **3** lead to a slight reduction of the difference between the symmetric and asymmetric stretching vibrations. The *ortho*- and *meta*- substitutions lead only to smaller effects than those observed for the *para*-substituted compounds (comparable to the order of magnitude observed for compound **3**). It can be concluded that their electronic effects on the attached MTO moiety therefore is on average less pronounced than that of the substituents in the *para* position.

NMR spectroscopy

A selection of the NMR data of complexes **1** - **10** is shown in Table 4. ^1H NMR spectra show only slight changes from the non-coordinated MTO to Schiff base coordinated MTO, especially in the case of adducts **1** - **4**. The proton signals of the MTO moiety show practically the same chemical shift in all cases, whereas the -OH group proton signal is shifted and significantly broadened in case of adducts **5** -**10** (in CDCl_3 at room temperature). Further experiments were carried out at different temperatures (223, 253, 273, 293 and 323 K) in order clarify the reason for this broadening. These experiments

show that at low temperatures the -OH signal of the complexes resembles that of the free ligand in terms of peak shape and chemical shift, indicating that the coordination of the ligand to MTO - as well as the position of the phenolic proton - could be affected by a temperature dependent equilibrium in solution. In support of this hypothesis, it should be noted that the use of other solvents than chloroform show important differences in the chemical shift of the phenolic H atom of the coordinated Schiff base, ranging from minor changes in its intensity and chemical shift (benzene) to the complete disappearance of the peak (methanol).

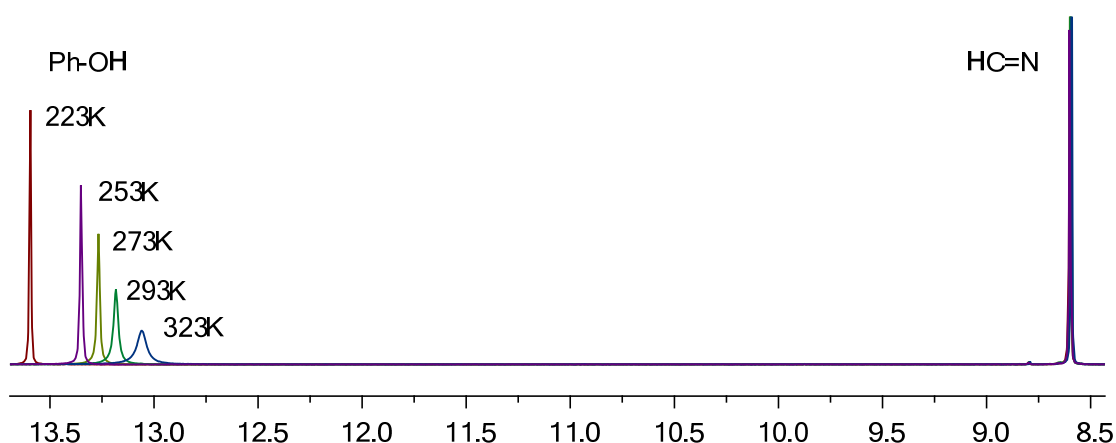


Figure 10 $^1\text{H-NMR}$ comparative of compound **6** at different temperatures, comparing both the phenolic (left) and iminic (right) proton signals.

The ^{13}C NMR data show also a slight downfield shift in the MTO methyl carbon ranging from 0.9 to 0.1 ppm, this shift being more pronounced in the case of compounds **1**, **2** and **5**. It can not be excluded that the bulky substituents in the case of the complexes **3**, **4** and **10** may be responsible for the observed weakening of the Re-O bond, which translates into minor changes in MTO carbon and proton NMR signals. Similar conclusions were previously drawn with respect to the interactions of MTO with sterically hindered pyridines.(66)

The use of ^{17}O labelled MTO has proven to be a useful tool in establishing the position of the oxygen atoms.(23, 67) Axially coordinated oxygen is usually quite distinguished by its chemical shift from equatorial oxygen atoms. This variation is particularly obvious at low temperatures, since the influence of exchange phenomena is reduced. In order to follow the behaviour of the adducts described in this work under these conditions, a number of ^{17}O NMR experiments were carried out at different temperatures, using deuterated chloroform as solvent. Despite a broadening of the ^{17}O signal at 223 K, only

a single signal can be obtained. As seen in the ^1H NMR experiments (see above), this would be in agreement with a fast equilibrium in solution.

| Compound | $\delta_{\text{MTO-CH}_3}$ | | $\delta_{\text{N-(O)-H}}$ | | |
|------------|----------------------------|------|---------------------------|----------------------|-------|
| | $\delta(^1\text{H})$ | | $\delta(^{13}\text{C})$ | $\delta(^1\text{H})$ | |
| | CDCl_3 | DMSO | CDCl_3 | CDCl_3 | DMSO |
| MTO | 2.63 | 1.91 | 19.03 | - | - |
| 1 | 2.59 | - | 19.46 | 15.48 | - |
| 2 | 2.50 | - | 19.88 | 15.49 | - |
| 3 | 2.58 | - | 19.26 | 15.72 | - |
| 4 | 2.62 | - | 19.09 | 15.40 | - |
| 5 | 2.63 | - | - | 13.07 | - |
| 6 | 2.60 | - | 19.52 | 13.22 | - |
| 7 | 2.61 | 1.91 | - | 13.49 | 13.37 |
| 8 | 2.60 | 1.90 | - | 13.52 | 13.30 |
| 9 | - | 1.90 | - | - | 13.41 |
| 10 | 2.62 | - | 19.11 | 13.22 | - |

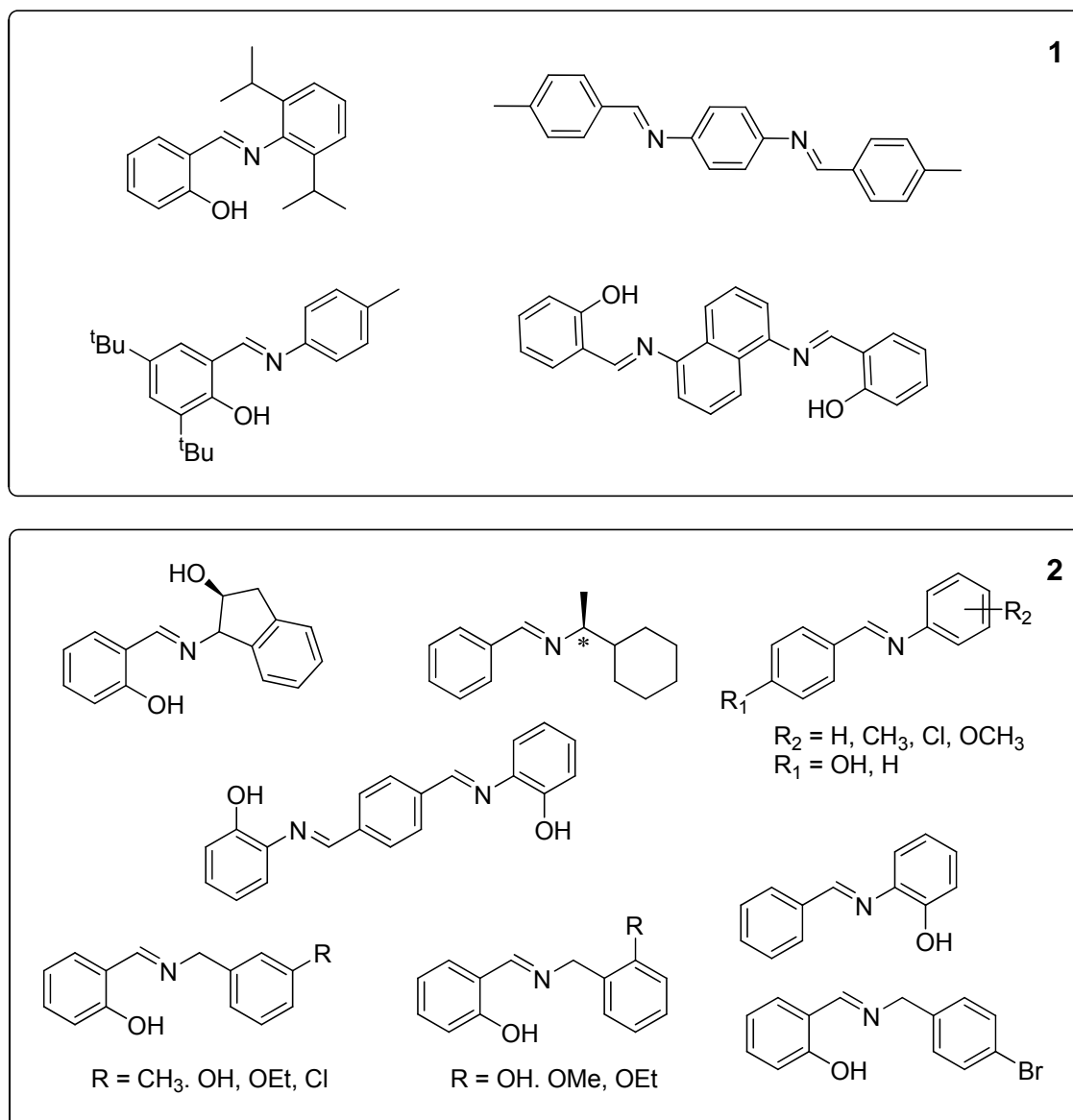
Table 4 Selected ^1H and ^{13}C NMR data of MTO complexes in CDCl_3 and DMSO.

The CI-MS spectra show, in all cases, the peaks of MTO and the ligands separately. In addition, the molecular peak of the complete molecule can only be seen in the case of complex **1**. These observations point to comparatively weak interactions between MTO and the respective Schiff base ligands, but the behaviour is in principle not uncommon, since it has also been observed and noted for MTO Lewis base adducts under the same conditions.^(45, 64)

6.2.2 Schiff base adducts of MTO: a comparative study of their stability

Besides the described compounds **1 - 6**, several other Schiff bases as ligands for MTO were tested. While some of these ligands did not react with MTO, others lead to instable products, decomposing either in solution or during the drying procedure while evaporating the solvent.

A comparison of these failed attempts with the compounds that could be isolated reveals that Schiff bases must share some common features in order to lead to the formation of reasonably stable MTO adducts. First of all, their stability clearly depends on a variety of electronic effects within the Schiff base. Thus, only structures seen in Scheme 1 have been successfully isolated.



Scheme 11 Selection of some of the Schiff bases reacted with MTO (1:1, ether or THF, 20 °C). They either do not react with MTO (1) or yield unstable adducts, which decompose either in solution or during the removal of the solvent (2).

The Re atom interacts with the O atom of the salicyl / 2-hydroxynaphthyl moiety, which after proper rearrangement via intramolecular H bonding forms a conjugated system similar to that of the free ligand. Experimental evidence supports that these interactions are mainly responsible for the stability of the adducts.(68)

Accordingly, all attempts to synthesise stable adducts with ligands where either no OH moiety is present or where the OH group is placed in other positions, do not lead to isolable products. Decomposition is observed when Schiff bases without an aniline moiety are applied. This observation originates very likely from the changed stability of the conjugated system in the latter case.

Besides these electronic effects, steric effects also seem to play a key role in the adduct formation. Bulky substituents in the *meta* position of the -OH substituted phenyl ring and/or in the *ortho*-substituted benzilidene aniline ring, obviously hinder the MTO coordination. In the specific reaction of salicylidene(2,5-dimethyl)aniline with MTO, a catalytically applicable, yet highly unstable adduct is obtained. Its 2-hydroxynaphthyl counterpart (compound **4**), however, has been isolated and successfully as a catalyst. Furthermore, a number of bidentate Schiff bases (i.e., derivatives of terephthal dialdehyde, 1,6-diaminonaphthalene, etc.), which could allow more than one MTO molecule to coordinate, yield either unstable adducts or do not react at all. THF was used as solvent due to the low solubility of these ligands in ether. This might have resulted in a competition for the free coordination sites at MTO between the coordinating solvent THF and the Schiff base and may therefore have contributed to the non availability of adducts of MTO with the afore mentioned Schiff bases.

6.2.3 X-ray structures of compounds 5-10

Figures 11-15 show the solid-state structures of complexes **5-9**. These display a distorted trigonal-bipyramidal geometry, the methyl group of MTO being either in *cis* or *trans* position with respect to the Schiff base.

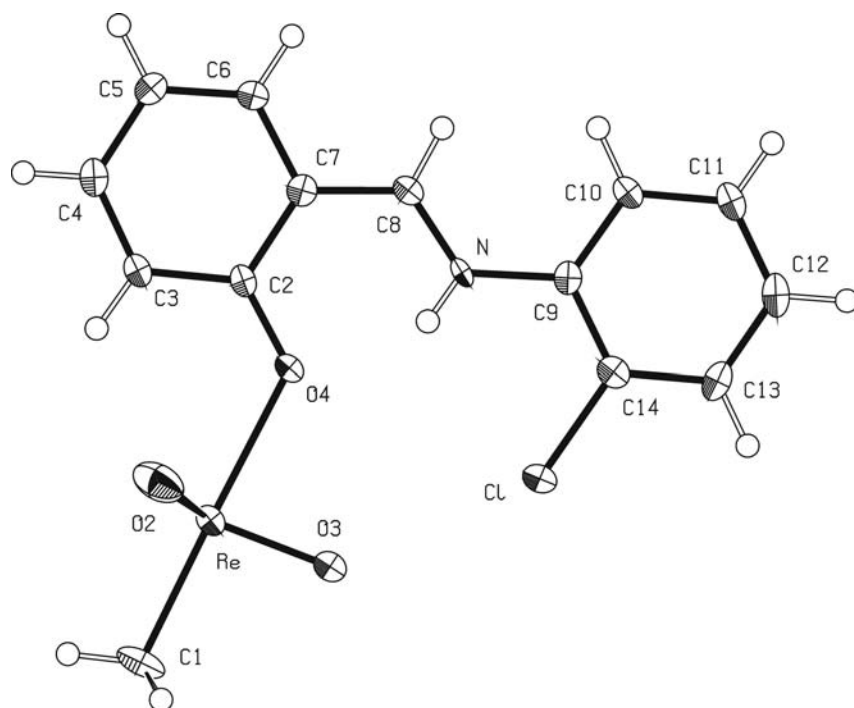


Figure 11 ORTEP style plot of compound **5** in the solid state. Thermal ellipsoids are drawn at the 50% probability level. The molecule is located on a mirror plane.

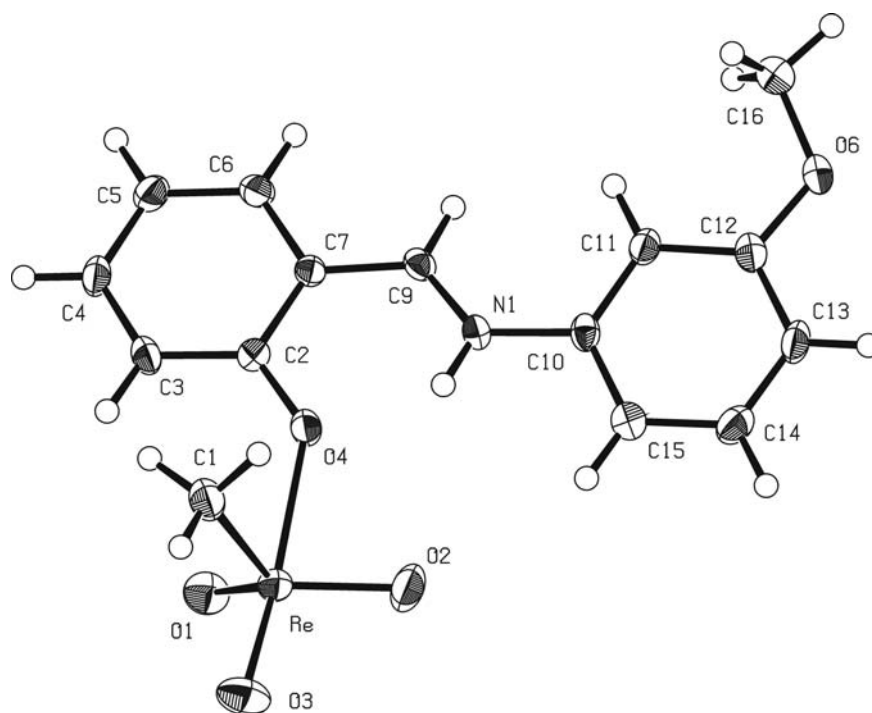


Figure 12 ORTEP style plot of compound **6** in the solid state. Thermal ellipsoids are drawn at the 50% probability level.

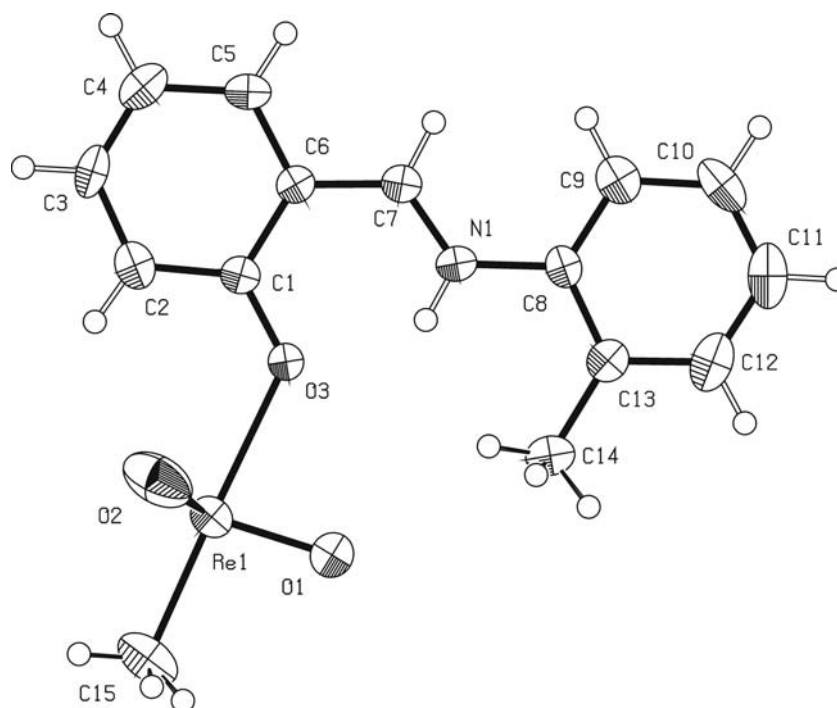


Figure 13 ORTEP style plot of compound **7** in the solid state. Thermal ellipsoids are drawn at the 50% probability level. The molecule is located on a mirror plane.

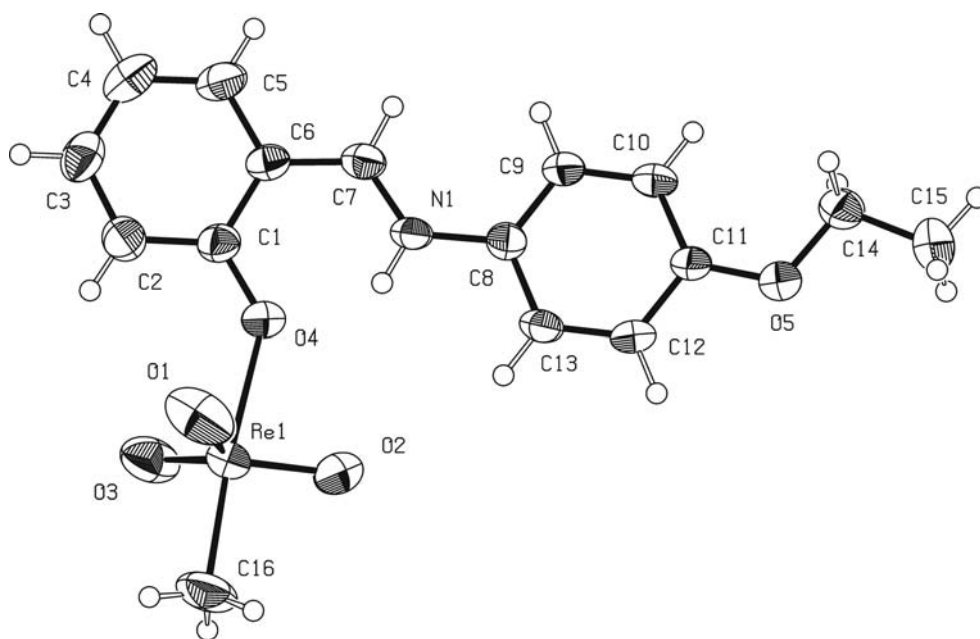


Figure 14 ORTEP style plot of compound **8** in the solid state. Thermal ellipsoids are drawn at the 50% probability level.

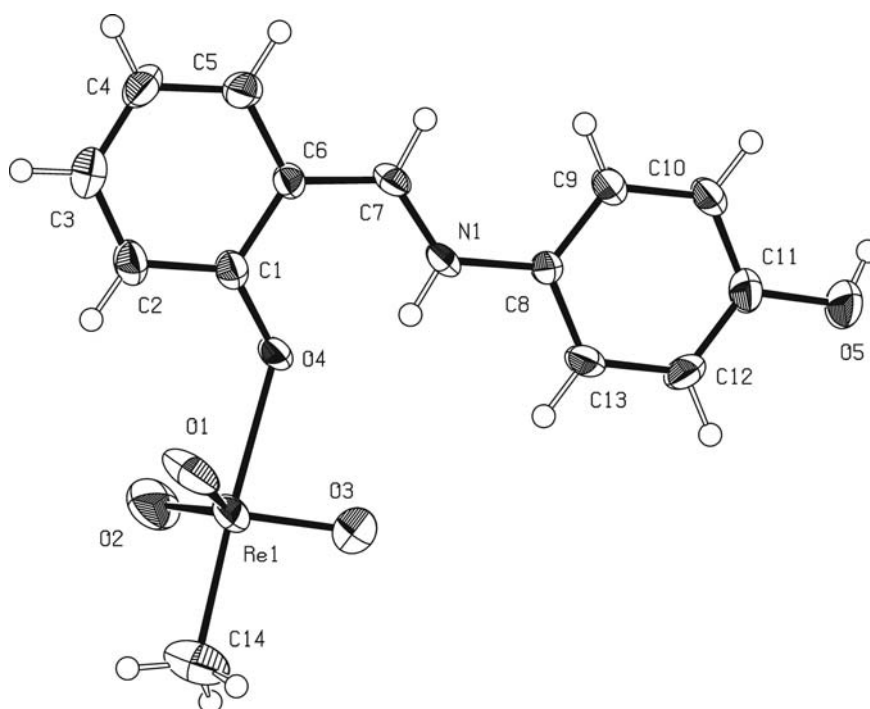


Figure 15 ORTEP style plot of compound **9** in the solid state. Thermal ellipsoids are drawn at the 50% probability level.

Compound **6** shows only a *cis*-positioning of the methyl group with respect to the coordinating Schiff base ligand at the Re atom; thus, the methyl group and two oxo ligands occupy the equatorial position while the donating phenolic group and the remaining oxo ligand occupy the axial positions. As reported previously, very few MTO adducts with such an arrangement of the ReO₃ moiety have been described.(1, 2, 17, 69). Recent crystallographic studies of compound **10** show that in the case of this adduct, both the *cis* and *trans* isomers (**10a** and **10b**) coexist in the unit cell.(70) The ORTEP plot of the structure is depicted below.

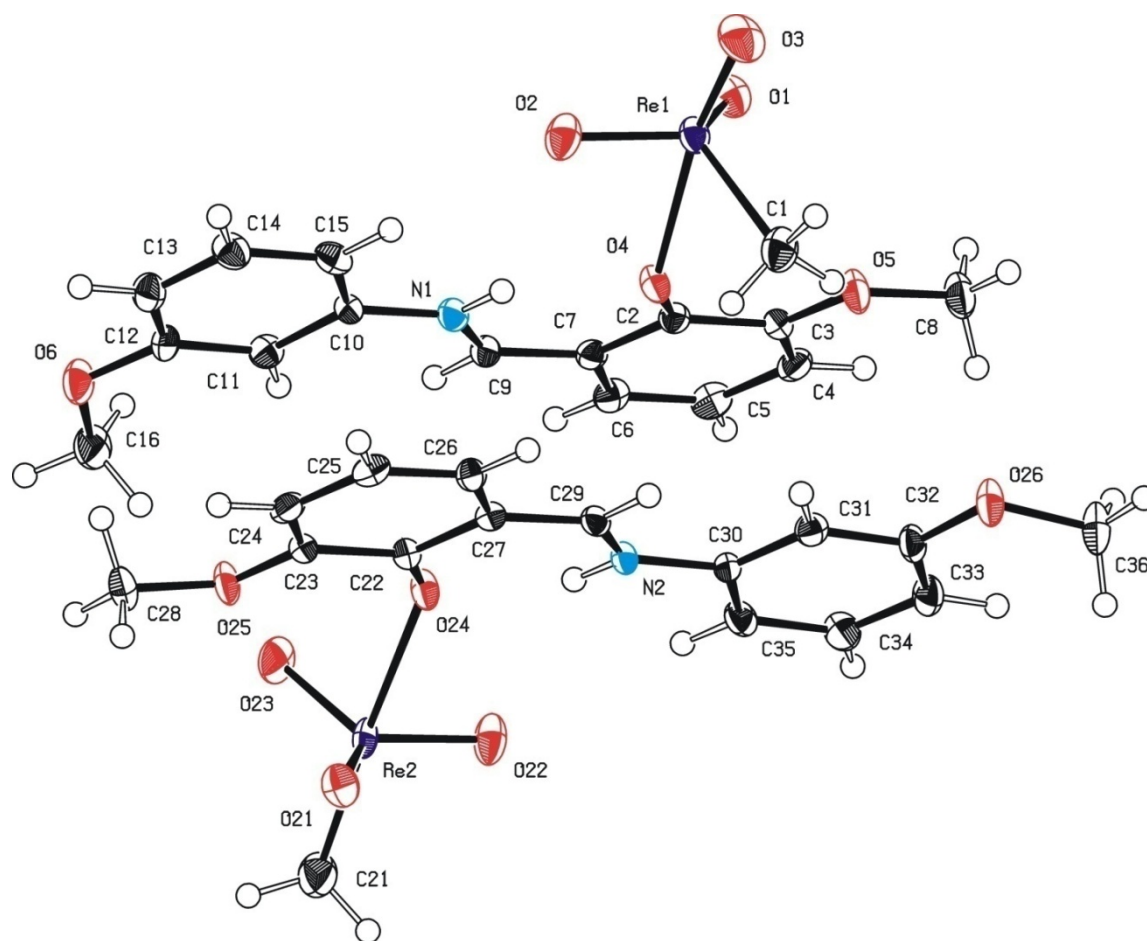


Figure 16 ORTEP style plot of molecules **10a** and **10b** of compound **1** in the solid state. Thermal ellipsoids are drawn at the 50% probability level.

It must be noted that the previously synthesised Schiff base adduct with a *para*-OMe substituent also displays a *cis*-configuration (see Figure 9 and reference (58)) However, and due to the recent studies on compound **10**, the reasons for this uncommon configuration might owe to packing reasons rather than to ligand or substituent influences.

| Compound | 5 | 6 | 7 |
|-----------------------------------|--|--|--|
| Empirical formula | C ₁₄ H ₁₃ Cl N O ₄ Re | C ₁₅ H ₁₆ N O ₅ Re | C ₁₅ H ₁₆ N O ₄ Re |
| Formula weight | 480.91 | 476.50 | 460.49 |
| Crystal system | Orthorhombic | Triclinic | Monoclinic |
| Space group | Pnma | P $\bar{1}$ | P2 ₁ /m |
| Unit cell parameter | a = 9.9098(4) Å b = 6.4517(3) Å c = 22.6637(14) Å α = 90° β = 90° γ = 90° | a = 8.4120(2) Å b = 8.8998(2) Å c = 10.4936(3) Å α = 78.9701(9)° β = 85.5727(9)° γ = 75.9375(15)° | a = 9.904(2) Å b = 6.6370(13) Å c = 12.081(2) Å α = 90° β = 110.198(3)° γ = 90° |
| Volume | 1449.01(13) Å ³ | 747.60(3) Å ³ | 745.3(2) Å ³ |
| Z, Calculated density | 4, 2.204 mg/m ³ | 2, 2.117 mg/m ³ | 2, 2.052 mg/m ³ |
| Absorption coefficient | 8.584 mm ⁻¹ | 8.150 mm ⁻¹ | 8.167 mm ⁻¹ |
| Crystal size (mm) | 0.15×0.51×0.61 | 0.20×0.30×0.33 | 0.3×0.30×0.24 |
| Colour | red | orange | red |
| θ data range collection | 4.11 to 26.71° | 1.98 to 25.24° | 1.80 to 25.02° |
| Reflections collected | 20593, 1669 | 16099, 2689 | 3145 / 1433 |
| /unique | [R(int) = 0.0121] | [R(int) = 0.035] | [R(int) = 0.0670] |
| Goodness-of-fit on F ² | 1.087 | 1.151 | 1.018 |
| Final R indices[I>2σ(I)] | R ₁ = 0.0229, wR ₂ = 0.0609 | R ₁ =0.0159, wR ₂ =0.0384 | R ₁ = 0.0323 wR ₂ = 0.0764 |
| R indices(all data) | R ₁ = 0.0229, wR ₂ = 0.0609 | R ₁ =0.0159, wR ₂ =0.0384 | R ₁ = 0.0355 wR ₂ = 0.0785 |

Table 5 X-ray crystal data, data collection parameters, and refinement parameters of compounds **5-7**.

| Compound | 8 | 9 | 10 |
|-----------------------------------|--|---|---|
| Empirical formula | C ₁₆ H ₁₈ N O ₅ Re | C ₁₄ H ₁₄ N O ₅ Re | C ₁₄ H ₁₄ N O ₅ Re |
| Formula weight | 490.51 | 462.46 | 506.52 |
| Crystal system | Triclinic | Monoclinic | Triclinic |
| Space group | P-1 | P2 ₁ /c | P $\bar{1}$ |
| Unit cell parameter | a = 8.7989(13) Å b = 9.9414(14) Å c = 10.9315(15) Å α = 116.959(2)° β = 98.219(2)° γ = 94.460(2)° | a = 6.8678(11) Å b = 22.432(3) Å c = 9.5822(14) Å α = 90° β = 97.319(3)° γ = 90° | a = 11.4383(1) Å b = 11.9898(1) Å c = 12.8468(4) Å α = 94.4663(4)° β = 102.1709(4)° γ = 106.9578(5)° |
| Volume | 832.5(2) Å ³ | 1464.2(4) Å ³ | 1628.96(3) Å ³ |
| Z, Calculated density | 2, 1.957 mg/m ³ | 4, 2.098 mg/m ³ | 4, 2.065 |
| Absorption coefficient | 7.322 mm ⁻¹ | 8.319 mm ⁻¹ | 7.492 mm ⁻¹ |
| Crystal size (mm) | 0.26×0.24×0.18 | 0.26×0.20×0.18 | 0.25×0.48×0.66 |
| Colour | orange | red | red |
| θ data range collection | 2.13 to 25.02° | 1.82 to 26.39° | 1.64 to 25.42 |
| Reflections collected | 4196 / 2900 | 8133 / 2991 | 35534 / 5524 |
| /unique | [R(int) = 0.0432] | [R(int) = 0.0784] | [R(int) = 0.057] |
| Goodness-of-fit on F ² | 1.068 | 0.999 | 1.108 |
| Final R indices[I>2σ(I)] | R ₁ = 0.0496, wR ₂ = 0.1217 | R ₁ = 0.0451, wR ₂ = 0.1111 | R ₁ = 0.0214, wR ₂ = 0.0244 |
| R indices(all data) | R ₁ = 0.0520, wR ₂ = 0.1263 | R ₁ = 0.0553, wR ₂ = 0.1178 | R ₁ = 0.0544, wR ₂ = 0.0557 |

Table 6 X-ray crystal data, data collection parameters, and refinement parameters of compounds **8-10**. Additional data for compound **10** is available via reference (**70**).

| | 5 | 6 | 7 | 8 | 9 |
|---------------------------|----------|----------|-----------|----------|----------|
| Re–O _{terminal} | 1.708(4) | 1.714(3) | 1.693(6) | 1.697(6) | 1.690(6) |
| | 1.717(3) | 1.721(2) | 1.697(5) | 1.701(6) | 1.714(5) |
| | 1.717(3) | 1.724(2) | 1.697(5) | 1.703(6) | 1.719(6) |
| Re–O _{bridge} | 2.286(3) | 2.166(3) | 2.309(5) | 2.234(6) | 2.271(4) |
| Re–CH ₃ | 2.116(5) | 2.116(3) | 2.089(10) | 2.073(9) | 2.098(8) |
| C–O _{bridge} | 1.316(5) | 1.320(4) | 1.315(9) | 1.324(9) | 1.311(7) |
| C _{methylene} –N | 1.310(6) | 1.301(4) | 1.301(9) | 1.295(9) | 1.305(7) |
| C _{aryl} –N | 1.416(6) | 1.419(4) | 1.438(10) | 1.416(9) | 1.418(8) |

Table 7 Selected bond lengths (Å) of compounds **5–9**.

| | 5 | 6 | 7 | 8 | 9 |
|---|------------|------------|----------|-----------|----------|
| O _{terminal} –Re–O _{terminal} | 119.04(10) | 103.77(13) | 117.7(4) | 118.3(4) | 118.1(3) |
| | 119.04(10) | 103.49(13) | 119.6(2) | 119.1(43) | 119.2(3) |
| | 119.63(14) | 119.34(12) | 119.6(2) | 119.9(4) | 120.4(3) |
| O _{terminal} –Re–CH ₃ | 94.9(2) | 89.15(13) | 95.4(2) | 94.6(5) | 94.5(3) |
| | 95.08(12) | 116.87(12) | 95.4(2) | 95.6(4) | 94.5(3) |
| | 95.08(12) | 116.63(12) | 96.6(4) | 96.0(4) | 96.2(3) |
| O _{terminal} –Re–O _{bridge} | 83.81(15) | 80.04(11) | 82.0(3) | 79.5(3) | 81.3(2) |
| | 85.54(10) | 85.51(10) | 85.3(2) | 86.8(3) | 86.3(2) |
| | 85.54(10) | 166.23(11) | 85.3(2) | 87.6(3) | 87.2(2) |
| O _{bridge} –Re–CH ₃ | 178.75(17) | 77.48(12) | 178.6(3) | 175.4(3) | 177.5(3) |

Table 8 Selected bond angles (°) of compounds **5–9**. Values for compound **6** reflect its *cis*-configuration.

The ReO₃ fragment has a pseudotetrahedral geometry. Re–C distances for compounds **5–9**, are 2.116(5), 2.116(3), 2.089(10), 2.073(9), and 2.098(8) Å respectively, all longer than free MTO ($d(\text{Re–C}) = 2.063(2)$ Å).⁽⁵⁾ This effect is already known from Lewis base adducts of MTO. It contributes to the higher lability of the Re–CH₃ bond and accordingly, adducts of MTO are generally somewhat less stable than the non-coordinated organometallic compound alone. The Re–O bond distances range between 2.166(3) (compound **6**) and 2.271(4) Å (compound **9**) and are in agreement with the results obtained for the previously synthesised adducts and the obtained IR data.^(58, 70) These distances are significantly shorter than the average Re–O bond distance, as found in many other donor adducts of organorhenium(VII) oxides.^(36, 38, 60, 71) It should be noted that the *cis*-configured adducts display the shortest Re–O bridged bond distances, as seen in the case of **6** and the previously synthesised para-OMe substituted Schiff base adduct.⁽⁵⁸⁾

In the case of the recently characterised compound **10**, both the *cis* and *trans* isomers, which are organised in pairs, can be seen within the unit cell. Bond distances and angles are in general within the expected range for both isomers. Thus, Re–O distances range from 2.218(2) Å (*cis* isomer) to 2.295(2) Å (*trans* isomer). However, it has to be noted that the latter is the longest distance observed to date for this type of Schiff base

adducts. Intramolecular interactions have been suggested as being responsible for the observation of both isomers.(60, 38, 36, 71) Scheme 2 shows the unit cell of the compound, in which it is possible to see that the piling of *cis* and *trans* structures could help minimising the sterical hindrance of the methyl groups. Moreover, the distance between aromatic rings in these *cis-trans* pairs ranges between 3.5 and 3.7 Å, suggesting that so-called π -stacking interactions.(72, 73) might also be of certain importance in this case.

The position of the proton

The position of the phenolic proton has been a matter of discussion for the Schiff base adducts of MTO. X-ray studies display this proton bound to the iminic N based on atomic electronic density, as shown in the structural drawings. Iminic bond distances lie also within the usual range in all compounds, but seem to be slightly elongated ($\sim 0.05\text{\AA}$). NMR and IR data show the OH signals both broadened and shifted to higher fields and the C=N stretching bands significantly blue-shifted due to the formation of a conjugated system. Additional NMR experiments have shown that the broadening and shifting of the phenolic proton signal is temperature dependant, being completely reversed at low temperatures. This is also in agreement with the experimental data, in which the synthesis of MTO-Schiff base adducts was not achieved at temperatures below 0 °C.

Hence, it can be concluded that the phenolic proton of compounds **5-10**, whereas being clearly bound to the N in the solid state due to the abovementioned conjugating effect is apparently fluxional in solution. Although no X-ray data is available for compounds **1-4**, experimental data suggests that the same conclusions can be drawn for these adducts. To the best of our knowledge - with the sole exception of our previously published results on MTO Schiff base adducts (58) - such behaviour is unprecedented for similar compounds. In order to find out more clearly about the nature of the N-H interactions, neutron diffraction experiments have been planned.

6.2.4 Application in epoxidation catalysis

Compounds **1-10** were examined as catalysts for the epoxidation of cyclooctene with hydrogen peroxide. Further details of the catalytic reaction are given in the experimental section. In the case of cyclooctene as the substrate, no significant amounts of epoxide

are formed in the absence of catalyst, and no by-products (such as diols) were detected during the course of the reaction.

The ratio of catalyst : substrate : oxidant was 1 : 100 : 200 in all cases, using mesitylene as internal standard.

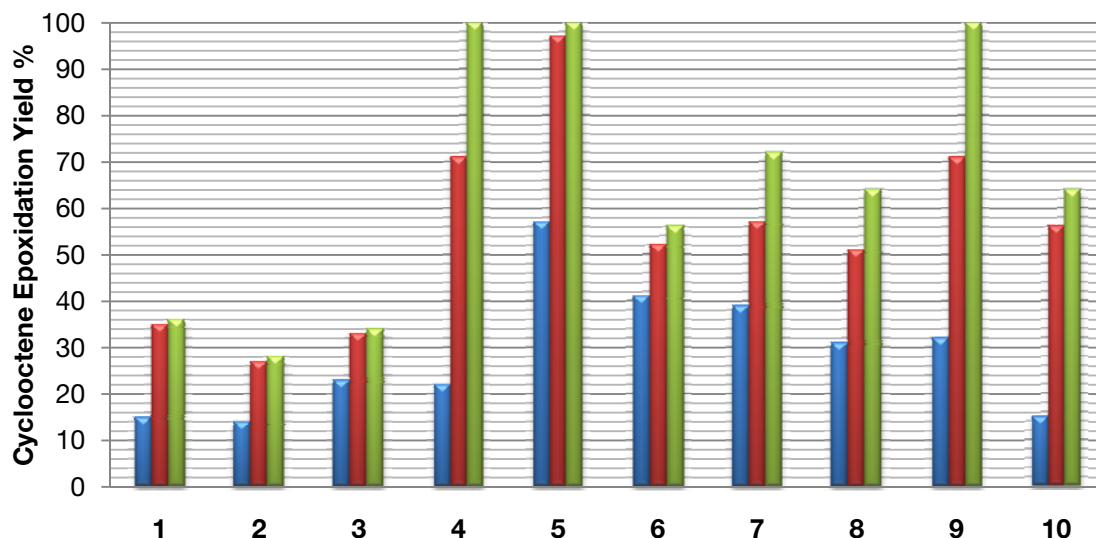


Figure 17 Yield of cyclooctene epoxide after 1h (blue bars), 4 h (red bars) and 24 h (green bars) of compounds **1-10** as catalysts and H₂O₂ as oxidant (catalyst : substrate : oxidant = 1 : 100 : 200; reaction temperature: 20 °C).

((2-hydroxynaphthalen-1-yl)methylene)aniline derivatives

Compounds **1-3** show low catalytic activity achieving yields not higher than 40 % during the first 24 h. On the contrary, complex **4** affords a 70 % yield within 4 h, reaching 100 % after 24 h. All complexes do not decompose in solution for 2 - 3 days. A possible explanation may be the dilution of the reaction mixture in dichloromethane.

(salicylidene)aniline derivatives

As expected from the results obtained with compound **4**, the catalytic activity and stability in solution for compound **5** is very high, exceeding 75 % yield after 4 h and achieving 100 % after 24h. The TOF for this compound is 400 h⁻¹. Compounds **6-8** afford moderate conversions, with TOFs ranging from 150 to 250 h⁻¹.

Compound **10** affords lower conversion (56 % yield after 4 h, 64 % after 24 h) and starts decomposing in solution after one hour reaction time. This adduct was also tested at lower catalyst concentrations (catalyst : substrate : oxidant ratio of 1 : 1000 :

2000). Although the TOF value is moderately high (140 h^{-1}), the reaction reaches only low yields after 4 h (10%).

It should be pointed out that, apart from compounds **1-10**, some of the above mentioned Schiff bases exhibit catalytic activity when reaction takes place with MTO *in situ*. However, in all these cases decomposition of MTO occurs during the first hours of the catalytic reaction. Kinetic NMR studies in which different MTO : Schiff Base ratio have been applied show that an excess of ligand and concentrated reaction mixtures increase decomposition and reduce the catalytic activity of the adducts. This is in contrast to the behaviour of Lewis base adducts of MTO, where pyridine based ligands accelerate the catalytic reactions significantly, when applied in larger excess. (36, 38, 60, 71)

Compounds **5-9** were also tested in the epoxidation of 1-octene and styrene. Both are terminal olefins, and yield usually much worse results than cycloalkenes such as cyclooctene. 1-octene is epoxidised in moderate to high yields by all tested compounds, achieving conversions up to 84% in the case of compound **7**. No diol formation was observed. On the other hand, oxidations with styrene as substrate yield moderate amounts of styrene oxide during the first two hours; however, the reaction proceeds further toward the diol, with the latter species becoming predominant after 4 hours and being the only detectable product after 1 day.

| Compound | 1-octene epoxidation | | | | Styrene epoxidation | | |
|----------|----------------------|---------------|-------------|----------|---------------------|-------------|----------|
| | Time (h) | Substrate (%) | Epoxide (%) | Diol (%) | Substrate (%) | Epoxide (%) | Diol (%) |
| 5 | 2 | 61.5 | 38.5 | 0 | 55.3 | 40.7 | 4 |
| | 4 | 54 | 46 | 0 | 26.2 | 28.4 | 45.4 |
| | 24 | 46.6 | 53.4 | 0 | 0 | 0 | 100 |
| 6 | 2 | 58 | 42 | 0 | 39.7 | 36.3 | 24 |
| | 4 | 45.6 | 54.4 | 0 | 16.1 | 0 | 83.9 |
| | 24 | 25 | 75 | 0 | 0 | 0 | 100 |
| 7 | 2 | 58.7 | 41.3 | 0 | 56 | 40.5 | 3.5 |
| | 4 | 46.7 | 53.3 | 0 | 35.1 | 28.8 | 36.1 |
| | 24 | 16.3 | 83.7 | 0 | 0 | 0 | 100 |
| 8 | 2 | 67.9 | 32.1 | 0 | 26.2 | 28.4 | 45.4 |
| | 4 | 63.8 | 36.2 | 0 | 9.8 | 0 | 90.2 |
| | 24 | 57.9 | 42.1 | 0 | 0 | 0 | 100 |
| 9 | 2 | 61.5 | 38.5 | 0 | 39.1 | 30.2 | 30.7 |
| | 4 | 52.3 | 47.7 | 0 | 14.1 | 0 | 85.9 |
| | 24 | 36.8 | 63.2 | 0 | 0 | 0 | 100 |

Table 9 Catalytic activities of compounds **5-9** in the epoxidation of 1-octene and styrene.

6.3 Conclusions

A number of Schiff bases which apply to certain electronic and steric requirements afford stable complexes with distorted trigonal bipyramidal structures on reaction with MTO in an equimolar fashion. The Schiff base ligands are either arranged in a *cis* or a *trans* positions with respect to the Re bound methyl moiety. The crystallographic data show that in some cases the molecules can adopt both positions in the solid state, most likely because of packing requirements and π -stacking interactions. However, none of those conformations are kept in solution due to temperature-dependent equilibria, as has been suggested by NMR experiments. As seen in the catalytic experiments, Schiff base ligands have an important influence on the performance of the complexes in catalysis. Depending on the substituents, and especially on their positions in the aromatic rings, the Schiff bases can behave in different fashion, from being highly stable against the catalytic oxidative conditions to decomposing within the first minutes of the reaction.

Given the ready availability and stability of the title complexes, together with the good catalytic performance of some, they are good alternatives to the – in many cases - less stable MTO N-donor complexes as epoxidation catalysts. As the latter, the Schiff base adducts can also be prepared and applied *in situ*. In contrast to the N-donor adducts no pronounced ligand excess is necessary to achieve high yields and selectivities in olefin epoxidation catalysis. High ligand : MTO ratios even reduce the catalytic activity by inducing complex decomposition. Future applications of these adducts should include both their immobilisation to enable catalyst recyclisation and the introduction of chirality in the system.

References cited in this chapter

- (1) Kühn, F. E.; Santos, A. M.; Herrmann, W. A. *Dalton Trans.* **2005**, 2483-2491.
- (2) Kühn, F. E.; Jain, K. R.; Zhou, M. *Rare Metals* **2006**, 25, 411-421.
- (3) Mertis, K.; Williamson, D. H.; Wilkinson, G. *J. Chem. Soc. Dalton Trans.* **1975**, 607-611.
- (4) Beattie, I. R.; Jones, P. J. *Inorg. Chem.* **1979**, 18, 2318-2319.
- (5) Herrmann, W. A.; Serrano, R.; Bock, H. *Angew. Chem. Int. Ed.* **1984**, 23, 383.
- (6) Herrmann, W. A.; Fischer, R. W.; Marz, D. W. *Angew. Chem. Int. Ed. Engl.* **1991**, 30, 1638-1641.
- (7) Schrock, R. R.; Parshall, G. W. *Chem. Rev.* **1976**, 76, 243-268.
- (8) Herrmann, W. A. *J. Organomet. Chem.* **1995**, 500, 149-174.
- (9) Herrmann, W. A. *Angew. Chem. Int. Ed. Engl.* **1988**, 27, 1297-1313.
- (10) de Bellefon, C. M.; Herrmann, W. A.; Kiprof, P.; Whitaker, C. R. *Organometallics* **1992**, 11, 1072-1081.
- (11) Herrmann, W. A.; Kuchler, J. G.; Weichselbaumer, G.; Herdtweck, E.; Kiprof, P. *J. Organomet. Chem.* **1989**, 372, 351-370.
- (12) Herrmann, W. A.; Kühn, F. E.; Fischer, R. W.; Thiel, W. R.; Romão, C. C. *Inorg. Chem.* **1992**, 31, 4431-4432.
- (13) Herrmann, W. A.; Rost, A. M. J.; Mitterpleiniger, J. K. M.; Szesni, N.; Sturm, S.; Fischer, R. W.; Kühn, F. E. *Angew. Chem. Int. Ed.* **2007**, 46, 7301-7303.
- (14) Tosh, E.; Mitterpleiniger, J. K. M.; Rost, A. M. J.; Veljanovski, D.; Herrmann, W. A.; Kühn, F. E. *Green Chem.* **2007**, 9, 1296-1298.
- (15) Herrmann, W. A. *J. Organomet. Chem.* **1990**, 382, 1-18.
- (16) Kühn, F. E.; Scherbaum, A.; Herrmann, W. A. *J. Organomet. Chem.* **2004**, 689, 4149-4164.
- (17) Romão, C. C.; Kühn, F. E.; Herrmann, W. A. *Chem. Rev.* **1997**, 97, 3197-3246.
- (18) Herrmann, W. A.; Fischer, R. W.; Correia, J. D. G. *J. Mol. Catal.* **1994**, 94, 213-223.
- (19) Adam, W.; Herrmann, W. A.; Lin, J.; Saha-Möller, C. R.; Fischer, R. W.; Correia, J. D. G. *Angew. Chem. Int. Ed. Engl.* **1994**, 33, 2475-2477.
- (20) Herrmann, W. A.; Weskamp, T.; Zoller, J. P.; Fischer, R. W. *J. Mol. Catal. A: Chem.* **2000**, 153, 49-52.
- (21) Goti, A.; Cardona, F.; Soldaini, G. *Org. Synth.* **2005**, 81, 204.
- (22) Herrmann, W. A.; Zoller, J. P.; Fischer, R. W. *J. Organomet. Chem.* **1999**, 579, 404-407.

- (23) Herrmann, W. A.; Fischer, R. W.; Scherer, W.; Rauch, M. U. *Angew. Chem. Int. Ed.* **1993**, *32*, 1157–1160.
- (24) Herrmann, W. A.; Fischer, R. W.; Rauch, M. U.; Scherer, W. *J. Mol. Catal.* **1994**, *86*, 243–266.
- (25) Al-Ajlouni, A. M.; Espenson, J. H. *J. Am. Chem. Soc.* **1995**, *117*, 9243–9250.
- (26) Al-Ajlouni, A. M.; Espenson, J. H. *J. Org. Chem.* **1996**, *61*, 3969–3976.
- (27) Espenson, J. H. *Chem. Commun.* **1999**, *6*, 479.
- (28) Owens, G. S.; Arias, J.; Abu-Omar, M. M. *Catal. Today* **2000**, *55*, 317–363.
- (29) Abu-Omar, M. M.; Hansen, P. J.; Espenson, J. H. *J. Am. Chem. Soc.* **1996**, *118*, 4966–4974.
- (30) Scheidt, E.; Miller, R.; Helbig, C.; Eickerling, G.; Mayr, F.; Herrmann, R.; Schwab, P.; Scherer, W. *Physica B* **2006**, *378–380*, 1132–1133.
- (31) Herrmann, R.; Tröster, K.; Eickerling, G.; Helbig, C.; Hauf, C.; Miller, R.; Mayr, F.; von Nidda, H. K.; Scheidt, E.; Scherer, W. *Inorg. Chim. Acta* **2006**, *359*, 4779–4788.
- (32) Bouh, A. O.; Espenson, J. H. *J. Mol. Cat. A: Chem.* **2003**, *200*, 43–47.
- (33) Li, M.; Espenson, J. H. *J. Mol. Cat. A: Chem.* **2004**, *208*, 123–128.
- (34) Jain, K. R.; Kühn, F. E. *J. Organomet. Chem.* **2007**, *692*, 5532–5540.
- (35) Adam, W.; Saha-Moller, C. R.; Weichold, O. *J. Organomet. Chem.* **2000**, *65*, 2897–2899.
- (36) Goti, A.; Cardona, F.; Soldaini, G.; Crestini, C.; Fiani, C.; Saladino, R. *Adv. Synth. Cat.* **2006**, *348*, 476–486.
- (37) Bianchini, G.; Crucianelli, M.; Crestini, C.; Saladino, R. *Top. Catal.* **2006**, *40*, 221–227.
- (38) Bianchini, G.; Crucianelli, M.; Canevali, C.; Crestini, C.; Morazzoni, F.; Saladino, R. *Tetrahedron* **2006**, *62*, 12326–12333.
- (39) Saladino, R.; Andreoni, A.; Neri, V.; Crestini, C. *Tetrahedron* **2005**, *61*, 1069–1075.
- (40) Herrmann, W. A.; Roesky, P. W.; Kühn, F. E.; Scherer, W.; Kleine, M. *Angew. Chem. Int. Ed.* **1993**, *32*, 1714–1716.
- (41) Herrmann, W. A.; Weichselbaumer, G.; Herdtweck, E. *J. Organomet. Chem.* **1989**, *372*, 371–389.
- (42) Rudolph, J.; Reddy, K. L.; Chiang, J. P.; Sharpless, K. B. *J. Am. Chem. Soc.* **1997**, *119*, 6189–6190.
- (43) Adolfsson, H.; Copéret, C.; Chiang, J. P.; Yudin, A. K. *J. Org. Chem.* **2000**, *65*, 8651–8658.
- (44) Copéret, C.; Adolfsson, H.; Sharpless, K. B. *Chem. Commun.* **1997**, 1565–1566.
- (45) Kühn, F. E.; Santos, A. M.; Roesky, P. W.; Herdtweck, E.; Scherer, W.; Gisdakis, P.; Yudanov, I. V.; Di Valentin, C.; Rösch, N. *Chem. Eur. J.* **1999**, *5*, 3602–3615.

- (46) Herrmann, W. A.; Kratzer, R. M.; Ding, H.; Thiel, W. R.; Glas, H. *J. Organomet. Chem.* **1998**, *555*, 293-295.
- (47) Ferreira, P.; Xue, W.; Bencze, E.; Herdtweck, E.; Kühn, F. E. *Inorg. Chem.* **2001**, *40*, 5834-5841.
- (48) Köstlmeier, S.; Naszulov, V. A.; Herrmann, W. A.; Rösch, N. *Organometallics* **1997**, *16*, 1786-1792.
- (49) Adam, W.; Mitchell, C. M. *Angew. Chem. Int. Ed. Engl.* **1996**, *35*, 533-535.
- (50) Kühn, F. E.; Zhao, J.; Herrmann, W. A. *Tetrahedron: Asymmetry* **2005**, *16*, 3469-3479.
- (51) Cunha-Silva, L.; Gonçalves, I. S.; Pillinger, M.; Xue, W.; Rocha, J.; Teixeira-Dias, J. J. C.; Kühn, F. E. *J. Organomet. Chem.* **2002**, *656*, 281-287.
- (52) Takacs, J.; Kiprof, P.; Riede, J.; Herrmann, W. A. *Organometallics* **1990**, *9*, 782-787.
- (53) Takacs, J.; Kiprof, P.; Kuchler, J. G.; Herrmann, W. A. *J. Organomet. Chem.* **1989**, *1*, C1-C5.
- (54) Zhu, Z.; Al-Ajlouni, A. M.; Espenson, J. H. *Inorg. Chem.* **1996**, *35*, 1408-1409.
- (55) Haider, J. J.; Kratzer, R. M.; Herrmann, W. A.; Zhao, J.; Kühn, F. E. *J. Organomet. Chem.* **2004**, *689*, 3735-3740.
- (56) Herrmann, W. A.; Rauch, M. U.; Artus, G. R. J. *Inorg. Chem.* **1996**, *35*, 1988-1991.
- (57) Kühn, F. E.; Rauch, M. U.; Lobmaier, G. M.; Artus, G. R. J.; Herrmann, W. A. *Chem. Ber.* **1997**, *130*, 1427-1431.
- (58) Zhou, M.; Zhao, J.; Li, J.; Yue, S.; Bao, C.; Mink, J.; Zang, S.; Kühn, F. E. *Chem. Eur. J.* **2007**, *13*, 158-166.
- (59) González-Arellano, C.; Corma, A.; Iglesias, M.; Sánchez, F. *Adv. Synth. Cat.* **2004**, *346*, 1758-1764.
- (60) González-Arellano, C.; Corma, A.; Iglesias, M.; Sánchez, F. *Chem. Commun.* **2005**, 1990-1992.
- (61) González-Arellano, C.; Gutiérrez-Puebla, E.; Iglesias, M.; Sánchez, F. *Eur. J. Inorg. Chem.* **2004**, 1955-1962.
- (62) Comas-Vives, A.; González-Arellano, C.; Corma, A.; Iglesias, M.; Sánchez, F.; Ujaque, G. *J. Am. Chem. Soc.* **2006**, *128*, 4756-4765.
- (63) González-Arellano, C.; Corma, A.; Iglesias, M.; Sánchez, F. *Adv. Synth. Cat.* **2004**, *346*, 1316-1328.
- (64) Herrmann, W. A.; Kühn, F. E.; Mattner, M. R.; Artus, G. R. J.; Geisberger, M. R.; Correia, J. D. G. *J. Organomet. Chem.* **1997**, *538*, 203-209.
- (65) Capapé, A.; Zhou, M.; Zang, S.; Kühn, F. E. *J. Organomet. Chem.* **2008**, *693*, 3240-3244.
- (66) Wang, W.; Espenson, J. H. *J. Am. Chem. Soc.* **1998**, *120*, 11335-11341.

- (67) Herrmann, W. A.; Roesky, P. W.; Kuehn, F. E.; Elison, M.; Artus, G.; Scherer, W.; Romao, C. C.; Lopes, A.; Basset, J. *Inorg. Chem.* **1995**, *34*, 4701-4707.
- (68) Bin-Bin, L.; Yong-Qing, Q.; Zhong-Min, S.; Shi-Ling, S.; Ji-Kang, F. *Chem. J. Chinese Universities.* **2001**, *22*, 1551-1554.
- (69) Herrmann, W. A.; Kühn, F. E. *Acc. Chem. Res.* **1997**, *30*, 169-180.
- (70) Zhou, M.; Zang, S.; Herdtweck, E.; Kühn, F. E. *J. Organomet. Chem.* **2008**, *693*, 2473-2477.
- (71) Rost, A. M. J.; Schneider, H.; Zoller, J. P.; Herrmann, W. A.; Kühn, F. E. *J. Organomet. Chem.* **2005**, *690*, 4712-4718.
- (72) Hunter, C. A.; Sanders, J. K. M. *J. Am. Chem. Soc.* **1990**, *112*, 5525-5534.
- (73) Braga, D.; Grepioni, F.; Desiraju, G. R. *Chem. Rev.* **1998**, *98*, 1375-1405.

**III. SYNTHESIS AND CATALYTIC
APPLICATIONS OF
CYCLOPENTADIENYL MOLYBDENUM
AND TUNGSTEN ALKYL COMPOUNDS**

Synthesis and Catalytic Applications of Cyclopentadienyl Molybdenum and Tungsten Alkyl Compounds

Despite their earlier start-up, the history of organo-molybdenum(VI) oxides is far less spectacular than that of the organorhenium(VII) oxides, lacking a “star” compound such as MTO. This is at least in part due to the early success of a plethora of at least partially ill defined molybdenum compounds in industrial catalysis, such as those conforming the Halcon and Arco processes.ⁱ Hence, it seemed quite unnecessary to synthesise *sensitive* organo-molybdenum species for catalytic applications, considering that such straightforward and stable compounds as $\text{Mo}(\text{CO})_6$ could be applied as homogeneous oxidation catalysts in the presence of TBHP. During the last years, the increasing concern over the synthesis of more selective catalysts has encouraged revisiting previously synthesised organometallic species which, as MTO, were at first considered mere curiosities. As a result, a number of Mo and W organometallic oxides have been tested in catalysis, showing promising capabilities and quickly becoming important fields of research in organometallic chemistry. This part will concentrate in the recent synthesis of organometallic Mo oxides, especially those containing a η^5 -coordinated cyclopentadienyl rings and their applications in olefin epoxidation catalysis. Parallely, the much similar, though less relevant tungsten systems will be also studied. Moreover, the current research in *ansa* derivatives will be emphasised, as well as its potential applications in enantioselective catalysis.

ⁱ See section 2.2.1

7. High Valent Organometallic Oxides of Molybdenum and Tungsten as Epoxidation Catalysts

Following their previous research of in η^5 -cyclopentadienyl compounds of Feⁱⁱ, Fischer *et al.* first reported the oxidation of CpV(CO)₄ to CpVOCl₂, followed by the formation of tetrameric CpCr oxides.(1-4) A few years later, Green and Cousins first reported the formation of small amounts of CpMoO₂Cl while studying the properties of alkyl carbonyls.(5-7). This discovery, along with the unexpected stability of the complex, prompted the investigation of similar species.

It was some time later when the first compounds with Mo-C σ -bonds were reported.(8) These compounds have been further stabilised by adding donor bases. Its related species, together with the abovementioned Cp derivatives have become the most relevant high valent Mo systems used in as catalysts in epoxidation reactions.(9)

This chapter will introduce both species, first the molybdenum dioxo complexes of formula MoO₂R₂L₂ (R = alkyl, halogen; L = donor ligand) and then the CpMo derivatives (carbonyls and oxidised derivatives). Apart from putting special attention into the most relevant enantioselective catalytic systems, the synthesis, characterisation and catalytic properties of the latter will be also studied, especially in the case of the alkyl derivatives of formula CpMo(CO)₃R (R = methyl, *ansa* bridge). In parallel, the much similar tungsten derivatives will also, when necessary, be properly introduced and compared with its molybdenum counterparts. It must be noted that the catalytic properties of the former species are in general much more moderate.

ⁱⁱ i.e., Ferrocenyl compounds

7.1 Dioxomolybdenum complexes

The MoO_2^{2+} moiety constitutes the pillar of all high valent molybdenum species employed in catalysis. As it will be observed throughout this chapter, this fragment and its peroxy derivatives are present in both organometallic and non-organometallic species.

7.1.1 Non-organometallic molybdenum dioxo compounds. Adducts with donor ligands

A significant number of Mo dioxo compounds are synthesised from MoO_2X_2 ($\text{X} = \text{Cl}, \text{Br}$) species, which at their turn are synthesised from MoO_2 and the respective halides via oxidative addition. Molybdenum species prefer octahedral environmentsⁱⁱⁱ, and the distortedly tetrahedral MoO_2X_2 species readily coordinate two solvent molecules when dissolved in THF, DMF, DMSO, acetonitrile, etc.⁽¹⁰⁾ Due to the similarity with Re(VII) oxides, which proved to be excellent oxidation catalysts, these species have been object of extensive studies. It has been observed that these compounds can be further stabilised with donor bases (utterly displacing the weakly donor solvent molecules).

A number of donor ligands form successful adducts with Mo dioxo compounds, including phosphine oxides, sulphur complexes, alkoxides, siloxils, glycols, siloxanes, pyridines, amines, etc.^{iv}

N-donor bases

MoO_2X_2 compounds have been found to form stable adducts with a plethora of N-donor bases, including diamines, chelate N-donor ligands, pyridines, pyrazolpyridines and Schiff bases.

ⁱⁱⁱ In addition, both oxygen ligands are in a *cis*-position with respect to the other in order to avoid competing for the same p and d orbitals, hence magnifying the π -bonding to the metal.

^{iv} A comprehensive review on this topic, including a detailed description of the to-date reported complexes can be found in the Ph.D. thesis of Dr. Jin Zhao (Technische Universität München, 2005).

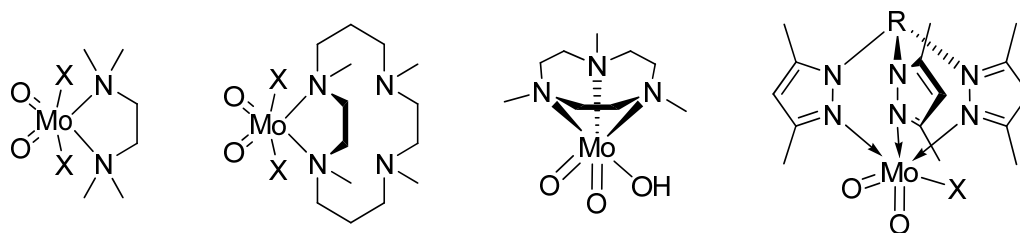


Figure 1 Some examples of MoO_2X_2 N-donor adducts (X = halogen).

O-donor bases

Oxygen donor compounds (see Section 5.4 for a view on the closely related MTO derivatives) are occasionally used as ligands for Mo dioxo compounds. Most results are inscribed within the field of optically active complexes, and will be introduced in the next sections.

7.1.2 Organometallic derivatives with M-C σ bonds

Heyn and Hoffmann were the first to report a σ -bound molybdenum dioxo compound, $\text{MoO}_2(\text{mes})_2$ (mes = 2,4,6-trimethylbenzyl) by reaction of the abovementioned MoO_2Cl_2 with mesitylmagnesium bromide.(8)

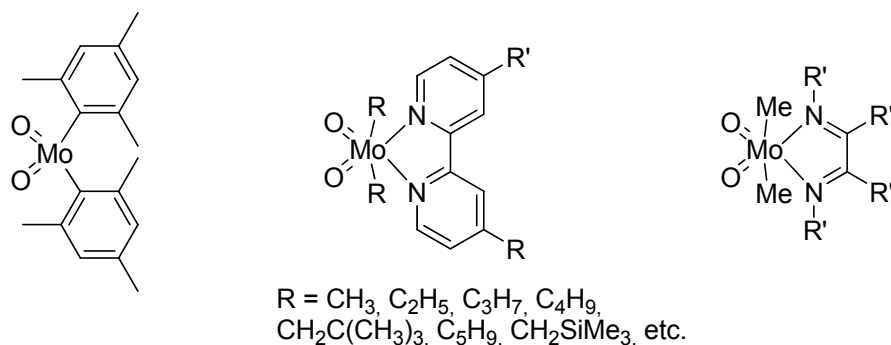


Figure 2 Various examples of σ -bound Mo-C dioxo compounds, including the first reported compound of its kind (left).

During the following years, many related compounds have been successfully synthesised, including N-donor adducts, especially those derived of 4,4'-bipyridine. A recent, comprehensive review from our group summarises the synthesis, characterisation and catalytic activity of σ -alkyl bound dioxo molybdenum compounds.(9)

Due to their importance in the present work, the much more studied π -bonded complexes, in special η^5 -derivatives will be discussed separately in Section 7.2.

7.1.3 Chiral derivatives

The great number of potential ligands available for the MoO_2^{2+} moiety includes many chiral derivatives. Many of these reported systems draw inspiration from Sharpless' Tartrate and Jacobsen's salen catalysts.(11, 12) During the last two decades, a number of chiral dioxomolybdenum compounds have been synthesised. The comprehensive review of Kühn et al (13) covers the most significant literature concerning both organorhenium and organomolybdenum chiral complexes. Some significant examples are included in Figure 3. Preferred approaches include the use of polydentate donor ligands coordinating in [O, O], [N, O], [N, N], [N, N, O] fashions, amongst others. Most of these complexes have been applied in epoxidation catalysis. Siderophore *cis*-dioxomolybdenum (VI) complexes have been also reported. In this case, azotochelin and other biologically inspired ligands, along with modified natural products such as sugar and menthyl derivatives (Figure 3) readily form chiral complexes with Mo oxides.(14-16)

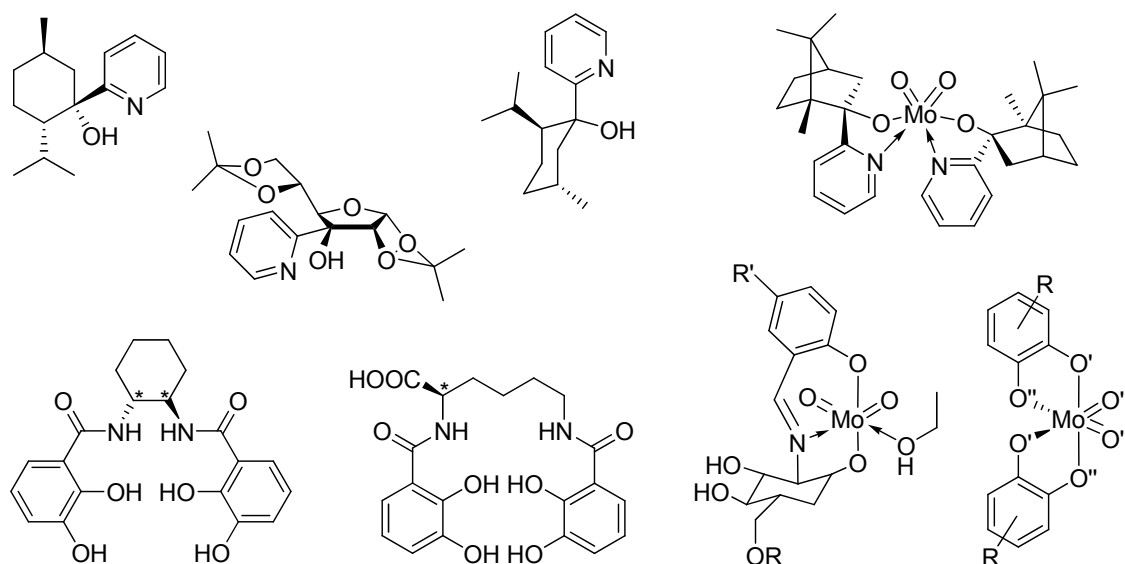


Figure 3 A selection of asymmetric ligands (left) and two examples of the chiral Mo-dioxo compounds (right).

7.1.4 Application in epoxidation catalysis

As it happens with other transition metal oxides, many Mo(VI) species display remarkable catalytic activities in certain oxidation reactions. Due to their similar structures, obvious comparisons with methyltrioxorhenium (VII) have arisen; whereas certain Mo species can surpass MTO in terms of selectivity and catalytic activity, they display rather poor performances - even at high temperatures - when using H₂O₂ as oxidant. This owes to the reduced stability of the compound in aqueous media. Therefore, catalytic studies usually employ alkylhydroperoxides such as TBHP.(10) σ -bound alkyl derivatives generally afford worse results than non-organometallic derivatives. It must be noted that compounds of formula MoO₂R₂(bpy) (R = Me, Et) have been found to catalyse ROMP (Ring Opening Metathesis Polymerisation) using MeMgBr as cocatalyst.(9)

Asymmetric Epoxidation

The success of Sharpless *et al.* in Mo, V and especially Ti-catalysed asymmetric epoxidation of allylic alcohols prompted similar studies with neighbouring transition metals, amongst them molybdenum oxides. Yamada *et al.* treated MoO₂(acac)₂ with alkylphedrine, obtaining ees up to 33%.(17) The reaction of the same oxide with excess *N*-methylprolinol afforded species that were also found to induce chirality, achieving moderate to low enantiometric excesses.(18)

The application of chiral dioxomolybdenum (VI) adducts in catalysis is relatively recent. The first promising results were reported by Herrmann *et al.*, in which a chiral 2'-pyridinyl alcohol derivatives afforded moderate enantiomeric excesses.(19) Sugar derived chiral Schiff bases have been also found to moderately induce asymmetric β -methylstyrene epoxidation.(14) Similarly, certain bis(oxazoline) and pyridyl alcoholate adducts were also found to induce chirality with the same substrate, although the obtained ees were generally low.

On the other hand, enantiomeric excesses up to 75% have been recently obtained by Kühn, Romão *et al.* using chiral diimines (Figure 4). However, these results come at the expense of very low conversions.(20) In a recent paper, the group of Romão has reported the synthesis of Mo and W (VI) BINOL complexes and their application in oxidation reactions, including sulphoxidations and asymmetric epoxidation. In the latter case, the conversions and ees obtained were very poor.(21)

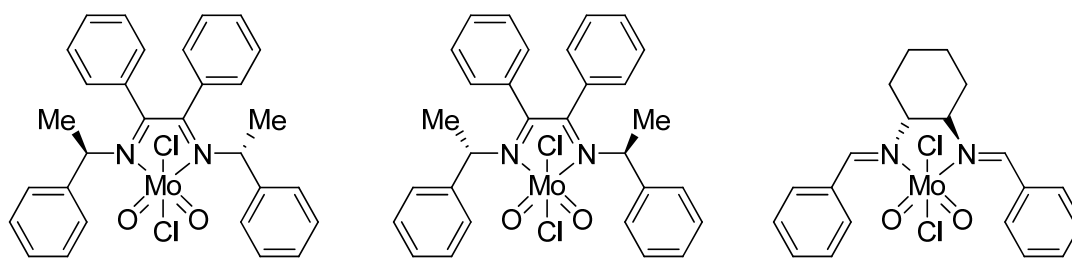


Figure 4 Chiral diimine bis(chloro)dioxomolybdenum complexes (From (20)).

7.1.5 Tungsten derivatives

In comparison with molybdenum derivatives, tungsten oxides have been much less studied. This owes to their higher costs and reduced catalytic activity. Despite these facts, the compounds display certain advantages over their Mo counterparts, most notably an improved stability.

Application in epoxidation catalysis

The most significant difference of W oxides in comparison with its Mo counterparts is their reported catalytic oxidation capabilities using H_2O_2 as oxidant. However, only a small number of publications reporting its applications in epoxidation catalysis can be found in the literature. Payne and Smith first reported the catalytic activity of tungstic acid in the hydroxylation of cyclohexene with water peroxide more than half century ago.(22) After a few further attempts, Sharpless and Kirshenbaum *rediscovered* the WO_4^{2-} moiety as a feasible catalytic species for the aqueous epoxidation of α,β -unsaturated acids with H_2O_2 .(23) In 1992, Noyori *et al.* reported yet another tungsten-based catalytic epoxidation system based on Na_2WO_4 dihydrate, (aminomethyl)-phosphonic acid and methyltri-*n*-octylammonium hydrogensulfate in a 2:1:1 molar ratio, employing aqueous hydrogen peroxide (30%) as oxidant and using either toluene or no organic solvents at all.(24) This system has proved extremely active in epoxidation of terminal alkenes such as 1-octene, achieving almost quantitative conversions after 4 hours and displaying high selectivities towards the epoxide.

Soon after the catalytic activity of molybdenum oxides of general formula $\text{MoO}_2\text{X}_2\text{L}_2$ was discovered, several groups attempted the synthesis of similar W derivatives.(25) Whereas the latter generally display lower catalytic activity in the epoxidation of various substrates with alkyhydroperoxides, it has been found that they clearly outperform Mo-

based catalysts when using hydrogen peroxide as the oxidising agent. Recent studies have reported the synthesis and catalytic applications of W oxo-peroxo derivatives with dppmO_2 (diphenylphosphinomethane oxide) donor ligands, which show promising activities in the epoxidation of cyclooctene with H_2O_2 .(26)

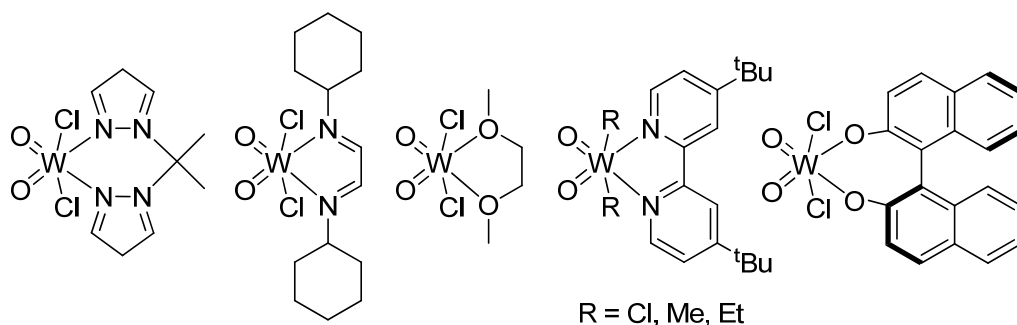


Figure 5 Several examples of synthesised W dioxo compounds with donor ligands.

7.2 η^5 -Cyclopentadienyl compounds^v

The cyclopentadienyl group is possibly one of the most significant ligands in organometallic chemistry - both from a historical as well as a synthetic point of view. Of all its possible coordination modes, the η^5 arrangement has been classically the most common, due to its firm bonding and inert character towards either nucleophilic or electrophilic reagents.(27)



Figure 6 From left to right: η^1 , η^3 and η^5 coordination modes of the cyclopentadienyl ligand to a given metal.

Apart from the well known metallocenes (such as ferrocene, which decisively contributed to the development of organometallic chemistry in the early fifties),(1) attention has been drawn to half sandwich compounds of formula CpML_n (28), L being carbonyl, halide, oxo and oxo-peroxo groups, amongst others. The two latter groups

^v Tungsten species are occasionally featured alongside its molybdenum counterparts. Though this section will concentrate on the latter, CpW compounds will be mentioned when necessary.

have aroused attention in the last years due to their catalytic capabilities. These oxides will be discussed in the present work, as well as their most common precursors, in special carbonyl compounds.

7.2.1 Cyclopentadienyl Carbonyl metal derivatives

As it has been discussed in previous sections, the active catalytic species in olefin oxidation are organometallic oxides containing the metal in a high oxidation state.⁽²⁹⁾ Due to their stability and relatively easy synthesis, cyclopentadienyl carbonyl compounds have become the most common precursors for these high valent CpM species (M = Mo, W).⁽³⁰⁾ The well established two-step synthesis of these compounds – both the alkyl and halide derivatives – uses $\text{Mo}(\text{CO})_6$ and the respective cyclopentadienides in high yields.⁽³¹⁾ Despite the versatility of this method, certain Cp derivatives of Mo and W cannot be synthesised from molybdenum hexacarbonyl. To put an example, in the next sections the synthesis of *ansa*-bridged Cp compounds will be introduced; these species precise of much more labile metallic precursors in order to facilitate both the coordination of the cyclopentadienyl moiety as well as the formation of the metallorganic bridge. A common approach in order to afford these species is to “activate” the metal carbonyls by displacing the strongly bonded CO molecules with N-donor ligands.

Precursors for the synthesis of CpMo compounds

As it has been mentioned above, the synthesis of most CpMo derivatives can be carried out with $\text{Mo}(\text{CO})_6$, whereas certain alkyl derivatives (such as the *ansa* derivatives) demand the use of more labile ligands. Tris-acetonitrile compounds of molybdenum and tungsten are known since the 60ies.⁽³²⁾ Due to the lability of the CH_3CN ligands, they are employed in a number of reactions, especially in the formation of CpMo allyl and alkyl derivatives (complete).^(33, 34) These precursors are, however, highly sensitive to both moisture and air and are generally impurified by highly reactive by-products that hamper subsequent reactions^{vi}. In order to minimise these problems, chelate triamine precursors such as pentamethyldiethylenetriamine (PMTA) have been more recently introduced. Amongst many other advantages, they display an improved solubility in

^{vi} This fact will discussed in chapter 10.

polar solvents and are much easier to handle. These compounds were successfully applied as reagents for the synthesis of certain metallic clusters.(35-37)

Angelici *et al.* improved the synthesis of the PMTA precursor, which apart from forming the $M(CO)_3(RCN)_3$ derivatives in high yields and purities can react with various phosphines as well as with benzene to form η^6 -aryl tricarbonyl derivatives.(38) In the latter case, a strong Lewis acid (such as BF_3) is used to activate the phenyl moiety.

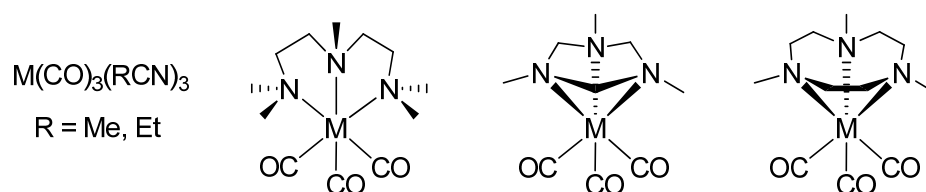


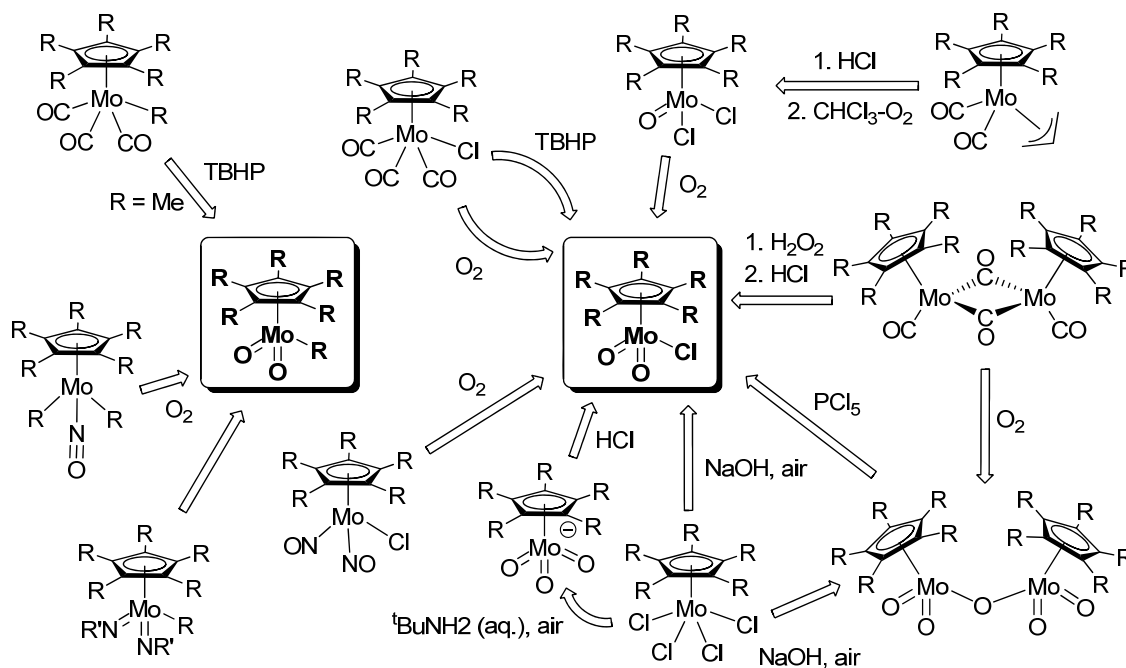
Figure 7 Precursors for the synthesis of cyclopentadienyl Mo and W complexes. From left to right, $M(CO)_3PMTA$, $M(CO)_3Me_3tach$, $M(CO)_3Me_3tacn$.

The use of cyclic tridentate amines such as trimethyltriazacyclohexane^{vii} has also been reported.(39-41) These products have shown a significant advantage over the PMTA derivatives due to the facial conformation of the chelate ligand, which make these compounds interesting precursors for the synthesis of *fac*- $M(CO)_3L_3$ complexes (L = phosphine, (CH_3CN) , etc.).

7.2.2 Cyclopentadienyl oxo-metal derivatives

Despite their enhanced stability, η^5 -Cp organometallic compounds were originally considered to lose the cyclopentadienyl moiety under oxidative conditions. The pioneering work of Fischer *et al.* in the 50ies on CpCr and CpV oxides from its respective metallocenes or half-sandwich carbonyls, proved otherwise.(42) Concerning the present work, attention must be drawn to the significant research of Cousins and Green, who prepared many Mo cyclopentadienyl oxo derivatives using molecular oxygen as oxidant. Both discoveries considerably raised the interest in organometallic high-oxidation state transition metal compounds and its potential applications. Hence, a plethora of these compounds has been synthesised during the last decades, including the already mentioned $(\eta^5-C_5R_5)ReO_3$ (R = Me or H), $(\eta^5-C_5H_5)ReOMe_2$, $(\eta^5-C_5H_5)WO(C_2H_2)Me$, $(\eta^5-C_5H_5)WO(C_2SiMe_3)$ and $(\eta^5-C_5R_5)VOCl_2$, amongst others.(42-46)

^{vii} As it has been seen in previous sections, there are many reported N-donor chelate complexes of Re and Mo oxides with triazacyclononanes.



Scheme 2 A selection of the obtention methods of CpMo dioxo complexes reported in the literature (from (9, 43, 47-50) and references cited therein).

There are many reports with regard to the synthesis of organometallic molybdenum (VI) oxides. Scheme 2 summarises the most significant procedures used in the synthesis of $(\text{CpR}_5)\text{Mo}$ dioxo species ($\text{R} = \text{H}, \text{Me}, \text{etc.}$). It was recently shown that MoCp carbonyl species are easily oxidised via TBHP when used as precatalysts for certain oxidations.⁽⁵¹⁾ Hence, and due to the difficult and isolation of the CpMo (VI) active species, the *in situ* generation of this species during the catalytic reaction is a much preferred approach.⁽³⁰⁾ This will be seen in the next chapters.

Oxo-peroxo species

Apart from the dioxo derivatives, cyclopentadienyl Mo (and W) complexes can be further oxidised to yield the respective oxo-peroxo species.^(45, 52) These compounds and their implications in oxidation catalysis are of special importance in the present manuscript and will be discussed in Chapter 8.

7.2.3 Chiral derivatives

Whereas a plethora of MoO_2R_2 adducts with chiral moieties have been thoroughly examined, there are not many examples of CpMo chiral systems. This is mainly due to the late application of such compounds in catalysis. Our laboratories recently reported

the synthesis of a both menthol-Cp and chiral *ansa*-bridged derivatives (see Figure 8).(53, 54) Since these systems are closely related to the experimental work presented in this manuscript, they will be examined in detail in chapters 9, 10 and 11, along with the most recent advances in the area.

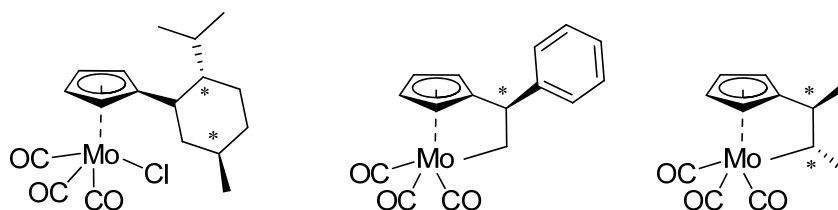


Figure 8 Recent examples of CpMo precatalysts with chiral moieties.

7.2.4 Application in epoxidation catalysis

In parallel to the more known $\text{MoO}_2\text{R}_2\text{L}$ derivatives, CpMo complexes (and W to a lesser extent) have been also studied and their catalytic properties examined.(55) These compounds have shown interesting features in the field of epoxidation catalysis, as reported for related organometallic oxides.(56) During the last years, many $(\text{CpR}_5)\text{Mo}$ ($\text{R} = \text{H}, \text{Me}, \text{Bz}, \text{Ph}$) compounds have been applied in olefin epoxidation. The obtained results are in some cases on par (and even surpassing) MTO-based catalysts. One of the major advantages of cyclopentadienyl Mo and W oxo-derivatives is that they can be synthesised from their carbonyl precursors using alkylhydroperoxides such as TBHP. Since the same peroxides are used as an oxygen source in catalytic epoxidation reactions, the precatalyst can be oxidised *in situ*, conveniently forming the catalytically active species without having to isolate it first. The research group of C. C. Romão reported a detailed study of $\text{Cp}'\text{Mo}(\text{CO})_3\text{Cl}$ species as precatalyst for olefin epoxidation.(30, 51) In general, the results reported to date favour the abovementioned halide derivatives over the alkyl compounds. Moreover, benzyl pentasubstituted cyclopentadienyl ligands have afforded the best cyclooctene epoxidation catalytic performances, achieving TOFs up to 21000 h^{-1} . (1 : 10000 : 20000 catalyst : substrate : oxidant ratio). Chiral CpMo carbonyl derivatives have recently been applied as precatalysts in prochiral olefin epoxidation, obtaining rather low yields and enantiomeric excesses.(53, 54, 57) Some of these catalytic reactions have been revisited in the present work. Due to their reduced activity, related tungsten species have rarely been applied in catalysis. In a recent publication, alkyl and *ansa* bridged CpW carbonyls were

tested as catalysts in cyclooctene epoxidation.⁽⁵⁸⁾ Significant results were only achieved for a reaction temperature of 90 °C^{viii}.

7.2.5 Heterogenisation of cyclopentadienyl molybdenum compounds. Applications in ionic liquids

Despite the numerous studies on related compounds, the use of CpMo systems in catalysis is still in its infancy. Hence, the few reported heterogenised cyclopentadienyl molybdenum complexes are relatively recent.⁽⁴⁷⁾ Grafting of the compounds have been achieved via the Cp ring and the σ -bound alkyl moiety. The majority of the work originates from the research of Sakthivel, Zhao and Kühn, and includes various supports (MCM, SBA, zeolites, etc).^(54, 59-65) The catalytic performance of these systems, though inferior in comparison with its homogeneous counterparts, is remarkable at least.

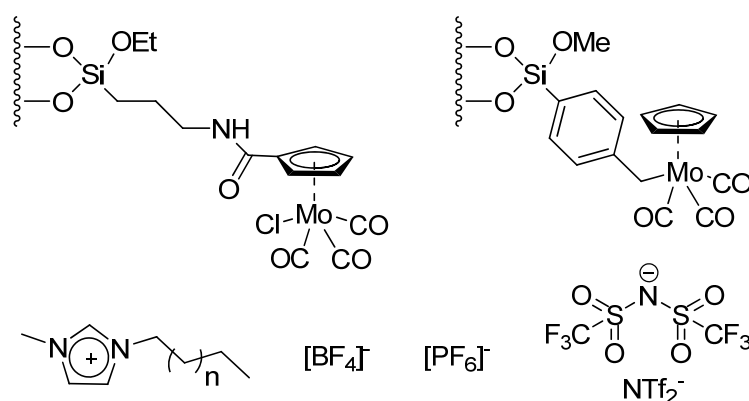


Figure 9 Some examples of heterogenised CpMo(CO)₃R compounds (above). Below, a selection of RTIL, including BMIM (n = 1), C₈MIM (n = 5) and its counteranions.

Certain room temperature ionic liquids (IL or RTIL) have been also applied as solvents in epoxidation, using (CpR₅)Mo(CO)₃X (R = H, Me; X = Me, Cl).⁽⁶⁶⁾ Amongst them, the use of [BMIM]NTf₂ has afforded activities comparable to those of the homogeneous systems.

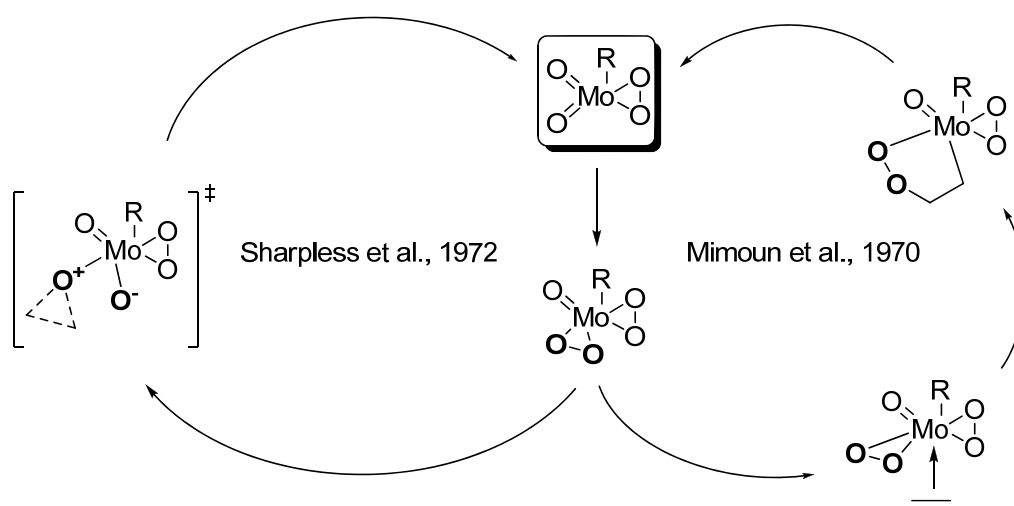
^{viii} Reactions with Mo compounds are usually carried out at 55 °C.

7.3 Mechanistic implications in the epoxidation reaction. A comparative

Once the synthesis and the catalytic activity of the organometallic Mo oxides was well established, it was found imperative to study its mechanistic features, with the aim of comparing the molybdenum species with the well known MTO epoxidation system.(67-71) The number of mechanistic reports on Mo-catalysed epoxidation is, however, rather low. The following chapter will present the mechanisms proposed to date, either for MoO_2R_2 or for CpMoO_2 systems.

7.3.1 Mechanistic features of molybdenum dioxo species. The Mimoun and Sharpless mechanisms

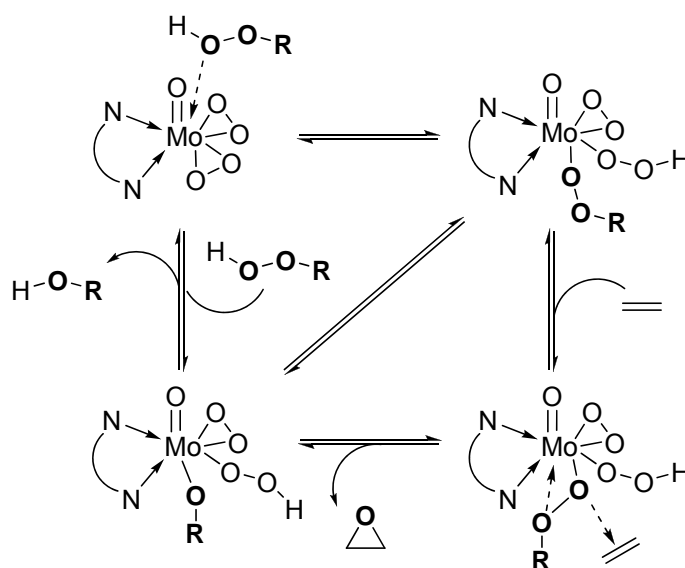
Despite the few reports on the oxidation catalysis performed by molybdenum oxides, two mechanistic systems were already proposed in the early 70ies, first by Mimoun and later by Sharpless.(72, 73) The main difference between both systems (depicted in Scheme 3) lies primarily within the mechanism of the oxygen transfer and the coordination of the olefin to the catalytic species – either directly to the metal centre or through one of the Mo-bound oxygen atoms.



Scheme 3 The two possible mechanistic pathways for the Mo catalysed epoxidation reaction.

Sharpless carried out ^{18}O labelling experiments and observed that the marked peroxo-complexes did not contain any of the labelled oxygen atoms in the epoxidised products. Thus, it was proposed that the peroxide would coordinate to the central atom and

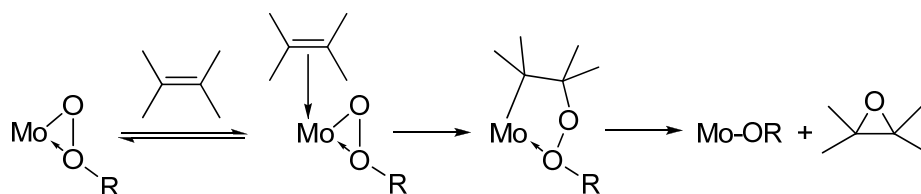
transfer the oxygen atom to the substrate via a concerted mechanism. In 1997, Thiel studied the mechanistic features of seven-coordinate oxobisperoxo molybdenum complexes with chelating pyrazolylpyridine ligands.⁽⁷⁴⁾ The proposed mechanism (Scheme 4) followed a Sharpless-like mechanism, with the hydroperoxide directly bound to the metal centre and the olefin coordinating via the α -O of the peroxide; again, the peroxy moiety was not involved in the oxygen transfer mechanism. Further studies on related species, including DFT calculations, have been also reported, drawing similar conclusions.⁽⁷⁵⁾



Scheme 4 The epoxidation mechanism in seven-coordinated Mo bisperoxo compounds.

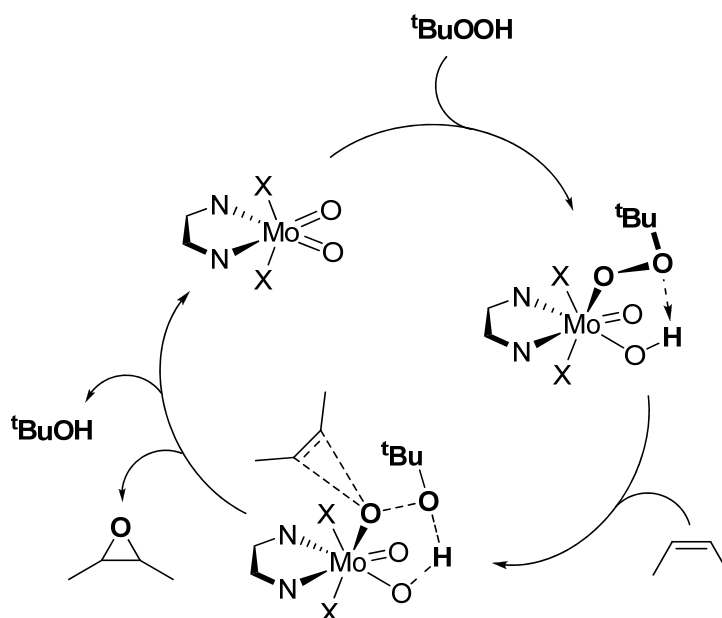
MoO₂X₂L₂ species

The first studies on the oxidation mechanism of dioxomolybdenum (VI) species were reported in 1983 by Mimoun *et al.* (Scheme 5).⁽⁷²⁾ In their study, the authors compared the results obtained with different oxidants such as H₂O₂, Ph₃COOH and ^tBuOOH. The results, including ¹⁸O labelling, highlighted the difference between ^tBuOOH and Ph₃COOH as oxidants, regarding the former a much preferred choice of oxidant. In agreement with Sharpless' studies, the proposed mechanism ruled out the formation of a peroxy-intermediate, but still favoured the formation of a cyclic intermediate containing the olefin and the coordinated alkylperoxide.



Scheme 5 Proposed olefin epoxidation mechanism catalysed by $t\text{BuOOH}$.

In 2002, Kühn *et al.* presented a detailed study on $\text{MoO}_2\text{X}_2\text{L}$ species (L = octahedral bipyridine and bipyrimidine), including DFT calculations for the epoxidation mechanism with these complexes.⁽⁷⁶⁾ This mechanism (Scheme 6) closely resembles that proposed by Thiel, ruling out the formation of the “pseudocycle” proposed by Mimoun.



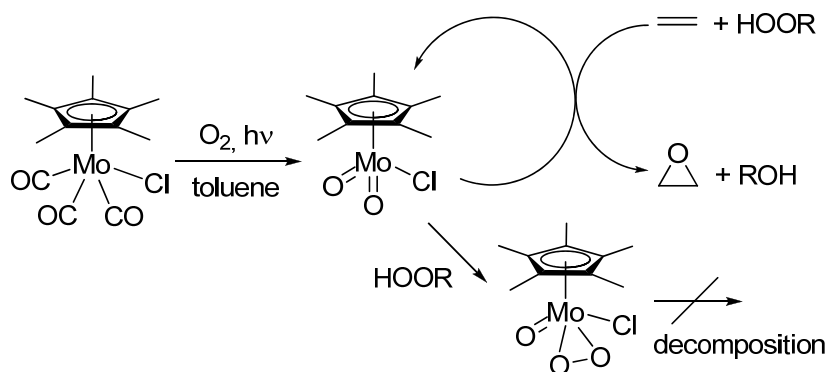
Scheme 6 The epoxidation mechanism for $\text{MoO}_2\text{X}_2\text{L}_2$ complexes (X = Halogen, L_2 = bidentate N-donor ligand, as proposed by Kühn *et al.*

7.3.2 Cyclopentadienyl derivatives. Catalytic activity of dioxo and oxo-peroxo species

Unlike other related oxides, the olefin mechanism catalysed by CpMo oxides has not been studied in detail. In the case of the well studied MTO, peroxy derivatives have been shown to be the active catalysts and metal attached η^2 -peroxy groups react with olefins already when applied stoichiometrically.^(67, 69, 77, 78)

In 1991, Trost and Bergman studied the epoxidation reaction catalysed by $(\text{Cp}^*)\text{MoO}_2\text{Cl}$.⁽⁷⁹⁾ In this system, the dioxo species was found to be primarily active,

whereas the oxo-peroxo derivative decomposes explosively; hence, this species was considered responsible for the loss of activity of the catalyst (see Scheme 7 below). Compounds of formula $Cp^*Mo(CO)_3R$ and their oxidation products have not yet been examined in comparable detail, particularly with respect to mechanistic implications, and no active species beyond the Mo(VI)-dioxo species has been found or proposed to date.(48, 80) However, catalytic results show that their activity is considerable and, in contrast to MTO, they are both easier to derivatise and immobilise.(9, 29, 44, 45, 49, 53, 57-59, 81-84)



Scheme 7 Proposed epoxidation mechanism for $Cp^*Mo(CO)_3Cl$ (from (79)).

8. Kinetic Studies on the Oxidation of η^5 -Cyclopentadienyl Methyl Tricarbonyl Molybdenum(II) and the Use of its Oxidation Products as Olefin Epoxidation Catalysts

In this chapter, a detailed examination of the reaction mechanism of $\text{CpMo}(\text{CO})_3\text{R}$ -based olefin epoxidation with TBHP as the oxidising agent is presented, based on kinetic experiments. It involves a comprehensive investigation of the system starting with 1) the tricarbonyl, 2) the dioxo, and 3) the oxo peroxy compounds after adding excess TBHP in the presence and in absence of olefin. Detailed kinetic studies have also been carried out on the activity of an oxo peroxy derived active species with respect to olefin epoxidation with TBHP.

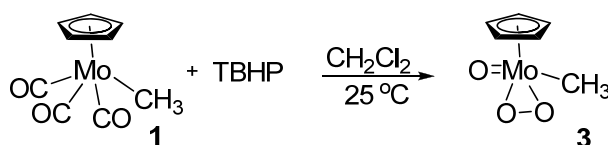
8.1 Abstract

The oxidation of $\eta^5\text{-CpMo}(\text{CO})_3\text{CH}_3$ (**1**) with excess *tert*-butylhydroperoxide (TBHP) initially yields the dioxo derivative $\eta^5\text{-CpMoO}_2\text{CH}_3$ (**2**), which further reacts with TBHP forming $\eta^5\text{-CpMoO}(\text{O}_2)\text{CH}_3$ (**3**). The solid state structure of **3** has been determined by single crystal X-ray diffraction. Detailed kinetic studies have been carried out on the oxidation of **1** with TBHP as an oxidising agent and on the catalytic activities of the resulting oxidation products, **2** and **3** in olefin epoxidation. In the absence of oxidant, none of the molybdenum species is able to transfer an O-atom to an olefin. However, both Mo(VI) species act as catalysts for the epoxidation of olefins with TBHP through the formation of active intermediates. It has been found that compound **3** reacts with excess TBHP to give an active intermediate, which exists in equilibrium with the catalyst precursor **3** with a K_{eq} close to one. This intermediate is slowly formed in a reversible

initial step. It reacts rapidly with an olefin, while it decomposes in absence of olefin. Furthermore, the kinetic results indicate the formation of another active intermediate, originating from **2** that is 3-5 times more active than the active intermediate formed from **3** in epoxidation catalysis. A mechanistic scheme is proposed, based on the kinetic results.

8.2 Results and discussion

The title compound $\text{CpMo}(\text{CO})_3\text{CH}_3$ (**1**) was synthesised and purified using a slightly modified literature method.⁽³¹⁾ When the carbonyl compound is treated with a TBHP excess of at least 5 equivalents in dichloromethane, the Mo(VI)oxo-peroxo complex (**3**) is formed and can be isolated in good yields.



Scheme 8 Synthesis of the Mo(VI) oxo-peroxo compound (**3**).

Compound **3** was characterised by UV-Vis, IR and NMR spectroscopy (see experimental section), and the solid state molecular structure was determined by single crystal X-ray diffraction (see Figure 10 and Appendix A).

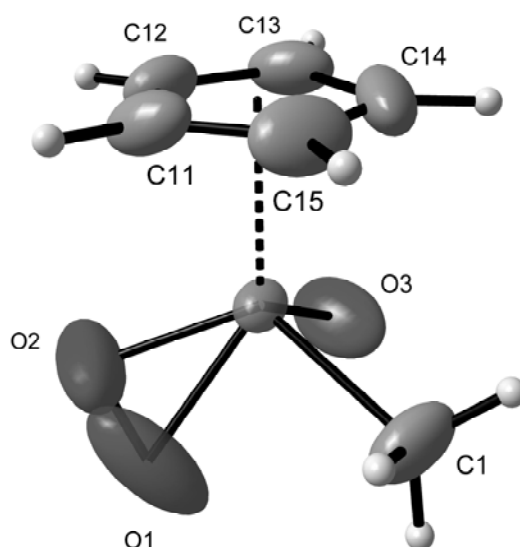


Figure 10 ORTEP style plot of compound **3** in the solid state. Thermal ellipsoids are drawn at the 50% probability level. Details of the single crystal X-ray diffraction studies are given in the supporting information.

The single crystal X-ray crystallographic analysis of compound **3** reveals a slightly distorted “three-legged piano stool” conformation, in which the midpoint of the peroxo ligand is one of the legs of the piano stool. Two other structurally characterised Mo oxo-peroxo compounds and three W(VI)-oxoperoxo compounds of composition $\text{Cp}'\text{WO}(\text{O}_2)(\text{CH}_2\text{SiMe}_3)$ and $\text{Cp}^*\text{WO}(\text{O}_2)\text{Cl}$ have a similar structural arrangement.(48, 52, 79)

8.2.1 Kinetic studies

Reaction of $\text{CpMo}(\text{CO})_3\text{CH}_3$ (**1**) with TBHP

The reaction of **1** with TBHP was carried out at room temperature and followed by NMR (in dry CDCl_3) and UV-vis (in dry CH_2Cl_2) spectroscopy, respectively. The changes in the chemical shifts of the Cp and/or the methyl protons in the NMR spectra are particularly informative. When 0.06 mmol of **1** and 10 equivalents of TBHP are mixed in 0.5 ml CDCl_3 , the reaction starts immediately. The Cp signal of the carbonyl compound at 5.27 ppm decreases with time and a new signal at 6.33 ppm appears. The area of this new signal reaches a maximum after 15 min whereas the carbonyl compound peak is reduced to around 60% of its original size. The reduction of the signal at 6.33 ppm is associated with the build up of a new signal at 6.29 ppm. After 2 hours, the Cp signal of the carbonyl compound and the Cp signal at 6.33 ppm disappear completely and only the signal at 6.29 ppm remains. The signal intensity-time curves are shown in Figure 11A. The ^{95}Mo NMR examination shows similar results. After 2 h, the ^{95}Mo signal of **1** at -1424 ppm vanishes completely, and a new peak at -609 ppm, which has been assigned to the complex **3** is the only one observed.(9) An intermediate forming and disappearing in the same time frame as for the ^1H -NMR experiments is observed at -346 ppm.

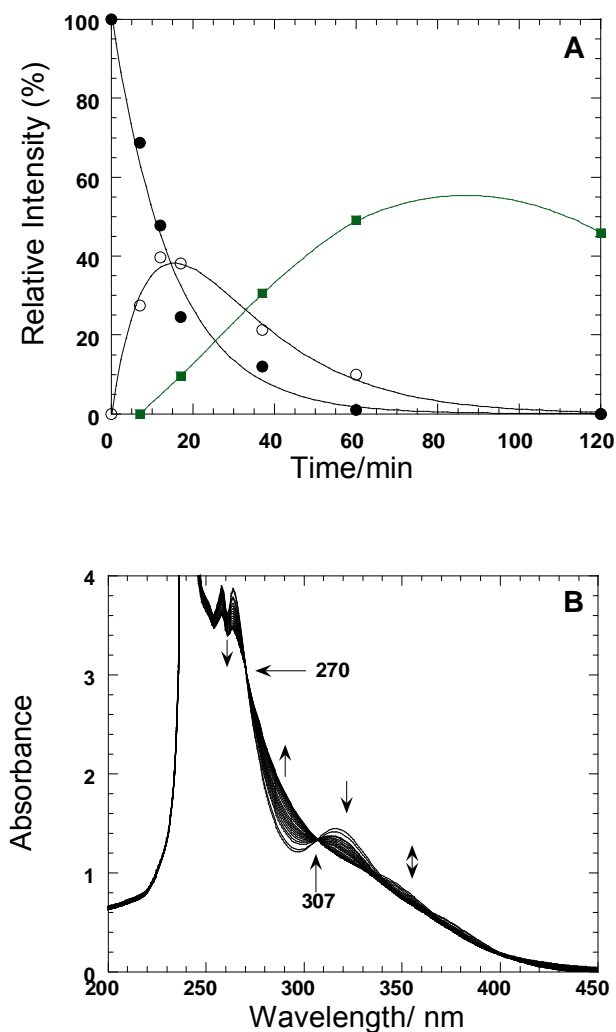
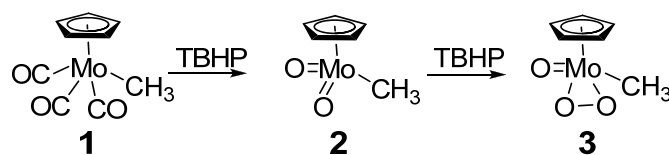


Figure 11 (A) The changes in the relative peak intensities with time of **1** (●) (at $\delta = 5.27$ ppm), and its products **2** (○) (at $\delta = 6.33$ ppm) and **3** (■) (at $\delta = 6.29$ ppm) during the reaction of **1** (0.06 mmol) with 10 eq. TBHP in CDCl_3 at 20 °C. (B) UV-vis spectral changes (at 6 min intervals for the first hour and then every 10 min) for the reaction of **1** (0.33 mM) with TBHP (10 eq.) in CH_2Cl_2 at 20 °C.

An experiment was designed to examine the intermediate compound (at 6.33 ppm), which is usually formed shortly after mixing TBHP with the carbonyl compound and later disappears. The above reaction was repeated and quenched after 15 min by adding MnO_2 . The filtrate was evaporated to dryness and extracted with diethyl ether to give a yellow solid. The product was analysed by ^1H and ^{95}Mo NMR spectroscopy. The ^1H NMR spectrum shows a signal at 6.33 ppm and a signal at 1.45 ppm with 5:3 relative intensities, respectively. The ^{95}Mo NMR shows one signal at -346 ppm. A similar reaction profile can be obtained if the reaction is carried out in C_6D_6 under the same conditions and the chemical shifts match with the NMR data for the dioxo-Mo(VI) compound, $\text{CpMoO}_2\text{CH}_3$ (**2**).⁽⁸⁰⁾ These results suggest that the formation of **3** from the

reaction of the carbonyl compound **1** with TBHP proceeds via compound **2**, as shown in Scheme 9.



Scheme 9 Proposed reaction pathway for the oxidation of compound **1**.

In the NMR experiments described above, the yield of compound **3** is less than 60% (with respect to **1**), due to a side reaction which forms an insoluble precipitate (hence explaining the decrease in the Cp signal's intensity observed in the NMR experiments). This was isolated as a blue solid, containing 42.3 % of Mo, 18.7 % of C and 2.9 % of H. Further characterisation attempts were unsuccessful due to its insolubility in all common solvents. The blue solid can also not be redissolved by adding excess of TBHP. It has been further tested as a catalyst in olefin epoxidation, and was found to be completely inactive, even after prolonged reaction times. The yield of compound **3** can be increased by increasing the TBHP:**1** ratio, suggesting that the major reaction pathway, which leads to the relatively stable product **3** is favoured. The side reaction pathway is totally suppressed with the addition of a substrate in the catalytic reaction. The reaction progress was also followed by UV-Vis spectroscopy with different concentrations and catalyst/TBHP ratios in CH_2Cl_2 . **1** has strong absorptions at $\lambda_{\text{max}} = 256, 267$ and 316 nm, and a shoulder peak at $\lambda_{\text{max}} \sim 370$ nm. When the carbonyl complex (0.33 mM) is treated with a 10-fold excess of TBHP at room temperature, the absorbance at 316 nm decreases with time and the absorbance in the range 207 – 270 nm increases to give two clear isosbestic points at 307 and 270 nm (Figure 11B). These changes in absorbance are due to the formation of complex **2**. The reaction of **2** with TBHP proceeds leading to an additional absorbance decrease in the range 307 - 335 nm and a slight increase in the absorbance in the range 335 - 400 nm, due to the formation of compound **3**. However, the isosbestic points due to this change are not all entirely clear, a possible explanation, based on further experimental evidence is given in the next subchapter. It is noteworthy, however, that under UV experimental conditions no precipitate was observed, possibly due to the higher TBHP excess that may decrease catalyst decomposition or side reactions.

The intensity-time curves and the changes in the UV-absorbance with time can be used to determine the rate constants for the oxidation of the carbonyl compound **1** with TBHP to yield **2** and the formation of **3** from compound **2**. In the presence of excess TBHP, the reactions follow pseudo-first-order kinetics, and the decrease in the intensity of the signal at 5.27 ppm (Cp protons of the carbonyl compound) with time fits to a first-order exponential decay equation ($I_t = I_\infty + (I_0 - I_\infty) \exp(-k_\psi t)$). The value of the observed-first-order rate constant was obtained from this fitting to be $k_\psi = (1.12 \pm 0.15) \times 10^{-3} \text{ s}^{-1}$. This indicates that the reaction is first-order with respect to the concentration of **1**. The build up and the decay of the signal intensity at 6.33 ppm (Cp protons of **2**) was fitted to a biexponential (build up and decay) equation to determine the pseudo-first-order constants for the formation of **2**, ($k_f = (1.25 \pm 0.35) \times 10^{-3} \text{ s}^{-1}$) and for its reaction with TBHP ($k_r = (8.5 \pm 0.3) \times 10^{-4} \text{ s}^{-1}$). The rate constant k_f is also valid for the reaction of the carbonyl compound with TBHP and is in accordance with the value obtained above from the time-dependent decrease of the carbonyl signal. These kinetic results confirm the observations made, when **2** is prepared from **1** in the presence of excess TBHP. The oxoperoxo compound **3** starts appearing immediately after **2** is formed because the two rate constants for the formation of **2** and its reaction with TBHP to produce **3** are comparable.

Previous studies on CpMo(CO)₃Cl-type compounds indicate that the Mo-dioxo moiety is rapidly formed in the case of the Cl containing compounds but reacts more slowly with additional TBHP to yield the final Mo-oxoperoxo product. (52, 46, 48, 80, 79) From the results obtained here, it appears that the presence of a methyl group instead of a chloro ligand does not strongly affect the initial oxidation rate from Mo(II) to Mo(VI). However, the presence of a methyl group seems to significantly enhance the displacement rate of the oxo with the peroxo group on the Mo(VI) centre. This difference in behaviour of the Mo(VI) species between the Cl and the CH₃ derivative seems to become more pronounced in the further reaction between compound **3** and TBHP, where compound **3** can be transformed to an active species (**I**, see Scheme 11), while the Cl derivative has been reported not to form an active catalyst in the presence of TBHP. (52, 44, 79)

Reaction of CpMoO(O₂)CH₃ (3**) with TBHP**

When **3** reacts with a large excess of TBHP (>100 eq) in the absence of an olefin, a slight change of its UV-vis spectra occurs. After mixing a 0.3 mM solution of **3** in CH₂Cl₂ (total volume 3 mL) with 0.15 mmol TBHP at room temperature, the absorbance at 335

nm decreases exponentially with time and levels off after ca. 20 minutes. By adding more TBHP, the absorbance decreases further but never becomes zero even with very high TBHP excess (~1500 eq), as shown in Figure 12. This must be due to the formation of an intermediate (**I**) which exists in equilibrium with **3**.



The equilibrium constant and the extinction coefficient of the intermediate were determined from the variation of the equilibrium absorbance with [TBHP] using Equation. 1. This equation is derived from the equilibrium expression and the mass-balance equation ($[\text{Mo}]_{\text{T}} = [\mathbf{3}] + [\text{I}]$). A complete derivation of Equation 1 is shown in Appendix A.

$$\frac{\text{Abs}_{\text{eq}}}{[\text{Mo}]_{\text{T}}} = \varepsilon_{\text{I}} + \frac{(\varepsilon_{\text{p}} - \varepsilon_{\text{I}})}{1 + K_{\text{eq}}[\text{TBHP}]} \quad (1)$$

where Abs_{eq} is the absorbance at equilibrium, $[\text{Mo}]_{\text{T}}$ is the initial concentration of **3**, ε_{I} and ε_{p} are the extinction coefficients of the intermediate and **3**, respectively.

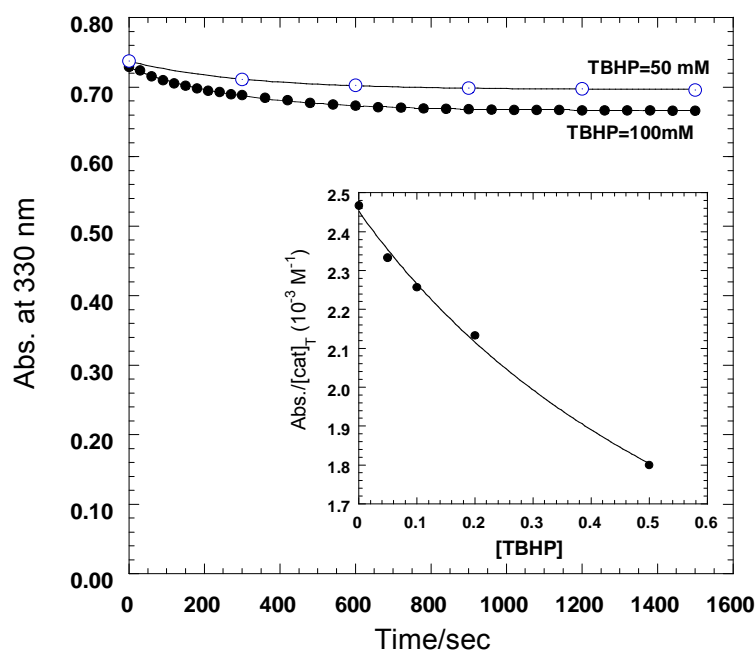


Figure 12 Changes in absorbance with time at 330 nm for the reaction of **3** with TBHP in CH_2Cl_2 at 20 °C. The inset shows a plot of $\text{Abs}_{\text{eq}}/[\text{Mo}]_{\text{T}}$ against [TBHP], the solid line represents the calculated values based on Eq. 1 with $K_{\text{eq}} = 1.23$, $\varepsilon_{\text{I}} = 748 \text{ M}^{-1}\text{cm}^{-1}$ and $\varepsilon_{\text{p}} = 2460 \text{ M}^{-1}\text{cm}^{-1}$.

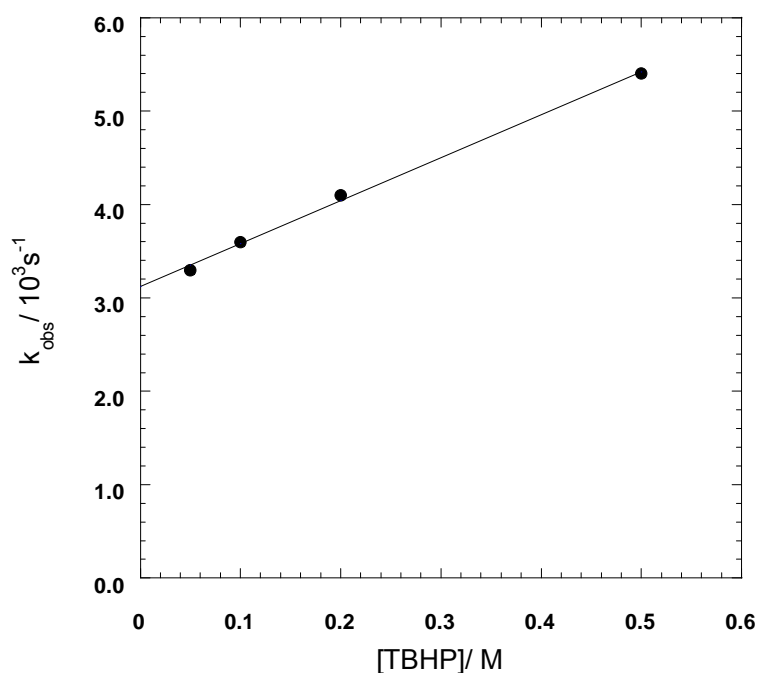


Figure 13 A plot of the observed-first-order rate constant (k_{obs}) against [TBHP] for the reaction of **3** (0.3 mM) with TBHP in CH_2Cl_2 at 20 °C.

The absorbance-time curves in Figure 12 are exponential, and fit to a 1st-order exponential equation, $A_t = A_\infty + (A_0 - A_\infty) \exp(-k_\psi t)$, to determine the values of k_ψ at each [TBHP]. The observed-first-order rate constants (k_ψ) vary linearly with [TBHP] in a relatively large intercept (Figure 13).

Since the reaction between TBHP and **3** is reversible, the observed-rate constant is the sum of the forward and the reverse rate constant. With TBHP being present in large excess over the catalyst, the observed-rate constant can be expressed as:

$$k_\psi = k_p[\text{TBHP}] + k_{-p} \quad (2)$$

Therefore, the intercept of the straight line represents the value of the reverse rate constant ($k_{-p} = 3.2 \cdot 10^{-3} \pm 2 \cdot 10^{-4} \text{ s}^{-1}$), and the slope expresses the forward rate constant ($k_p = 4.7 \cdot 10^{-3} \pm 3 \cdot 10^{-4} \text{ M}^{-1} \text{ s}^{-1}$). The value of the equilibrium constant ($K_{\text{eq}} = 1.47 \pm 0.36$) calculated from these kinetic data agrees with the value ($K_{\text{eq}} = 1.23$) obtained from Equation 1 within the experimental error range of these measurements. After the equilibrium is established, a slow decrease in the absorbance continues with time, probably due to the decomposition of the catalytic system, in the absence of olefin and increases with the TBHP concentration and the solvent polarity. (59)

8.2.2 Catalytic epoxidation

Epoxidations starting from $\text{CpMo}(\text{CO})_3\text{CH}_3$ (**1**)

Since the olefin does not react with TBHP without the catalyst being present, no corrections were needed for the uncatalysed process. In the presence of an olefin, the epoxide is formed and the conversion to the epoxide proceeds to completion. Figure 14 shows the time resolved formation of cyclooctene oxide in an NMR experiment initially started with **1** (0.05 mmol), TBHP (0.6 mmol) and cyclooctene (0.44 mmol) in CDCl_3 at 20 °C. When TBHP was added last to a mixture of the catalyst and the olefin, the epoxide appears slowly in the first 10 minutes of the reaction. The rate then increases and becomes linear in the next 20 minutes, and the build-up continues exponentially.

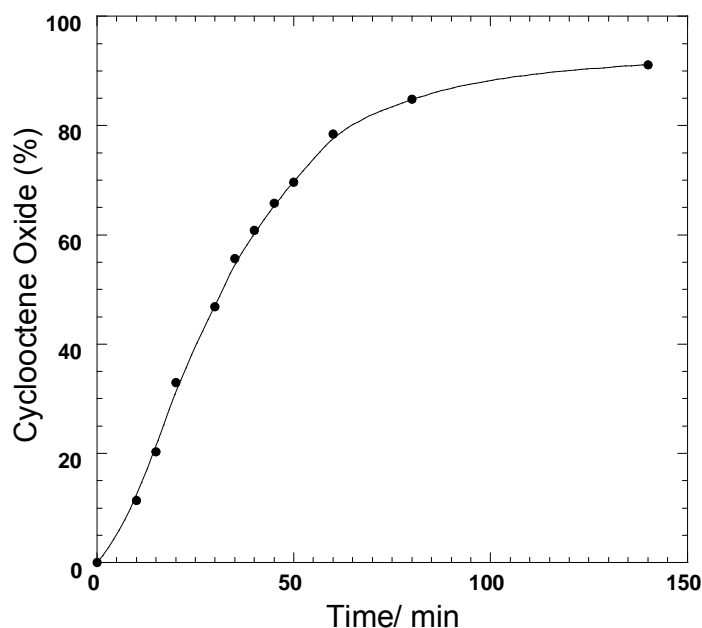


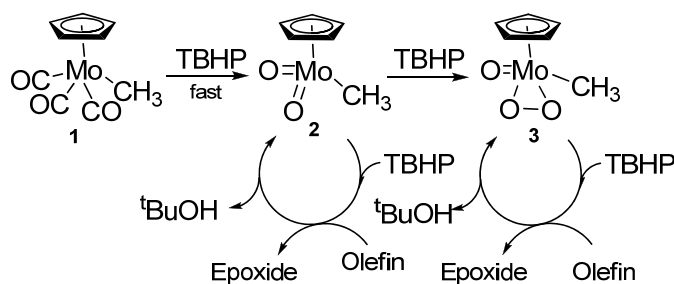
Figure 14 Yield of cyclooctene oxide against time. The reaction was carried out using 0.44 mmol cyclooctene, 0.6 mmol TBHP and 0.05 mmol **1** in CDCl_3 at 20 °C.

This kinetic behaviour is typical for a catalytic reaction where the catalyst precursor initially reacts with the oxidant to produce the active species in rates slower or similar to the rate of the reaction of the active species with the substrate. In addition, the reaction rate in the later stages of the reaction becomes slower, indicating that the catalyst is (at least) partially deactivated. It has been previously reported that the accumulation of *t*-BuOH as a byproduct deactivates the catalyst, most likely by adduct formation.^(9, 29, 48, 49, 58, 59, 80-82) In this catalytic system, **1** reacts with TBHP to form **2** and **3**. One

or both of them could be the active species, directly epoxidising the olefin or acting as catalysts to activate TBHP toward epoxidation. To get further insight on the catalytic cycle, **3** was isolated and its activity tested with different substrates (cyclooctene, β -methylstyrene and β -methoxystyrene).

In the absence of TBHP, both Mo(VI) species are inactive toward the epoxidation of cyclooctene and β -methoxystyrene at room temperature. However, when excess TBHP is added, the catalytic reaction proceeds. The epoxidation of cyclooctene and β -methylstyrene leads to the corresponding epoxides only, whereas the oxidation of β -methoxystyrene produces benzaldehyde. Similar behaviour was observed for the oxidation of β -methoxystyrene with Re(VII)-peroxo species as a catalyst. The reaction initially produces the epoxide, which is not stable due to the electron donating ability of the methoxy group, and undergoes C-C bond cleavage leading to benzaldehyde as the final product.⁽⁶⁷⁾

A general pathway (Scheme 10) for this catalytic reaction can thus be proposed, involving three Mo species: the carbonyl (**1**), the dioxo (**2**), and the oxo-peroxo (**3**) complexes. Kinetically, it is possible to investigate the proposed pathways by studying each species separately.

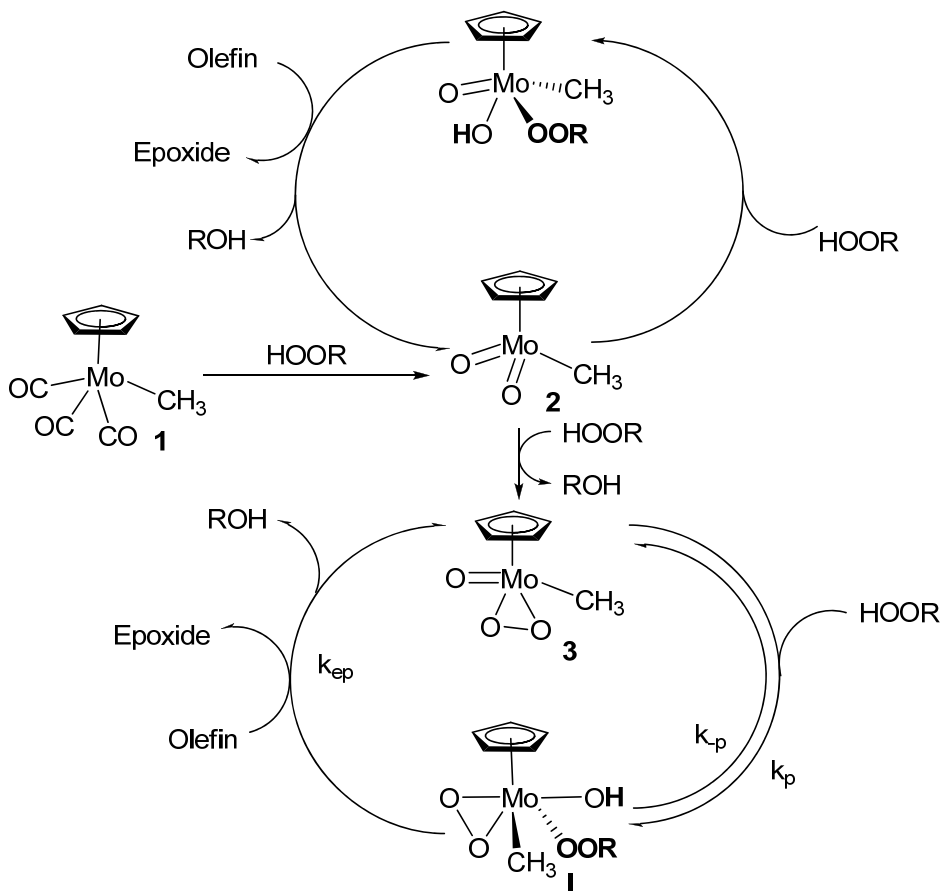


Scheme 10 General reaction scheme for the oxidation of **1** by TBHP and the epoxidation activity of the oxidation products, **2** and **3**.

Epoxidations utilising $\text{CpMoO(O)}_2\text{CH}_3$ (**3**)

Compound **3** was found to catalyse the epoxidation of cyclooctene and styrene with TBHP as oxidising agent at room temperature. Figure 15 shows the change in the absorbance with time at 265 nm due to the epoxidation of β -methoxystyrene by the TBHP/**3** system. In the absence of TBHP, the olefin is not oxidised, nor does it react in any form with **3** (when **3** was mixed with cyclooctene or β -methoxystyrene no changes were observed by NMR and UV spectroscopy). However, as discussed above, UV experiments show that **3** reacts with TBHP in the absence of olefin. This suggests that

the epoxidation of the olefin is carried out by an active intermediate **I**, which is formed by the reaction of **3** with TBHP (Scheme 11).



Scheme 11 General mechanism for the oxidation of CpMo(CO)₃CH₃ (1) and catalytic activity of the resulting complexes in the presence of TBHP.

Although both homolytic and heterolytic activation of peroxides by metal catalysts is possible, activation of TBHP by a homolytic cleavage of the O-O bond (which would generate reactive radicals, such as RO· or HO·) does not occur due to the reaction insensitivity against oxygen. Also, the olefin reactivity, which was found to increase with the olefin nucleophilicity rather than with the radical stability, does not support a radical mechanism. Furthermore, radical mechanisms have not been proposed by the previous studies on epoxidations catalysed by similar Mo compounds.^(79, 85, 74, 75, 86, 72) Therefore, it appears reasonable to assume that the reactive intermediate (**I**), in equilibrium with the catalyst, transfers an O-atom to the olefin to form the epoxide and regenerate the catalyst (Scheme 11).

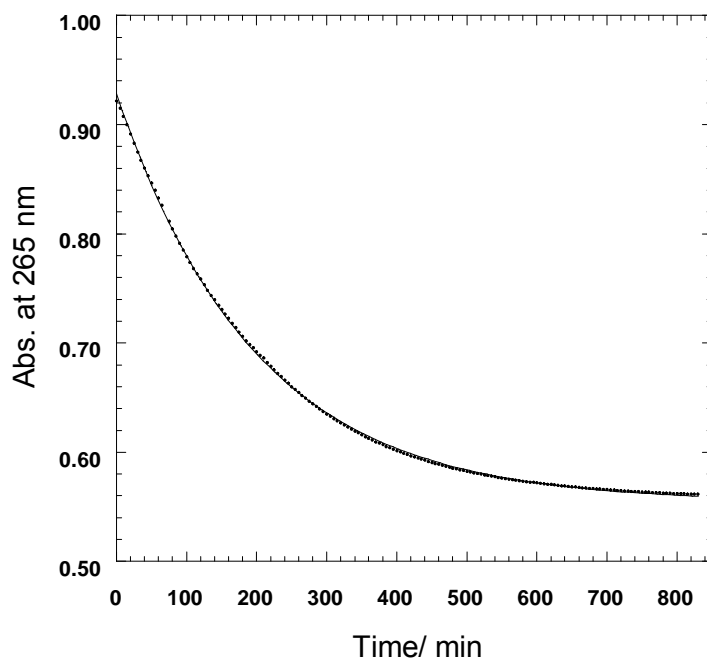


Figure 15 The absorbance-time curve at 265 nm for the oxidation of β -methoxystyrene (0.1 mM) with TBHP (10 mM) catalysed by **3** (0.4 mM) in CH_2Cl_2 at 20 °C.

During the catalytic reaction, the concentration of **I** can be defined by either a steady-state approximation or a pre-equilibrium condition. The epoxidation rate according to Scheme 4 is expressed by Equation 3:

$$\text{rate} = \frac{-d[\text{olefin}]}{dt} = k_{\text{ep}}[\text{olefin}][\text{I}] \quad (3)$$

If the rate equation is derived by means of a steady-state approximation for **I** with the mass balance expression, $[\text{Mo}]_{\text{T}} = [\text{3}] + [\text{I}]$, the rate of the reaction can be written as follows^{ix}:

$$\text{rate} = \frac{k_{\text{ep}}k_{\text{p}}[\text{olefin}][\text{TBHP}][\text{Mo}]_{\text{T}}}{k_{\text{-p}} + k_{\text{p}}[\text{TBHP}] + k_{\text{ep}}[\text{olefin}]} \quad (4)$$

The kinetics of the epoxidation of β -methoxystyrene with TBHP catalysed by **3** were investigated by following the absorbance change due to the consumption of β -methoxystyrene and the formation of the product(s) in the region 260-270 nm. Kinetic

^{ix} Derivation for this equation is included in the Appendix.

measurements were carried out with a constant concentration of β -methoxystyrene of 0.1 mM and a constant [TBHP] of 10 mM. The concentration of **3** was varied in the range 0.1 - 0.5 mM. Reaction mixtures were prepared in a spectrophotometric cell, the last added reagent being TBHP. The initial rates (i.r.) were calculated from the first 5% of the curves by using Equation 5.

$$\text{initial rate} = (1/b\Delta\varepsilon_\lambda) * \Delta\text{Abs}_i / \Delta t \quad (5)$$

where b is the optical path length and $\Delta\varepsilon_\lambda$ is the total change in the molar absorptivity at λ , and ΔAbs_i is the initial change in the absorbance.

The variation of the initial rate with the catalyst concentration is presented in Figure 16 and shows a linear dependence on $[\text{Mo}]_T$ as expected from Equation 4. Using the determined values of k_p and k_{-p} ($0.0047 \text{ M}^{-1}\text{s}^{-1}$ and 0.0032 s^{-1} , respectively) and the initial concentrations of β -methoxystyrene and TBHP, the value of k_{ep} ($\sim 16 \text{ M}^{-1}\text{s}^{-1}$) was determined from the slope.

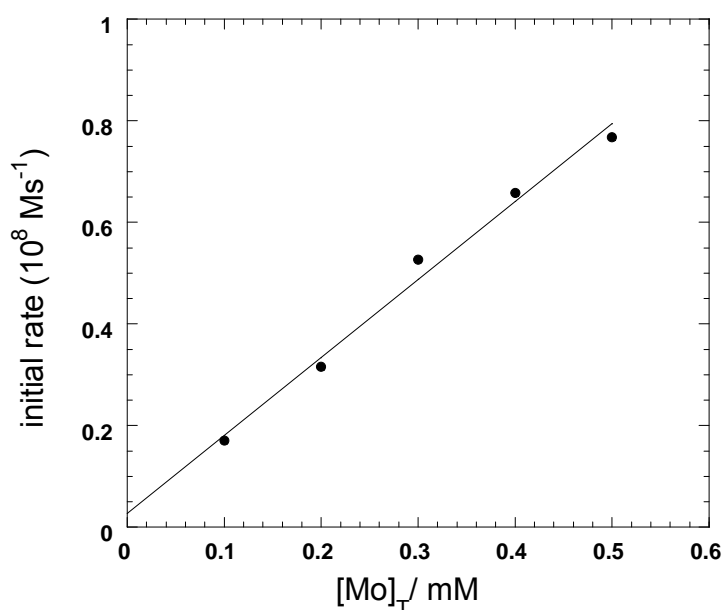


Figure 16 Linear variation of the oxidation initial rate of β -methoxystyrene against $[\text{Mo}]_T$ in CH_2Cl_2 at 20 °C. [TBHP] = 10 mM, [β -methoxystyrene] = 0.1 mM.

Kinetic measurements were also carried out with a constant $[\text{Mo}]_T$ (**3**) of 0.4 mM and a constant concentration of β -methoxystyrene of 0.1 mM, varying the concentration of TBHP in the range 5-500 mM. A low concentration of β -methoxystyrene was used to

allow direct measurement of the absorbance change, since β -methoxystyrene has a very strong absorptivity in the UV region ($\epsilon_{265} \sim 2 \times 10^4 \text{ M}^{-1} \text{ cm}^{-1}$). A plot of the initial rate against [TBHP] is shown in Figure 16. At low [TBHP] ($\leq 20 \text{ mM}$), the initial rate varies linearly and is first-order with respect to [TBHP]. The order decreases with increasing [TBHP]. This kinetic behaviour agrees with the rate law derived based on a steady-state approximation (Equation 4). Fitting the data in Figure 17 to Equation 4 using the known values of k_p ($= 0.0047 \text{ M}^{-1} \text{ s}^{-1}$) and k_{-p} ($= 0.0032 \text{ s}^{-1}$), leads to the epoxidation rate constant ($k_{ep} = 18.3 \pm 3.8 \text{ M}^{-1} \text{ s}^{-1}$). This value of k_{ep} is close to the value estimated above from varying the concentration of the catalyst.

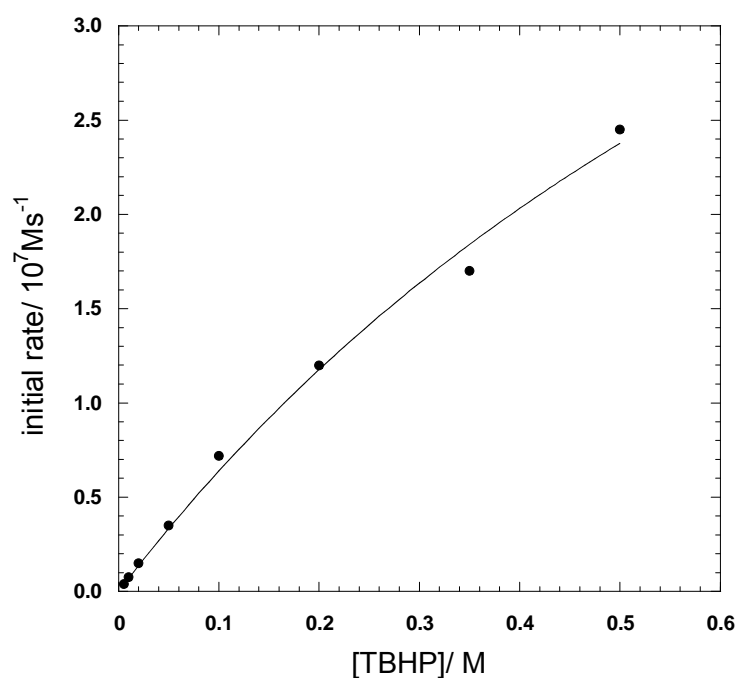


Figure 17 Variation of the oxidation initial rate of β -methoxystyrene (0.1 mM) with TBHP catalysed by **3** (0.4 mM) in CH_2Cl_2 at 20 °C. The data was fitted to Eq. 4 with the values of k_p ($= 0.0047 \text{ M}^{-1} \text{ s}^{-1}$) and k_{-p} ($= 0.0032 \text{ s}^{-1}$) being held constant, and k_{ep} ($= 18.3 \pm 3.8 \text{ M}^{-1} \text{ s}^{-1}$) being varied.

The reactions of *trans*- β -methylstyrene (UV method) and cyclooctene (NMR method) were studied similarly, and the values of k_{ep} for their epoxidation with TBHP catalysed by **3** are 0.5 and 1.3 $\text{M}^{-1} \text{ s}^{-1}$, respectively. These results show that the epoxidation rate constant (k_{ep}) increases with the olefin nucleophilicity:



β -methoxystyrene is the most nucleophilic olefin among the examined substrates (due to the presence of an OCH_3 group), and it is ca. 15 times more reactive than cyclooctene.(67-69, 76, 87-89)

Additionally, the epoxidation reaction is stereoselective. When *trans*- β -methylstyrene is oxidised, only the *trans* epoxide is obtained. Epoxidations that occur by an external attack of the nucleophilic olefin onto the electrophilic oxygen of the M-alkylperoxo (or M-peroxo) group by a concerted O-transfer step are usually stereoselective, and coordination of the olefin to the metal centre prior to the oxygen transfer step is less likely happening.(53, 57, 59)

Epoxidation catalysed by $\text{CpMoO}_2\text{CH}_3$ (**2**)

The profile of the reaction between **1** (0.05 M), cyclooctene (0.44 M) and TBHP (0.6 M) in CDCl_3 at 20 °C (Figure 4) indicates the presence of at least two catalytic systems formed from the initial Mo(II) precursor. Each catalyst activates TBHP (through an active intermediate) for the epoxidation of an olefin (as shown in Scheme 3). It was not possible to study the catalytic activity of **2** separately, because in addition to the epoxidation reaction, **2** also reacts with TBHP to form **3**, which also catalyses the epoxidation of olefin as shown above. However, the values of the rate constants for the reactions of **1** with TBHP to yield **2** and **3** were determined in the absence of the olefin under the same conditions and the rate constants for the epoxidation of cyclooctene by the TBHP / **3** catalytic system (k_p , k_p and k_{ep} in Scheme 4) were determined separately. Therefore, it is possible to estimate the relative rates of the epoxidation reactions by **2** from reactions initially started with the precursor **1** (see Appendix A). An initial rate method with the olefin existing in much higher concentration than the catalyst and TBHP was used. The initial rates were calculated from the initial 2-5% conversion of the olefin. Under these conditions, **3** is not involved, and the rate constant for the epoxidation of an olefin by **2**/TBHP was estimated. For cyclooctene, the epoxidation rate constant for reactions catalysed by compound **2** are 3-5 times higher than those catalysed by compound **3** under the same conditions, which might originate from the slightly different structure of the intermediates. This shows that **2** is more active than **3**. However, when TBHP is present in large excess over the olefin and the catalyst formation of **3** from **2** occurs at the beginning of the catalytic reaction, most of the epoxidation is carried out by the active species formed from **3** rather than that from **2**.

8.3 Conclusions

Based on detailed kinetic studies and experimental evidences, the mechanism shown in Scheme 11 has been proposed for the catalytic olefin epoxidation promoted by the precursor $\text{CpMo}(\text{CO})_3\text{CH}_3$ (**1**). In the presence of excess alkyl hydroperoxide (TBHP), $\text{CpMo}(\text{O})_2\text{CH}_3$ (**2**) and $\text{CpMo}(\text{O})(\text{O}_2)\text{CH}_3$ (**3**) are formed. Whereas the isolated compound **3** is inactive for stoichiometric epoxidation of cyclooctene and styrenes, epoxidation with **3** does proceed in the presence of TBHP under formation of a reactive species **I**. The kinetic results of the variation of the reaction rate with the alkyl hydroperoxide are consistent with the formation of a σ -alkylperoxo intermediate species as has been postulated for other Mo(VI) based catalyst systems.(67-69, 76, 87-89) In the presence of excess olefin, the catalytic system is stable and the major pathway is the catalytic epoxidation reaction. As far as it can be concluded from the published literature, $\text{CpMo}(\text{CO})_3\text{CH}_3$ differs in several aspects from the previously examined $\text{CpMo}(\text{CO})_3\text{Cl}$ with respect to its reaction behaviour and applicability as catalyst. Work is currently undertaken in our laboratories to examine the apparently different catalytic behaviour of the Cl derivative in more detail.

Related alkyl derived compounds such as Mo and W cyclopentadienyl *ansa*-complexes, which display similar epoxidation capabilities, will be studied in the next chapter. The catalytic mechanism of this species is also being object of study, paying special attention the the similarities with the $\text{CpMo}(\text{CO})_3\text{CH}_3$ system.

9. *ansa* Compounds

Intramolecular coordination compounds are a most significant research topic in organometallic chemistry. Amongst them, *ansa* complexes have aroused special attention.(90, 91) In these compounds, a cyclopentadienyl fragment containing a chain-like substituent coordinates to the metal via both the Cp ring and the terminal fragment of the chain, forming a handle-like structure in the process (hence the name “*ansa*”). The terminal moiety can be either a donor species (phosphine, amine, etc.) or an alkyl, aryl and even another cyclopentadienyl fragment (see Figure 18).

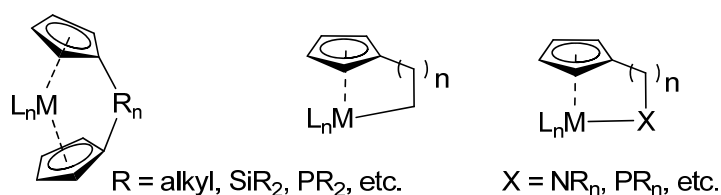


Figure 18 General structure of *ansa* coordinated compounds.

During the last decades, a vast number of *ansa* compounds have been reported.(92) They can be roughly divided between those that include either a heteroatom or a C coordinated to the metal via the *ansa* fragment. This chapter will summarise the most significant compounds of this family, paying special attention to those who display prominent catalytic activities.

9.1 Classification

As it has been mentioned above, the concept of *ansa* bridged compounds includes an enormous variety of organometallic species. Though the work presented herein deals with half-sandwich, η^5 -cyclopentadienyl- η^1 -alkyl compounds, it is interesting to highlight the most prominent species of this ever-growing class of complexes, including both bent metallocenes and heteroatomic bridged compounds.

9.1.1 *ansa* bridged bent metallocenes

Shortly after the discovery of ferrocene and the establishment of its sandwich structure with parallel rings, the first bis-cyclopentadienyl^x metal complexes with inclined angles to one another were synthesised. Amongst other properties, these compounds allowed the coordination of additional ligands to the metal.(93) During the last decades, a wealth of related complexes was reported. It was found that bent metallocenes (especially titanocenes and zirconocenes) are powerful catalytic species in olefin polymerisation; thus, they are regarded as a valid alternative to the well established, heterogeneous Ziegler-Natta catalysts.(94) The bent structures may allow the inclusion of a bridge between both cyclopentadienyl moieties. These *ansa* metallocenes have been profusely studied due to their potential applications in asymmetric olefin polymerisation catalysis.(95, 96) Moreover, these complexes can undergo ring opening polymerisation (ROP), forming the respective *poly(metallocenes)*, which are interesting novel materials.(97)

9.1.2 Heteroatomic “half-sandwich” *ansa* compounds. *Constrained geometry catalysts*

In parallel with their bent-metallocene counterparts, the so-called constrained geometry catalysts (CGC) have been widely studied in the last two decades due to their promising performances in copolymerisation reactions. Most of the available literature deals with Ti and Zr derivatives, which form heteroatomic bridges with a variety of species (see Figure 19). These systems - which are also applied in olefin polymerisation - are commonly synthesised from fulvene derivatives, forming structures of the type Cp-R₁-R₂ (where R₁ = C,Si, R₂ = N, P and R₂ is bound to the metal centre).(98) The properties of the bridge can be tuned depending on the nature of the members of the *ansa* fragment, further allowing the synthesis of highly selective catalysts. Other CGCs can be synthesised from amino substituted fulvene derivatives, allowing the insertion of vinylidene groups.(99)

Certain CpMo carbonyls have been also found to form heteroatomic *ansa* bridges with N-donor atoms. The lability of the Mo-N bond, however, promotes dimerisation

^x Apart from cyclopentadienyl, certain moieties such as indenyl and fluorenyl form bent metallocenes as well.

reactions.(100) Similar structures with cyclopentadienyl vanadium moieties have been recently reported.(101)

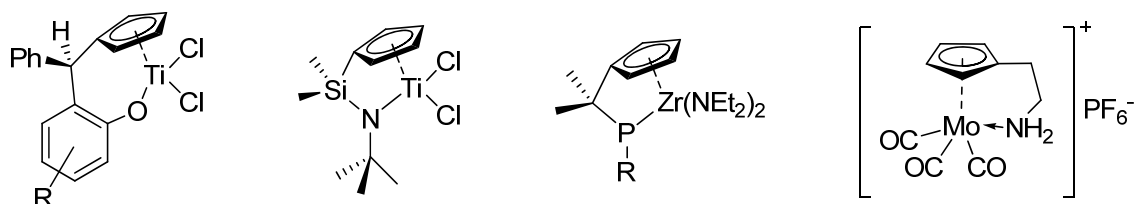
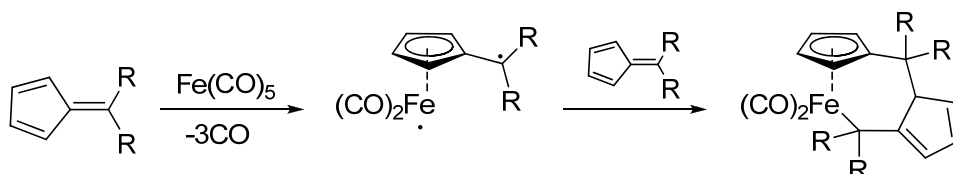


Figure 19 A selection of half sandwich heteroatomic *ansa* compounds.

9.1.3 M-C *ansa* compounds

To the best of our knowledge, Weiss *et al.* were the first to report a cyclopentadienyl *ansa* bridged complex from the reaction of iron carbonyl and pentafulvene.(102) Further studies by Weiss, Behrens *et al.* reported the synthesis of similar complexes with iron and ruthenium.(103-106) These compounds have been occasionally revisited, including reactions with difbenzofulvalene derivatives.(107)



Scheme 12 A possible reaction pathway to form an iron *ansa* carbonyl (from **(104)**).

The pioneering research of Eilbracht *et al.* with *spiro* ligands (108) as substitutes for the fulvene moiety generated a number of novel metallorganic $\eta^5\text{-}\eta^1$ σ M-C complexes, including molybdenum and tungsten derivatives. The next chapter will concentrate on this group of complexes, paying special attention to the latter compounds and highlighting its promising catalytic applications.

9.2 *ansa* compounds of Mo and W as oxidation catalysts

Following the research of Weiss and Behrens, Eilbracht *et al.* comprehensively studied the reactions of *spiro* compounds with different carbonyl compounds, including $\text{Ni}(\text{CO})_4$,

$\text{Fe}(\text{CO})_5$ and $\text{M}(\text{CO})_3(\text{CH}_3\text{CN})_3$ ($\text{M} = \text{Mo}, \text{W}$).⁽¹⁰⁹⁻¹²¹⁾ Amongst many other reactions, Eilbracht concentrated both on the synthesis of the bridged derivatives as well as on the ring cleavage or carbonyl insertion within the *ansa* bridge (see Figure 20).

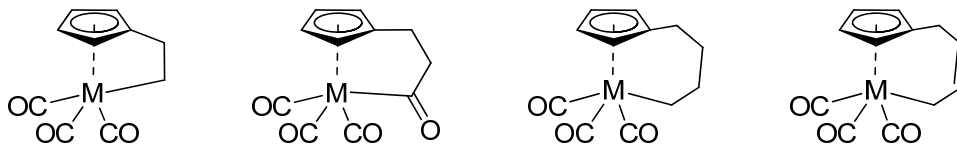


Figure 20 Selection of *ansa*-bridged compounds synthesised by Eilbracht *et al.*

The work of Eilbracht with Mo and W derivatives was revisited on few occasions, including studies with indenyl and fluorenyl derivatives. In this case, the metal centre can coordinate in both η^5 and η^6 fashions; the latter, however, do not form the expected insertion, *ansa* bridged products.^(122, 123)

10. Stable and Catalytically Active *ansa* Compounds With Cycloalkyl Moieties as Bridging Units

A plethora of catalyst systems based on Mo and W have been extensively studied and applied in asymmetric epoxidation catalysis, but have been found to give only moderate ee values at best.(14, 19, 124-133) These can be improved by performing the catalytic experiments at lower temperatures, leading in all cases to a significant loss of activity.(20, 75, 79) In the last years, CpM(CO)₃R compounds (M = Mo, W, R = halogen, alkyl) have been thoroughly examined in epoxidation catalysis. Amongst these, *ansa*-type complexes, which had first been described by Eilbracht *et al.* in the late 1970ies, have aroused attention due to their potential applications in the field of asymmetric catalysis.(53, 57, 84, 95, 96, 101, 109-112, 134-139)

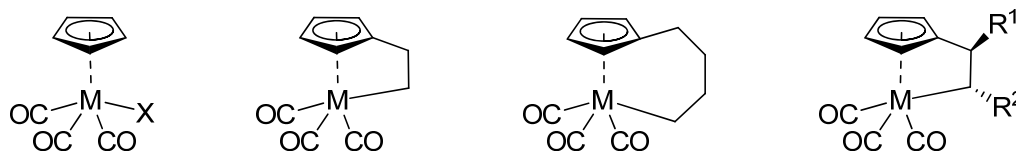


Figure 21 General catalysts of the type CpM(CO)₃R and *ansa*-CpM(CO)₃R. M = Mo, W; R = Cl, CH₃, CH₂CH₃; R¹ = Ph, CH₃, R² = H, CH₃.

Continuing the work of Zhao *et al.* carried out in our laboratories,(53, 57, 58) the next chapter will study the first representatives of a series of new molybdenum and tungsten *ansa* complexes with cycloalkyl moieties as exceptionally stable bridging units, as well as the use of these complexes as catalysts for olefin epoxidation reactions at room temperature. For the sake of comparison, a number of previously reported complexes will be also studied and their catalytic properties tested.

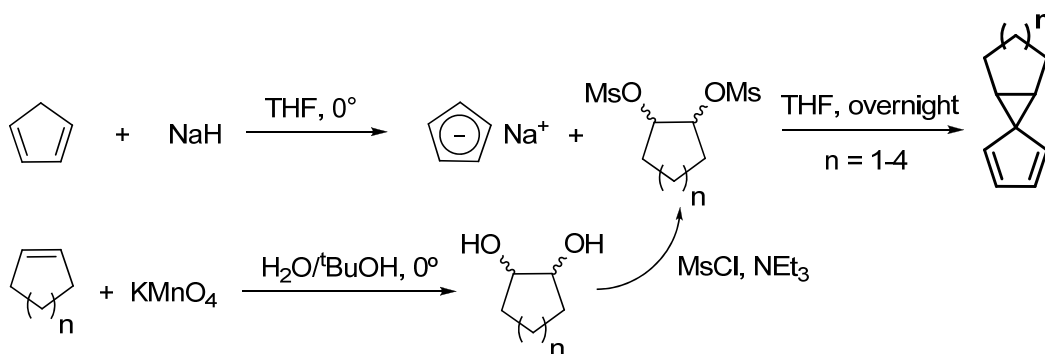
10.1 Abstract

Compounds $[\text{Mo}(\eta^5\text{-C}_5\text{H}_4(\text{CH}(\text{CH}_2)_n)\text{-}\eta^1\text{-CH})(\text{CO})_3]$ and $[\text{W}(\eta^5\text{-C}_5\text{H}_4(\text{CH}(\text{CH}_2)_3)\text{-}\eta^1\text{-CH})(\text{CO})_3]$ (**2a**, **3a** $n=3$; **2b**, **3b** $n=4$; **2c**, **3c** $n=5$; **2d**, **3d** $n=6$) were synthesised by reacting spiroligands **1a-d** with $\text{M}(\text{CO})_3(\text{CH}_3\text{CN})_3$ or $\text{M}(\text{CO})_3\text{L}$ ($\text{M} = \text{Mo}, \text{W}$; $\text{L} = \text{Me}_3\text{tach}, \text{PMTA}$). NMR spectroscopy as well as X-ray diffraction studies confirm the formation of the intramolecular *ansa* bridge. The complexes display a remarkable stability in the solid state (stable up to 180 °C under air in thermogravimetric studies) and are very active catalysts at room temperature (Mo compounds) or moderate temperatures (W compounds) in olefin epoxidation. In the case of cyclooctene, TOFs up to 3600 h^{-1} are obtained. Moreover, the catalysts display a high selectivity in the epoxidation of *cis*- and *trans*-stilbene. In addition, the novel complexes were compared with previously synthesised related compounds, displaying comparable (if not better) catalytic performances.

10.2 Results and discussion

10.2.1 Synthesis and characterisation of the spiroligands **1a-d**

Reaction of the respective bis(methanesulfonate)cycloalkyls with NaCp in THF was carried out following known reaction procedures,⁽¹³⁴⁾ and resulted in the novel spiroannulated dienes **1a-d**. In contrast to more simple spirodienes such as spiro[2.4]hepta-4,6-diene, these oily compounds cannot be distilled, but are obtained in good yields and purities via pentane extraction.



Scheme 13 Synthesis of the spiroligands **1a-d**.

$^1\text{H-NMR}$ data (see Figure 22 for the ^1H spectrum of ligand **1a**) show a group of signals in the range between 6 and 6.6 ppm, corresponding to the cyclopentadienyl moiety. Moreover, a second multiplet can be observed between 2.2 and 2.6 ppm; this has been assigned to the cycloalkyl protons next to the *ipso* carbon, which are slightly shifted to lower fields due to the effect of the Cp fragment. On the other hand, the ^{13}C NMR displays four signals in the 125-145 ppm range and a fifth signal at ca. 50 ppm corresponding to the *ipso* carbon. CI mass spectroscopy shows one strong signal corresponding to the molecular peak of the complexes. Minor polymerisation byproducts (mostly dimeric species), as well as a fragment with $[\text{M}^+] = 66$ (assigned to the Cp fragment) can also be observed.

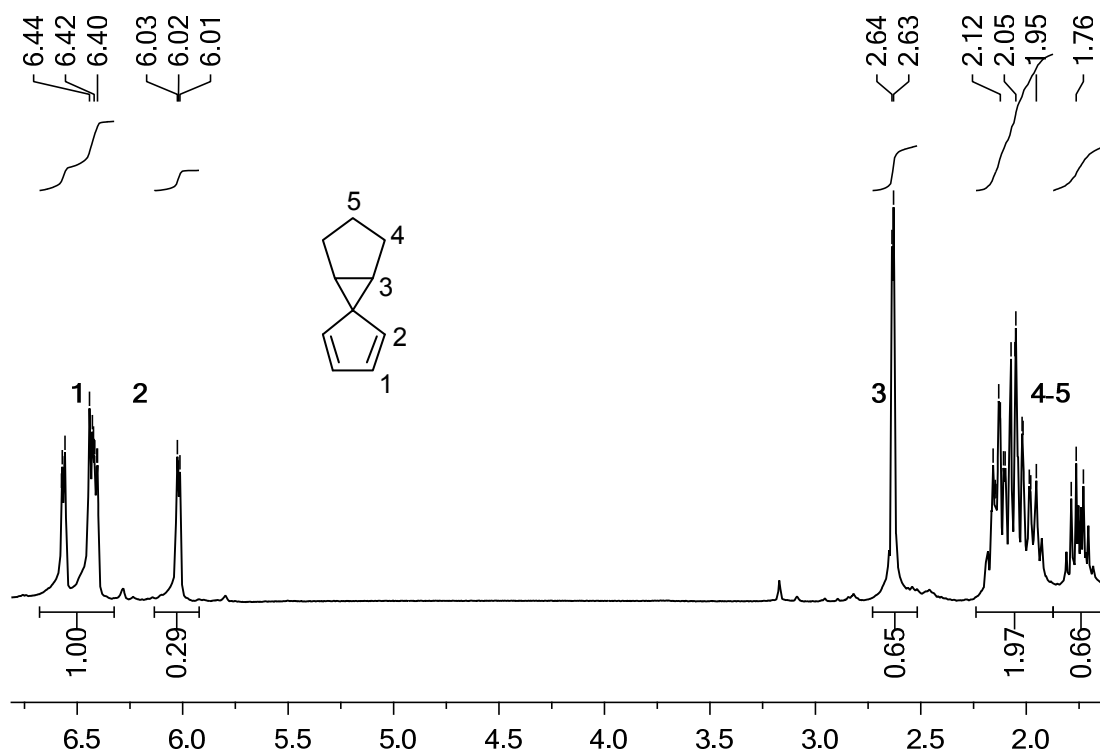


Figure 22 ^1H NMR spectra (solvent: CDCl_3) of compound **1a**, showing the Cp system (6.6 - 6.0ppm) and the cycloalkyl fragment (2.6 - 1.7ppm) signals.

10.2.2 Synthesis of the *ansa* compounds **2a-d**

The obtained spiroligands were reacted with $\text{M}(\text{CO})_3(\text{CH}_3\text{CN})_3$ ($\text{M} = \text{Mo}, \text{W}$) in THF to afford the complexes $[\text{Mo}(\eta^5\text{-C}_5\text{H}_4(\text{CH}(\text{CH}_2)_3)\text{-}\eta^1\text{-CH})(\text{CO})_3]$ (**2a**) and $[\text{W}(\eta^5\text{-C}_5\text{H}_4(\text{CH}(\text{CH}_2)_3)\text{-}\eta^1\text{-CH})(\text{CO})_3]$ (**2b**) in moderate yields. On the other hand, compounds **2b-d** and **3b-d** were obtained in either low (**2b-d**, **3b**) or trace yields (**3c-d**). In light of these results, a new synthetic method was developed.

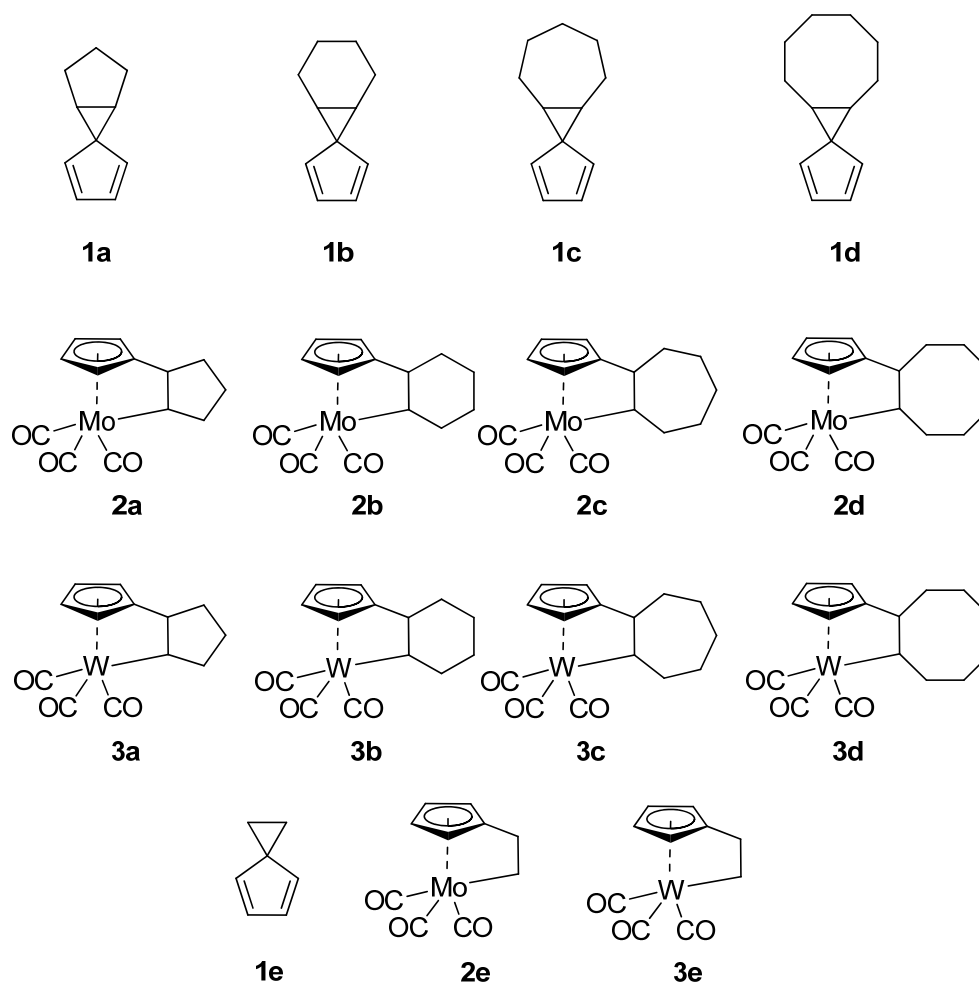
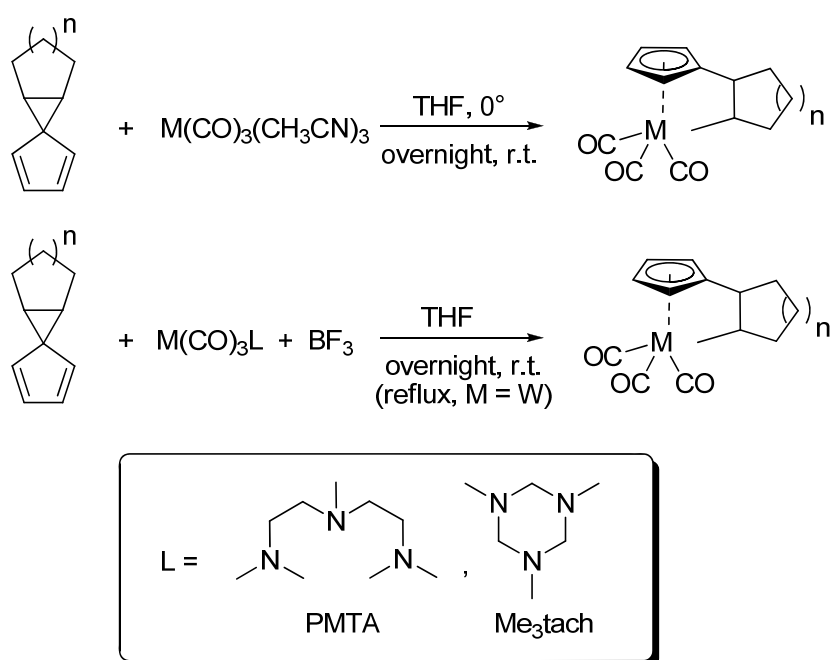


Figure 23 Diagram of the novel C₂-spiro ligands and ansa compounds (below, the previously synthesised ethylene-bridged compounds, **2e** and **3e**).

Improved synthetic procedure

In order to optimise the reaction, an improved pathway involving chelate metal precursors with terdentate amines was developed. The amines used were pentamethyldiethylenediamine PMTA and trimethyltriazocyclohexane (Me₃tach), and the precursors were synthesised according to published procedures.(38-40) In comparison to their acetonitrile counterparts, these compounds show an improved stability and a much higher purity, avoiding the formation of highly reactive carbonyls which are common during the synthesis of M(CO)₃(CH₃CN)₃.(40)

The reaction proceeds at room temperature after adding a strong Lewis acid such as BF₃. In the case of the bulkier W derivatives, however, overnight reflux is needed for the reaction to take place. The reaction can be easily monitored with the change of colour of the mixture, which turns from a yellow suspension to a dark-orange red solution.



Scheme 14 Synthesis of *ansa* complexes **2a-d**, showing both the original (above) and the improved (below) synthetic methods.

Moreover, the *ansa* complexes obtained with this method have little to no impurities. With the previously employed methods, the hexane/pentane extracts were contaminated with unstable species which can lead to the utter decomposition of the target compound.

Comparative studies show that Me₃tach derivatives display a better activity than PMTA complexes. This might owe to the facial disposition of the chelating amine, in contrast to the meridional disposition of the PMTA derivative.(38, 40)

The same synthetic route was also applied for previously synthesised *ansa* compounds, such as $[\text{M}(\eta^5\text{-C}_5\text{H}_4(\text{CH}_2)_2\text{-}\eta^1\text{-CH})(\text{CO})_3]$ (M= Mo (**2e**), W (**3e**)), obtaining the target compounds in better yields and purities.(135) This is particularly striking in the case of compound **2e**, which was originally considered to be thermally unstable, but can be stored for hours at room temperature and under air without visible decomposition.(135) NMR characterisation of **2e** (see Appendix B), along with the preliminary X-ray diffraction studies seen in Figure 24 confirm this fact.

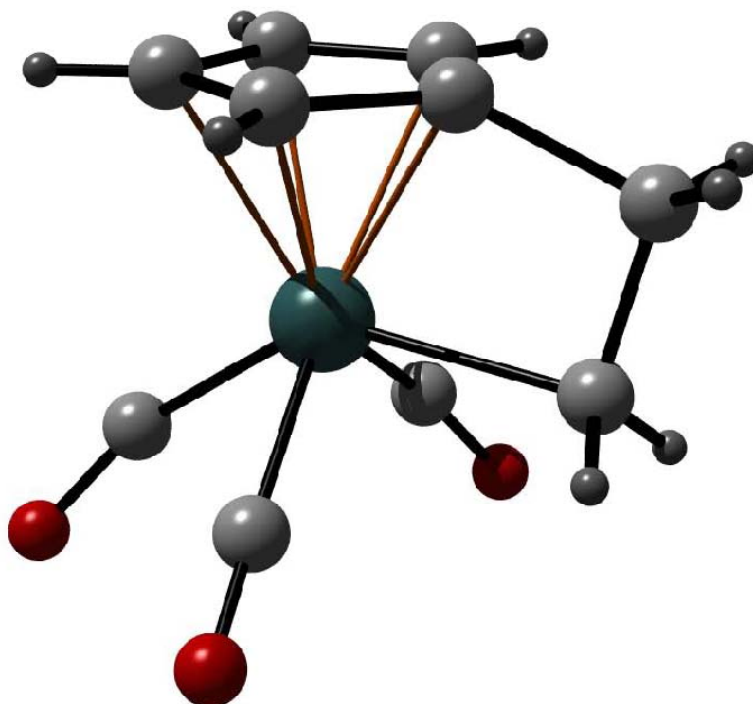


Figure 24 Ball and stick model for the preliminary X-ray structure of compound **2e**.

10.2.3 Properties and characterisation

The colour of the complexes ranges from bright orange (**2a**, **3a**) to bright red (**2b**, **2d**) or dark red (**2c**, **3b-d**). All compounds are slightly sensitive towards light and moisture, but show an improved stability in comparison to previously synthesised *ansa* compounds. Thus, **2a-d** can be handled at room temperature under air for some hours without decomposition in the solid state, whereas **3a-d** can be stored indefinitely under air. **2b** and, to a lesser extent, **2a**, **2c** and **2d** have been shown to decompose faster when exposed to light in solution. It was however not possible to quantify the decomposition rate of the complexes using UV spectroscopy.

Study of the stability. Thermogravimetric studies

TG-MS measurements for **2a** show a first decomposition step at 140 °C by loss of the carbonyl ligands according to a sharp MS signal for 28 m/z. For **2b**, the starting temperature of decomposition is 180 °C. The other compounds show a similar trend, ranging from 120-160 °C (Mo species) and 140-180 °C (W species). This is in agreement with the observed stability of the compounds under air and moisture.

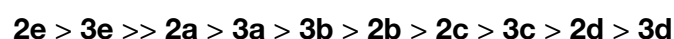
Mass spectroscopy

CI mass spectroscopy shows both the molecular peaks of the *ansa* compounds, as well as the M-CO fragments for the molybdenum species. Due to their enhanced stability, only the molecular peak is observed for most tungsten derivatives.

NMR spectroscopy. COSY experiments

Relevant NMR data for compounds **2a-d** and **3a-d** are included in Table 1. NMR spectra for **2a** and **3a** are included in Figures 25-29^{xi}. ¹H-NMR for **2a-2d** show a group of multiplets at in the range between 5.0 and 5.3 ppm, which are attributed to the four protons of the cyclopentadienyl moiety, indicating a cleavage of the spirocycle and the insertion of the metal into one of the C_{diene}-C bonds, forming a η⁵-coordinated cyclopentadienyl moiety and a η¹-coordinated metal-carbon bond. This is further confirmed by the shift of the Cp-CH proton signal, which appears between 2.9 and 3.4 ppm. On the other hand, the proton bound to the η¹-coordinating carbon displays a chemical shift of δ = 0.4-0.8 ppm due to the deshielding effect of the metal centre. The effect of the cycloalkyl moiety, however, significantly shifts this signal to lower fields, as inferred when comparing these values with those for the ethylene bridged compounds **2e** and **3e**.

This tendency is observed for the rest of the obtained complexes, with the size of the alkyl ring and the metal centre playing an important role in the shift of the *ansa*-C proton (see below, organised from higher to lower fields):



The effect of the substituents is also observed in both the 2-phenyl- and the 1,2-dimethyl-substituted derivatives previously synthesised in our group. The reported values for the C_{ansa} protons are also in agreement with the results obtained herein.⁽⁵³⁾

Both ¹³C-NMR and two-dimensional COSY experiments support these assignments. ¹³C-NMR for compound **2a-2d** shows four different signals in the range between δ = 90 – 86 ppm, attributed to the four non-substituted cyclopentadienyl carbons, and a low intensity signal at δ = 80-70 ppm, corresponding to the cyclopentadienyl carbon bearing the *ansa*-cyclopentadienyl unit. The η¹-bound carbon is found in the range within -12

^{xi} NMR spectra of all the obtained complexes, including the previously commented spiro ligands, are available in Appendix B.

(**2d**) and -27 (**2a**) ppm, and the values are in agreement with those obtained in the ^1H -NMR experiments. Moreover, the rather elusive carbonyl signals can be observed at 201.3 ppm (see Figure 26). CO signals usually appear between 190 and 230 ppm.

2D-COSY experiments (see Figures 27 and 29 for the obtained bidimensional spectra of complexes **2a** and **3a**) show two separate spin systems, one for the four protons of the Cp moiety and other for the *ansa* fragment. The interactions between the members of the *ansa* ring are observed in all cases.

Similar values are generally observed for the tungsten complexes (see NMR spectra of **2b** in Figures 25-27). In this case, the ^{13}C signals of the metal bound carbon are generally shifted to higher fields than its Mo counterparts (-24 to -38 ppm)

^{95}Mo NMR of compounds **2a-2d** shows the molybdenum signals at $\delta = -1389$, -1400, -1413, and -1668 ppm, respectively. These values are consistent with previously reported *ansa* compounds.(53, 57) To further confirm this fact, ^{95}Mo NMR experiments were performed with the previously reported compound **2e**, showing a peak at -1395 ppm.

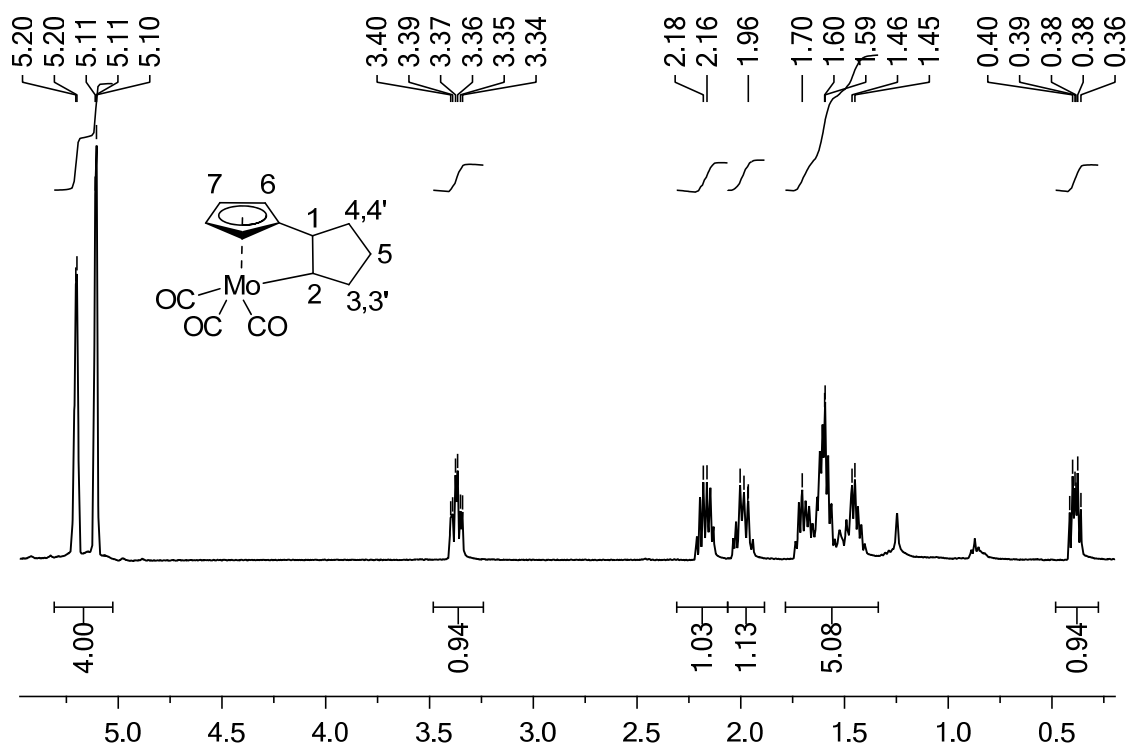


Figure 25 ^1H NMR spectra of compound **2a**.

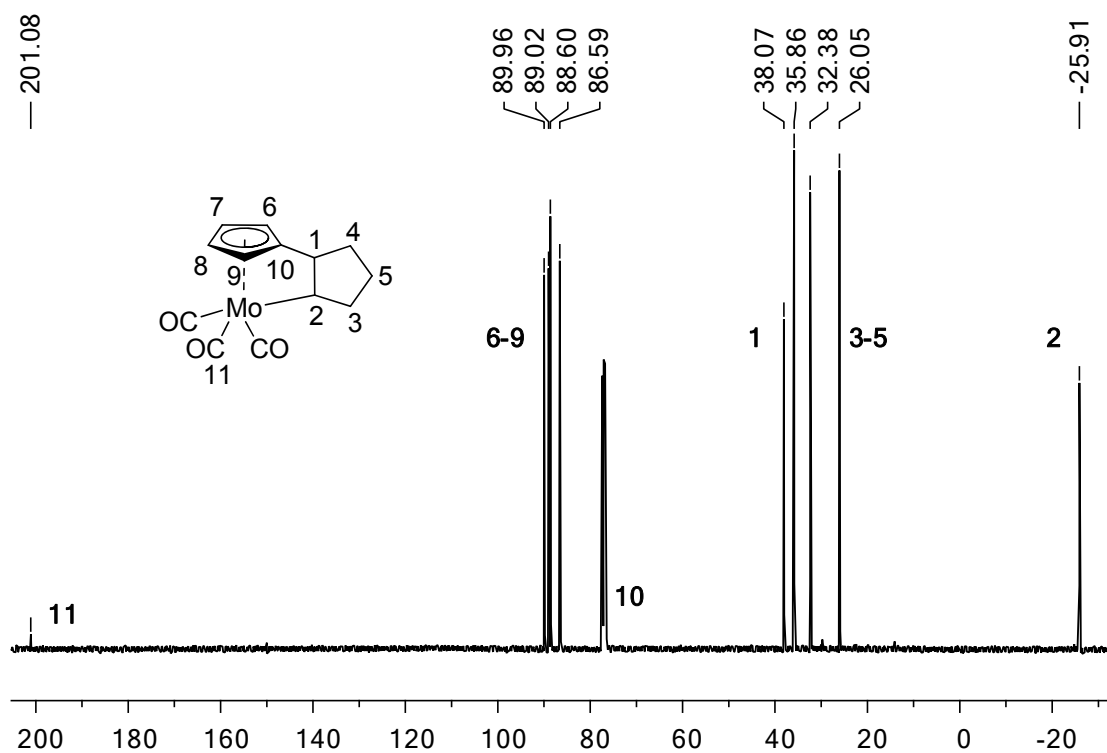


Figure 26 ^{13}C NMR spectra of compound **2a**. The CO signal is observed in the left part of the spectra.

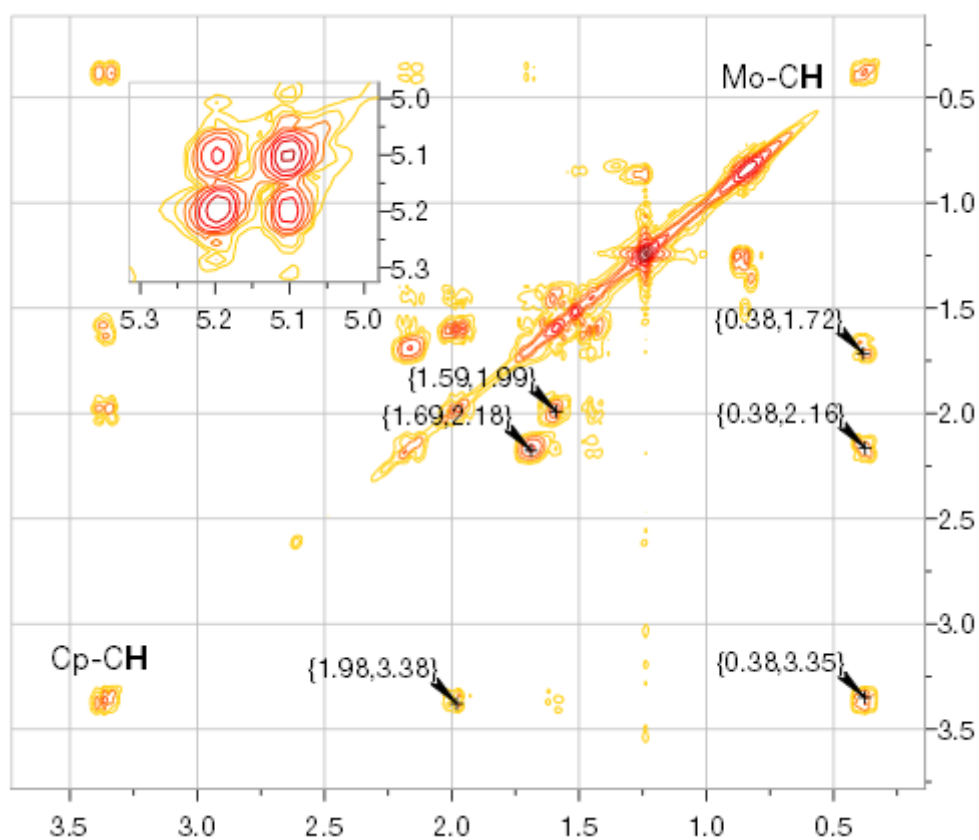


Figure 27 2D-COSY of **2a**, showing both the cyclopentadienyl (upper left corner) and the *ansa* cyclopentyl spin systems.

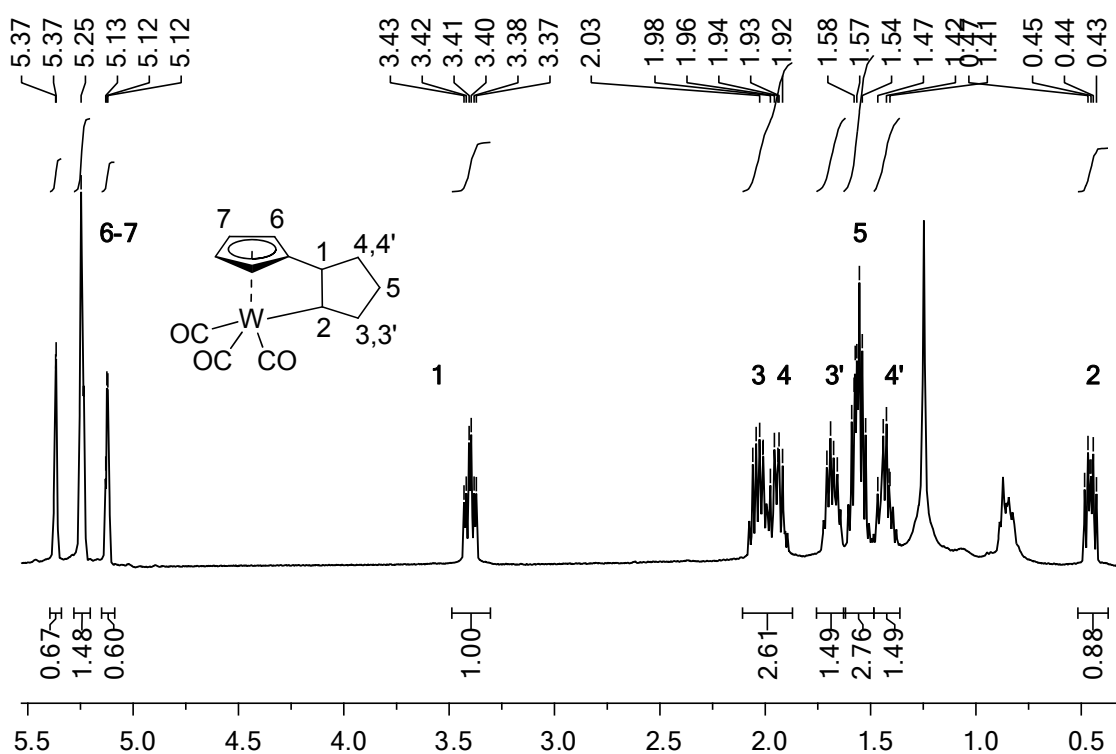


Figure 28 ^1H NMR spectra of compound **3a**.

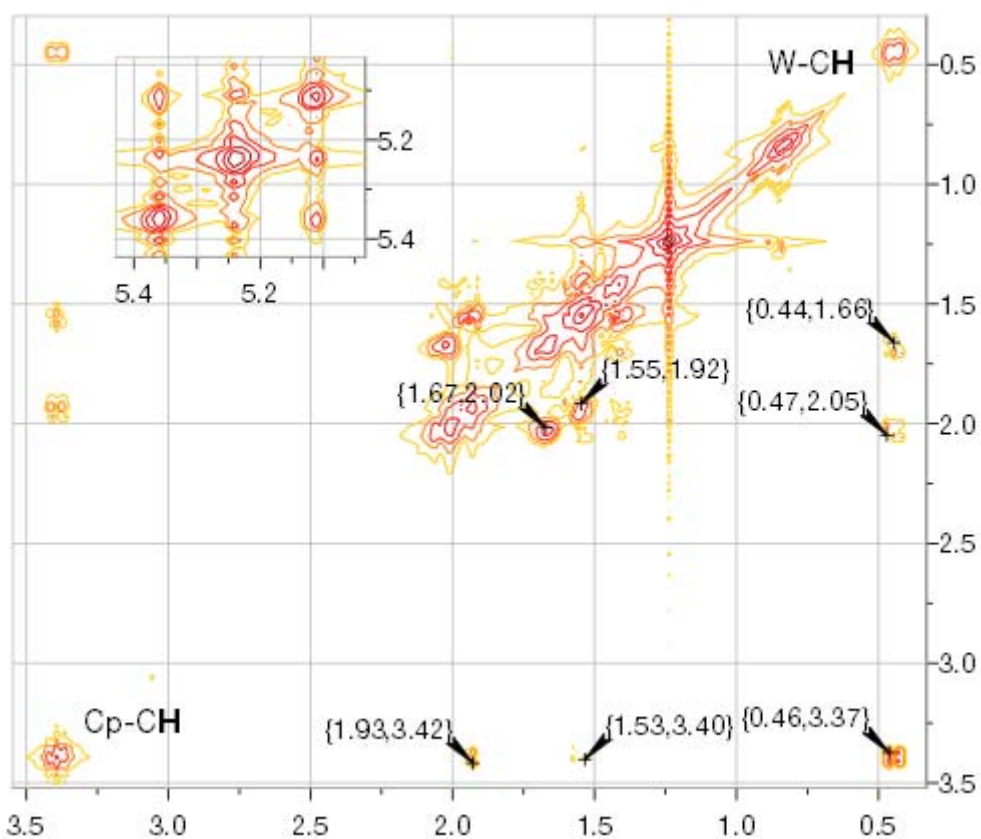


Figure 29 2D-COSY of **3a**, showing both the cyclopentadienyl (upper left corner) and the ansa cyclopentyl spin systems.

| Compound | ¹ H | | ¹³ C | | ⁹⁵ Mo |
|-----------|----------------|-------|-----------------|--------|------------------|
| | Cp-CH | M-CH | Cp-CH | M-CH | |
| 2a | 3.38 | 0.40 | 76.6 | -25.9 | -1389 |
| 2b | 3.11 | 0.72 | 72.2 | -22.1 | -1400 |
| 2c | 2.95 | 0.74 | 73.5 | -15.9 | -1413 |
| 2d | 3.17 | 0.80 | 73.0 | -12.0 | -1668 |
| 2e | 2.94 | -0.42 | 67.0 | -49.7 | -1395 |
| 3a | 3.40 | 0.46 | 80.2 | -38.0 | - |
| 3b | 3.11 | 0.68 | 75.6 | -36.1 | - |
| 3c | 2.99 | 0.77 | 76.9 | -24.30 | - |
| 3d | 3.25 | 0.81 | 76.6 | -25.29 | - |
| 3e | 2.91 | -0.25 | 70.9 | -61.7 | - |

Table 1 Selected NMR data for the new cycloalkyl *ansa*-compounds. In italic, the previously synthesised ethylene-bridged complexes.

10.2.4 X-ray structures of compounds **2a**, **3a** and **2b**

Compounds **2a**, **3a** and **2b** were characterised by X-ray crystallography. All complexes display a distorted four-legged stool structure similar to that established for analogous complexes.(53, 57, 135)

Whereas only one of the possible enantiomers - (S,R)-[Mo(η^5 -C₅H₄(CH(CH₂)₄)- η^1 -CH)(CO)₃] - is clearly observed in the case of compound **2b**, complexes **2a** and **3a** display a mixture of isomers (**a** and **a'**) depending on the conformation of the cycloalkyl ring (either a distorted envelope or a distorted half-chair conformations). In the latter cases, however, the *ansa* bridge still displays an (S,R) configuration.

Tables 3 and 4 show a selection of bond distances and angles for all the obtained structures. As expected, the cyclopentadienyl ligand is coordinated in a η^5 -fashion, inferred from the total value of the angles at the ring and the distances from the central atom to each of the carbon atoms (ranging from 2.304(5) to 2.3394(14)Å) and to the Cp centroid (ranging from 1.977 to 1.981 Å). Both C-O distances (ca. 1.14 Å) and M-C-O angles (ca. 177-180°) are well within the expected values for this kind of compounds.

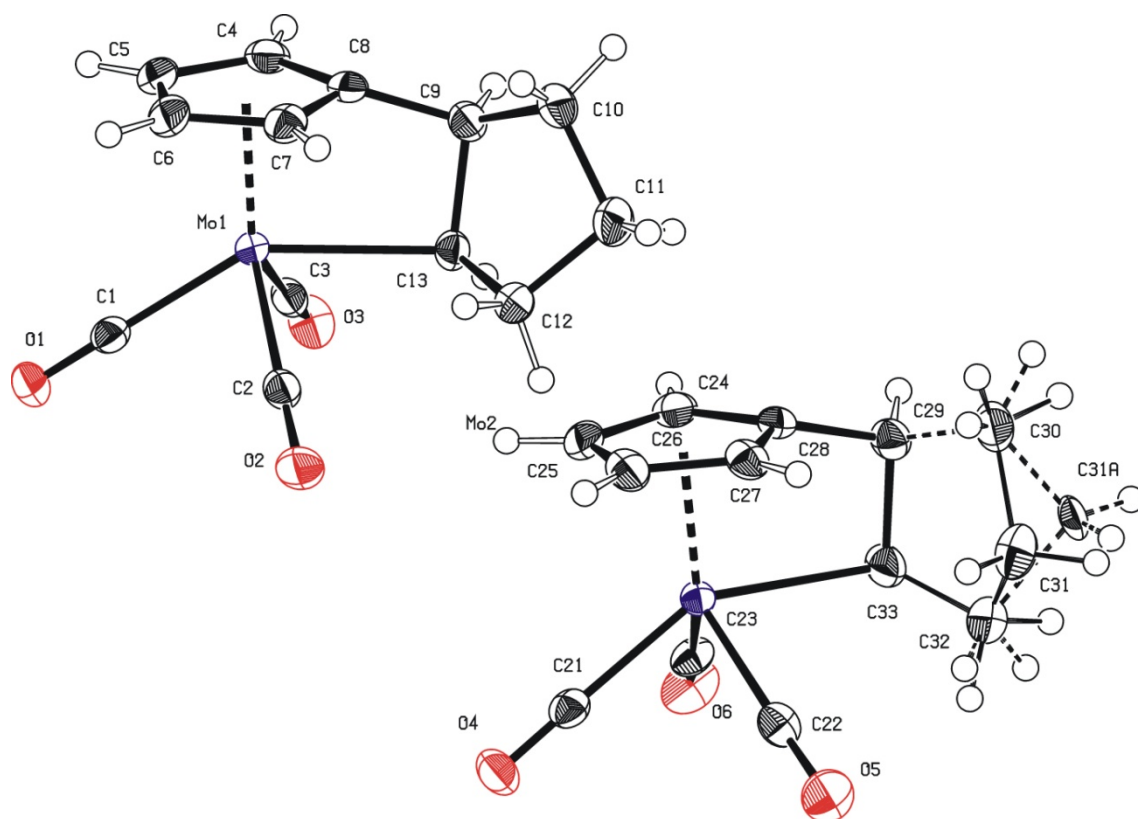


Figure 30 Crystal structure of compound **2a**.

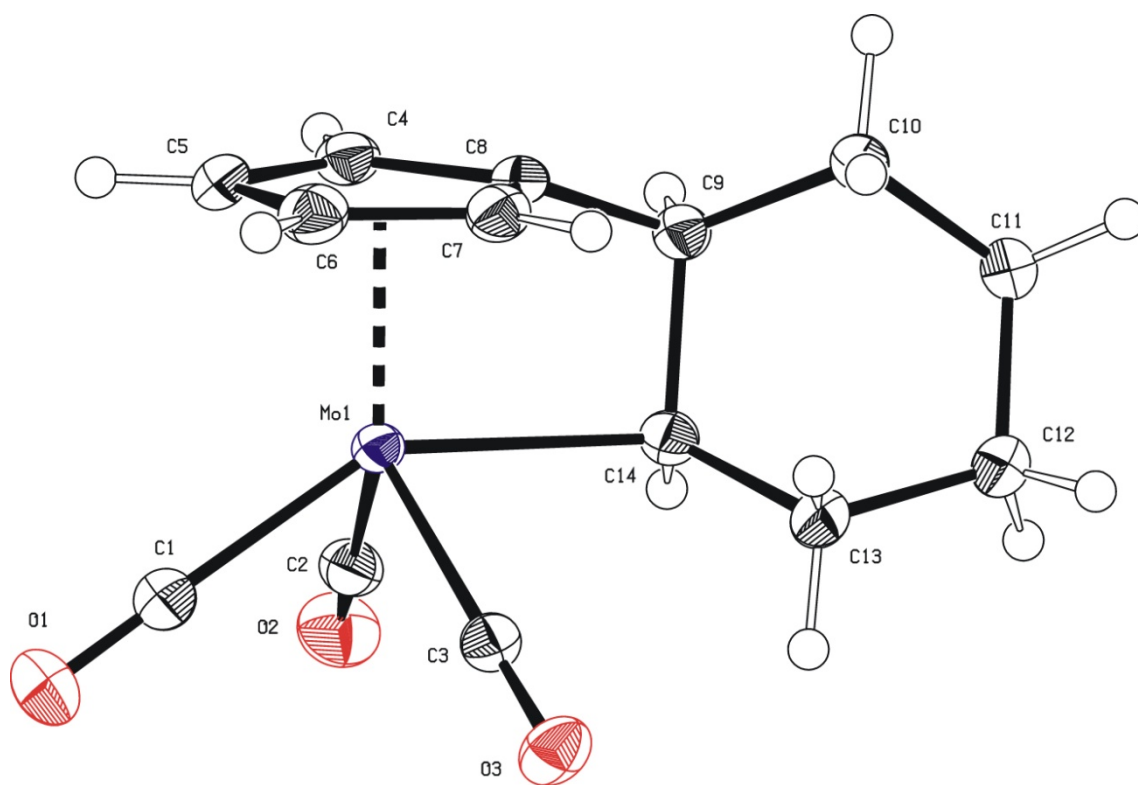


Figure 31 Crystal structure of compound **2b**.

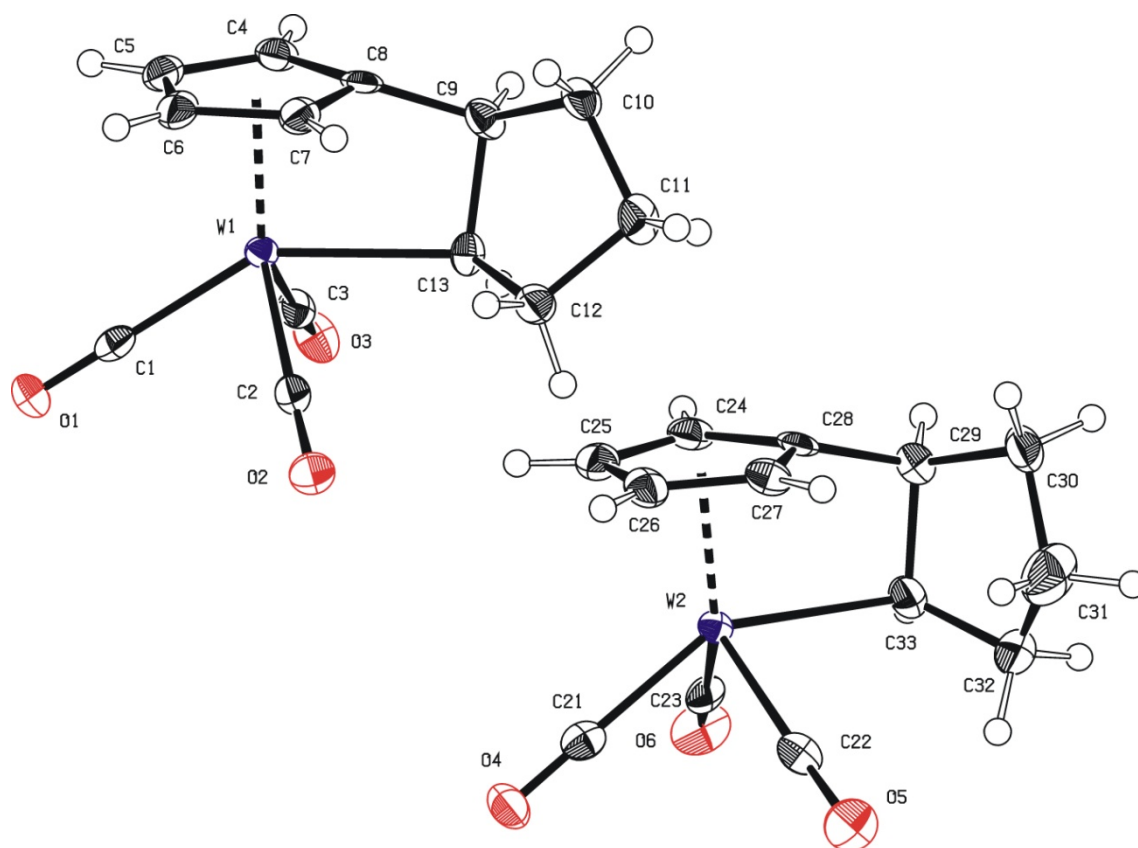


Figure 32 Crystal structure of compound **3a**.

The greatest difference between the obtained **a** and **a'** isomers lies within the observed Mo-C distance values, which differ in approximately 0.04 Å. Moreover, the terminal cycloalkyl fragment is found to shift between two different conformations, affecting the configuration of the *ansa* bridge with respect to the metal centre.

Apart from **2a** and **3a**, preliminary X-ray diffraction studies on complex **3b** (see Figure 33 for the ORTEP diagram) suggest that both the R,R and the R,S diastereomers crystallise. Whereas the obtained $C_{p_{\text{centroid}}}-W$ and $W-C_{\text{ansa}}$ distances lie within the expected values (1.99 Å and 2.34 Å, respectively), most ellipsoids near the *ansa* bridge are significantly broader than usual. This is particularly clear when observing the carbon atom next to the C_{ansa} , and further indicates that the obtained crystal is in fact a mixture of different isomers. These results contradict previous studies with related bridged compounds, which considered that the synthesis of the *ansa* complexes was enantioselective.⁽⁵³⁾ It seems, however, that certain enantiomers (such as in the case of **3b**) are preferably crystallised. This result, coupled with the fact that an asymmetric carbon is directly attached to the metal centre makes these new compounds promising candidates in asymmetric epoxidation reactions.

| Compound | 2a | 2b | 3a |
|--|--|--|---|
| Formula | C ₁₃ H ₁₂ MoO ₃ | C ₁₄ H ₁₄ MoO ₃ | C ₁₃ H ₁₂ WO ₃ |
| Formula Weight | 312.17 | 326.19 | 400.07 |
| Crystal System | Monoclinic | Monoclinic | Monoclinic |
| Space Group | C2/c (No. 15) | P21/n (No.14) | C2/c (No. 15) |
| a,b,c (Å) | 24.3045(6), 13.3776(4), 14.8051(4) | 7.7140(3), 13.3671(6), 12.2217(5) | 24.290(5), 13.415(3), 14.817(3) |
| α, β, γ (°) | 90, 97.0970(13), 90 | 90, 96.273(2), 90 | 90, 96.847(6), 90 |
| V [Å ³] | 4776.8(2) | 1252.68(9) | 4793.7(18) |
| Z | 16 | 4 | 16 |
| D (calc) [g·cm ⁻³] | 1.736 | 1.730 | 2.217 |
| μ (MoKα) [mm ⁻¹] | 1.090 | 1.043 | 9.631 |
| F (000) | 2496 | 656 | 3008 |
| Crystal Size [mm] | 0.10 x 0.30 x 0.41 | 0.10 x 0.10 x 0.24 | 0.03 x 0.18 x 0.43 |
| Temperature (K) | 123 | 123 | 123 |
| Radiation [Å] | MoKα 0.71073 | MoKα 0.71073 | MoKα 0.71073 |
| θ Min-Max [°] | 2.8, 25.4 | 2.3, 30.6 | 1.7, 25.4 |
| Dataset | -29:29; -14:14; -17:17 | -11:11; -17:17; -17:17 | -29:29; -14:15; -17:17 |
| Tot., Uniq. Data, R(int) | 67622, 4175, 0.032 | 32779, 3691, 0.038 | 14937, 4345, 0.039 |
| Observed data [I > 2.0σ(I)] | 3983 | 3509 | 3886 |
| N _{ref} , N _{par} | 4175, 317 | 3691, 163 | 4345, 307 |
| R, wR ₂ , S | 0.0258, 0.0690, 1.32 ¹ | 0.0191, 0.0493, 1.06 ² | 0.024, 0.0655, 1.03 ³ |
| Max. and Av. Shift/Error | 0.00, 0.00 | 0.00, 0.00 | 0.00, 0.00 |
| Min. and Max. Resd. | -0.70, 1.37 | -0.48, 0.54 | -0.99, 1.29 |
| Dens. [e/Å ³] | | | |
| 1: w = 1/[s ² (F _o ²) + (0.0340P) ² + 6.7318P] where P = (F _o ² + 2F _c ²)/3 | | | |
| 2: w = 1/[s ² (F _o ²) + (0.0177P) ² + 0.9030P] where P = (F _o ² + 2F _c ²)/3 | | | |
| 3: w = 1/[s ² (F _o ²) + (0.0307P) ² + 21.5575P] where P = (F _o ² + 2F _c ²)/3 | | | |

Table 2 Crystal data, data collection and refinement parameters for structures **2a**, **2b** and **3a**.

| | 2a | 2a' | 2b | 3a | 3a' |
|---------------------------|----------|----------|------------|----------|----------|
| M-CO | 2.019(2) | 2.016(2) | 2.0128(15) | 2.014(5) | 2.014(6) |
| | 1.985(2) | 1.987(3) | 1.9921(15) | 1.987(5) | 1.982(5) |
| | 1.990(2) | 1.985(2) | 1.9885(14) | 1.998(5) | 1.991(5) |
| M-C _{ansa} | 2.372(2) | 2.408(3) | 2.4011(13) | 2.353(5) | 2.398(4) |
| M-Cp _{centroid} | 1.977 | 1.978 | 1.981 | 1.981 | 1.982 |
| M-Cp (CH) | 2.324(3) | 2.316(3) | 2.3279(14) | 2.330(5) | 2.318(5) |
| | 2.335(2) | 2.330(2) | 2.3389(15) | 2.337(5) | 2.334(5) |
| | 2.336(2) | 2.337(2) | 2.3394(14) | 2.333(5) | 2.339(5) |
| | 2.305(2) | 2.314(2) | 2.3065(14) | 2.304(5) | 2.317(5) |
| M-Cp (C _{ansa}) | 2.293(2) | 2.294(2) | 2.2945(12) | 2.306(5) | 2.301(5) |
| (C-C) _{ansa} | 1.551(3) | 1.549(3) | 1.5517(18) | 1.564(7) | 1.562(7) |
| Cp-C _{ansa} | 1.510(3) | 1.509(3) | 1.5133(19) | 1.503(7) | 1.516(7) |

Table 3 Selected bond distances (in Å) for compounds **2a**, **3a** (and their respective isomers) and **2b**.

| | 2a | 2a' | 2b | 3a | 3a' |
|---|------------|------------|------------|------------|------------|
| M-C _{ansa} -C _{ansa} | 96.30(13) | 96.03(14) | 95.91(8) | 96.9(3) | 96.7(3) |
| Cp _C -C _{ansa} -C _{ansa} | 100.50(17) | 101.51(19) | 100.95(10) | 100.2(4) | 100.7(4) |
| Cp _{CH} -Cp _C -C _{ansa} | 124.0(2) | 123.5(2) | 123.55(13) | 124.1(5) | 123.5(5) |
| | 124.3(2) | 125.0(2) | 124.69(13) | 123.9(5) | 125.5(5) |
| CO _{trans} -M-C _{ansa} | 146.37(8) | 146.82(9) | 146.15(5) | 146.19(17) | 146.46(18) |
| CO _{cis} -M-C _{ansa} | 78.49(9) | 80.06(9) | 75.38(5) | 79.04(18) | 80.68(18) |
| | 78.51(9) | 76.24(10) | 81.29(5) | 78.9(2) | 76.5(2) |
| CO _{cis} -M-CO _{trans} | 80.45(10) | 80.34(10) | 80.98(6) | 79.9(2) | 79.9(2) |
| | 80.10(10) | 80.94(10) | 79.46(6) | 79.9(2) | 80.6(2) |
| CO _{cis} -M-CO _{cis} | 100.88(10) | 99.54(10) | 100.26(6) | 101.8(2) | 100.7(2) |

Table 4 Selected bond angles (in °) for compounds **2a**, **3a** (and their respective isomers) and **2b**.

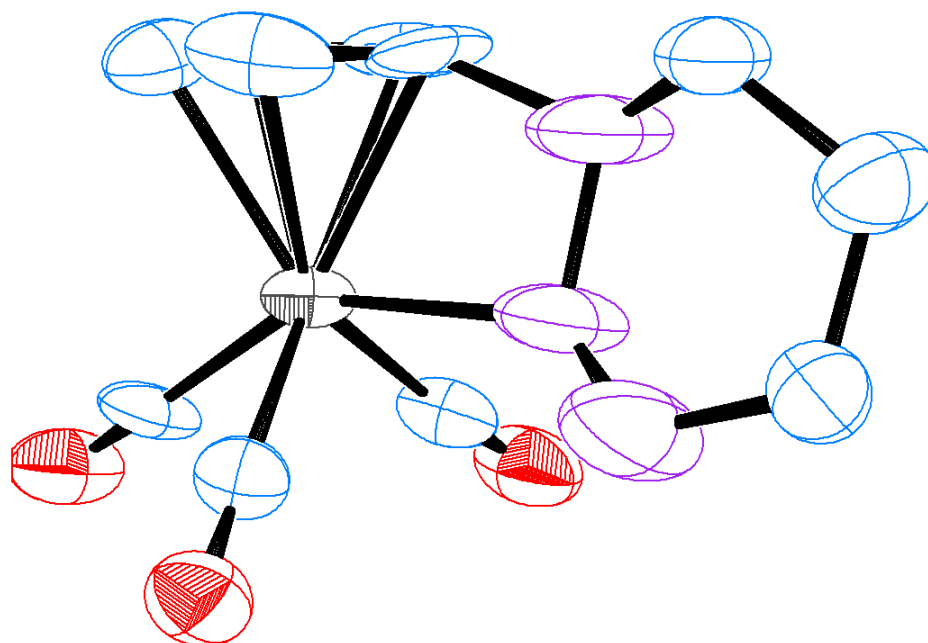


Figure 33 ORTEP plot for the preliminary X-ray structure of compound **3b**. The position of the atoms (especially those in the vicinity of the *ansa* cycloalkyl ring, see purple ellipsoids) could not be properly determined.

10.2.5 Application in epoxidation catalysis

All complexes were tested in the epoxidation of *cis*-cyclooctene, 1-octene, *cis*-stilbene and *trans*-stilbene, with *tert*-butyl hydroperoxide (TBHP) as the oxidant and under air at room temperature (Mo and W derivatives) and at 55 °C (W derivatives). A catalyst:oxidant:substrate ratio of 1 : 200 : 100 was used for all reactions except stated otherwise.

Cyclooctene

Being the most common epoxidation substrate in the literature, cyclooctene was exhaustively tested with the novel *ansa* compounds. Since there are no comparable experiments in the literature, compounds **2e** and $\text{CpMo}(\text{CO})_3\text{R}$ (R = Cl, Me) were also tested. Catalytic data are summarised in Figures 34-37 (Legend: MoC2 = **2e**; MoC5 = **2a**; MoC6 = **2b**; MoC7 = **2c**; MoC8 = **2d**; WC2 = **3e**; WC5 = **3a**; WC6 = **3b**; WC7 = **3c**; WC8 = **3d**; $\text{CpMo}(\text{CO})_3\text{Cl}$ = **MoCl**; $\text{CpMo}(\text{CO})_3\text{Me}$ = **MoMe**).

Upon addition of TBHP, the solution turned light yellow, owing to the oxidation of the carbonyl compound to yield the catalytically active species, as described previously.^(14, 19, 51, 58, 76, 124-133, 140-142) An induction period can be observed during the first minutes of the reaction, especially in the case of the less active catalytic species. This owes to the *in situ* formation of the abovementioned active species^{xii}. A similar behaviour has been reported for related complexes.^(30, 143)

The reaction mixture was analysed via GC-MS. Additional data is provided in the experimental section.

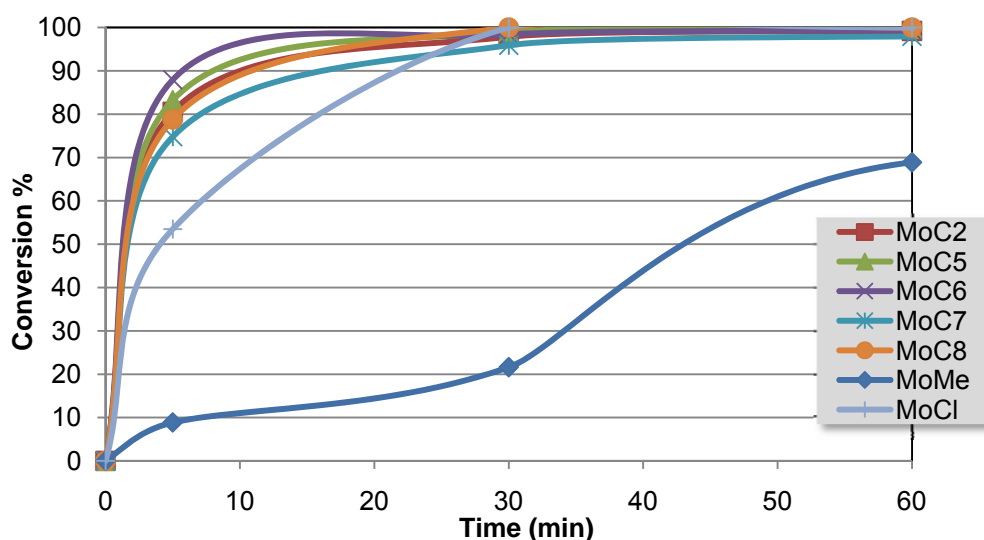


Figure 34 Catalytic epoxidation of *cis*-cyclooctene at room temperature with compounds **2a-e** and the previously reported $\text{CpMo}(\text{CO})_3\text{Me}$ (**MoMe**) and $\text{CpMo}(\text{CO})_3\text{Cl}$ (**MoCl**). Catalyst:oxidant:substrate ratio 1 : 200 : 100.

Compounds **2a-2e** were found to be highly active catalysts for the epoxidation of cyclooctene at room temperature, surpassing the activities of both the methyl and chloro derivatives (see Figure 34) Quantitative conversions (90 - 100 %) are reached

^{xii} This induction period can be seen occasionally as a small curve in the Figures: this owes mostly to the slight experimental error for the 5 min samples.

after 30 min. On the other hand, compounds **3a-3e** display a much more modest catalytic activity at r.t. – a result which was otherwise expected, since W derivatives are generally worse catalysts than their Mo analogues. Hence, a further series of experiments was carried out at 55 °C.^{xiii} A comparison between both series of experiments is featured in Figure 35. The obtained catalytic activities – both in the case of Mo and W derivatives - clearly outperform previous results.(58) The calculated turnover frequencies range between 250 and 750 h⁻¹ (**2d** and **2a**, respectively), which is within the range of other non-*ansa* cyclopentadienyl molybdenum alkyls such as CpMo(CO)₃Me.(*ibid.*)

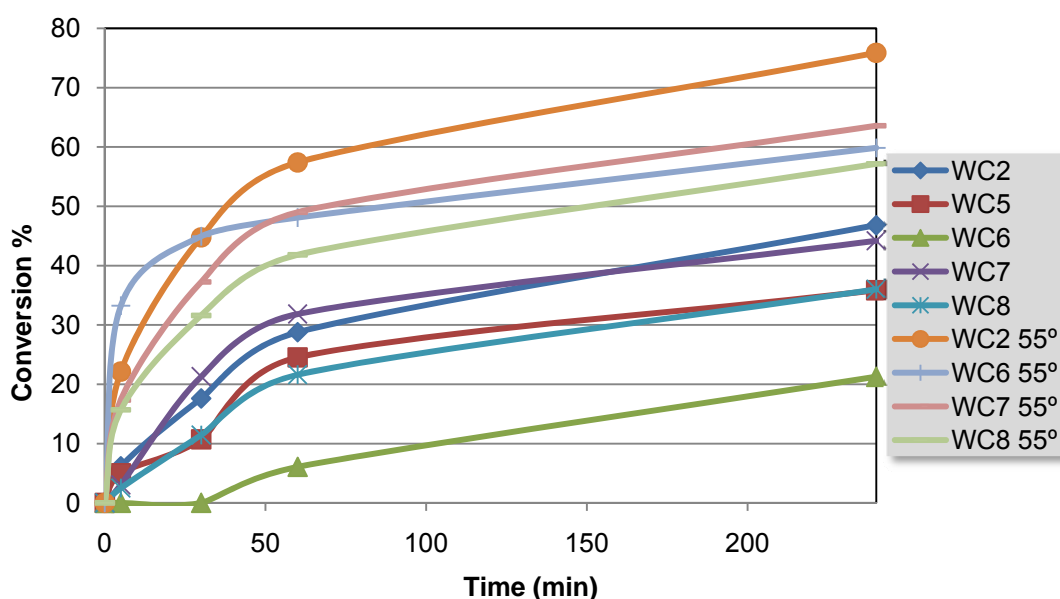


Figure 35 Catalytic epoxidation of *cis*-cyclooctene at room temperature and at 55 °C with compounds **3a-e** and the previously reported CpMo(CO)₃Me (**MoMe**). Catalyst:oxidant:substrate ratio 1 : 200 : 100.

Additional experiments were carried out using a 1 : 2000 : 1000 ratio of **2a**, **2b** and **2e**. In this case, a TOF of 3650 h⁻¹ is obtained for the former, whereas **2b** displays a reduced catalytic activity. In another experiment, a ratio of 2 : 20000 : 10000 was used for **2a**. Although moderate conversions (ca. 60 %) were obtained after 24 h, the catalytic activity of the compound was, in overall, very low.

^{xiii} Previous publication report experiments carried out at 90°C. This temperature, however, is also the decomposition temperature of TBHP; hence, this fact (coupled with the reduced stability of the catalyst against moisture and high temperatures) could be responsible for the reduced activity of the W catalysts observed therein.

In order to properly compare the novel catalysts with those reported in the literature, the epoxidation reactions were performed at 55 °C. In most cases, the catalytic activity was either reduced or did not change in comparison with the r.t. experiments. Moreover, the catalyst clearly decomposed within the first hour of the reaction.

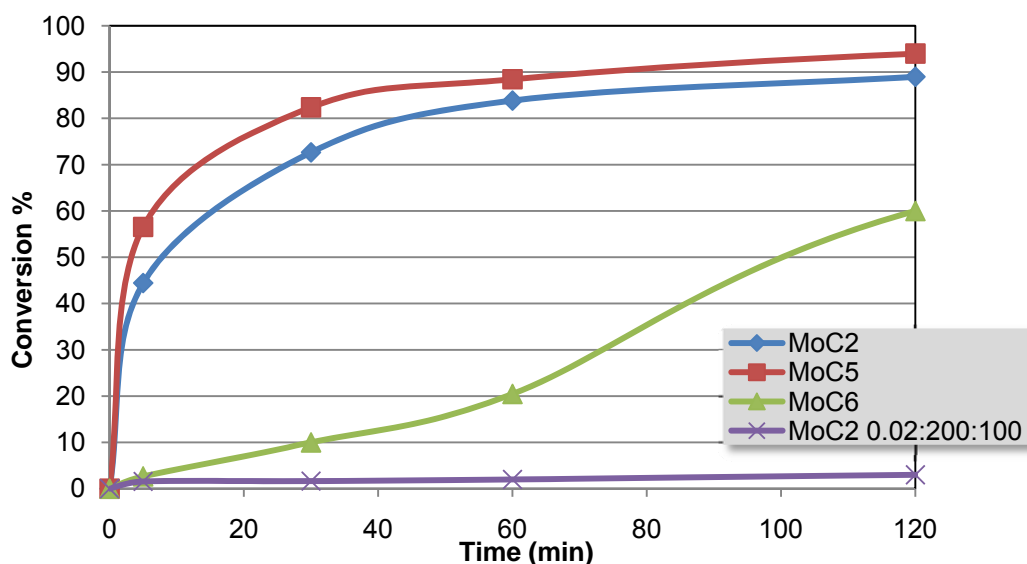


Figure 36 Catalytic epoxidation of *cis*-cyclooctene at room temperature with compounds **2a**, **2b** and **2e** with lower substrate ratios (cat:ox:subs ratio 0.1 : 200 : 100 unless otherwise stated).

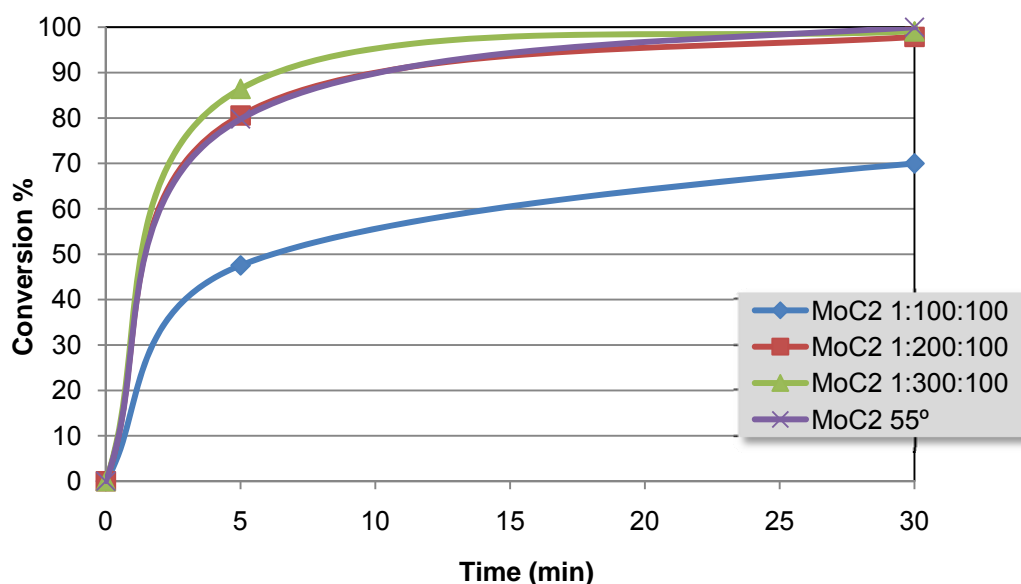


Figure 37 Comparative of the catalytic activity of compound **2e**.

The catalyst:oxidant:substrate ratio has also been found to influence the catalytic activity. Thus, using 1 molar equivalent of oxidant (instead of 2) significantly reduces the

catalytic activity of the complex, whereas 3 molar equivalents do not accelerate the reaction significantly.

In order to test the stability of the catalytic species, further amounts of substrate were added after the first run (using **2e** as catalyst). It was shown that the catalyst remained active after 4 catalytic runs, with a moderate drop in the activity. Further experiments with the more stable W derivatives, as well as a comparative between all the tested catalysts are currently underway.

1-Octene, *cis*- and *trans*-stilbene

Experiments with 1-octene afford moderate yields (40 % the case of **2a**), although no diols were detected during the course of the experiment. Moreover, **2a** is found to be a highly stereoselective catalyst in the epoxidation of *cis*- and *trans*-stilbene, affording the respective epoxides with almost quantitative *cis/trans* ratios. These results rule out the possibility of the catalyst following a radical mechanism, as it has been reported for related species^{xiv}.(144) Compound **2b**, on the other hand, has been found to form only the *trans*-epoxide from both olefinic substrates. Further studies are currently underway in our group.

2a, **2b** and **2e**, were also tested in the epoxidation of glycidol and the course of the reaction monitored via NMR experiments (CDCl₃ as solvent, r.t., 1 : 200 : 100 catalyst : oxidant : substrate ratio). Preliminary results showed that a significant amount of epoxide (ca. 15-20 % conversion) was formed after 4 h of reaction in the case of **2a**. Moreover, no diol formation was observed. Further experiments include the use of the isolated, optically active catalysts in asymmetric epoxidation of glycidol as well as other prochiral substrates (such as β-methylstyrene).

10.3 Conclusions

New molybdenum and tungsten *ansa* complexes (**2a-2d** and **3a-3d**, respectively) with cycloalkyl units as the *ansa* bridge have been synthesised by the reaction of spiro

^{xiv} It must be noted that a number of experiments using butylated hydroxyanisole (BHA) as radical scavenger in the catalytic reaction were performed with compounds 2a-2d. Unfortunately, the obtained results were not conclusive.

annulated dienes **1a-d** with $M(\text{CO})_3(\text{CH}_3\text{CN})_3$, $M(\text{CO})_3(\text{Me}_3\text{tach})$ and $M(\text{CO})_3\text{PMTA}$ ($M = \text{Mo}, \text{W}$), the latter being a much preferred synthetic approach. The complexes have been characterised by ^1H , ^{13}C , ^{95}Mo and two-dimensional COSY NMR experiments. X-ray structures of compounds **2a**, **2b** **3a** and preliminary structures of compounds **2e** and **3b** confirm the obtained spectroscopic data. In comparison to previously reported *ansa* compounds of Mo and W, these complexes show an improved thermal stability and can be stored under air for long periods of time. Catalytic epoxidation with *cis*-cyclooctene, 1-octene, *cis*-stilbene and *trans*-stilbene as substrate and TBHP as oxidant show that **2a-2d** are highly active and stereoselective epoxidation catalysts, achieving TOFs up to 3600 h^{-1} at room temperature. Since **3a-3d** show only moderate activities with *cis*-cyclooctene as substrate at room temperature, higher reaction temperatures are required for it to afford high product yields.

Further research in the field of *ansa* compounds, both synthetical and catalytic, is currently underway in our group.

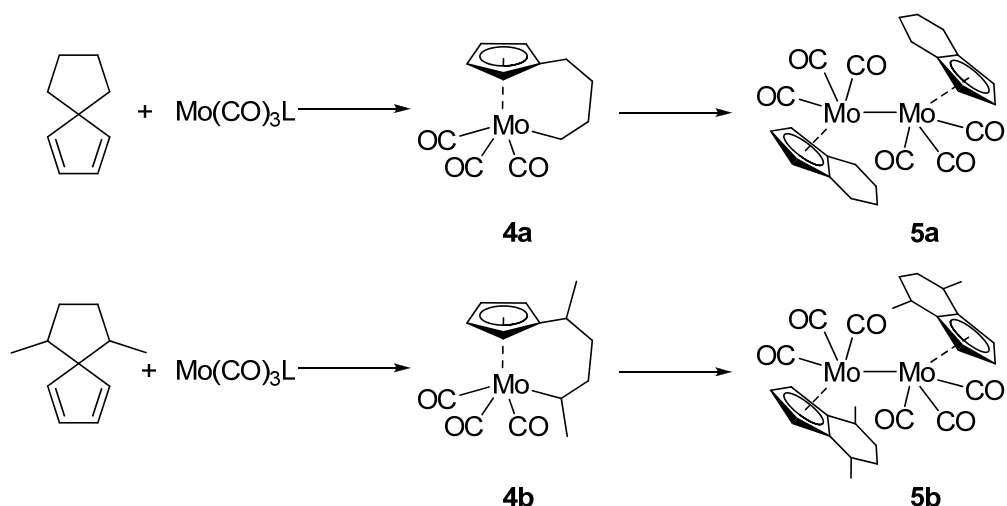
11. Current Research. New *ansa* Derivatives

11.1 *ansa*-C₄ compounds. Dimer formation

Due to the rather difficult reproducibility of the reaction, the previously reported [Mo(η^5 -C₅H₄(CH₂)₄- η^1 -CH)(CO)₃] and similar related compounds are being object of further synthetic studies. Although they should theoretically be more stable than the C₂-*ansa* derivatives, these compounds could not be isolated as described in the literature.⁽⁵⁷⁾ Instead, a dark red-purple solid was formed independently of the synthetic method applied^{xv}. NMR studies of this product suggest that it consists of a mixture of both the *ansa* monomer and a dimeric species with bis(tetrahydroindenyl) moieties coordinating to the metal centres.^{xvi} According to Eilbracht *et al.*, who detected a similar byproduct when reacting W(CO)₃(CH₃CN)₃ with spiro[4.4]nona(1,3)diene, this dimer should originate from the *ansa* monomer, as depicted in Scheme 16.⁽¹¹²⁾ Recent studies on similar CpMo dimeric species are also in agreement with the data provided herein.⁽¹⁰⁰⁾ Similar results have been observed when attempting the synthesis of [Mo(η^5 -C₅H₄(CH₂)₄- η^1 -CH)(CO)₃] (**4b**). Preliminary catalytic tests show that these dimers display a moderate catalytic activity, achieving yields up to 40-50 % in the epoxidation of cyclooctene. It must be noted that the formation of related *ansa* C₂ derivatives can be ruled out; in this case, the fused cyclopentadienyl moiety would suffer from a stronger ring strain.

^{xv} i.e., using Mo(CO)₃(CH₃CN)₃, Mo(CO)₃(PMTA) or Mo(CO)₃(Me₃tach) as metal precursors

^{xvi} See Appendix B for spectra of compounds **4a-b** and **5a-b**.



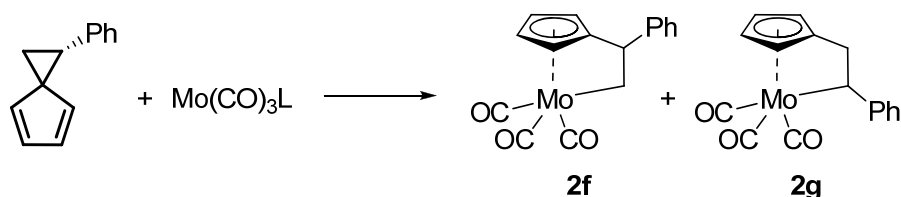
Scheme 16 formation of bimetallic tetrahydroindenyl compounds, originally postulated by Eilbracht *et al.*

11.2 Synthesis and catalytic applications of highly enantioselective *ansa* compounds

The success of the abovementioned cycloalkyl *ansa* compounds has prompted our research towards similar derivatives. The current work is mostly concentrated in the synthesis of related *ansa* species with enhanced chiral inducing capabilities.

11.2.1 Revisiting the epoxidation catalysis of *ansa* compounds

The results shown in the previous sections have highlighted the above-average catalytic activities of the *ansa* derivatives at moderate temperatures (room temperature for Mo derivatives, 55 °C for W derivatives), which in most cases clearly outperform previously obtained results due to the partial decomposition of the catalyst in the catalytic solution at high temperatures.



Scheme 17 Synthesis of compounds **2f** and **2g**.

These facts have prompted us to revisit the previously synthesised *ansa* compounds, especially those with alleged chiral capabilities.

$\text{Mo}(\eta^5\text{-C}_5\text{H}_4((\text{CHPh})\text{CH}_2)\text{-}\eta^1\text{-CH})(\text{CO})_3$, one of the most prominent synthetic attempts of a chiral Mo *ansa*-compound, was reported in 2006 by Zhao *et al.* (53) The authors reported that only one compound (that with the phenyl substituent in α position with respect to the Cp ring) was formed, due to sterical effects and relative stability toward ring-opening reactions (such as β -elimination). Recent studies have shown that the other possible insertion product is also formed in significant proportions. $^1\text{H-NMR}$ and 2D-COSY experiments (shown in Figures 16 and 17) of the majority **2g** isomer display significant differences in the chemical shift of the *ansa* bridge protons. In light of the promising results of related complexes, these compounds are currently under investigation, both from a synthetic point of view as well as from an asymmetric catalysis perspective.

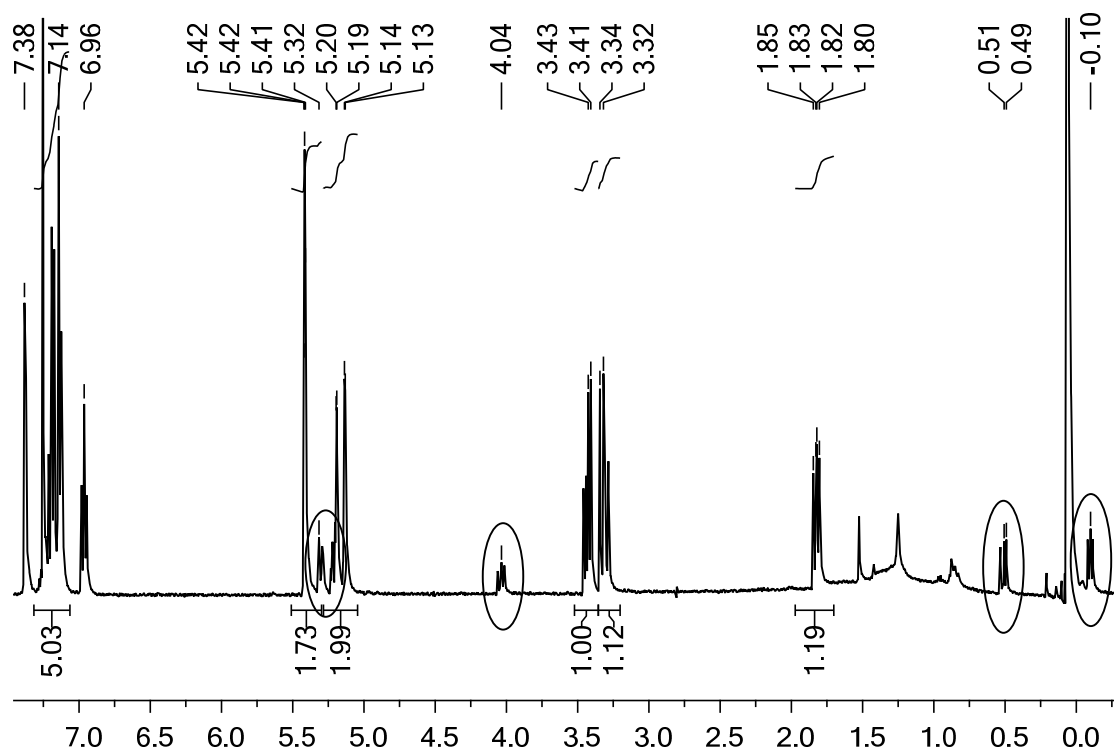


Figure 38 ^1H NMR spectra of compounds **2f** (minor isomer, circled) and **2g**.

To this respect, the preliminary results obtained in the epoxidation of allyl alcohol to glycidol, along with the X-ray studies presented in Section 10.2.4 have prompted the application of the synthesised *ansa* compounds in this direction.

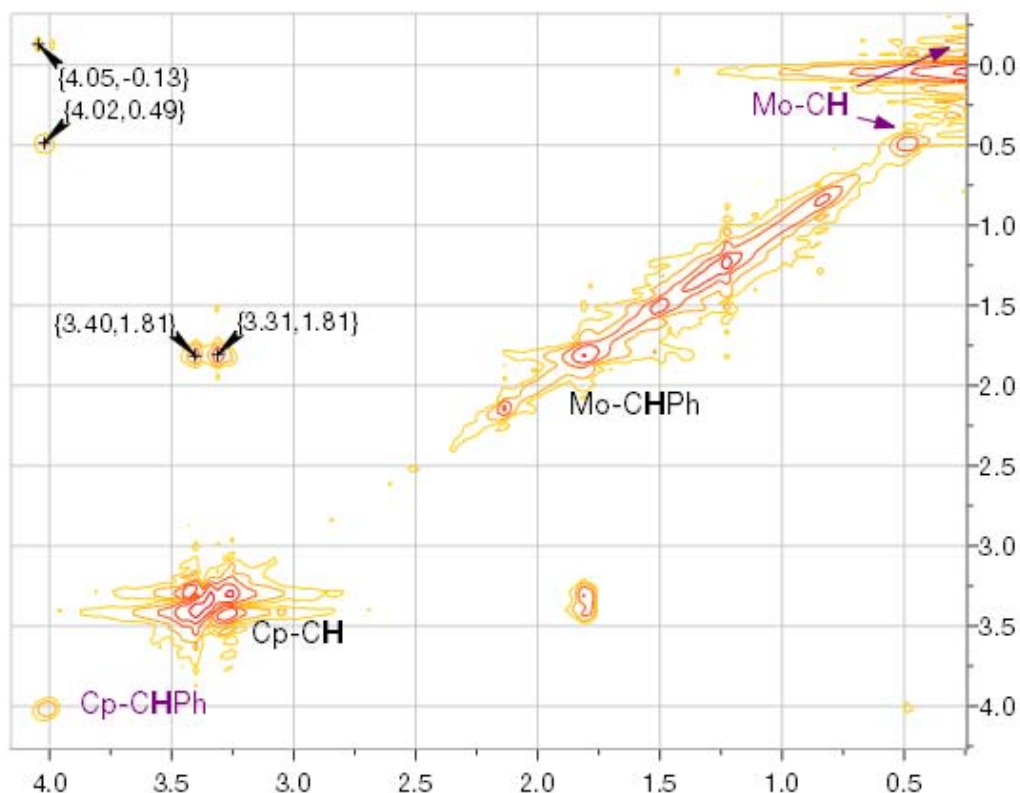


Figure 39 2D-COSY NMR spectra of compounds **2f** (minor isomer, in magenta) and **2g**, showing the interactions between the *ansa*-bridge protons of each compound.

11.2.2 Use of the menthyl moiety as a chiral inducing agent

The previous work of Abrantes *et al.* dealing with menthyl-Cp Mo carbonyls and their application as epoxidation catalysts⁽⁵⁴⁾ has prompted the development of related species. Since the authors pointed out that the low enantiomeric species obtained in the epoxidation of *trans*- β -methylstyrene could result of the free rotation of the cyclopentadienyl ring, it has been suggested that immobilising the menthyl-Cp moiety via an *ansa* bridge could dramatically enhance the chiral induction properties of the catalyst.

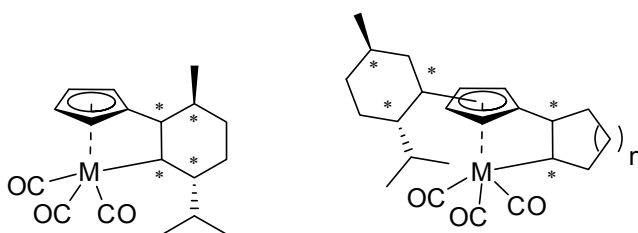
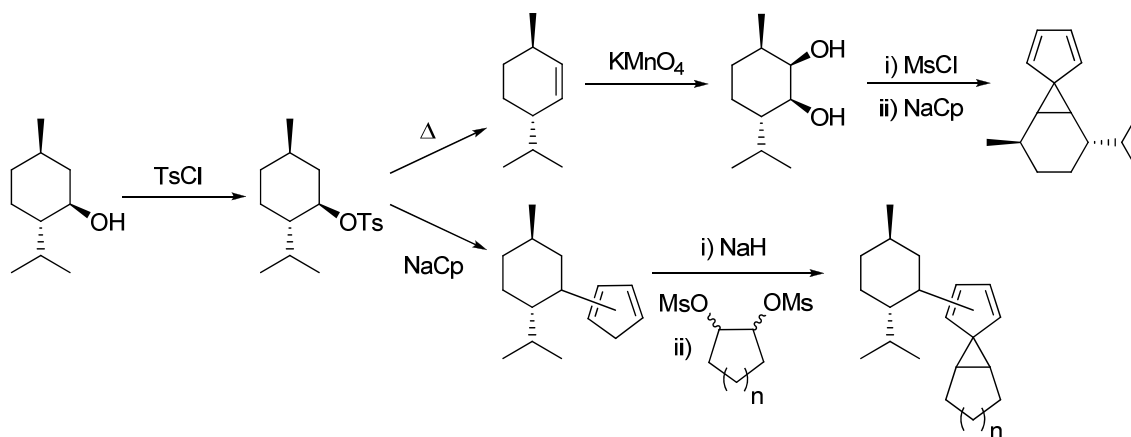


Figure 40 *ansa* menthyl derivatives.

The promising results shown by the *ansa* cycloalkyl derivatives in enantioselective catalysis has prompted us to synthesise menthyl-Cp substituted derivatives of compounds **2a**, **2b** and **2e** as well as to incorporate the menthyl fragment as the *ansa* cycloalkyl ring itself (see Figure 40 and Scheme 18).



Scheme 18 Synthesis of menthyl derivatives, including the synthesis of *cis*-menthenediol to afford the respective spiro ligand (above) and the synthesis of a menthyl-Cp cycloalkyl spiro ligand (below).

Our group has recently synthesised the spiro menthyl derivatives of ligands **1a**, **1b** and **1e** (**1g**, **1h** and **1i**, see Figure 41)^{xvii}. The ¹H-NMR spectra shows a number of isomers, depending on the position of the menthyl substituent and the cycloalkyl ring.

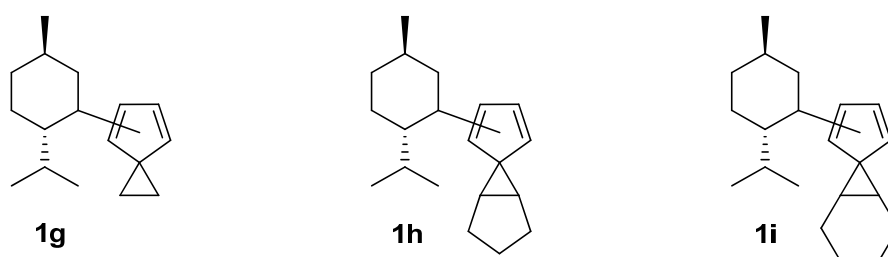


Figure 41 Spiro menthyl derivatives synthesised in our group.

1g and **1h** have been reacted without further purification with $\text{Mo}(\text{CO})_3(\text{Me}_3\text{tach})$. The obtained compounds (dark red oily products) have been characterised by ¹H and ¹³C experiments, as well as 2D COSY experiments. Surprisingly, no signals are observed in the expected C_{ansa} range. A reason for these results might be the formation of a dimeric structure. Mass spectroscopy partly supports these conclusions: apart from a molecular

^{xvii} The ¹H spectra of compound **1g** is featured in section A.1 of the Appendix

peak corresponding to $[M-CO]^+$, a group of smaller peaks which could be assigned to the dimeric species $[2M-CO]^+$, $[2M-2CO]^+$ and $[2M-3CO]^+$ are observed.

The obtained complexes have been also applied as catalysts in the epoxidation of cyclooctene. Preliminary results have shown that the obtained compounds do display catalytic activity, albeit with moderate to low conversions.

11.2.3 Other alkyl ansa derivatives

Apart from the abovementioned menthyl derivatives, a series of new ansa derivatives have been designed. Bicyclic derivatives might be a source for sterically demanding ansa compounds. Thus, our group has synthesised mesylated norbornandiol from the well known norbornene. Attempts to successfully form the spiro ligand from this bicyclic diol in good yields and purities are currently underway.

On the other hand, compounds with quaternary carbons (such as catechol and bi(cyclopentane)-1,1'-diol) in the ansa bridge could feature an improved stability. However, first attempts have not been successful due to the high sensitivity of the obtained mesyl derivatives.

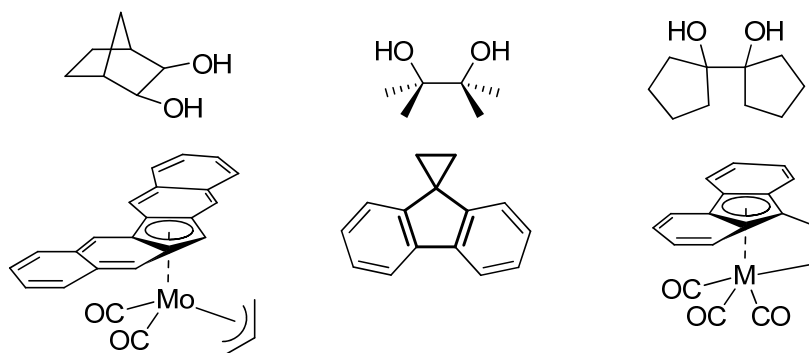


Figure 42 Selection of diols as possible ansa moieties (above). Below: the compound reported by Thiel *et al.*, a spiro derivative of fluorenyl and its expected ansa derivative.

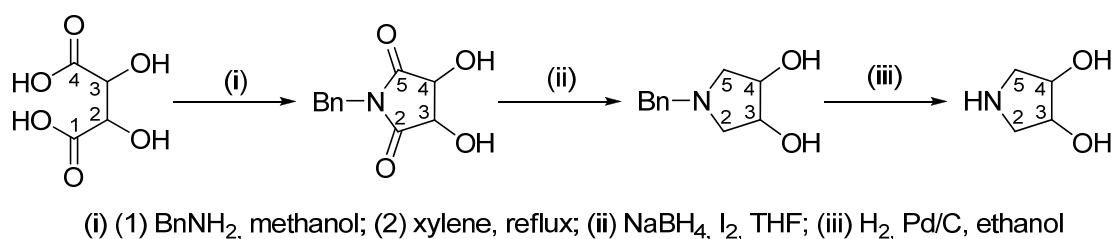
Indenyl and fluorenyl Mo and W derivatives (with or without ansa bridges) are known since the mid 80ies.(122, 123) Further attempts include menthyl-substituted indene spiro ligands, which have been found to form highly chiral rhodium heteroatomic ansa complexes.(145)

More recently, Thiel *et al.* synthesised a Mo dibenzofluorenyl (dbf) derivative (Figure 42, lower left corner).(146) It was found that the diphenyl fragments are bent with respect to the Cp moiety, hindering the rotation of the dbf ligand.

In light of these results, our group is currently attempting the synthesis of indenyl and fluorenyl *ansa* derivatives. However, these compounds display a reduced stability with donor solvents such as THF. Moreover, the metal centre can coordinate either to the phenyl or the cyclopentadienyl moieties, further hindering metal insertion to form the expected *ansa* derivatives.

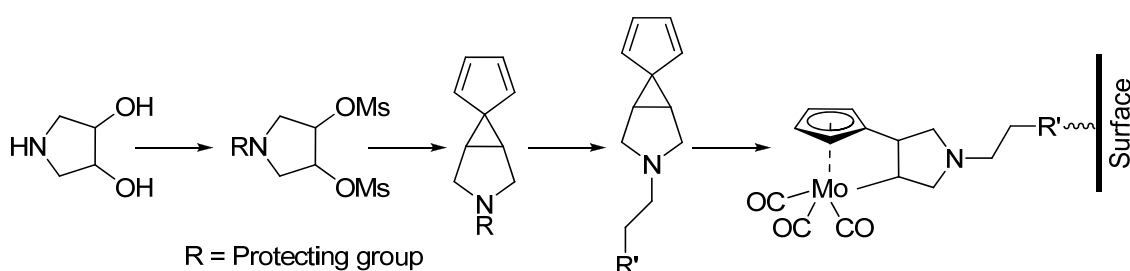
11.2.4 Heterogenisation of the cycloalkyl *ansa* compounds. Synthesis of 3,4-dihydroxypyrrolidines

The stability of the reported compounds has aroused the possibility of functionalising the *ansa* cycloalkyl ring in order to graft it to a surface. A promising candidate, pyrrolidine 3,4-diol, has been synthesised using published procedures (see Scheme 19).(147)



Scheme 19 Synthesis of pyrrolidine-3,4-diol (from (147)).

So far, the substituted pyrrolidine synthesised in step *ii* has afforded the spiro derivative in low yields and purities. The main reason for this fact is the reaction of the benzylic moiety with the strongly basic cyclopentadienide moiety, generating the spiro derivative of the pyrrolidinediol moiety. Current research aims for the synthesis of the latter product, using its deprotonated or protected form to form the expected spiro ligand. A scheme summarising this ongoing work is included below.



Scheme 20 Proposed heterogenisation of the *ansa* compound.

11.2.5 Mechanistic studies

The mechanistic studies of $\text{CpMo}(\text{CO})_3\text{Me}$ reported in the present work have given some insight in the particularities of the epoxidation reaction with alkyl derivatives.⁽¹⁴³⁾ As it has been observed in Chapter 10, our current research with *ansa* compounds is strongly concentrated on studying the catalytic capabilities of these novel compounds. Since many comparisons have been done with the $\text{CpMo}(\text{CO})_3\text{Me}$ systems, our group is trying to isolate the oxidated derivatives of the cycloalkyl *ansa* complexes. So far, it has been observed that the oxidation reaction of the carbonyl species is highly exothermic (which would account for the reduced induction time in comparison with both the chloro and the alkyl derivatives). Moreover, preliminary NMR studies during the catalytic reaction have detected signals in the range for related Cp-M species, which further proves that the *ansa* species are involved in the oxidation reaction. This conclusion rules out the proposed *in situ* formation of non-organometallic molybdenum oxides, which would be the main catalytic species.⁽⁸²⁾

References cited in this chapter

- (1) Fischer, E. O. *Angew. Chem.* **1955**, *67*, 475-482.
- (2) Fischer, E. O.; Vigoureux, S. *Chem. Ber.* **1958**, *91*, 1342-1344.
- (3) Fischer, E. O.; Ulm, K.; Fritz, H. P. *Chem. Ber.* **1960**, *93*, 2167-2173.
- (4) Cotton, F. A.; Wilkinson, G. Z. *Z. Naturforsch.* **1954**, *9b*, 417.
- (5) Cousins, M.; Green, M. L. H. *J. Chem. Soc.* **1963**, 889-895.
- (6) Cousins, M.; Green, M. L. H. *J. Chem. Soc.* **1964**, 1567-1572.
- (7) Cousins, M.; Green, M. L. H. *J. Chem. Soc.* **1969**, 16-19.
- (8) Heyn, B.; Hoffmann, R. Z. *Chem.* **1976**, *16*, 195.
- (9) Kühn, F. E.; Santos, A. M.; Abrantes, M. *Chem. Rev.* **2006**, *106*, 2455-2475.
- (10) Kühn, F. E.; Santos, A. M.; Gonçalves, I. S.; Romão, C. C.; Lopes, A. D. *Appl. Organomet. Chem.* **2001**, *15*, 43-50.
- (11) Katsuki, T.; Martín, V. *Org. React.* **1996**, *48*, 1-299.
- (12) Katsuki, T. *Synlett* **2003**, *3*, 281-297.
- (13) Kühn, F. E.; Zhao, J.; Herrmann, W. A. *Tetrahedron: Asymmetry* **2005**, *16*, 3469-3479.
- (14) Zhao, J.; Zhou, X.; Santos, A. M.; Herdtweck, E.; Romão, C. C.; Kühn, F. E. *Dalton Trans.* **2003**, 3736-3742.
- (15) Duhme-Klair, A.; Vollmer, G.; Mars, C.; Fröhlich, R. *Angew. Chem. Int. Ed.* **2000**, *39*, 1626-1628.
- (16) Bellemin-Laponnaz, S.; Coleman, K. S.; Osborn, J. A. *Polyhedron* **1999**, *18*, 2533-2536.
- (17) Yamada, S.; Mashiko, T.; Terashima, S. *J. Am. Chem. Soc.* **1977**, *99*, 1988-1990.
- (18) Coleman-Kammula, S.; Duim-Koolstra, E. T. *J. Organomet. Chem.* **1983**, *246*, 53-56.
- (19) Herrmann, W. A.; Haider, J. J.; Fridgen, J.; Lobmaier, G. M.; Spiegler, M. *J. Organomet. Chem.* **2000**, *603*, 69-79.
- (20) Gago, S.; Rodríguez-Borges, J. E.; Teixeira, C.; Santos, A. M.; Zhao, J.; Pillinger, M.; Nunes, C. D.; Petrovski, Z.; Santos, T. M.; Kühn, F. E.; Romão, C. C.; Gonçalves, I. S. *J. Mol. Cat. A: Chem.* **2005**, *236*, 1-6.
- (21) Pontes da Costa, A.; Reis, P. M.; Gamelas, C.; Romão, C. C.; Royo, B. *Inorg. Chim. Acta* **2008**, *361*, 1915-1921.
- (22) Payne, G. B.; Smith, C. W. *J. Org. Chem.* **1957**, *22*, 1682-1685.
- (23) Kirshenbaum, K. S.; Sharpless, K. B. *J. Org. Chem.* **1985**, *50*, 1979-1982.

- (24) Sato, K.; Aoki, M.; Ogawa, M.; Hashimoto, T.; Noyori, R. *J. Org. Chem.* **1996**, *61*, 8310-8311.
- (25) Kühn, F. E.; Xue, W.; Al-Ajlouni, A. M.; Santos, A. M.; Zang, S.; Romão, C. C.; Eickerling, G.; Herdtweck, E. *Inorg. Chem.* **2002**, *41*, 4468-4477.
- (26) Jimtaisong, A.; Luck, R. L. *Inorg. Chem.* **2006**, *45*, 10391-10402.
- (27) Crabtree, R. H. *The Organometallic Chemistry of the Transition Metals*; 4th ed.; Wiley, **2005**; p. 538.
- (28) King, R. B.; Bisnette, M. B. *J. Organomet. Chem.* **1967**, *8*, 287-297.
- (29) Romão, C. C.; Kühn, F. E.; Herrmann, W. A. *Chem. Rev.* **1997**, *97*, 3197-3246.
- (30) Valente, A. A.; Seixas, J. D.; Gonçalves, I. S.; Abrantes, M.; Pillinger, M.; Romão, C. C. *Catal. Lett.* **2005**, *101*, 127-130.
- (31) Zybill, C. E. In *Synthetic Methods of Organometallic and Inorganic Chemistry*; Herrmann, W. A., Ed.; Georg Thieme Verlag: Stuttgart - New York, **1997**; Vol. 8, p. 103.
- (32) Tate, D. P.; Knipple, W. R.; Augl, J. M. *Inorg. Chem.* **1962**, *1*, 433-434.
- (33) Faller, J. W.; Lambert, C. *Tetrahedron* **1985**, *41*, 5755-5760.
- (34) Edelmann, F.; Behrens, P.; Behrens, S.; Behrens, U. *J. Organomet. Chem.* **1986**, *310*, 333-355.
- (35) Ellis, J. E.; Rochfort, G. L. *Organometallics* **1982**, *1*, 682-689.
- (36) Lin, J. T.; Ellis, J. E. *J. Am. Chem. Soc.* **1983**, *105*, 6252-6258.
- (37) Lin, J. T.; Yeh, S. K.; Lee, G. H.; Wang, Y. *J. Organomet. Chem.* **1989**, *361*, 89-99.
- (38) Zanotti, V.; Rutar, V.; Angelici, R. J. *J. Organomet. Chem.* **1991**, *414*, 177-191.
- (39) Armanasco, N. L.; Baker, M. V.; North, M. R.; Skelton, B. W.; White, A. H. *J. Chem. Soc., Dalton Trans.* **1998**, 1145-1149.
- (40) Baker, M. V.; North, M. R. *J. Organomet. Chem.* **1998**, *565*, 225-230.
- (41) Armanasco, N. L.; Baker, M. V.; North, M. R.; Skelton, B. W.; White, A. H. *J. Chem. Soc., Dalton Trans.* **1997**, 1363-1368.
- (42) Bottomley, F. *Polyhedron* **1992**, *11*, 1707-1731.
- (43) Roesky, H. W.; Haiduc, I.; Hosmane, N. S. *Chem. Rev.* **2003**, *103*, 2579-2595.
- (44) Faller, J. W.; Ma, Y. *J. Organomet. Chem.* **1988**, *340*, 59-69.
- (45) Faller, J. W.; Ma, Y. *J. Organomet. Chem.* **1989**, *368*, 45-56.
- (46) Faller, J. W.; Ma, Y. *Organometallics* **1988**, *7*, 559-561.
- (47) Freund, C.; Abrantes, M.; Kühn, F. E. *J. Organomet. Chem.* **2006**, *691*, 3718-3729.
- (48) Legzdins, P.; Phillips, E. C.; Rettig, S. J.; Sánchez, L.; Trotter, J.; Yee, V. C. *Organometallics* **1988**, *7*, 1877-1878.
- (49) Radius, U.; Wahl, G.; Sundermeyer, J. Z. *Anorg. Allg. Chem.* **2004**, 848-857.

- (50) Kühn, F. E.; Santos, A. M.; Herrmann, W. A. *Dalton Trans.* **2005**, 3566-3571.
- (51) Abrantes, M.; Santos, A. M.; Mink, J.; Kühn, F. E.; Romão, C. C. *Organometallics* **2003**, *22*, 2112-2118.
- (52) Chakraborty, D.; Bhattacharjee, M.; Krätzner, R.; Siefken, R.; Roesky, H. W.; Usón, I.; Schmidt, H. *Organometallics* **1999**, *18*, 106-108.
- (53) Zhao, J.; Herdtweck, E.; Kühn, F. E. *J. Organomet. Chem.* **2006**, *691*, 2199-2206.
- (54) Abrantes, M.; Sakthivel, A.; Romão, C. C.; Kühn, F. E. *J. Organomet. Chem.* **2006**, *691*, 3137-3145.
- (55) Bunker, M. J.; Green, M. L. H. *J. Chem. Soc. Dalton Trans.* **1981**, 847-851.
- (56) Sheldon, R. A.; Van Doorn, J. A. *J. Catal.* **1973**, *31*, 427-437.
- (57) Zhao, J.; Jain, K. R.; Herdtweck, E.; Kühn, F. E. *Dalton Trans.* **2007**, *47*, 5567-5571.
- (58) Zhao, J.; Santos, A. M.; Herdtweck, E.; Kühn, F. E. *J. Mol. Catal. A: Chem.* **2004**, *222*, 265-271.
- (59) Zhao, J.; Sakthivel, A.; Santos, A. M.; Kühn, F. E. *Inorg. Chim. Acta* **2005**, *358*, 4201-4207.
- (60) Sakthivel, A.; Zhao, J.; Hanzlik, M.; Kühn, F. E. *Dalton Trans.* **2004**, 3338-3341.
- (61) Sakthivel, A.; Zhao, J.; Hanzlik, M.; Chiang, A. S. T.; Herrmann, W. A.; Kühn, F. E. *Adv. Synth. Catal.* **2005**, *347*, 473-483.
- (62) Sakthivel, A.; Zhao, J.; Kühn, F. E. *Catal. Lett.* **2005**, *102*, 115-119.
- (63) Sakthivel, A.; Zhao, J.; Raudaschl-Sieber, G.; Kühn, F. E. *J. Organomet. Chem.* **2005**, *690*, 5105-5112.
- (64) Sakthivel, A.; Zhao, J.; Kühn, F. E. *Microporous and Mesoporous Materials* **2005**, *86*, 341-348.
- (65) Sakthivel, A.; Zhao, J.; Raudaschl-Sieber, G.; Hanzlik, M.; Chiang, A. S. T.; Kühn, F. E. *Appl. Catal. A: General* **2005**, *281*, 267-273.
- (66) Kühn, F. E.; Zhao, J.; Abrantes, M.; Sun, W.; Afonso, C. A. M.; Branco, L. C.; Gonçalves, I. S.; Pillinger, M.; Romão, C. C. *Tetrahedron Letters* **2005**, *46*, 47-52.
- (67) Al-Ajlouni, A. M.; Espenson, J. H. *J. Am. Chem. Soc.* **1995**, *117*, 9243-9250.
- (68) Al-Ajlouni, A. M.; Espenson, J. H. *J. Org. Chem.* **1996**, *61*, 3969-3976.
- (69) Espenson, J. H. *Chem. Commun.* **1999**, *6*, 479.
- (70) Bouh, A. O.; Espenson, J. H. *J. Mol. Catal. A: Chem.* **2003**, *200*, 43-47.
- (71) Li, M.; Espenson, J. H. *J. Mol. Catal. A: Chem.* **2004**, *208*, 123-128.
- (72) Chaumette, P.; Mimoun, H.; Saussine, L.; Fischer, J.; Mitschler, A. *J. Organomet. Chem.* **1983**, *250*, 291-310.
- (73) Chong, A. O.; Sharpless, K. B. *J. Org. Chem.* **1977**, *42*, 1587-1590.

- (74) Thiel, W. R. *J. Mol. Catal. A: Chem.* **1997**, *117*, 449-454.
- (75) Wahl, G.; Kleinhenz, D.; Schorm, A.; Sundermeyer, J.; Stowasser, R.; Rummey, C.; Bringmann, G.; Fickert, C.; Kiefer, W. *Chem. Eur. J.* **1999**, *5*, 3237-3251.
- (76) Kühn, F. E.; Groarke, M.; Bencze, É.; Herdtweck, E.; Prazeres, A.; Santos, A. M.; Calhorda, M. J.; Romão, C. C.; Gonçalves, I. S.; Lopes, A. D.; Pillinger, M. *Chem. Eur. J.* **2002**, *8*, 2370-2383.
- (77) Herrmann, W. A.; Fischer, R. W.; Scherer, W.; Rauch, M. U. *Angew. Chem. Int. Ed.* **1993**, *32*, 1157-1160.
- (78) Herrmann, W. A.; Fischer, R. W.; Rauch, M. U.; Scherer, W. *J. Mol. Catal.* **1994**, *86*, 243-266.
- (79) Trost, M. K.; Bergman, R. G. *Organometallics* **1991**, *10*, 1172-1178.
- (80) Legzdins, P.; Phillips, E. C.; Sánchez, L. *Organometallics* **1989**, *8*, 940-949.
- (81) Robin, T.; Montilla, F.; Galindo, A.; Ruiz, C.; Hartmann, J. *Polyhedron* **1999**, *18*, 1485-1490.
- (82) Pratt, M.; Harper, J. B.; Colbran, S. B. *Dalton Trans.* **2007**, 2746-2748.
- (83) Bottomley, F.; Boyle, P. D.; Chen, J. *Organometallics* **1994**, *13*, 370-373.
- (84) Honzicek, J.; Almeida Paz, F. A.; Romão, C. C. *Eur. J. Inorg. Chem.* **2007**, 2827-2838.
- (85) Sheldon, R. A. *Recl. Trav. Chim.* **1973**, *92*, 253.
- (86) Poli, R. *Chem. Eur. J.* **2004**, *10*, 332-341.
- (87) Hroch, A.; Gemmecker, G.; Thiel, W. R. *Eur. J. Inorg. Chem.* **2000**, 1107-1114.
- (88) Veiros, L. F.; Prazeres, A.; Costa, P. J.; Romão, C. C.; Kühn, F. E.; Calhorda, M. J. *Dalton Trans.* **2006**, *11*, 1383-1389.
- (89) Al-Ajlouni, A.; Valente, A.; Nunes, C. D.; Pillinger, M.; Santos, A. M.; Zhao, J.; Romão, C. C.; Gonçalves, I. S.; Kühn, F. E. *Eur. J. Inorg. Chem.* **2005**, 1716-1723.
- (90) Omae, I. *Coord. Chem. Rev.* **1982**, *42*, 31-54.
- (91) Omae, I. *Coord. Chem. Rev.* **1988**, *83*, 137-167.
- (92) Raith, A.; Altmann, P.; Kühn, F. E. *Coord. Chem. Rev.* **2009**, *in press*.
- (93) Green, J. C. *Chem. Soc. Rev.* **1998**, *27*, 263-271.
- (94) Brintzinger, H. H.; Fischer, D.; Mülhaupt, R.; Rieger, B.; Waymouth, R. M. *Angew. Chem. Int. Ed. Engl.* **1995**, *34*, 1143-1170.
- (95) Gómez-Ruiz, S.; Polo-Cerón, D.; Prashar, S.; Fajardo, M.; Cruz, V. L.; Ramos, J.; Hey-Hawkins, E. *J. Organomet. Chem.* **2008**, *693*, 601-610.
- (96) Wang, H.; Kehr, G.; Fröhlich, R.; Erker, G. *Angew. Chem. Int. Ed.* **2007**, *46*, 4905-4908.
- (97) Manners, I. *Can. J. Chem.* **1998**, *76*, 371-381.
- (98) Wang, C.; Kehr, G.; Wedeking, K.; Fröhlich, R. *Organometallics* **2005**, *24*, 4760-4773.
- (99) Kunz, D.; Erker, G.; Fröhlich, R.; Kehr, G. *Eur. J. Inorg. Chem.* **2000**, 409-416.

- (100) Avey, A.; Weakley, T. J. R.; Tyler, D. R. *J. Am. Chem. Soc.* **1993**, *115*, 7706-7715.
- (101) Liu, G.; Lu, X.; Gagliardo, M.; Beetstra, D. J.; Meetsma, A.; Hessen, B. *Organometallics* **2008**, *27*, 2316-2320.
- (102) Weiss, E.; Hübel, W. *Chem. Ber.* **1962**, *95*, 1186-1196.
- (103) Behrens, U.; Weiss, E. *J. Organomet. Chem.* **1974**, *73*, C64-C66.
- (104) Behrens, U.; Weiss, E. *J. Organomet. Chem.* **1975**, *96*, 399-433.
- (105) Behrens, U.; Weiss, E. *J. Organomet. Chem.* **1975**, *96*, 435-450.
- (106) Behrens, U.; Karnatz, D.; Weiss, E. *J. Organomet. Chem.* **1976**, *117*, 171-182.
- (107) Waldbaum, B. R.; Kerber, R. C. *Inorg. Chim. Acta* **1999**, *291*, 109-126.
- (108) Wilcox Jr., C. F.; Craig, R. R. *J. Am. Chem. Soc.* **1961**, *83*, 3866-3871.
- (109) Eilbracht, P. *Chem. Ber.* **1976**, *109*, 1429-1435.
- (110) Eilbracht, P.; Dahler, P.; Mayser, U.; Henkes, E. *Chem. Ber.* **1980**, *113*, 1033-1046.
- (111) Eilbracht, P. *J. Organomet. Chem.* **1976**, *120*, C37-C38.
- (112) Eilbracht, P.; Dahler, P. *J. Organomet. Chem.* **1977**, *127*, C48-C50.
- (113) Eilbracht, P.; Mayser, U.; Tiedtke, G. *Chem. Ber.* **1980**, *113*, 1420-1430.
- (114) Eilbracht, P.; Mayser, U. *Chem. Ber.* **1980**, *113*, 2211-2220.
- (115) Eilbracht, P.; Dahler, P.; Tiedtke, G. *J. Organomet. Chem.* **1980**, *185*, C25-C28.
- (116) Eilbracht, P. *Chem. Ber.* **1976**, *109*, 3136-3141.
- (117) Eilbracht, P.; Fassmann, W.; Diehl, W. *Chem. Ber.* **1985**, *118*, 2314-2329.
- (118) Eilbracht, P.; Dahler, P. *J. Organomet. Chem.* **1977**, *135*, C23-C25.
- (119) Eilbracht, P.; Dahler, P. *J. Organomet. Chem.* **1977**, *135*, C23-C25.
- (120) Braun, S.; Dahler, P.; Eilbracht, P. *J. Organomet. Chem.* **1978**, *146*, 135-141.
- (121) Eilbracht, P.; Dahler, P. *Chem. Ber.* **1980**, *113*, 542-554.
- (122) Novikova, L. N.; Ustynyuk, N. A.; Zvorykin, V. E.; Dneprovskaya, L. S.; Ustynyuk, Y. A. *J. Organomet. Chem.* **1985**, *292*, 237-243.
- (123) Ustynyuk, N. A.; Novikova, L. N.; Zvorykin, V. E.; Kravtsov, D. N.; Ustynyuk, Y. A. *J. Organomet. Chem.* **1988**, *338*, 19-28.
- (124) Kühn, F. E.; Santos, A. M.; Lopes, A. D.; Gonçalves, I. S.; Rodríguez-Borges, J. E.; Pillinger, M.; Romão, C. C. *J. Organomet. Chem.* **2001**, *621*, 207-217.
- (125) Berkessel, A.; Kaiser, P.; Lex, J. *Chem. Eur. J.* **2003**, *9*, 4746-4756.
- (126) Gonçalves, I. S.; Santos, A. M.; Romão, C. C.; Pillinger, M.; Ferreira, P.; Rocha, J.; Kühn, F. E. *J. Organomet. Chem.* **2001**, *626*, 1-10.
- (127) Tucker, C. E.; Davenport, K. G.; US 5618958, **1997**.
- (128) Sabater, M. J.; Domint, M. E.; Corma, A. *J. Catal.* **2002**, *210*, 192-197.
- (129) Zhou, X.; Zhao, J.; Santos, A. M.; Kühn, F. E. *Z. Naturforsch.* **2004**, *59b*, 1223-1228.

- (130) Cross, R. J.; Newman, P. D.; Peacock, R. D.; Stirling, D. *J. Mol. Cat. A: Chem.* **1999**, *144*, 273-284.
- (131) Fridgen, J.; Herrmann, W. A.; Eickerling, G.; Santos, A. M.; Kühn, F. E. *J. Organomet. Chem.* **2004**, *689*, 2752-2761.
- (132) Valente, A. A.; Gonçalves, I. S.; Lopes, A. D.; Rodríguez-Borges, J. E.; Pillinger, M.; Romão, C. C.; Rocha, J.; García-Mera, X. *New J. Chem.* **2001**, *25*, 959-964.
- (133) Haider, J. J.; Kratzer, R. M.; Herrmann, W. A.; Zhao, J.; Kühn, F. E. *J. Organomet. Chem.* **2004**, *689*, 3735-3740.
- (134) Ciruelos, S.; Englert, U.; Salzer, A.; Bolm, C.; Maischak, A. *Organometallics* **2000**, *19*, 2240-2242.
- (135) Amor, F.; Royo, P.; Spaniol, T. P.; Okuda, J. *J. Organomet. Chem.* **2000**, *604*, 126-131.
- (136) Barretta, A.; Chong, K. S.; Cloke, F. G. N.; Feigenbaum, A.; Green, M. L. H. *J. Chem. Soc. Dalton Trans.* **1983**, 861-864.
- (137) Barretta, A.; Cloke, F. G. N.; Feigenbaum, A.; Green, M. L. H.; Gourdon, A.; Prout, K. *Chem. Commun.* **1981**, 156-158.
- (138) Doppiu, A.; Englert, U.; Salzer, A. *Inorg. Chim. Acta* **2003**, *350*, 435-441.
- (139) Ciruelos, S.; Doppiu, A.; Englert, U.; Salzer, A. *J. Organomet. Chem.* **2002**, *663*, 183-191.
- (140) Thiel, W. R.; Priermeier, T. *Angew. Chem. Int. Ed. Engl.* **1995**, *34*, 1737-1738.
- (141) Abrantes, M.; Valente, A.; Pillinger, M.; Gonçalves, I. S.; Rocha, J.; Romão, C. C. *J. Catal.* **2002**, *209*, 237-244.
- (142) Martins, A. M.; Romão, C. C.; Abrantes, M.; Azevedo, M. C.; Cui, J.; Dias, A. R.; Duarte, M. T.; Lemos, M. A.; Lourenço, T.; Poli, R. *Organometallics* **2005**, *24*, 2582-2589.
- (143) Al-Ajlouni, A. M.; Veljanovski, D.; Capapé, A.; Zhao, J.; Herdtweck, E.; Calhorda, M. J.; Kühn, F. E. *Organometallics* **2009**, *28*, 639-645.
- (144) Sweany, R. L.; Comberrel, D. S.; Dombourian, M. F.; Peters, N. A. *J. Organomet. Chem.* **1981**, *216*, 57-63.
- (145) Kataoka, Y.; Iwato, Y.; Yamagata, T.; Tani, K. *Organometallics* **1999**, *18*, 5423-5425.
- (146) Pammer, F.; Sun, Y.; May, C.; Wolmershäuser, G.; Kelm, H.; Krüger, H.; Thiel, W. R. *Angew. Chem. Int. Ed.* **2007**, *46*, 1270-1273.
- (147) Rejman, D.; Kocialka, P.; Budešínský, M.; Pohl, R.; Rosenberg, I. *Tetrahedron* **2007**, *63*, 1243-1253.

IV. EXPERIMENTAL SECTION

12. Synthesis and Catalytic Applications of MTO Schiff Base Complexes (Chapter 6)

12.1 Materials and methods

All preparations and manipulations were performed using standard Schlenk techniques under an argon atmosphere. However, in the case of **1** - **3** the synthesis can be carried out under air without decomposition of the products. Solvents were dried by standard procedures (*n*-hexane and Et₂O over Na/benzophenone; CH₂Cl₂ over CaH₂), distilled under argon and kept over molecular sieves. Elemental analyses were performed with a Flash EA 1112 series elemental analyser. ¹H, ¹³C NMR and ¹⁷O NMR were measured in CDCl₃ with a Mercury-VX 300, a Varian 270 and 400 or a 400 MHz Bruker Avance DPX-400 spectrometers. IR spectra were recorded with a Perkin Elmer FT-IR spectrometer using KBr pellets as the IR matrix. CI mass spectra (isobutene as CI gas) were obtained with a Finnigan MAT 90 mass spectrometer. Catalytic runs were monitored by GC methods on a Varian CP-3800 instrument equipped with a FID and a VF-5ms column or on a Hewlett-Packard instrument HP 5890 Series II equipped with a FID, a Supelco column Alphasex 120 and a Hewlett-Packard integration unit HP 3396 Series II. The Schiff base ligands were prepared as described previously.⁽¹⁻³⁾.

12.2 Synthesis of the Schiff base adducts

Compounds **1**–**10** were prepared as follows: A solution of [(CH₃)ReO₃] (0.2 g, 0.8 mmol) in diethyl ether (5 mL) was added dropwise to an equally concentrated solution of ligand (0.8 mmol) in diethyl ether (5 mL) whilst stirring at room temperature. After 20-30 min the yellow-orange solution-mixture was dried (compounds **1** - **4**) or concentrated to about 3

mL (**5 - 10**) under oil pump vacuum and the orange/red precipitate recrystallised from a CH_2Cl_2 /hexane mixture.

1: Yield: 82 %. ^1H NMR (400 MHz, CDCl_3 , 25°C): $\delta = 15.46$ (d, $^4J_{(\text{H-H})} = 2.75$, 1H, C-OH), 9.31 (d, $^4J_{(\text{H-H})} = 3.7$, 1H, CH=N), 8.1-7.1 (m, H aryl), 2.59 (s, 3H, CH_3 -MTO). ^{13}C NMR (100.28 MHz, CDCl_3): $\delta = 171.26$ (C-OH), 154.13 (CH=N), 144.61, 136.90, 129.71, 129.40, 128.14, 126.56, 123.55, 122.51, 120.12, 118.74, 108.70 (aryl-C), 19.46 (CH_3 -MTO). IR (KBr): see Tables 1 and 2. MS (CI): m/z (%) 498.1 [M^+], 250.9 [M^+ -MTO], 248.9 [M^+ -L]. Elemental analysis calcd. (%) for $\text{C}_{18}\text{H}_{16}\text{NO}_4\text{Re}$ (496.53): C 43.54, H 3.25, N 2.82; Found: C 43.84, H 3.24, N 2.81.

2: Yield: 80 %. ^1H NMR (400 MHz, CDCl_3 , 25°C): $\delta = 15.49$ (d, $^4J_{(\text{H-H})} = 3.7$, 1H, C-OH), 9.23 (d, $^4J_{(\text{H-H})} = 4.9$, 1H, CH=N), 8.1-7.0 (m, H-aryl), 2.50 (s, 3H, CH_3 -MTO), 2.38 (s, 1H, Ph- CH_3). ^{13}C -NMR (100.28 MHz, CDCl_3): $\delta = 171.87$ (C-OH), 153.72 (CH=N), 141.33, 137.19, 136.66, 133.31, 130.29, 129.37, 128.10, 127.06, 123.43, 122.69, 119.77, 118.62 (aryl-C), 70.57, 26.48, 20.99 (CH_3 -Ph), 19.88 (CH_3 -MTO). IR(KBr): see Tables 1 and 2. MS (CI): m/z (%) 262.1 [M^+ -MTO], 251.0 [M^+ -L]. Elemental analysis calcd. (%) for $\text{C}_{19}\text{H}_{18}\text{NO}_4\text{Re}$ (510.56): C 44.70, H 3.55, N 2.74; Found: C 45.07, H 3.53, N 2.69.

3: Yield: 94 %. ^1H NMR (270 MHz, CDCl_3 , 25°C): $\delta = 15.72$ (d, $^4J_{(\text{H-H})} = 5.6$, 1H, C-OH), 9.26 (d, $^4J_{(\text{H-H})} = 5.8$, 1H, CH=N), 8.1-7.0 (m, H-aryl), 2.58 (s, 1H, CH_3 -MTO), 2.45-2.42 (s, 2H, Ph- CH_3). ^{13}C -NMR (100.28 MHz, CDCl_3): $\delta = 172.51$ (C-OH), 153.13 (CH=N), 137.15, 130.96, 129.39, 128.11, 127.24, 123.44, 122.98, 118.66, 117.72, 108.71 (aryl-C), 21.15, 17.70 (CH_3 -Ph), 19.26 (CH_3 -MTO). IR(KBr): see Tables 1 and 2. MS (CI): m/z (%) 276.1 [M^+ -MTO], 250.9 [M^+ -L]. Elemental analysis calcd. (%) for $\text{C}_{20}\text{H}_{20}\text{NO}_4\text{Re}$ (524.58): C 45.79, H 3.84, N 2.67; Found: C 45.69, H 3.76, N 2.63.

4: Yield: 75 %. ^1H NMR (400MHz, CDCl_3 , 25°C): $\delta = 15.40$ (d, $^4J_{(\text{H-H})} = 3.2$, 1H, C-OH), 9.39 (d, $^4J_{(\text{H-H})} = 3.2$, 1H, CH=N), 8.1-7.1 (m, H-aryl), 2.62 (s, 1H, CH_3 -MTO). ^{13}C -NMR (100.28 MHz, CDCl_3): $\delta = 168.97$ (C-OH), 155.60 (CH=N), 143.23, 136.83, 133.09, 130.38, 129.43, 128.16, 127.88, 127.50, 127.14, 123.73, 121.71, 118.96, 118.67, 109.22 (C-aryl), 19.09 (CH_3 -MTO). IR(KBr): see Tables 1 and 2. MS (CI): m/z (%) 282.0 [M^+ -MTO], 250.9 [M^+ -L]. Elemental analysis calcd. (%) for $\text{C}_{18}\text{H}_{15}\text{ClNO}_4\text{Re}$ (552.2): C 40.72, H 2.85, N 2.64, Cl 6.68; Found: C 40.53, H 2.84, N 2.44, Cl 6.78.

5: (colour: red) Yield: 85 %; $^1\text{H-NMR}$ (400 MHz, CDCl_3 , RT): δ = 13.07 (s, 1H; NH), 8.70 (s, 1H; CH=N), 7.51-7.34 (m, 6H; Ph), 7.11-6.94 (m, 2H; Ph), 2.63 ppm (s, 3H; MTO- CH_3); IR (KBr): see Table 1; MS (70eV, Cl): m/z (%): 232.00 (100) [$\text{C}_{13}\text{H}_{10}\text{ClNO}+\text{H}^+$] $^+$, 336.0 (13.53), 463.0 (3.19); elemental analysis: calcd (%) for $\text{C}_{14}\text{H}_{13}\text{ClNO}_4\text{Re}$ (480.92): C 34.96, H 2.72, N 2.91; found: C 35.07, H 2.77, N 2.95.

6: (colour: orange) Yield: 86 %; $^1\text{H-NMR}$ (300 MHz, CDCl_3 , RT): δ =13.25 (s, 1H; NH), 8.60 (s, 1H; CH=N), 7.40-7.25 (m, 3H; Ph), 7.03-6.82 (m, 5H;Ph), 3.84 (3H, s, OCH_3), 2.60 ppm(3H, s, MTO- CH_3); IR(KBr): see Tables 1; MS (70eV, Cl): m/z (%): 228.1 (100) [$\text{C}_{14}\text{H}_{13}\text{NO}_2+\text{H}^+$] $^+$, 251.0 (48.15) [$\text{CH}_3\text{ReO}_3+\text{H}^+$] $^+$; elemental analysis: calcd (%) for $\text{C}_{15}\text{H}_{16}\text{NO}_5\text{Re}$ (476.50): C 37.82, H 3.36, N 2.94; found: C 37.99, H 3.24, N 2.88.

7: (colour: red) Yield: 78 %; $^1\text{H-NMR}$ (400 MHz, CDCl_3 , RT): δ =13.49 (s, 1H; NH), 8.61 (s, 1H; CH=N), 7.45-7.28 (m, 3H; Ph), 7.23-7.10 (m, 4H; Ph), 6.97-6.94(m, 1H; Ph), 2.61 (s, 3H; MTO- CH_3), 2.40 ppm (s, 3H; CH_3); IR (KBr): see Table 1; MS (70eV, Cl): m/z (%): 212.10 (100) [$\text{C}_{14}\text{H}_{13}\text{NO}+\text{H}^+$] $^+$, 250.1 (1.52) [CH_3ReO_3] $^+$; elemental analysis: calcd (%) for $\text{C}_{15}\text{H}_{16}\text{O}_4\text{NRe}$ (461.06): C 39.12, H 3.50, N 3.04; found: C 39.17, H 3.57, N 3.09.

8: (colour: orange) Yield: 80 %; $^1\text{H-NMR}$ (300 MHz, CDCl_3 , RT): δ =13.43 (s, 1H; NH), 8.60 (s, 1H; CH=N), 7.38-7.26 (m, 4H; Ph), 7.03-6.90 (m, 4H; Ph), 4.08-4.03 (q, 2H; CH_2), 2.60 (s, 3H; MTO- CH_3), 1.45-1.42 (t, 3H; CH_3); IR (KBr): see Table 1; MS (70eV, Cl): m/z (%): 242.1 (100) [$\text{C}_{15}\text{H}_{15}\text{NO}_2+\text{H}^+$] $^+$, 298.1 (25.54), 483.0 (11.78); elemental analysis: calcd (%) for $\text{C}_{16}\text{H}_{18}\text{O}_5\text{NRe}$ (490.52) C 39.18, H 3.70, N 2.86; found: C 39.19, H 3.74, N 2.94.

9: (colour: red) Yield: 82 %; $^1\text{H-NMR}$ (400 MHz, DMSO, RT): δ =13.41 (s, 1H; NH), 9.66 (s, 1H; OH), 8.90 (s, 1H; CH=N), 7.60-7.57 (m, 1H; Ph), 7.38-7.30 (m, 3H; Ph), 6.97-6.82 (m, 4H; Ph), 1.90 ppm (s, 3H, MTO- CH_3); IR (KBr): see Tables 2 and 3 (p. 67); MS (70eV, Cl): m/z (%): 212.1 (68.32) [$\text{C}_{13}\text{H}_{11}\text{NO}_2+\text{H}^+$] $^+$, 251.0 (60.02) [$\text{CH}_3\text{ReO}_3+\text{H}^+$] $^+$; elemental analysis: calcd (%) for $\text{C}_{14}\text{H}_{14}\text{O}_5\text{NRe}$ (462.47): C 36.36, H 3.05, N 3.03; found: C 36.41, H 3.09, N 3.05.

10: (colour: red) Yield 79 % $^1\text{H-NMR}$ (CDCl_3 , 300MHz, 25°C, ppm): δ = 13.63 (C-OH, s, 1H), 8.62 (CH=N, s, 1H), 7.32-6.83 (aryl-H, m, 7H), 3.94 (Ph- OCH_3 , s, 3H), 3.85 (Ph- OCH_3 , s, 3H), 2.62 (Re- CH_3 , s, 3H); $^{13}\text{C-NMR}$ (CDCl_3 , 100.28 MHz, 25°C, ppm): δ = 196.59 (C-OH), 162.73, 160.49 (CH=N), 151.51, 149.48, 130.14, 123.83, 118.51, 114.86, 113.27, 112.62, 107.01 (C-aryl), 56.20, 55.38 (O- CH_3), 19.11 (Re- CH_3); IR(KBr, $\nu[\text{cm}^{-1}]$):

1646s ν (CH=N), 1500s, 1488s, 1371m, 1297m ν (C-OH), 1266s, 1142m, 1006m ν_s (Re=O), 931s, 917vs ν_{as} (Re=O), 742s, 555m; CI-MS (70 eV): m/z =258.1 [M^+ -MTO], 251.0 [M^+ -L]; elemental analysis: calcd (%) for $C_{16}H_{18}NO_6Re$ (506.52): C, 37.94; H, 3.58; N, 2.77; found: C, 38.49; H, 3.47; N, 2.70.

12.3 X-ray crystal determination of compounds 5-9

Complexes 5 and 6

General: Preliminary examination and data collection were carried out on an area detecting system (**5**: STOE IPDS 2T; **6**: NONIUS κ -CCD device) at the window of a rotating anode (NONIUS FR591) and graphite monochromated Mo- K_α radiation ($\lambda = 0.71073$ Å). Data collections were performed at 173 K (OXFORD CRYOSYSTEMS). Reflections were integrated, corrected for Lorentz, polarisation, absorption effects, and arising from the scaling procedure for latent decay. The structures were solved by a combination of direct methods and difference Fourier syntheses. All non-hydrogen atoms were refined with anisotropic displacement parameters. All hydrogen atoms were calculated in ideal positions (**5**: riding model, $d_{C-H} = 0.95$ and 0.98 Å **6**: riding model, $d_{N-H} = 0.88$ Å and $d_{C-H} = 0.95$ and 0.98 Å). Isotropic displacement parameters were calculated from the parent carbon/nitrogen atom ($U_{iso(H)} = 1.2/1.5U_{eq(C)}$). Full-matrix least-squares refinements were carried out by minimising $w(F_o^2 - F_c^2)^2$ with the SHELXL-97 weighting scheme. The final residual electron density maps show no remarkable features. *Specials 5*: Small extinction effects were corrected with the SHELXL-97 procedure [$\epsilon = 0.0105(5)$]. The hydrogen atom located at the nitrogen atom was found in the final difference Fourier maps and was allowed to refine freely ($d_{N-H} = 0.80(7)$ Å). CCDC reference numbers 702104(5) (compound **5**), 702105(6) (compound **6**). (4-10)

Complexes 7-9

The diffraction data were obtained with a Bruker Smart 1000 CCD diffractometer operating at 50kV and 30mA using Mo- K_α radiation ($\lambda = 0.71073$ Å). Data collection was performed at 293 K with a diffraction measurement method and reduction was performed using the SMART and SAINT software with frames of 0.3° oscillation in the range $1.5 < \theta < 26.2^\circ$. An empirical absorption correction was applied using the

SADABS program. The structures were solved by direct methods and all non-hydrogen atoms were subjected to anisotropic refinement by full-matrix least squares on F^2 using the SHELXTL package. All hydrogen atoms were generated geometrically (C-H bond lengths fixed at 0.96 Å), assigned appropriate isotropic thermal parameters, and included in structure factor calculations in the final stage of F^2 refinement. CCDC reference numbers 648768 (Compound **7**), 648766 (Compound **8**), 648767 (Compound **9**). (11-14)

12.4 Catalytic reactions

Method A: *Cis-cyclooctene* (800 mg, 7.3 mmol), 1.00 g mesitylene (internal standard), H₂O₂ (30 % aqueous solution; 1.62 mL, 14.6 mmol) and 1 mol % (73 μmol) of compounds **1–10** or 0.1 mol % (7.3 μmol) of compound **5** as catalyst were mixed.

Method B: 1-octene (343.2 mg, 3.12 mmol), 429 mg mesitylene (internal standard), H₂O₂ (30 % aqueous solution) (0.64 mL, 6.24 mmol,) and 1 mol % (31.3 μmol) of catalyst (**5–9**) were mixed.

Method C: Styrene (250 mg, 2.39 mmol), 100 mg mesitylene (internal standard), H₂O₂ (30 % aqueous solution) (0.53 mL, 4.78 mmol,) and 1 mol % (24 μmol) of catalyst (**5–9**) were mixed.

Olefins, mesitylene (internal standard) and the catalysts were added to the reaction vessel under standard conditions and diluted in CH₂Cl₂. The reaction began with the addition of H₂O₂. The course of the reaction was monitored by quantitative GC analysis (cyclooctene and styrene) and GC-MS analysis (1-octene). Samples were taken in regular time intervals, diluted with CH₂Cl₂, and treated with a catalytic amount of MgSO₄ and MnO₂ to remove water and to destroy the excess of peroxide. The resulting slurry was filtered and the filtrate injected into a GC column. The conversion of cyclooctene, 1-octene, styrene and the formation of the corresponding oxides were calculated from calibration curves ($r^2 = 0.999$) recorded prior to the reaction course.

13. Kinetic Studies on the Oxidation of η^5 -Cyclopentadienyl Methyl Tricarbonyl Molybdenum(II) and the use of its Oxidation Products as Olefin Epoxidation Catalysts (Chapter 8)

13.1 Materials and methods

All preparations were carried out under an oxygen- and water-free argon atmosphere using standard Schlenk techniques. All solvents were derived from MBraun solvent purification system. Cyclooctene and -methoxystyrene (Aldrich) were used as received without further purifications. TBHP (Aldrich, 5.0-6.0 M solution in decane) was used after drying over molecular sieves to remove the residual water (< 4 % when received). IR spectra were measured with a JASCO FT-IR-460 Plus spectrometer using KBr pellets. NMR spectra were measured applying a JEOL 400 and 400-MHz Bruker Avance DPX-400 spectrometer. The UV spectra were measured on JASCO UV-Vis V-550 spectrophotometer.

13.2 Synthesis of $\text{CpMo}(\text{O}_2)\text{OCH}_3$

Complex **1** (1 mmol, 260 mg) was mixed with 10 eq TBHP (10 mmol) in 40 mL dichloromethane at room temperature. The oxidation continued for 3 h, and then MnO_2 was added to quench the reaction. After another 1 h stirring, the solution was filtrated to removed MnO_2 and any solid residue. Then the solvent was evaporated under vacuum at 0 °C. The pale yellow solid was washed three times with hexane (3x5 mL)

and dried under vacuum. Yield: 140 mg (63%). Elemental analysis (C, 32.06; H, 3.76) is in agreement with the calculated values for $C_6H_8O_3Mo$ (224.06): C, 32.17; H, 3.60. The spectral data of the pure compound are in agreement with those reported for the Mo-oxoperoxo compound, $CpMo(O)(O_2)CH_3$, prepared previously by the method of Legzdins.^(16, 15) IR (KBr, cm^{-1}): 3102s (Cp), 3064w, 2987w, 2943w, 2895w, 1633bw, 1454w, 1420m, 1169m, 1067m, 1029m, 1002m, 951vs ($\nu_{Mo=O}$), 931s, 877vs (ν_{O-O}), 849s, 831s, 774w, 748w, 575s, 565s (ν_{Mo-O}); 1H -NMR ($CDCl_3$, 400 MHz, rt., δ ppm): 6.29 (5H, s, Cp), 2.12 (3H, s, CH_3), ^{13}C -NMR (C_6D_6 , 100.28 MHz, rt. δ ppm): 109.3 (Cp), 24.7 (CH_3); ^{95}Mo -NMR (C_6D_6 , 26.07 MHz, rt. δ ppm): -609 ppm; ^{17}O NMR ($CDCl_3$, 54.26 MHz, rt. δ ppm): 869 (oxo), 359, 336 (peroxo).

13.3 Kinetic studies

Kinetic data were collected by using 1H NMR and UV methods. The epoxidation of cyclooctene was monitored by NMR, and the epoxidation of β -methoxystyrene was followed by UV spectrophotometric technique. In each case the temperature was controlled at 20 °C. (a) The reactions studied by 1H NMR were carried out in $CDCl_3$ in a total volume of 0.5-1.0 mL. The relative amounts of TBHP, the catalyst and cyclooctene were chosen with a concern for the requirements of the kinetic analysis which was carried out by a first-order or initial rate kinetic. The 1H -NMR spectra were recorded at 2 - 20 min increments over the 2 - 5 h reaction time. Under pseudo-first-order conditions, the changes in the intensity (I) of the cyclooctene signal(s) and/or the cyclooctene oxide with time were fit to a single exponential decay: $I_t = I_\infty + (I_0 - I_\infty) \exp(-k_p t)$. (b) In the spectrophotometric (UV) method, the reaction mixtures were prepared in the reaction cuvette (optical path = 1.0 cm, $V_T = 3.0$ mL) with the last component added being TBHP or the olefin. Some experiments were carried out in cuvettes with short optical paths (0.1-0.2 cm) to allow direct measurement of the absorbance changes during the reaction when the catalyst or β -methoxystyrene were varied, because both have high molar absorptivities and contribute a large absorbance background at the wavelengths used. The data were obtained by following the loss of the β -methoxystyrene (or *trans*- β -methylstyrene) absorption in the range between 260 - 270 nm. Initial rate and pseudo-first-order conditions applied in different protocols. In the latter case, the pseudo-first-order rate constants were evaluated by nonlinear least-

squares fitting of the absorbance-time curves to a single exponential equation, $A_t = A_\infty + (A_0 - A_\infty) \exp(-k_p t)$.

13.4 Crystal data of compound 3

Crystal data and details of the structure determination are presented in Table S1 and Figure S1. Suitable single crystals for the X-ray diffraction study were grown from diethyl ether. A clear yellow fragment was stored under perfluorinated ether, transferred in a Lindemann capillary, fixed, and sealed. Preliminary examination and data collection were carried out on a kappa-CCD device (NONIUS MACH3) with an Oxford Cryosystems cooling device at the window of a rotating anode (NONIUS FR591) with graphite monochromated Mo-K $_{\alpha}$ radiation ($\lambda = 0.71073 \text{ \AA}$). Data collection was performed at 173 K within the θ range of $3.45^\circ < \theta < 27.81^\circ$. A total of 5660 reflections were integrated, corrected for Lorentz polarisation, and, arising from the scaling procedure, corrected for latent decay and absorption effects. After merging ($R_{\text{int}} = 0.019$), 1711 [$l_o > 2\sigma(l_o)$] independent reflections remained and all were used to refine 94 parameters. The structure was solved by a combination of direct methods and difference-Fourier syntheses. All non-hydrogen atoms were refined with anisotropic displacement parameters. Methyl hydrogen atoms were calculated as a part of rigid rotating groups, with $d_{\text{C-H}} = 0.98 \text{ \AA}$ and $U_{\text{iso(H)}} = 1.5U_{\text{eq(C)}}$. Aromatic hydrogen atoms were placed in ideal positions and refined using a riding model with $d_{\text{C-H}} = 0.95 \text{ \AA}$ and $U_{\text{iso(H)}} = 1.2U_{\text{eq(C)}}$. Small extinction effects were corrected with the SHELXL-97 procedure [$\epsilon = 0.013(2)$]. Full-matrix least-squares refinements were carried out by minimising $\sum w(F_o^2 - F_c^2)^2$ with the SHELXL-97 weighting scheme and converged with $R1 = 0.0384$ [$l_o > 2\sigma(l_o)$], $wR2 = 0.0989$ [all data], $GOF = 1.094$, and shift/error < 0.001 . The final difference-Fourier map shows clearly a disorder which could not be resolved and modeled without a doubt. This fact is obvious, too, in the unusual high thermal displacement parameters and the positions of the two highest difference-Fourier peaks (Figure S2). As can be seen by Flack's Parameter $\epsilon = 0.51(15)$ the crystal is twinned and the refinements were completed with the TWIN / BASF option. All calculations were performed with the WINGX system, including the programs DIAMOND, PLATON, SHELXL-97, and SIR92.(4-10, 17)

| 3 | |
|---|--|
| formula | C ₆ H ₈ MoO ₃ |
| fw | 224.06 |
| colour / habit | yellow / fragment |
| cryst dimensions (mm ³) | 0.10 × 0.18 × 0.46 |
| cryst syst | Orthorhombic |
| space group | <i>P</i> 2 ₁ 2 ₁ 2 ₁ (no. 19) |
| <i>a</i> , Å | 6.5225(5) |
| <i>b</i> , Å | 7.9532(5) |
| <i>c</i> , Å | 13.9632(7) |
| <i>V</i> , Å ³ | 724.34(8) |
| <i>Z</i> | 4 |
| <i>T</i> , K | 173 |
| <i>D</i> _{calcd} , g cm ⁻³ | 2.055 |
| μ , mm ⁻¹ | 1.751 |
| F(000) | 440 |
| θ range, deg | 3.45 – 27.81 |
| Index ranges (h, k, l) | ±8, ±10, -10: 18 |
| no. of rflns collected | 5660 |
| no. of indep rflns / <i>R</i> _{int} | 1711 / 0.019 |
| no. of obsd rflns (<i>I</i> > 2 σ (<i>I</i>)) | 1662 |
| no. of data/restraints/params | 1711 / 0 / 94 |
| <i>R</i> 1 / <i>wR</i> 2 (<i>I</i> > 2 σ (<i>I</i>)) ^a | 0.0384 / 0.0984 |
| <i>R</i> 1 / <i>wR</i> 2 (all data) ^a | 0.0391 / 0.0389 |
| GOF (on <i>F</i> ²) ^a | 1.094 |
| Largest diff peak and hole (e Å ⁻³) | +1.23 / -0.72 |

^a*R*1 = $\Sigma(|F_o| - |F_c|) / \Sigma|F_o|$; *wR*2 = $\{\Sigma[w(F_o^2 - F_c^2)^2] / \Sigma[w(F_o^2)^2]\}^{1/2}$;
 GOF = $\{\Sigma[w(F_o^2 - F_c^2)^2] / (n-p)\}^{1/2}$

Table S1. Crystallographic Data for [Mo(η^5 -C₅H₅)O(O₂)CH₃] (**3**).

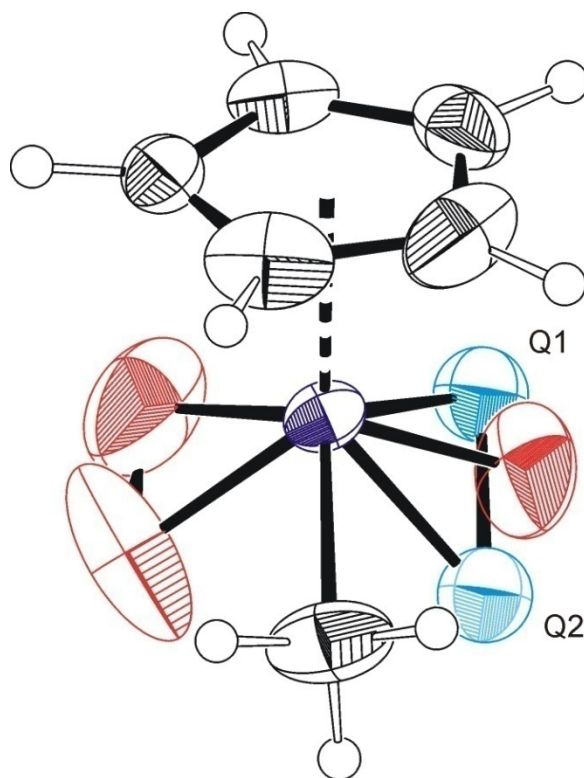


Figure S1 ORTEP style plot of compound **3** in the solid state showing the two highest difference-Fourier peaks Q1 (+1.23 e Å⁻³) and Q2 (+1.17 e Å⁻³).

14. Stable and Catalytically Active *ansa* Compounds with Cycloalkyl Moieties as Bridging Units (Chapter 10)

14.1 Materials and methods

All preparations and manipulations were performed using standard Schlenk techniques under an argon atmosphere. Solvents were dried by standard procedures (THF, n-hexane and Et₂O over Na/benzophenone; CH₂Cl₂ and pentane over CaH₂), distilled under an argon atmosphere and used immediately (THF) or kept over 4 Å molecular sieves. TBHP was purchased from Aldrich as 5.0–6.0 mol% solution in n-decane and used after drying over molecular sieves to remove the water (< 4% when received). Microanalyses were performed in the Mikroanalytisches Labor of the TU München in Garching. Thermogravimetric analyses were performed with a Netzsch TG 209 system at a heating rate of 5 °C min⁻¹ under an oxygen atmosphere. ¹H-, ¹³C- and ⁹⁵Mo-NMR spectra were recorded using a Jeol-JMX-GX 400 MHz or a Bruker Avance DPX-400 spectrometer. Mass spectra were recorded with a Finnigan MAT 311 A and a MAT 90 spectrometer. Catalytic runs were monitored by GC methods on a Varian CP-3800 instrument equipped with a FID and a VF-5ms column (*cis*-cyclooctene, 1-octene) or a Hewlett-Packard HP-6890 instrument with a mass selective detector and a DB-225 column (*cis*-stilbene, *trans*-stilbene). The cycloalkyl bis(methanesulfonates) were synthesised from their respective diols using published procedures.(18) (Cyclopentane- and cyclohexanediol purchased from Aldrich and used without further purification, cycloheptane- and cyclooctanediol were synthesised from the respective olefins via KMnO₄ dihydroxylation using previously reported procedures (19)). The metal precursors W(CO)₃(CH₃CN)₃, Mo(CO)₃(CH₃CN)₃, Mo(CO)₃(Me₃tach) and W(CO)₃(Me₃tach) were synthesised from the respective carbonyls according to published procedures.(20-22)

Compounds η^5 -cyclopentadienyltricarbonylmethylmolybdenum(II) and η^5 -

cyclopentadienyltricarbonylchloromolybdenum(II) were synthesised using modified literature procedures.(23)

14.2 Synthesis of the spiro ligands

1a-d were synthesised according to a modified literature procedure.(24) Freshly distilled cyclopentadiene (5 mL, 0.06 mol) was added to a suspension of NaH (1.9 g, 0.08 mol) in 200 mL THF at 0 °C. The flask was then cooled again to 0 °C and the respective bis(methanesulfonate) cycloalkyldiols (10 g, 0.04 mol) in 100 mL THF were added dropwise. The mixture was stirred overnight at r.t. and 20 mL of methanol were added to quench any excess of NaH and NaCp. After addition 100 ml of water, the THF layer was separated and the aqueous layer was washed with hexane (3 × 50 mL). The combined organic layers were washed with 100 mL water, 100 ml HCl (10%) and 100 mL water to obtain an orange-yellow solution. All the organic solvents were distilled off and the residue was extracted with pentane. After drying under high vacuum, the spiro ligand were obtained as bright yellow-orange oils and were used without further purification.

The previously reported spiro[2.4]hepta-4,6-diene and spiro[4.4]nona-1,3-diene (**1e**, **1f**) were synthesised according to published procedures.(25)

Spiro[4.2]-bicyclo[4.1]-deca-6,8-diene (1a) was obtained as a bright yellow oil ($\rho = 1.5 \text{ g/cm}^3$). Yield: 70%. $^1\text{H NMR}$ (400 MHz, CDCl_3 , 25 °C): $\delta = 6.56$ (m, 1H, Cp); 6.43 (m, 1H, Cp); 6.41 (m, 1H, Cp); 6.02 (m, 1H, Cp); 2.63 (m, 2H, Cp-CH); 2.2-1.9 (m, 5H, cyclopentyl); 1.75 (m, 1H, cyclopentyl). $^{13}\text{C NMR}$ (100.28 MHz, CDCl_3): $\delta = 140.17$, 132.76, 131.57, 126.87 (Cp); 48.37 (C_{spiro}); 36.09 (Cp-CH); 28.81, 24.80 (cycloalkyl). CI-MS: parent peak at $m/z = 133$ corresponding to $[\text{M}]^+$.

Spiro[bicyclo[4.1.0]heptane-7,1'-cyclopenta[2,4]diene] (1b) was obtained as a yellow oil ($\rho = 1.5 \text{ g/cm}^3$). Yield: 60%. $^1\text{H NMR}$ (400 MHz, CD_2Cl_2 , 25 °C): $\delta = 6.55$ (m, 2H, Cp); 6.35 (m, 1H, Cp); 6.04 (m, 1H, Cp); 2.29 (m, 2H, Cp-CH); 2.1-1.5 (m, 8H, cycloalkyl). $^{13}\text{C NMR}$ (100.28 MHz, CD_2Cl_2): $\delta = 142.86$, 133.09, 131.79, 126.74 (Cp); 48.81 (C_{spiro}); 32.33 (Cp-CH); 30.09, 27.16, 23.78, 22.44 (cycloalkyl). CI-MS: parent peak at $m/z = 147$ corresponding to $[\text{M}]^+$.

Spiro[bicyclo[5.1.0]octane-8,1'-cyclopenta[2,4]diene] (1c) was obtained as a yellow-orange oil ($\rho = 1.6 \text{ g/cm}^3$). Yield: 50%. $^1\text{H NMR}$ (400 MHz, CDCl_3 , 25°C): $\delta = 6.60$ (m, 1H, Cp); 6.45 (m, 1H, Cp); 6.37 (m, 1H, Cp); 6.02 (m, 1H, Cp); 2.26 (m, 2H, Cp-CH); 2.16 (m, 2H, cycloalkyl); 1.99 (m, 2H, cycloalkyl); 1.9-1.3 (m, 6H, cyclo). $^{13}\text{C NMR}$ (100.28 MHz, CDCl_3): $\delta = 140.78, 133.46, 131.18, 126.65$ (Cp); 50.48 (C_{spiro}); 38.75 (Cp-CH); 33.60, 32.71, 29.555, 29.03, 25.69 (cycloalkyl); CI-MS: parent peak at $m/z = 161$ corresponding to $[\text{M}]^+$.

Spiro[bicyclo[6.1.0]nonane-9,1'-cyclopenta[2,4]diene] (1d) was obtained as an orange oil ($\rho = 1.6 \text{ g/cm}^3$). Yield: 65%. $^1\text{H NMR}$ (400 MHz, CDCl_3 , 25°C): $\delta = 6.59$ (m, 1H, Cp); 6.40 (m, 1H, Cp); 6.36 (m, 1H, Cp); 6.08 (m, 1H, Cp); 2.40 (m, 2H, Cp-CH); 2.08 (m, 2H, cycloalkyl); 1.95 (m, 2H, cycloalkyl); 1.87 (m, 2H, cycloalkyl); 1.7-1.3 (m, 10H, cyclo). $^{13}\text{C NMR}$ (100.28 MHz, CDCl_3): $\delta = 141.09, 133.19, 131.25, 126.71$ (Cp); 47.13 (C_{spiro}); 42.13 (Cp-CH); 33.19, 29.69, 27.26, 26.64, 25.75, 24.81 (cycloalkyl); CI-MS: parent peak at $m/z = 175$ corresponding to $[\text{M}]^+$.

14.3 Synthesis of the Mo derivatives

Method A (Compounds 2a-d) The addition of spiro ligands **1a-d** (0.21 g, 1.6 mmol) to a 20 mL solution of $\text{Mo}(\text{CO})_3(\text{CH}_3\text{CN})_3$ (0.63 g, 1.6 mmol) produced a yellow suspension (0.63 g, 1.6 mmol) which was stirred overnight at 25°C . Volatiles were removed under vacuum, the sticky residue was extracted with hexane ($3 \times 15 \text{ mL}$), filtered, and the obtained orange filtrates were either concentrated and cooled to -30°C or evaporated in vacuo to afford complexes **2a-d**.

Method B (Compounds 2a-e) The addition of spiro ligands **1a-e** (0.21 g, 1.6 mmol) to a 20 mL solution of $\text{W}(\text{CO})_3(\text{Me}_3\text{Tach})$ (0.63 g, 1.6 mmol) produced a yellow suspension, which was stirred for 5 min before adding 0.25 g (3.8 mmol) of BF_3 . Volatiles were removed under vacuum, the sticky residue was extracted with pentane ($3 \times 15 \text{ mL}$), filtered, and the obtained orange filtrates were either concentrated and cooled to -30°C (**2a, 2b, 2e**) or dried in vacuum (**2c, 2d**) to afford the respective *ansa* compounds.

$[\text{Mo}(\eta^5\text{-C}_5\text{H}_4(\text{CH}(\text{CH}_2)_3)\text{-}\eta^1\text{-CH})(\text{CO})_3]$ (2a): Orange crystals were obtained. Yield: 70 %. $^1\text{H NMR}$ (400 MHz, CDCl_3 , 25°C): $\delta = 5.21$ (m, 2H, Cp); 5.12 (m, 2H, Cp); 3.38 (td, $^3\text{J}(\text{H-}$

$H_{\text{cyclopentyl}} = 9.4$, $^3J(\text{H-H}_{\text{Mo-C}}) = 4.2$, 1H, Cp-CH); 2.17 (m, 1H, cycloalkyl); 2.0 (m, 1H, cycloalkyl); 1.71 (m, 1H, cycloalkyl); 1.60 (m, 2H, cycloalkyl); 1.45 (m, 1H, cycloalkyl); 0.40 (dt, $^3J(\text{H-H}_{\text{cyclopentyl}}) = 9.8$, $^3J(\text{H-H}_{\text{Cp-CH}}) = 5.8$, Mo-CH). ^{13}C NMR (100.28 MHz, CDCl_3): $\delta = 231.0$, 201.1 (CO); 90.0, 89.0, 88.6, 86.6 (Cp); 76.6 (Cp-CH); 38.1, 35.9, 32.4, 26.1 (cycloalkyl); -25.9 (Mo-C). ^{95}Mo NMR (26 MHz, CDCl_3 , 25°C): -1389. CI-MS: parent peak at $m/z = 314$ corresponding to $[\text{M}]^+$, $m/z = 286$ corresponding to $[\text{M-CO}]^+$. Anal. calc. for $\text{C}_{13}\text{H}_{12}\text{O}_3\text{Mo}$ (312): C, 50.02; H, 3.87. Found: C, 49.62; H, 3.65%.

[Mo($\eta^5\text{-C}_5\text{H}_4(\text{CH}(\text{CH}_2)_4\text{)-}\eta^1\text{-CH})(\text{CO})_3$] (2b): Red crystals were obtained. Yield: 50 %. ^1H NMR (400 MHz, CDCl_3 , 25°C): $\delta = 5.39$ (m, 1H, Cp); 5.26 (m, 1H, Cp); 5.13 (m, 1H, Cp); 5.11 (m, 1H, Cp); 3.11 (td, $^3J(\text{H-H}_{\text{cyclohexyl}}) = 9.5$, $^3J(\text{H-H}_{\text{Mo-C}}) = 6.8$, 1H, Cp-CH); 1.91 (m, 1H, cycloalkyl); 1.71 (m, 1H, cycloalkyl); 1.7-1.4 (m, 6H, cycloalkyl); 0.74 (td, $^3J(\text{H-H}_{\text{cyclohexyl}}) = 9.8$, $^3J(\text{H-H}_{\text{Cp-CH}}) = 5.5$, 1H, Mo-CH). ^{13}C NMR (100.28 MHz, CDCl_3): $\delta = 223.3$ (CO); 90.24, 89.04, 88.75, 87.24 (Cp); 72.19 (Cp-ansa); 34.98, 30.11, 26.32, 25.75, 19.96 (cycloalkyl); -22.14 (Mo-C). ^{95}Mo NMR (26 MHz, CDCl_3 , 25°C): -1400.37. CI-MS: parent peak at $m/z = 328$ corresponding to $[\text{M}]^+$, $m/z = 300$ corresponding to $[\text{M-CO}]^+$.

[Mo($\eta^5\text{-C}_5\text{H}_4(\text{CH}(\text{CH}_2)_5\text{)-}\eta^1\text{-CH})(\text{CO})_3$] (2c): Dark red crystals were obtained. Yield: 40 %. ^1H NMR (400 MHz, CDCl_3 , 25°C): $\delta = 5.18$ (m, 1H, Cp); 5.13 (m, 1H, Cp); 5.11 (m, 1H, Cp); 4.99 (m, 1H, Cp); 2.96 (t, 1H, $^3J(\text{H-H}_{\text{cycloheptyl}}) = 9.8$, Cp-CH); 2.25 (m, 1H, cycloalkyl); 2.0-1.3 (m, 11H, cycloalkyl); 0.74 (tm, $^3J(\text{H-H}_{\text{cycloheptyl}}) = 9.8$, 1H, Mo-CH). ^{13}C NMR (100.28 MHz, CDCl_3): $\delta = 201.1$ (CO); 89.31, 88.42, 87.78, 85.21 (Cp); 73.53 (Cp-ansa); 39.22, 37.41, 34.49, 31.37, 30.41, 30.36, 29.78 (cycloalkyl); -15.90 (Mo-C). ^{95}Mo NMR (26 MHz, CDCl_3 , 25°C): -1412.64. CI-MS: parent peak at $m/z = 342$ corresponding to $[\text{M}]^+$, $m/z = 314$ corresponding to $[\text{M-CO}]^+$.

[Mo($\eta^5\text{-C}_5\text{H}_4(\text{CH}(\text{CH}_2)_6\text{)-}\eta^1\text{-CH})(\text{CO})_3$] (2d): Dark red crystals were obtained. Yield: 30 %. ^1H NMR (400 MHz, CDCl_3 , 25°C): $\delta = 5.18$ (m, 1H, Cp); 5.15 (m, 1H, Cp); 5.09 (m, 1H, Cp); 5.02 (m, 1H, Cp); 3.17 (m, 1H, Cp-CH); 2.12 (m, 1H, cycloalkyl); 1.71 (m, 1H, cycloalkyl); 1.7-1.3 (m, 11H, cycloalkyl); 0.80 (tm, $^3J(\text{H-H}_{\text{cyclooctyl}}) = 9.8$, 1H, Mo-CH). ^{13}C NMR (100.28 MHz, CDCl_3): $\delta = 231.9$ (CO); 89.26, 89.18, 88.26, 84.70 (Cp); 73.02 (Cp-ansa); 38.42, 34.40, 32.16, 30.49, 28.62, 26.07, 25.29 (cycloalkyl); -11.97 (Mo-C). ^{95}Mo NMR (26 MHz, CDCl_3 , 25°C): -1668.28. CI-MS: parent peak at $m/z = 356$ corresponding to $[\text{M}]^+$, $m/z = 328$ corresponding to $[\text{M-CO}]^+$.

14.4 Synthesis of the W derivatives

Method A (Compounds 3a and 3b) The addition of spiro ligands **1a** and **1b** (0.21 g, 1.6 mmol) to a 20 mL solution of $W(CO)_3(CH_3CN)_3$ (0.63 g, 1.6 mmol) produced a yellow suspension (0.63 g, 1.6 mmol) which was stirred overnight at 25 °C. The obtained orange solution was refluxed for 2 hours. Volatiles were removed under vacuum, the sticky residue was extracted with pentane (3 × 15 mL), filtered, and the obtained orange filtrates were concentrated and cooled to -30°C.

Method B (Compounds 3a-e) The addition of spiro ligands **1a-d** (0.21 g, 1.6 mmol) to a 20 mL solution of $W(CO)_3(Me_3Tach)$ (0.63 g, 1.6 mmol) produced a yellow suspension, which was stirred for 5 min before adding g (3.8 mmol) of $BF_3 \cdot THF$. The mixture was then refluxed overnight to afford a dark orange-red solution. Volatiles were removed under vacuum, the sticky residue was extracted with pentane (3 × 15 mL), filtered, and the obtained orange filtrates were either concentrated and cooled to -30 °C (**3a**, **3b**, **3e**) or dried in vacuum (**3c**, **3d**) to afford the respective *ansa* compounds.

[W(η^5 -C₅H₄(CH(CH₂)₃)- η^1 -CH)(CO)₃] · 3a: an orange powder was obtained. *Method A:* Yield: 35 %. *Method B:* Yield 60 % ¹H NMR (400 MHz, CDCl₃, 25 °C): δ = 5.37 (m, 1H, Cp); 5.25 (m, 2H, Cp); 5.12 (m, 1H, Cp); 3.40 (td, ³J(H-H_{cyclopentyl})= 9.4, ³J(H-H_{W-C})= 4.2, 1H, Cp-CH); 2.17 (m, 1H, cycloalkyl); 2.03 (m, 1H, cycloalkyl); 1.95 (m, 1H, cycloalkyl); 1.71 (m, 1H, cycloalkyl); 1.55 (m, 2H, cycloalkyl); 0.46 (dt, ³J(H-H_{cyclopentyl}) = 9.8, ³J(H-H_{Cp-CH}) = 5.8, W-CH). ¹³C NMR (100.28 MHz, CDCl₃): δ = 88.0, 87.8, 86.4, 84.6 (Cp); 80.2 (Cp-CH); 38.0, 36.1, 32.5, 26.3 (cycloalkyl); -38.2 (W-C). CI-MS: parent peak at *m/z* = 401 corresponding to [M]⁺ *m/z* = 373 corresponding to [M-CO]⁺. Anal. calc. for C₁₃H₁₂O₃W (403): C, 38.73; H, 3.75. Found: C, 38.57; H, 3.58%.

[W(η^5 -C₅H₄(CH(CH₂)₄)- η^1 -CH)(CO)₃] (3b): a red powder was obtained. *Method A:* Yield: 20 %. *Method B:* Yield 40 %. ¹H NMR (400 MHz, CDCl₃, 25 °C): δ = 5.51 (m, 1H, Cp); 5.27 (m, 2H, Cp); 5.13 (m, 1H, Cp); 3.11 (td, ³J(H-H_{cyclohexyl})= 10.2, ³J(H-H_{W-C})= 5.7, 1H, Cp-CH); 1.79 (m, 1H, cycloalkyl); 1.70 (m, 7H, cycloalkyl); 0.68 (td, ³J(H-H_{cyclohexyl}) = 10.8, ³J(H-H_{Cp-CH}) = 5.2, 1H, W-CH). ¹³C NMR (100.28 MHz, CDCl₃): δ = 191.2 (CO); 88.3, 87.5, 86.8, 84.9 (Cp); 75.6 (Cp-CH); 34.9, 30.0, 29.8, 25.8, 25.7, 19.5 (cycloalkyl); -36.1 (W-C). CI-MS: low intensity parent peak at *m/z* = 413.5 corresponding to [M]⁺ *m/z* = 385.5 corresponding to [M-CO]⁺.

[W(η^5 -C₅H₄(CH(CH₂)₅)- η^1 -CH)(CO)₃] (3c): a dark red powder was obtained. Yield: 30 %. ¹H NMR (400 MHz, CDCl₃, 25 °C): δ = 5.27 (m, 1H, Cp); 5.21 (m, 1H, Cp); 5.17 (m, 1H, Cp); 5.13 (m, 1H, Cp); 2.99 (td, ³J(H-H_{cycloheptyl})= 11.6, ³J(H-H_{W-C})= 3.0, 1H, Cp-CH); 2.14 (m, 1H, cycloalkyl); 2.01 (m, 1H, cycloalkyl); 1.86 (m, 1H, cycloalkyl); 1.75 (m, 1H, cycloalkyl); 1.5-1.0 (m, 7H, cycloalkyl); 0.77 (dt, ³J(H-H_{cycloheptyl}) = 11.6, ³J(H-H_{Cp-CH}) = 3.9, 1H, W-CH). ¹³C NMR (100.28 MHz, CDCl₃): δ = 222.28 (CO); 87.4, 86.4, 86.1, 83.3 (Cp); 76.9 (Cp-CH); 39.3, 37.7, 34.7, 31.6, 30.5, 29.8 (cycloalkyl); -24.3 (W-C). CI-MS: parent peak at m/z = 428.25 corresponding to [M]⁺.

[W(η^5 -C₅H₄(CH(CH₂)₆)- η^1 -CH)(CO)₃] (3d): a dark red powder was obtained. Yield: 40 %. ¹H NMR (400 MHz, CDCl₃, 25 °C): δ = 5.22 (m, 1H, Cp); 5.20 (m, 1H, Cp); 5.18 (m, 1H, Cp); 5.16 (m, 1H, Cp); 3.23 (td, ³J(H-H_{cycloheptyl})= 9.2, ³J(H-H_{W-C})= 2.4, 1H, Cp-CH); 2.10 (m, 1H, cycloalkyl); 1.8-1.3 (m, 11H, cycloalkyl); 0.83 (m, 1H, W-CH). ¹³C NMR (100.28 MHz, CDCl₃): δ = 222.1, 191.1 (CO); 87.3, 87.2, 86.5, 83.4 (Cp); 76.6 (Cp-CH); 38.4, 34.4, 32.3, 30.5, 28.79, 28.7, 26.0, 25.2 (cycloalkyl); -25.3 (W-C). CI-MS: parent peak at m/z = 442.5 corresponding to [M]⁺.

14.5 Application in epoxidation catalysis

The catalytic reactions were performed in air, within a reaction vessel equipped with a magnetic stirrer. *cis*-cyclooctene: 800 mg (7.3 mmol) of the olefin, 500 mg of mesitylene (internal standard) and 1 mol% (73 mol) of the catalysts (**2a**, **2b**) or 0.1 mol% (**2a**) were added to the reaction vessel and diluted in 20 ml CH₂Cl₂. 1-Octene: 410 mg (3.65 mmol) of the olefin, 250 mg of mesitylene (internal standard) and 1 mol% (36 μ mol) of the catalysts (**2a**, **2b**) were added to the reaction vessel and diluted in 10 ml CH₂Cl₂. *trans*-Stilbene: 660 mg (3.65 mmol) of the olefin, 500 mg of 4-methylbenzophenone (internal standard) and 1 mol% (36 mol) of the catalysts (**2a**, **2b**) were added to the reaction vessel and diluted in 10 ml CH₂Cl₂. *cis*-Stilbene: 200 mg (1.10 mmol) of the olefin, 100 mg of 4-methylbenzophenone (internal standard) and 1 mol% (11 mol) of the catalysts (**2a**, **2b**) were added to the reaction vessel and diluted in 10 ml CH₂Cl₂. The reaction begins with the addition of TBHP (5.5 M in *n*-decane). The course of the reaction was monitored by quantitative GC analysis. Samples taken were diluted with CH₂Cl₂ and treated with MgSO₄ and MnO₂ to remove water and destroy the excess of peroxide. The resulting slurry was filtered and the filtrate obtained was

injected into a GC column. The conversions of *cis*-cyclooctene, 1-octene, *cis*- and *trans*-stilbene and the formation of their respective oxides were calculated from calibration curves ($r^2 > 0.999$) recorded prior to the commencement of the reaction.

14.6 Crystal data of compound 2a

14.6.1 Bond distances (in Å)

| | | | | | |
|-----|-------|----------|------|-------|-----------|
| Mo1 | -C1 | 2.019(2) | Mo2 | -C21 | 2.016(2) |
| Mo1 | -C2 | 1.985(2) | Mo2 | -C22 | 1.987(3) |
| Mo1 | -C3 | 1.990(2) | Mo2 | -C23 | 1.985(2) |
| Mo1 | -C4 | 2.324(3) | Mo2 | -C24 | 2.316(3) |
| Mo1 | -C5 | 2.335(2) | Mo2 | -C25 | 2.330(2) |
| Mo1 | -C6 | 2.336(2) | Mo2 | -C26 | 2.337(2) |
| Mo1 | -C7 | 2.305(2) | Mo2 | -C27 | 2.314(2) |
| Mo1 | -C8 | 2.293(2) | Mo2 | -C28 | 2.294(2) |
| Mo1 | -C13 | 2.372(2) | Mo2 | -C33 | 2.408(3) |
| O1 | -C1 | 1.143(3) | O4 | -C21 | 1.144(3) |
| O2 | -C2 | 1.149(3) | O5 | -C22 | 1.148(3) |
| O3 | -C3 | 1.150(3) | O6 | -C23 | 1.148(3) |
| C4 | -C5 | 1.417(4) | C24 | -C25 | 1.409(4) |
| C4 | -C8 | 1.419(4) | C24 | -C28 | 1.424(4) |
| C5 | -C6 | 1.421(4) | C25 | -C26 | 1.418(4) |
| C6 | -C7 | 1.418(4) | C26 | -C27 | 1.423(3) |
| C7 | -C8 | 1.442(3) | C27 | -C28 | 1.433(4) |
| C8 | -C9 | 1.510(3) | C28 | -C29 | 1.509(3) |
| C9 | -C10 | 1.545(4) | C29 | -C30 | 1.538(4) |
| C9 | -C13 | 1.551(3) | C29 | -C33 | 1.549(3) |
| C10 | -C11 | 1.532(4) | C30 | -C31 | 1.577(5) |
| | | | C30 | -C31A | 1.444(13) |
| | | | C31A | -C32 | 1.670(13) |
| C11 | -C12 | 1.537(4) | C31 | -C32 | 1.462(5) |
| C12 | -C13 | 1.526(4) | C32 | -C33 | 1.494(4) |
| C4 | -H41 | 0.95 | C24 | -H241 | 0.95 |
| C5 | -H51 | 0.95 | C25 | -H251 | 0.95 |
| C6 | -H61 | 0.95 | C26 | -H261 | 0.95 |
| C7 | -H71 | 0.95 | C27 | -H271 | 0.95 |
| C9 | -H91 | 1.00 | C29 | -H291 | 1.00 |
| C10 | -H101 | 0.99 | C30 | -H301 | 0.99 |
| C10 | -H102 | 0.99 | C30 | -H302 | 0.99 |
| C11 | -H111 | 0.99 | C31 | -H311 | 0.99 |
| C11 | -H112 | 0.99 | C31 | -H312 | 0.99 |
| | | | C31A | -H313 | 0.99 |
| | | | C31A | -H314 | 0.99 |
| C12 | -H121 | 0.99 | C32 | -H321 | 0.99 |
| C12 | -H122 | 0.99 | C32 | -H322 | 0.99 |
| C13 | -H131 | 1.00 | C33 | -H331 | 1.00 |

14.6.2 Bond angles (in °)

| | | | | | | | |
|------|------|-------|------------|------|-------|-------|------------|
| C1 | -Mo1 | -C2 | 80.45(10) | C21 | -Mo2 | -C22 | 80.34(10) |
| C1 | -Mo1 | -C3 | 80.10(10) | C21 | -Mo2 | -C23 | 80.94(10) |
| C1 | -Mo1 | -C13 | 146.37(8) | C21 | -Mo2 | -C33 | 146.82(9) |
| C2 | -Mo1 | -C3 | 100.88(10) | C22 | -Mo2 | -C23 | 99.54(10) |
| C2 | -Mo1 | -C13 | 78.49(9) | C22 | -Mo2 | -C33 | 80.06(9) |
| C3 | -Mo1 | -C13 | 78.51(9) | C23 | -Mo2 | -C33 | 76.24(10) |
| Mo1 | -C1 | -O1 | 179.2(2) | Mo2 | -C21 | -O4 | 179.1(2) |
| Mo1 | -C2 | -O2 | 177.3(2) | Mo2 | -C22 | -O5 | 178.3(2) |
| Mo1 | -C3 | -O3 | 177.5(2) | Mo2 | -C23 | -O6 | 177.4(2) |
| C5 | -C4 | -C8 | 108.7(2) | C25 | -C24 | -C28 | 108.4(2) |
| C4 | -C5 | -C6 | 108.0(2) | C24 | -C25 | -C26 | 108.3(2) |
| C5 | -C6 | -C7 | 108.2(2) | C25 | -C26 | -C27 | 108.1(2) |
| C6 | -C7 | -C8 | 107.9(2) | C26 | -C27 | -C28 | 107.7(2) |
| C4 | -C8 | -C7 | 107.1(2) | C24 | -C28 | -C27 | 107.5(2) |
| C4 | -C8 | -C9 | 124.0(2) | C24 | -C28 | -C29 | 123.5(2) |
| C7 | -C8 | -C9 | 124.3(2) | C27 | -C28 | -C29 | 125.0(2) |
| C8 | -C9 | -C10 | 118.0(2) | C28 | -C29 | -C30 | 116.3(2) |
| C8 | -C9 | -C13 | 100.50(17) | C28 | -C29 | -C33 | 101.51(19) |
| C10 | -C9 | -C13 | 106.56(19) | C30 | -C29 | -C33 | 106.1(2) |
| C9 | -C10 | -C11 | 104.1(2) | C29 | -C30 | -C31 | 102.4(2) |
| C10 | -C11 | -C12 | 102.7(2) | C30 | -C31 | -C32 | 104.4(3) |
| | | | | C30 | -C31A | -C32 | 100.8(7) |
| C11 | -C12 | -C13 | 102.86(19) | C31 | -C32 | -C33 | 105.8(3) |
| Mo1 | -C13 | -C9 | 96.30(13) | Mo2 | -C33 | -C29 | 96.03(14) |
| Mo1 | -C13 | -C12 | 120.31(15) | Mo2 | -C33 | -C32 | 122.24(19) |
| C9 | -C13 | -C12 | 104.65(19) | C29 | -C33 | -C32 | 106.5(2) |
| C5 | -C4 | -H41 | 126.00 | C25 | -C24 | -H241 | 126.00 |
| C8 | -C4 | -H41 | 126.00 | C28 | -C24 | -H241 | 126.00 |
| C4 | -C5 | -H51 | 126.00 | C24 | -C25 | -H251 | 126.00 |
| C6 | -C5 | -H51 | 126.00 | C26 | -C25 | -H251 | 126.00 |
| C5 | -C6 | -H61 | 126.00 | C25 | -C26 | -H261 | 126.00 |
| C7 | -C6 | -H61 | 126.00 | C27 | -C26 | -H261 | 126.00 |
| C6 | -C7 | -H71 | 126.00 | C26 | -C27 | -H271 | 126.00 |
| C8 | -C7 | -H71 | 126.00 | C28 | -C27 | -H271 | 126.00 |
| C8 | -C9 | -H91 | 110.00 | C28 | -C29 | -H291 | 111.00 |
| C10 | -C9 | -H91 | 110.00 | C30 | -C29 | -H291 | 111.00 |
| C13 | -C9 | -H91 | 110.00 | C33 | -C29 | -H291 | 111.00 |
| C9 | -C10 | -H101 | 111.00 | C29 | -C30 | -H301 | 111.00 |
| C9 | -C10 | -H102 | 111.00 | C29 | -C30 | -H302 | 111.00 |
| C11 | -C10 | -H101 | 111.00 | C31 | -C30 | -H301 | 111.00 |
| C11 | -C10 | -H102 | 111.00 | C31 | -C30 | -H302 | 111.00 |
| H101 | -C10 | -H102 | 109.00 | H301 | -C30 | -H302 | 109.00 |
| | | | | C29 | -C30 | -H303 | 109.00 |
| | | | | C29 | -C30 | -H304 | 109.00 |
| | | | | C31 | -C30 | -H303 | 109.00 |
| | | | | C31 | -C30 | -H304 | 109.00 |
| | | | | H303 | -C30 | -H304 | 108.00 |
| C10 | -C11 | -H111 | 111.00 | C30 | -C31 | -H311 | 111.00 |
| C10 | -C11 | -H112 | 111.00 | C30 | -C31 | -H312 | 111.00 |
| C12 | -C11 | -H111 | 111.00 | C32 | -C31 | -H311 | 111.00 |

| | | | | | | | |
|------|------|-------|--------|------|-------|-------|--------|
| C12 | -C11 | -H112 | 111.00 | C32 | -C31 | -H312 | 111.00 |
| H111 | -C11 | -H112 | 109.00 | H311 | -C31 | -H312 | 109.00 |
| | | | | C30 | -C31A | -H313 | 112.00 |
| | | | | C30 | -C31A | -H314 | 112.00 |
| | | | | C32 | -C31A | -H313 | 112.00 |
| | | | | C32 | -C31A | -H314 | 112.00 |
| | | | | H313 | -C31A | -H314 | 109.00 |
| C11 | -C12 | -H121 | 111.00 | C31 | -C32 | -H321 | 111.00 |
| C11 | -C12 | -H122 | 111.00 | C31 | -C32 | -H322 | 111.00 |
| C13 | -C12 | -H121 | 111.00 | C33 | -C32 | -H321 | 111.00 |
| C13 | -C12 | -H122 | 111.00 | C33 | -C32 | -H322 | 111.00 |
| H121 | -C12 | -H122 | 109.00 | H321 | -C32 | -H322 | 109.00 |
| | | | | C31A | -C32 | -H323 | 110.00 |
| | | | | C31A | -C32 | -H324 | 110.00 |
| | | | | C33 | -C32 | -H323 | 110.00 |
| | | | | C33 | -C32 | -H324 | 110.00 |
| | | | | H323 | -C32 | -H324 | 108.00 |
| Mo1 | -C13 | -H131 | 111.00 | Mo2 | -C33 | -H331 | 110.00 |
| C9 | -C13 | -H131 | 111.00 | | | | |
| C12 | -C13 | -H131 | 111.00 | | | | |

14.7 Crystal data of compound 2b

14.7.1 Bond distances (in Å)

| | | | | | |
|-----|------|------------|-----|-------|------------|
| Mo1 | -C1 | 2.0128(15) | C9 | -C14 | 1.5517(18) |
| Mo1 | -C2 | 1.9921(15) | C10 | -C11 | 1.527(2) |
| Mo1 | -C3 | 1.9885(14) | C11 | -C12 | 1.5385(19) |
| Mo1 | -C4 | 2.3279(14) | C12 | -C13 | 1.5419(19) |
| Mo1 | -C5 | 2.3389(15) | C13 | -C14 | 1.517(2) |
| Mo1 | -C6 | 2.3394(14) | C4 | -H41 | 0.95 |
| Mo1 | -C7 | 2.3065(14) | C5 | -H51 | 0.95 |
| Mo1 | -C8 | 2.2945(12) | C6 | -H61 | 0.95 |
| Mo1 | -C14 | 2.4011(13) | C7 | -H71 | 0.95 |
| O1 | -C1 | 1.1438(19) | C9 | -H91 | 1.00 |
| O2 | -C2 | 1.1484(19) | C10 | -H101 | 0.99 |
| O3 | -C3 | 1.1473(18) | C10 | -H102 | 0.99 |
| C4 | -C5 | 1.418(2) | C11 | -H111 | 0.99 |
| C4 | -C8 | 1.425(2) | C11 | -H112 | 0.99 |
| C5 | -C6 | 1.422(2) | C12 | -H121 | 0.99 |
| C6 | -C7 | 1.422(2) | C12 | -H122 | 0.99 |
| C7 | -C8 | 1.4313(19) | C13 | -H131 | 0.99 |
| C8 | -C9 | 1.5133(19) | C13 | -H132 | 0.99 |
| C9 | -C10 | 1.525(2) | C14 | -H141 | 1.00 |

14.7.2 Bond angles (in °)

| | | | | | | | |
|-----|------|------|------------|------|------|-------|------------|
| C1 | -Mo1 | -C2 | 80.98(6) | Mo1 | -C8 | -C9 | 101.51(8) |
| C1 | -Mo1 | -C3 | 79.46(6) | C4 | -C8 | -C7 | 107.50(12) |
| C1 | -Mo1 | -C4 | 121.28(6) | C4 | -C8 | -C9 | 123.55(13) |
| C1 | -Mo1 | -C5 | 93.33(6) | C7 | -C8 | -C9 | 124.69(13) |
| C1 | -Mo1 | -C6 | 97.57(6) | C8 | -C9 | -C10 | 116.18(12) |
| C1 | -Mo1 | -C7 | 130.02(5) | C8 | -C9 | -C14 | 100.95(10) |
| C1 | -Mo1 | -C8 | 152.85(5) | C10 | -C9 | -C14 | 112.68(12) |
| C1 | -Mo1 | -C14 | 146.15(5) | C9 | -C10 | -C11 | 108.96(12) |
| C2 | -Mo1 | -C3 | 100.26(6) | C10 | -C11 | -C12 | 111.56(11) |
| C2 | -Mo1 | -C4 | 96.41(5) | C11 | -C12 | -C13 | 112.51(12) |
| C2 | -Mo1 | -C5 | 115.26(6) | C12 | -C13 | -C14 | 110.58(11) |
| C2 | -Mo1 | -C6 | 150.64(6) | Mo1 | -C14 | -C9 | 95.91(8) |
| C2 | -Mo1 | -C7 | 146.84(5) | Mo1 | -C14 | -C13 | 117.14(9) |
| C2 | -Mo1 | -C8 | 110.94(5) | C9 | -C14 | -C13 | 111.84(11) |
| C2 | -Mo1 | -C14 | 75.38(5) | Mo1 | -C4 | -H41 | 122.00 |
| C3 | -Mo1 | -C4 | 155.37(5) | C5 | -C4 | -H41 | 126.00 |
| C3 | -Mo1 | -C5 | 142.26(5) | C8 | -C4 | -H41 | 126.00 |
| C3 | -Mo1 | -C6 | 108.34(6) | Mo1 | -C5 | -H51 | 122.00 |
| C3 | -Mo1 | -C7 | 97.43(5) | C4 | -C5 | -H51 | 126.00 |
| C3 | -Mo1 | -C8 | 120.02(5) | C6 | -C5 | -H51 | 126.00 |
| C3 | -Mo1 | -C14 | 81.29(5) | Mo1 | -C6 | -H61 | 122.00 |
| C4 | -Mo1 | -C5 | 35.37(5) | C5 | -C6 | -H61 | 126.00 |
| C4 | -Mo1 | -C6 | 59.11(5) | C7 | -C6 | -H61 | 126.00 |
| C4 | -Mo1 | -C7 | 59.62(5) | Mo1 | -C7 | -H71 | 121.00 |
| C4 | -Mo1 | -C8 | 35.91(5) | C6 | -C7 | -H71 | 126.00 |
| C4 | -Mo1 | -C14 | 85.55(5) | C8 | -C7 | -H71 | 126.00 |
| C5 | -Mo1 | -C6 | 35.38(5) | C8 | -C9 | -H91 | 109.00 |
| C5 | -Mo1 | -C7 | 59.31(5) | C10 | -C9 | -H91 | 109.00 |
| C5 | -Mo1 | -C8 | 59.59(5) | C14 | -C9 | -H91 | 109.00 |
| C5 | -Mo1 | -C14 | 118.53(5) | C9 | -C10 | -H101 | 110.00 |
| C6 | -Mo1 | -C7 | 35.64(5) | C9 | -C10 | -H102 | 110.00 |
| C6 | -Mo1 | -C8 | 59.80(5) | C11 | -C10 | -H101 | 110.00 |
| C6 | -Mo1 | -C14 | 114.87(5) | C11 | -C10 | -H102 | 110.00 |
| C7 | -Mo1 | -C8 | 36.25(5) | H101 | -C10 | -H102 | 108.00 |
| C7 | -Mo1 | -C14 | 79.90(5) | C10 | -C11 | -H111 | 109.00 |
| C8 | -Mo1 | -C14 | 60.42(4) | C10 | -C11 | -H112 | 109.00 |
| Mo1 | -C1 | -O1 | 179.00(14) | C12 | -C11 | -H111 | 109.00 |
| Mo1 | -C2 | -O2 | 176.94(12) | C12 | -C11 | -H112 | 109.00 |
| Mo1 | -C3 | -O3 | 177.70(12) | H111 | -C11 | -H112 | 108.00 |
| Mo1 | -C4 | -C5 | 72.74(8) | C11 | -C12 | -H121 | 109.00 |
| Mo1 | -C4 | -C8 | 70.77(8) | C11 | -C12 | -H122 | 109.00 |
| C5 | -C4 | -C8 | 108.18(12) | C13 | -C12 | -H121 | 109.00 |
| Mo1 | -C5 | -C4 | 71.89(8) | C13 | -C12 | -H122 | 109.00 |
| Mo1 | -C5 | -C6 | 72.33(8) | H121 | -C12 | -H122 | 108.00 |
| C4 | -C5 | -C6 | 108.34(13) | C12 | -C13 | -H131 | 110.00 |
| Mo1 | -C6 | -C5 | 72.29(8) | C12 | -C13 | -H132 | 110.00 |
| Mo1 | -C6 | -C7 | 70.91(8) | C14 | -C13 | -H131 | 110.00 |
| C5 | -C6 | -C7 | 107.85(12) | C14 | -C13 | -H132 | 110.00 |
| Mo1 | -C7 | -C6 | 73.44(8) | H131 | -C13 | -H132 | 108.00 |
| Mo1 | -C7 | -C8 | 71.42(8) | Mo1 | -C14 | -H141 | 110.00 |

| | | | | | | | |
|-----|-----|-----|------------|-----|------|-------|--------|
| C6 | -C7 | -C8 | 108.11(13) | C9 | -C14 | -H141 | 110.00 |
| Mo1 | -C8 | -C4 | 73.32(8) | C13 | -C14 | -H141 | 110.00 |
| Mo1 | -C8 | -C7 | 72.33(7) | | | | |

14.8 Crystal data of compound 3a

14.8.1 Bond distances (in Å)

| | | | | | |
|-----|------|----------|-----|-------|----------|
| W1 | -C1 | 2.014(5) | C4 | -H41 | 0.95 |
| W1 | -C2 | 1.987(5) | C5 | -H51 | 0.95 |
| W1 | -C3 | 1.998(5) | C6 | -H61 | 0.95 |
| W1 | -C4 | 2.330(5) | C7 | -H71 | 0.95 |
| W1 | -C5 | 2.337(5) | C9 | -H91 | 1.00 |
| W1 | -C6 | 2.333(5) | C10 | -H101 | 0.99 |
| W1 | -C7 | 2.304(5) | C10 | -H102 | 0.99 |
| W1 | -C8 | 2.306(5) | C11 | -H112 | 0.99 |
| W1 | -C13 | 2.353(5) | C11 | -H111 | 0.99 |
| W2 | -C26 | 2.339(5) | C12 | -H122 | 0.99 |
| W2 | -C27 | 2.317(5) | C12 | -H121 | 0.99 |
| W2 | -C28 | 2.301(5) | C13 | -H131 | 1.00 |
| W2 | -C33 | 2.398(4) | C24 | -C25 | 1.403(8) |
| W2 | -C21 | 2.014(6) | C24 | -C28 | 1.431(8) |
| W2 | -C22 | 1.982(5) | C25 | -C26 | 1.432(8) |
| W2 | -C23 | 1.991(5) | C26 | -C27 | 1.409(7) |
| W2 | -C24 | 2.318(5) | C27 | -C28 | 1.433(7) |
| W2 | -C25 | 2.334(5) | C28 | -C29 | 1.516(7) |
| O1 | -C1 | 1.155(6) | C29 | -C30 | 1.547(8) |
| O2 | -C2 | 1.158(6) | C29 | -C33 | 1.562(7) |
| O3 | -C3 | 1.148(6) | C30 | -C31 | 1.551(9) |
| O4 | -C21 | 1.151(7) | C31 | -C32 | 1.483(9) |
| O5 | -C22 | 1.155(7) | C32 | -C33 | 1.509(8) |
| O6 | -C23 | 1.147(7) | C24 | -H241 | 0.95 |
| C4 | -C8 | 1.428(8) | C25 | -H251 | 0.95 |
| C4 | -C5 | 1.426(8) | C26 | -H261 | 0.95 |
| C5 | -C6 | 1.417(8) | C27 | -H271 | 0.95 |
| C6 | -C7 | 1.426(7) | C29 | -H291 | 1.00 |
| C7 | -C8 | 1.429(7) | C30 | -H301 | 0.99 |
| C8 | -C9 | 1.503(7) | C30 | -H302 | 0.99 |
| C9 | -C13 | 1.564(7) | C31 | -H311 | 0.99 |
| C9 | -C10 | 1.549(8) | C31 | -H312 | 0.99 |
| C10 | -C11 | 1.531(7) | C32 | -H321 | 0.99 |
| C11 | -C12 | 1.539(7) | C32 | -H322 | 0.99 |
| C12 | -C13 | 1.535(8) | C33 | -H331 | 1.00 |

14.8.2 Bond angles (in °)

| | | | | | | | |
|-----|-----|------|------------|-----|------|------|------------|
| C1 | -W1 | -C2 | 79.9(2) | C23 | -W2 | -C33 | 76.5(2) |
| C1 | -W1 | -C3 | 79.9(2) | C24 | -W2 | -C25 | 35.1(2) |
| C1 | -W1 | -C4 | 121.5(2) | C24 | -W2 | -C26 | 58.93(19) |
| C1 | -W1 | -C5 | 93.1(2) | C24 | -W2 | -C27 | 59.52(18) |
| C1 | -W1 | -C6 | 97.25(19) | C24 | -W2 | -C28 | 36.10(19) |
| C1 | -W1 | -C7 | 129.85(17) | C24 | -W2 | -C33 | 82.77(19) |
| C1 | -W1 | -C8 | 152.86(19) | C25 | -W2 | -C26 | 35.70(18) |
| C1 | -W1 | -C13 | 146.19(17) | C25 | -W2 | -C27 | 59.34(18) |
| C2 | -W1 | -C3 | 101.8(2) | C25 | -W2 | -C28 | 59.67(19) |
| C2 | -W1 | -C4 | 155.10(19) | C25 | -W2 | -C33 | 116.72(19) |
| C2 | -W1 | -C5 | 142.98(19) | C26 | -W2 | -C27 | 35.24(18) |
| C2 | -W1 | -C6 | 109.04(19) | C26 | -W2 | -C28 | 59.53(19) |
| C2 | -W1 | -C7 | 97.69(19) | C26 | -W2 | -C33 | 117.14(19) |
| C2 | -W1 | -C8 | 119.64(19) | C27 | -W2 | -C28 | 36.16(18) |
| C2 | -W1 | -C13 | 79.04(18) | C27 | -W2 | -C33 | 83.40(16) |
| C3 | -W1 | -C4 | 95.1(2) | C28 | -W2 | -C33 | 60.53(18) |
| C3 | -W1 | -C5 | 112.8(2) | W1 | -C1 | -O1 | 179.4(4) |
| C3 | -W1 | -C6 | 148.1(2) | W1 | -C2 | -O2 | 176.5(4) |
| C3 | -W1 | -C7 | 147.2(2) | W1 | -C3 | -O3 | 177.5(5) |
| C3 | -W1 | -C8 | 111.2(2) | C5 | -C4 | -C8 | 108.4(5) |
| C3 | -W1 | -C13 | 78.9(2) | W1 | -C4 | -C8 | 71.1(3) |
| C4 | -W1 | -C5 | 35.6(2) | W1 | -C4 | -C5 | 72.5(3) |
| C4 | -W1 | -C6 | 59.11(19) | W1 | -C5 | -C6 | 72.2(3) |
| C4 | -W1 | -C7 | 59.43(18) | C4 | -C5 | -C6 | 108.1(5) |
| C4 | -W1 | -C8 | 35.88(19) | W1 | -C5 | -C4 | 72.0(3) |
| C4 | -W1 | -C13 | 86.45(18) | W1 | -C6 | -C5 | 72.5(3) |
| C5 | -W1 | -C6 | 35.32(19) | W1 | -C6 | -C7 | 71.0(3) |
| C5 | -W1 | -C7 | 59.37(18) | C5 | -C6 | -C7 | 107.9(5) |
| C5 | -W1 | -C8 | 59.83(19) | W1 | -C7 | -C8 | 72.0(3) |
| C5 | -W1 | -C13 | 119.34(18) | C6 | -C7 | -C8 | 108.5(5) |
| C6 | -W1 | -C7 | 35.81(18) | W1 | -C7 | -C6 | 73.2(3) |
| C6 | -W1 | -C8 | 59.9(2) | W1 | -C8 | -C4 | 73.0(3) |
| C6 | -W1 | -C13 | 114.51(18) | C7 | -C8 | -C9 | 124.1(5) |
| C7 | -W1 | -C8 | 36.11(18) | W1 | -C8 | -C7 | 71.9(3) |
| C7 | -W1 | -C13 | 79.18(16) | W1 | -C8 | -C9 | 100.7(3) |
| C8 | -W1 | -C13 | 60.64(17) | C4 | -C8 | -C7 | 107.1(5) |
| C21 | -W2 | -C22 | 79.9(2) | C4 | -C8 | -C9 | 123.9(5) |
| C21 | -W2 | -C23 | 80.6(2) | C8 | -C9 | -C13 | 100.2(4) |
| C21 | -W2 | -C24 | 124.3(2) | C10 | -C9 | -C13 | 107.2(4) |
| C21 | -W2 | -C25 | 94.4(2) | C8 | -C9 | -C10 | 118.8(4) |
| C21 | -W2 | -C26 | 95.3(2) | C9 | -C10 | -C11 | 103.6(4) |
| C21 | -W2 | -C27 | 125.88(18) | C10 | -C11 | -C12 | 103.4(4) |
| C21 | -W2 | -C28 | 152.92(19) | C11 | -C12 | -C13 | 103.0(4) |
| C21 | -W2 | -C33 | 146.46(18) | W1 | -C13 | -C12 | 120.9(3) |
| C22 | -W2 | -C23 | 100.7(2) | C9 | -C13 | -C12 | 103.9(4) |
| C22 | -W2 | -C24 | 152.60(19) | W1 | -C13 | -C9 | 96.9(3) |
| C22 | -W2 | -C25 | 145.8(2) | W1 | -C4 | -H41 | 122.00 |
| C22 | -W2 | -C26 | 110.7(2) | C8 | -C4 | -H41 | 126.00 |
| C22 | -W2 | -C27 | 96.85(19) | C5 | -C4 | -H41 | 126.00 |
| C22 | -W2 | -C28 | 116.57(19) | C4 | -C5 | -H51 | 126.00 |

| | | | | | | | |
|------|------|-------|-----------|------|------|-------|----------|
| C22 | -W2 | -C33 | 80.68(18) | C6 | -C5 | -H51 | 126.00 |
| C23 | -W2 | -C24 | 96.5(2) | W1 | -C5 | -H51 | 122.00 |
| C23 | -W2 | -C25 | 111.7(2) | C7 | -C6 | -H61 | 126.00 |
| C23 | -W2 | -C26 | 147.1(2) | W1 | -C6 | -H61 | 122.00 |
| C23 | -W2 | -C27 | 150.7(2) | C5 | -C6 | -H61 | 126.00 |
| C23 | -W2 | -C28 | 114.5(2) | C6 | -C7 | -H71 | 126.00 |
| W1 | -C7 | -H71 | 121.00 | C27 | -C28 | -C29 | 125.5(5) |
| C8 | -C7 | -H71 | 126.00 | C28 | -C29 | -C30 | 116.0(4) |
| C8 | -C9 | -H91 | 110.00 | C28 | -C29 | -C33 | 100.7(4) |
| C10 | -C9 | -H91 | 110.00 | C30 | -C29 | -C33 | 105.9(4) |
| C13 | -C9 | -H91 | 110.00 | C29 | -C30 | -C31 | 103.5(4) |
| C9 | -C10 | -H102 | 111.00 | C30 | -C31 | -C32 | 105.2(5) |
| C11 | -C10 | -H101 | 111.00 | C31 | -C32 | -C33 | 105.4(4) |
| C9 | -C10 | -H101 | 111.00 | W2 | -C33 | -C29 | 96.7(3) |
| C11 | -C10 | -H102 | 111.00 | W2 | -C33 | -C32 | 122.4(4) |
| H101 | -C10 | -H102 | 109.00 | C29 | -C33 | -C32 | 106.2(4) |
| C10 | -C11 | -H111 | 111.00 | W2 | -C24 | -H241 | 122.00 |
| C12 | -C11 | -H112 | 111.00 | C25 | -C24 | -H241 | 126.00 |
| H111 | -C11 | -H112 | 109.00 | C28 | -C24 | -H241 | 126.00 |
| C10 | -C11 | -H112 | 111.00 | W2 | -C25 | -H251 | 121.00 |
| C12 | -C11 | -H111 | 111.00 | C24 | -C25 | -H251 | 126.00 |
| C11 | -C12 | -H121 | 111.00 | C26 | -C25 | -H251 | 126.00 |
| C13 | -C12 | -H121 | 111.00 | W2 | -C26 | -H261 | 122.00 |
| C13 | -C12 | -H122 | 111.00 | C25 | -C26 | -H261 | 126.00 |
| C11 | -C12 | -H122 | 111.00 | C27 | -C26 | -H261 | 126.00 |
| H121 | -C12 | -H122 | 109.00 | W2 | -C27 | -H271 | 121.00 |
| C9 | -C13 | -H131 | 111.00 | C26 | -C27 | -H271 | 126.00 |
| C12 | -C13 | -H131 | 111.00 | C28 | -C27 | -H271 | 126.00 |
| W1 | -C13 | -H131 | 111.00 | C28 | -C29 | -H291 | 111.00 |
| W2 | -C21 | -O4 | 179.3(4) | C30 | -C29 | -H291 | 111.00 |
| W2 | -C22 | -O5 | 178.1(4) | C33 | -C29 | -H291 | 111.00 |
| W2 | -C23 | -O6 | 177.2(5) | C29 | -C30 | -H301 | 111.00 |
| W2 | -C24 | -C25 | 73.1(3) | C29 | -C30 | -H302 | 111.00 |
| W2 | -C24 | -C28 | 71.3(3) | C31 | -C30 | -H301 | 111.00 |
| C25 | -C24 | -C28 | 108.9(5) | C31 | -C30 | -H302 | 111.00 |
| W2 | -C25 | -C24 | 71.8(3) | H301 | -C30 | -H302 | 109.00 |
| W2 | -C25 | -C26 | 72.3(3) | C30 | -C31 | -H311 | 111.00 |
| C24 | -C25 | -C26 | 107.7(5) | C30 | -C31 | -H312 | 111.00 |
| W2 | -C26 | -C25 | 72.0(3) | C32 | -C31 | -H311 | 111.00 |
| W2 | -C26 | -C27 | 71.6(3) | C32 | -C31 | -H312 | 111.00 |
| C25 | -C26 | -C27 | 108.2(5) | H311 | -C31 | -H312 | 109.00 |
| W2 | -C27 | -C26 | 73.2(3) | C31 | -C32 | -H321 | 111.00 |
| W2 | -C27 | -C28 | 71.3(3) | C31 | -C32 | -H322 | 111.00 |
| C26 | -C27 | -C28 | 108.3(5) | C33 | -C32 | -H321 | 111.00 |
| W2 | -C28 | -C24 | 72.6(3) | C33 | -C32 | -H322 | 111.00 |
| W2 | -C28 | -C27 | 72.5(3) | H321 | -C32 | -H322 | 109.00 |
| W2 | -C28 | -C29 | 102.1(3) | W2 | -C33 | -H331 | 110.00 |
| C24 | -C28 | -C27 | 106.9(5) | C29 | -C33 | -H331 | 110.00 |
| C24 | -C28 | -C29 | 123.5(5) | C32 | -C33 | -H331 | 110.00 |

14.9 Preliminary crystal data of compounds 2e and 3b

| Compound | 2e | 3b |
|--------------------------------|---|---|
| Formula | C ₁₀ H ₈ MoO ₃ | C ₁₄ H ₁₄ WO ₃ |
| Formula Weight | 272.10 | 414.09 |
| Space Group | Orthorhombic, P bcn | Monoclinic, P2 ₁ /n |
| Systematic Absences | 0kl: k≠2n; h0l: l≠2n? | 7.7140(3), 13.3671(6), 12.2217(5) |
| Cell Constants (pm) | a = 749.37(2) b = 1100.19(3) c = 1162.32(4) | a = 819.3(2) b = 1328.0(3) β = 98.851(4)° c = 1196.2(3) |
| V [pm ³] | 958.27(5)·10 ⁶ | 1286.0(5)·10 ⁶ |
| Z | 4 | 4 |
| D (calc) [g·cm ⁻³] | 1.886 | 2.139 |

References cited in this chapter

- (1) López, J.; Liang, S.; Ru, X. R. *Tetrahedron Lett.* **1998**, 39, 4199.
- (2) Boghaei, D. M.; Mohebi, S. *J. Mol. Catal. A: Chem.* **2002**, 179, 41.
- (3) Lin, B.; Qiu, Y.; Su, Z.; Sun, S.; Feng, J. *J. Chinese Universities* **2001**, 22, 1551.
- (4) Delft Data Collection Software for NONIUS alpha-CCD devices; The Netherlands, **2001**.
- (5) Otwinowski, Z.; Minor, W. *Methods in Enzymology* **1997**, 276, 307ff.
- (6) Altomare, A.; Cascarano, G.; Giacovazzo, C.; Guagliardi, A.; Burla, M. C.; Polidori, G.; Camalli, M. *J. Appl. Crystallogr.* **1994**, 27, 435-436.
- (7) *International Tables for Crystallography*; Wilson, A. J. C., Ed.; Kluwer Academic Publishers: The Netherlands, **1992**; Vol. Vol. C, pp. Tables 6.1.1.4, 4.2.6.8, and 4.2.4.2.
- (8) Sheldrick, G. M. *SHELXL-97* **1998**, Universität Göttingen, Göttingen, Germany.
- (9) Spek, A. L. *PLATON, A Multipurpose Crystallographic Tool*; Utrecht University: Utrecht, The Netherlands, **2007**.
- (10) Farrugia, L. J. *WinGX, Version 1.70.01*; **2005**.
- (11) Bruker Analytical X-ray Systems, Inc. *SMART V5.618 Software for the CCD Detector System*; Madison, WI, **1998**.
- (12) Bruker Analytical X-ray Systems, Inc. *SAINTPLUS, V6.45, A Software for the CCD Detector System*; Madison, WI, **1998**.
- (13) Blessing, R. H. *Acta Cryst. A* **1995**, A51, 33.
- (14) Sheldrick, G. M. *SHELXTL-97*. **1997**, Universität Göttingen, Göttingen, Germany.
- (15) Legzdins, P.; Phillips, E. C.; Sánchez, L. *Organometallics* **1989**, 8, 940-949.
- (16) Legzdins, P.; Phillips, E. C.; Rettig, S. J.; Sánchez, L.; Trotter, J.; Yee, V. C. *Organometallics* **1988**, 7, 1877-1878.
- (17) Brandenburg, K. *DIAMOND, Version 3.1d*; Crystal Impact GbR: Bonn, Germany, **2006**.
- (18) Ciruelos, S.; Englert, U.; Salzer, A.; Bolm, C.; Maischak, A. *Organometallics* **2000**, 19, 2240-2242.
- (19) Wiberg, K. B.; Saegbarth, K. A. *J. Am. Chem. Soc.* **1957**, 79, 2822-2824.
- (20) Armanasco, N. L.; Baker, M. V.; North, M. R.; Skelton, B. W.; White, A. H. *J. Chem. Soc., Dalton Trans.* **1998**, 1145-1149.
- (21) Baker, M. V.; North, M. R. *J. Organomet. Chem.* **1998**, 565, 225-230.
- (22) Ellis, J. E.; Rochfort, G. L. *Organometallics* **1982**, 1, 682-689.
- (23) Zybilla, C. E. In *Synthetic Methods of Organometallic and Inorganic Chemistry*; Herrmann, W. A., Ed.; Georg Thieme Verlag: Stuttgart - NewYork, **1997**; Vol. 8, p. 103.

- (24) Amor, F.; Royo, P.; Spaniol, T. P.; Okuda, J. *J. Organomet. Chem.* **2000**, 604, 126-131.
- (25) Wilcox Jr., C. F.; Craig, R. R. *J. Am. Chem. Soc.* **1961**, 83, 3866-3871.

V. APPENDIX

Appendix A: Supplementary Data for Chapter 8

A.1: Derivation of Equation 1

The absorbance at 335 nm (A_{335}) can be expressed as follows:

$$A_{335} = A_p + A_l = [\mathbf{3}] \cdot \varepsilon_p + [I] \cdot \varepsilon_l \quad (1)$$

where A_p and A_l are the absorbance of **3** and the intermediate (I), and ε_p and ε_l are their extinction coefficients, respectively.

With the total mass balance expression, $[Mo]_T = [\mathbf{3}] + [I]$, Eq. 1 can be written as follows:

$$A_{335} = [\mathbf{3}](\varepsilon_p - \varepsilon_l) + [Mo]_T \cdot \varepsilon_l \quad (2)$$

Using the equilibrium expression:

$$K_{eq} = [I]/[TBHP][\mathbf{3}] = ([Mo]_T - [\mathbf{3}])/([TBHP][\mathbf{3}]) \quad (3)$$

and therefore,

$$[\mathbf{3}] = [Mo]_T / (1 + K_{eq}[TBHP]) \quad (3a)$$

Replacing **3** in Eq. 2 by using Eq. 3a

$$A_{335} = (\varepsilon_p - \varepsilon_l)[Mo]_T / (1 + K_{eq}[TBHP]) + [Mo]_T \cdot \varepsilon_l \quad (4)$$

and

$$A_{335}/[Mo]_T = (\varepsilon_p - \varepsilon_l)/(1 + K_{eq}[TBHP]) + \varepsilon_l \quad (5)$$

A.2: Derivation of Equation 4

Based on Scheme 11, the rate of the alkene consumption is:

$$\text{rate} = \frac{-d[\text{alkene}]}{dt} = k_{ep}[\text{alkene}][\text{I}] \quad (1)$$

The change in the intermediate with time can be expressed:

$$\frac{d[\text{I}]}{dt} = k_p[\text{3}][\text{TBHP}] - k_{-p}[\text{I}] - k_{ep}[\text{alkene}][\text{I}] \quad (2)$$

Using the total mass balance expression, $[\text{Mo}]_T = [\text{3}] + [\text{I}]$, Eq. 2 becomes:

$$\frac{d[\text{I}]}{dt} = k_p[\text{TBHP}](\text{Mo}]_T - [\text{I}]) - k_{-p}[\text{I}] - k_{ep}[\text{alkene}][\text{I}] \quad (3)$$

Applying steady-state approximation on [I], $d[\text{I}]/dt = 0$, leads to:

$$[\text{I}]_{ss} = \frac{k_p[\text{TBHP}](\text{Mo}]_T}{k_{-p} + k_p[\text{TBHP}] + k_{ep}[\text{alkene}]} \quad (4)$$

Replacing the value of [I] in Eq. 1 by $[\text{I}]_{ss}$ above, the rate law equation becomes:

$$\text{rate} = \frac{-d[\text{alkene}]}{dt} = \frac{k_p k_{ep} [\text{alkene}] [\text{TBHP}] (\text{Mo}]_T}{k_{-p} + k_p [\text{TBHP}] + k_{ep} [\text{alkene}]} \quad (5)$$

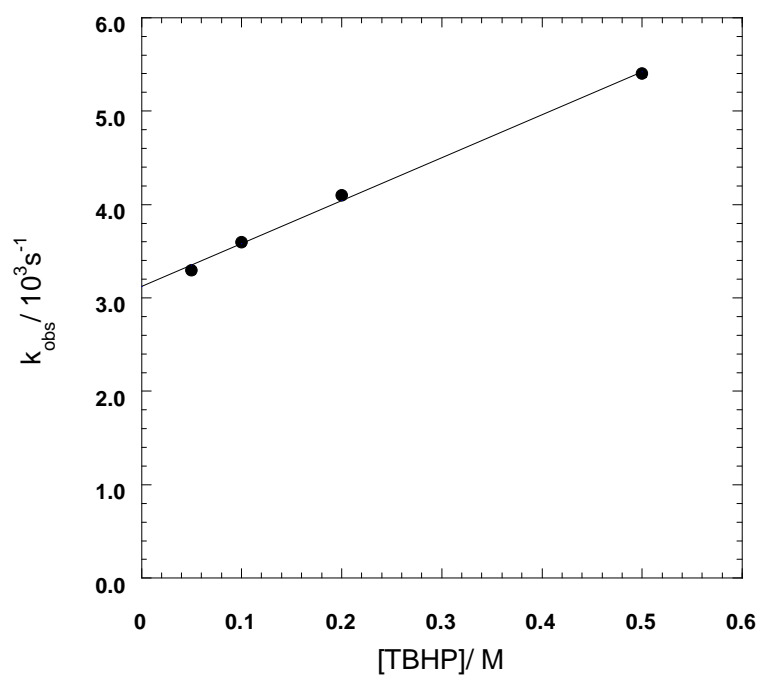


Figure A1. A plot of the observed-first-order rate constant (k_{obs}) against [TBHP] for the reaction of **3** (0.3 mM) with TBHP in CH_2Cl_2 at 20 °C.

Appendix B: NMR spectra of compounds from Chapter 10

^1H -, ^{13}C - and spectra were recorded using a Jeol-JMX-GX 400 MHz or a Bruker Avance DPX-400 spectrometer under r.t. and CDCl_3 unless stated otherwise, and treated with MestreNova v.5.3.0 (© Mestrelab Research S. L.).

B.1 Compounds 1a-1e

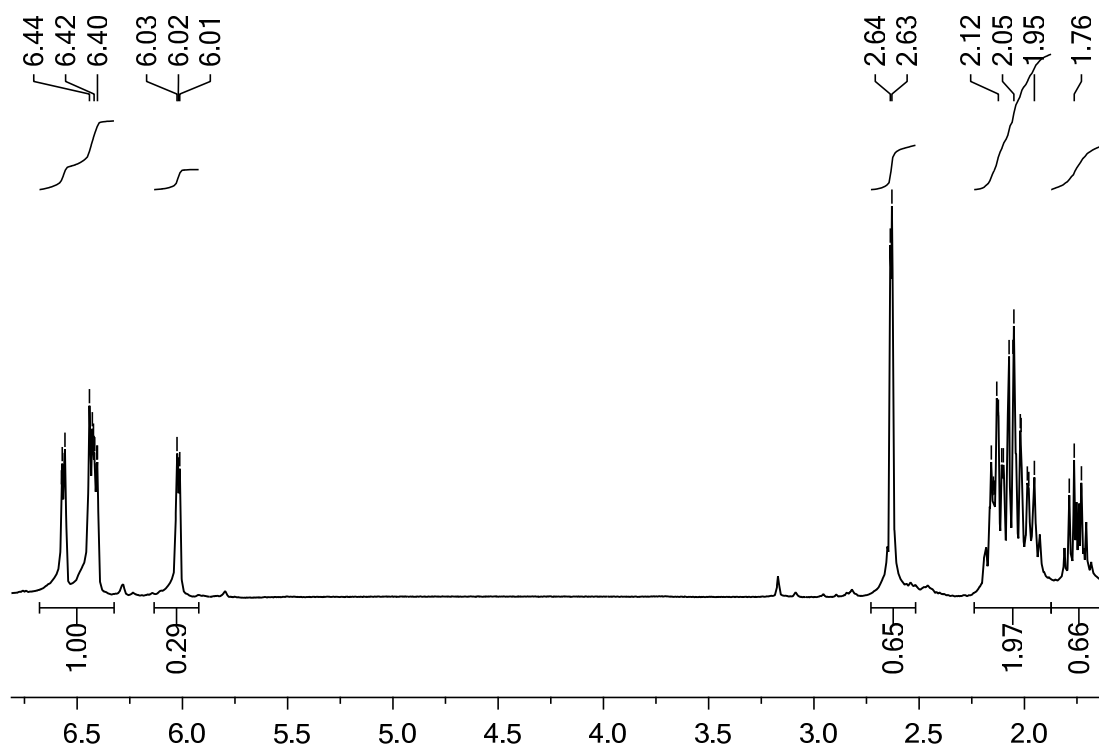


Figure B1 ^1H NMR spectra of compound 1a.

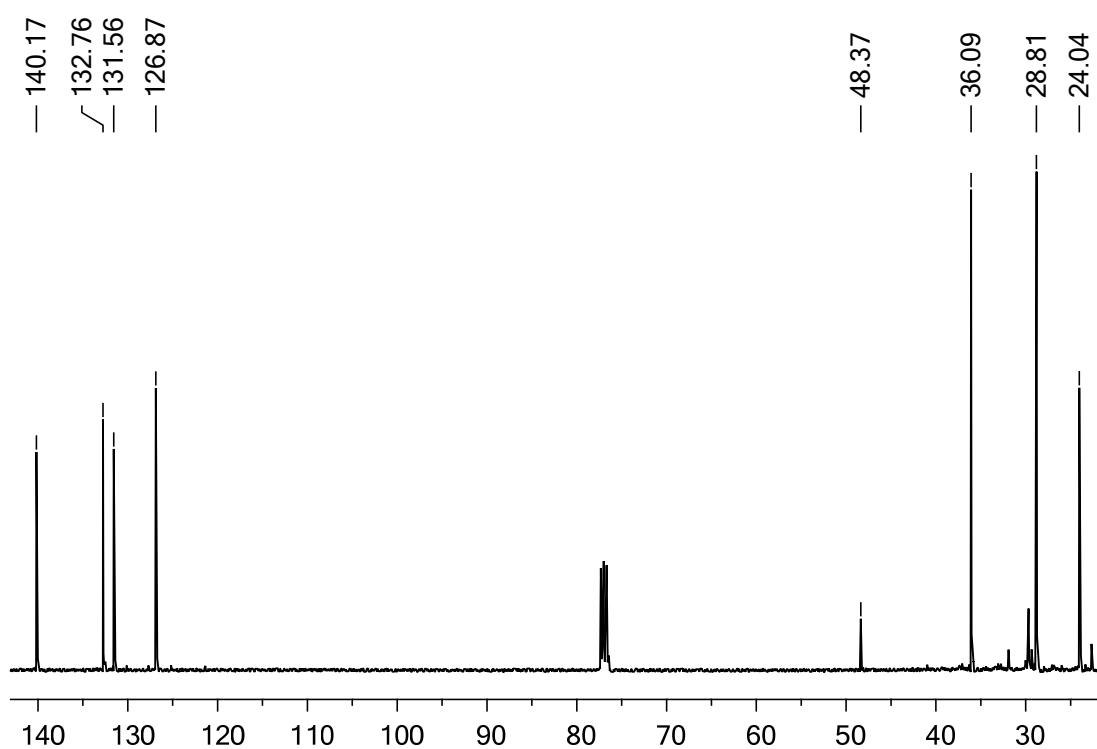


Figure B2 ¹H NMR spectra of compound **1a**.

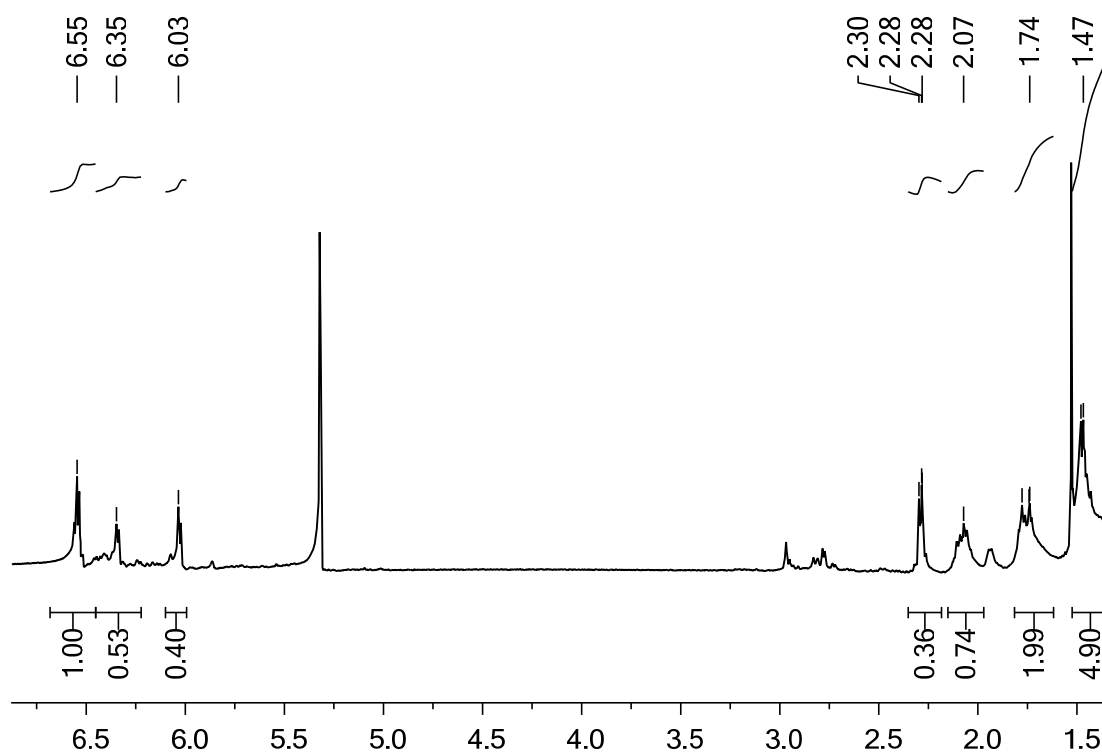
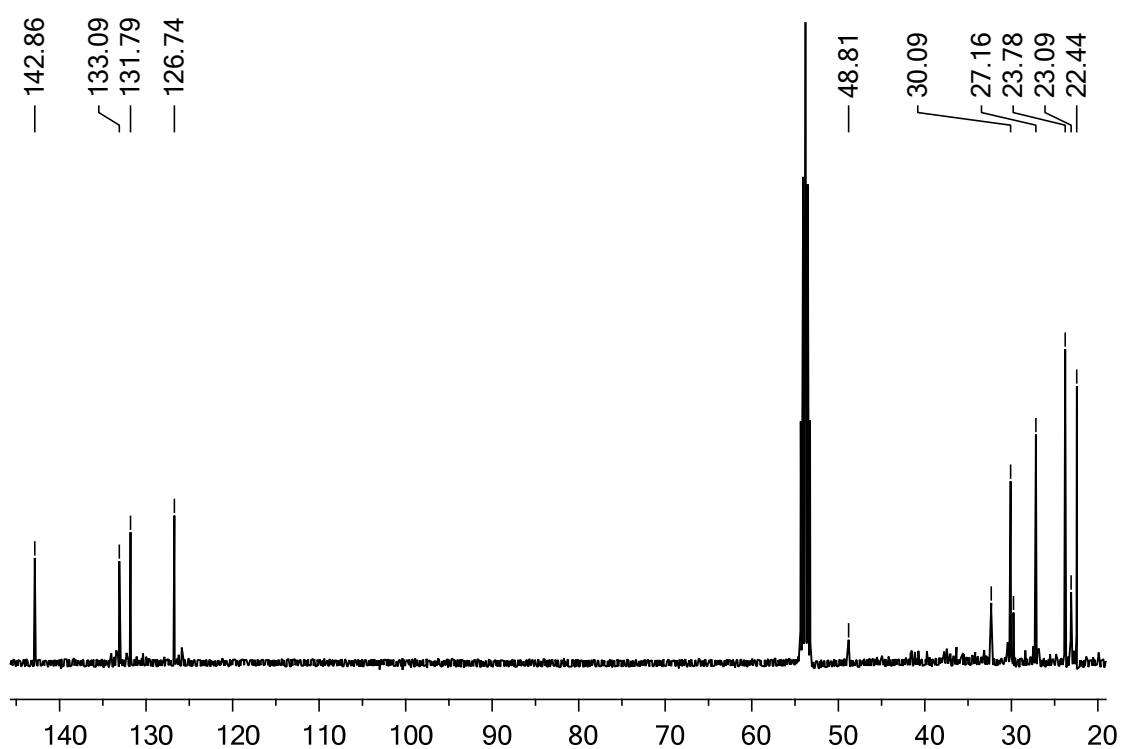
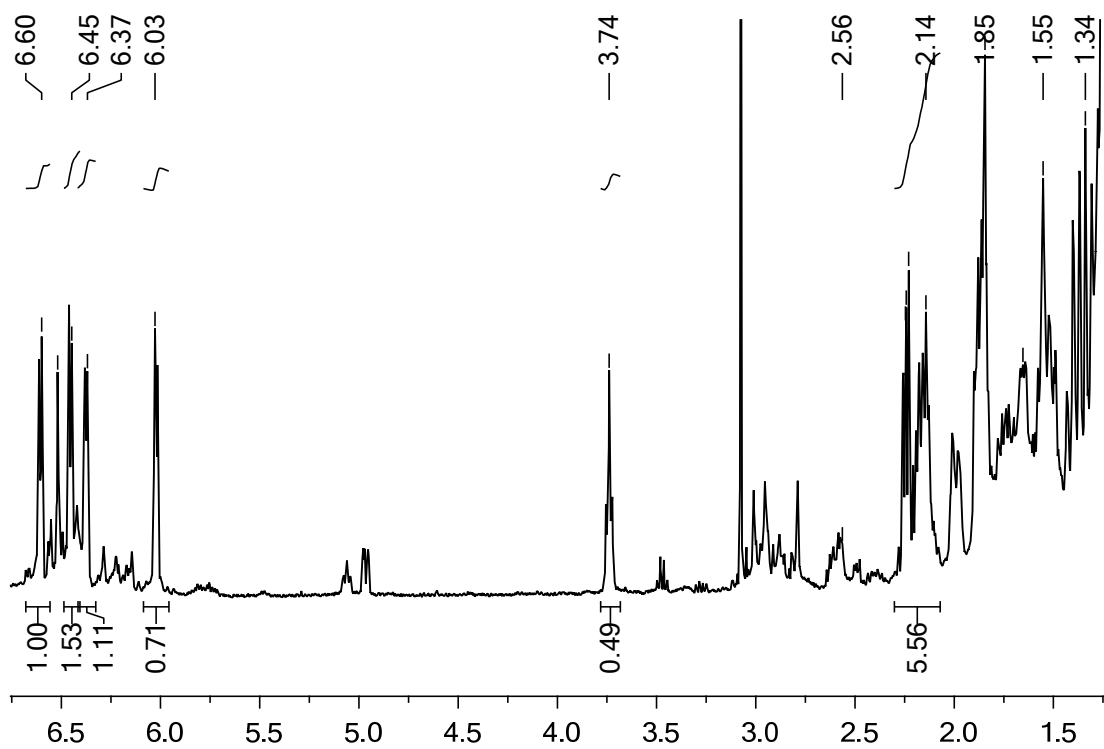
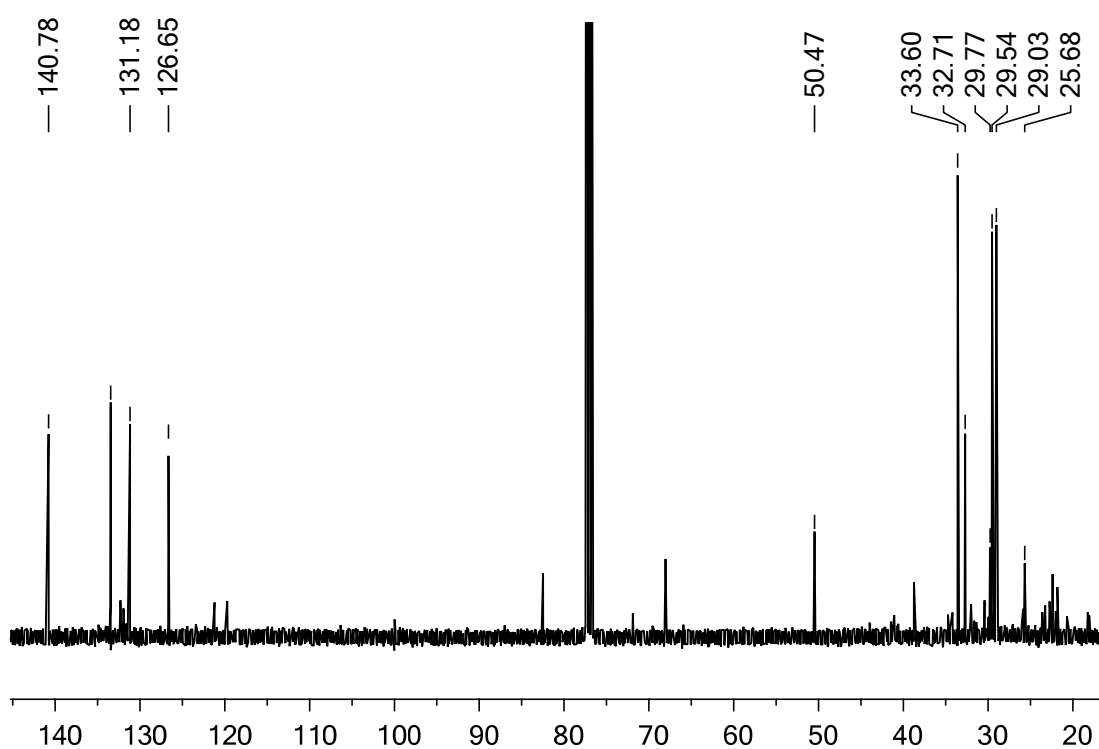
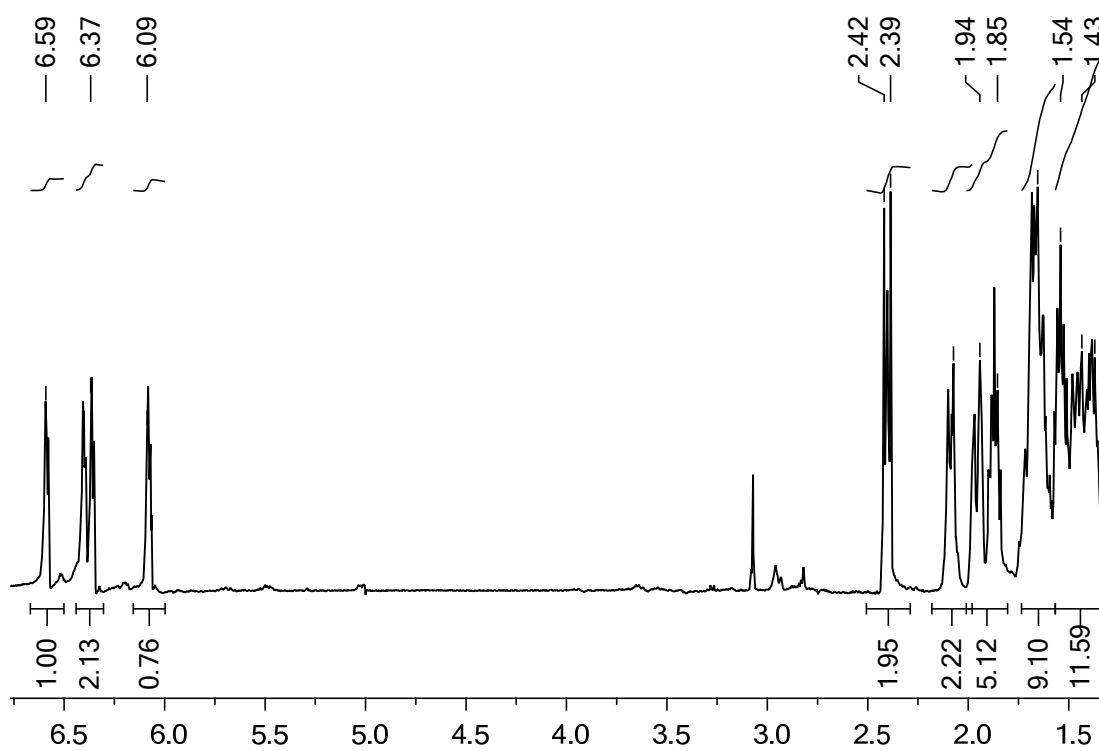


Figure B3 ¹H NMR spectra of compound **1b**.

Figure B4 ^{13}C NMR spectra of compound **1b**.Figure B5 ^1H NMR spectra of compound **1c**.

Figure B6 ^{13}C NMR spectra of compound **1c**.Figure B7 ^1H NMR spectra of compound **1d**.

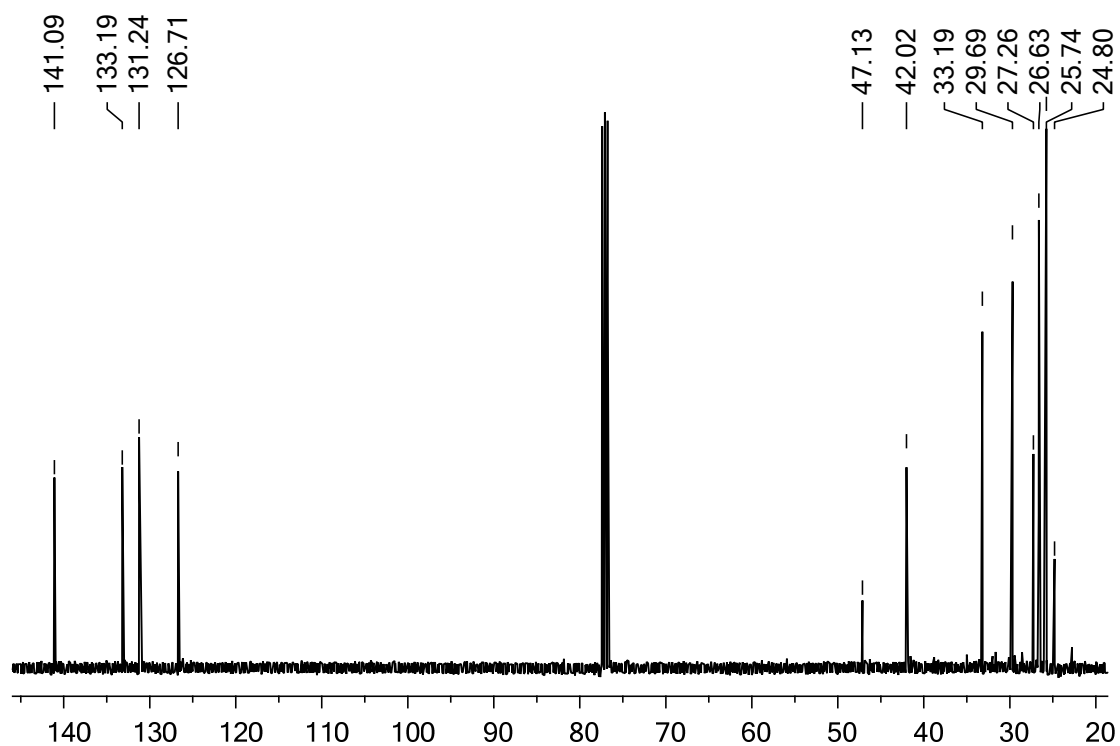


Figure B8 ^{13}C NMR spectra of compound **1d**.

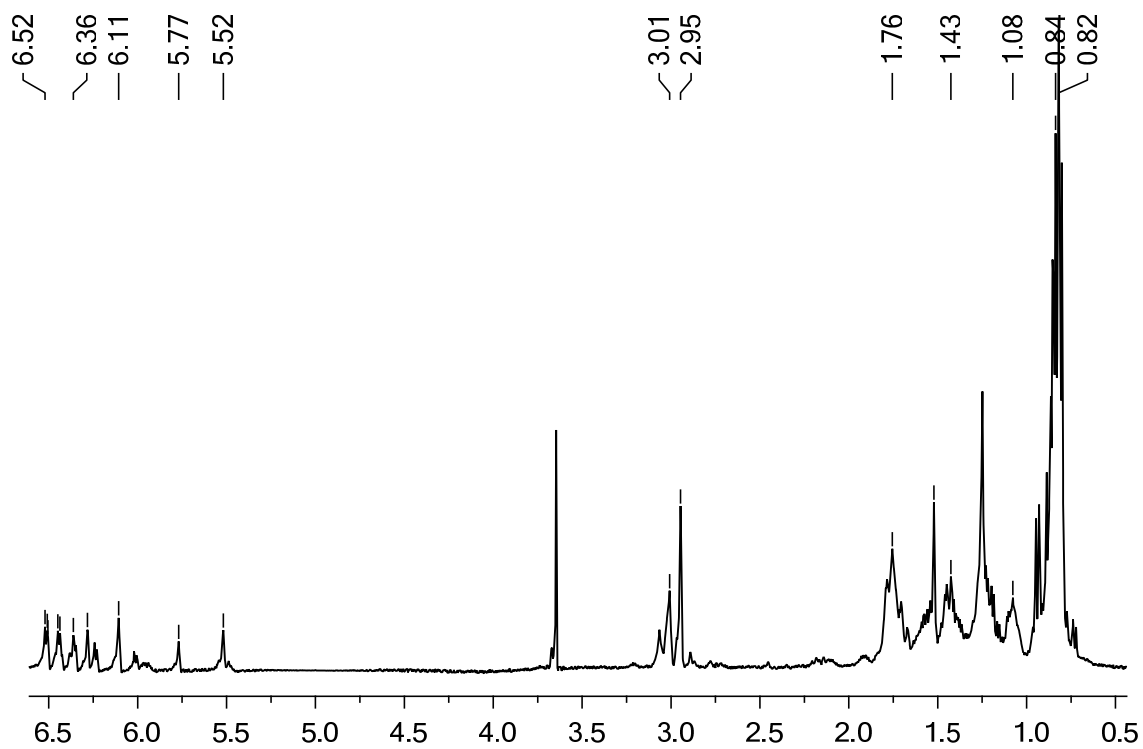
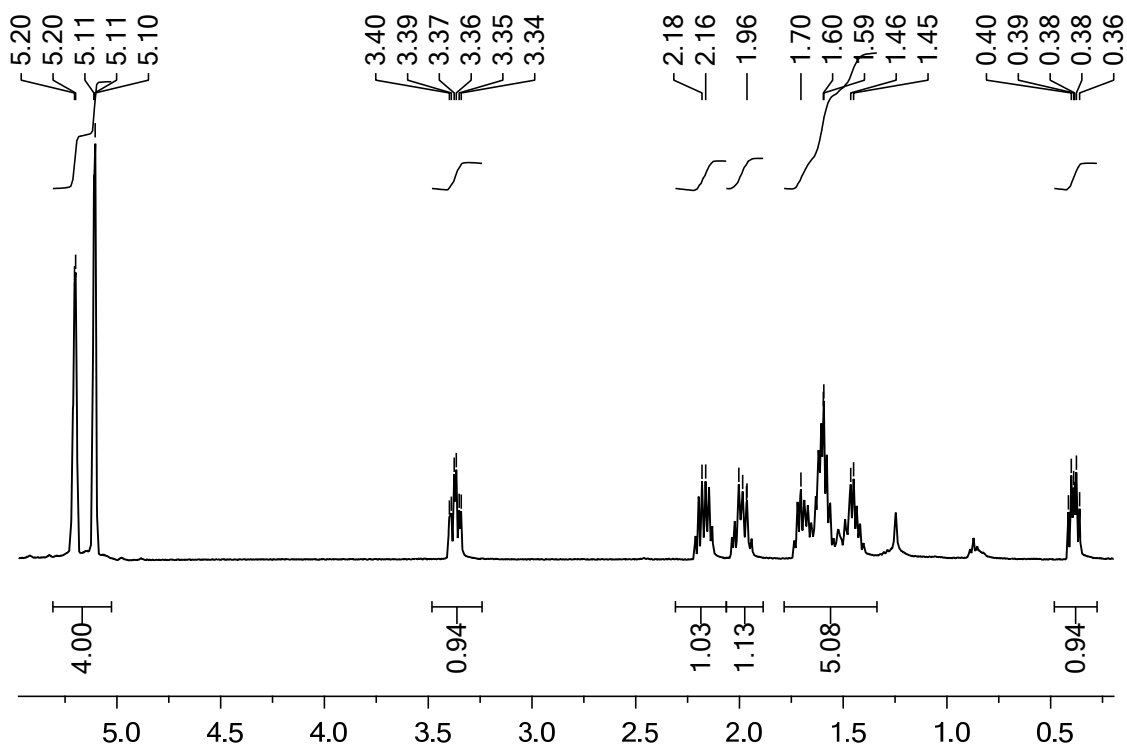
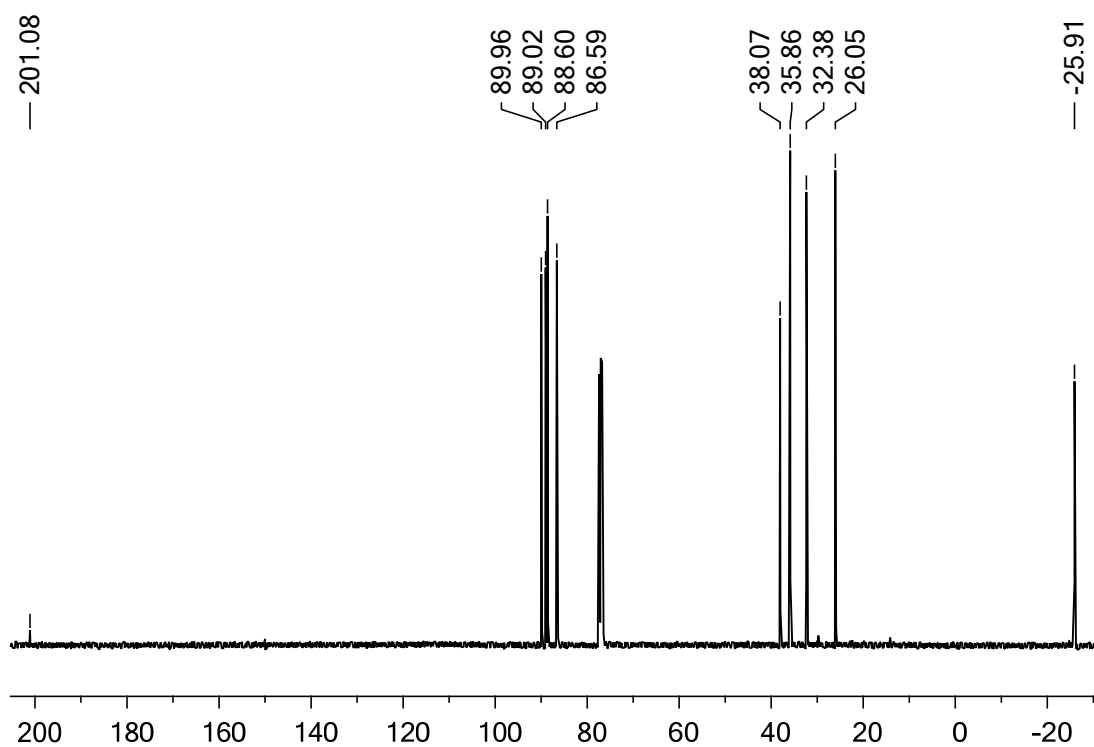


Figure B9 ^1H NMR spectra of compound **1g**.

B.2 Compounds 2a-2f**Figure B10** ¹H NMR spectra of compound 2a.**Figure B11** ¹³C NMR spectra of compound 2a.

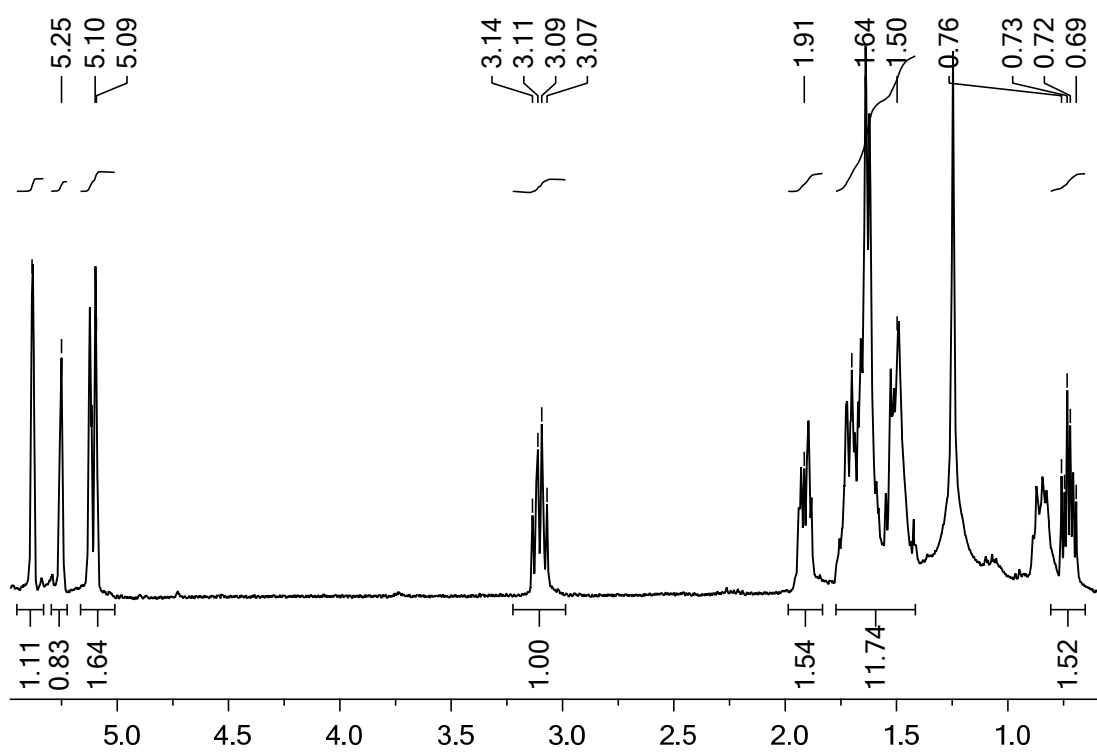


Figure B12 ¹H NMR spectrum of compound 2b.

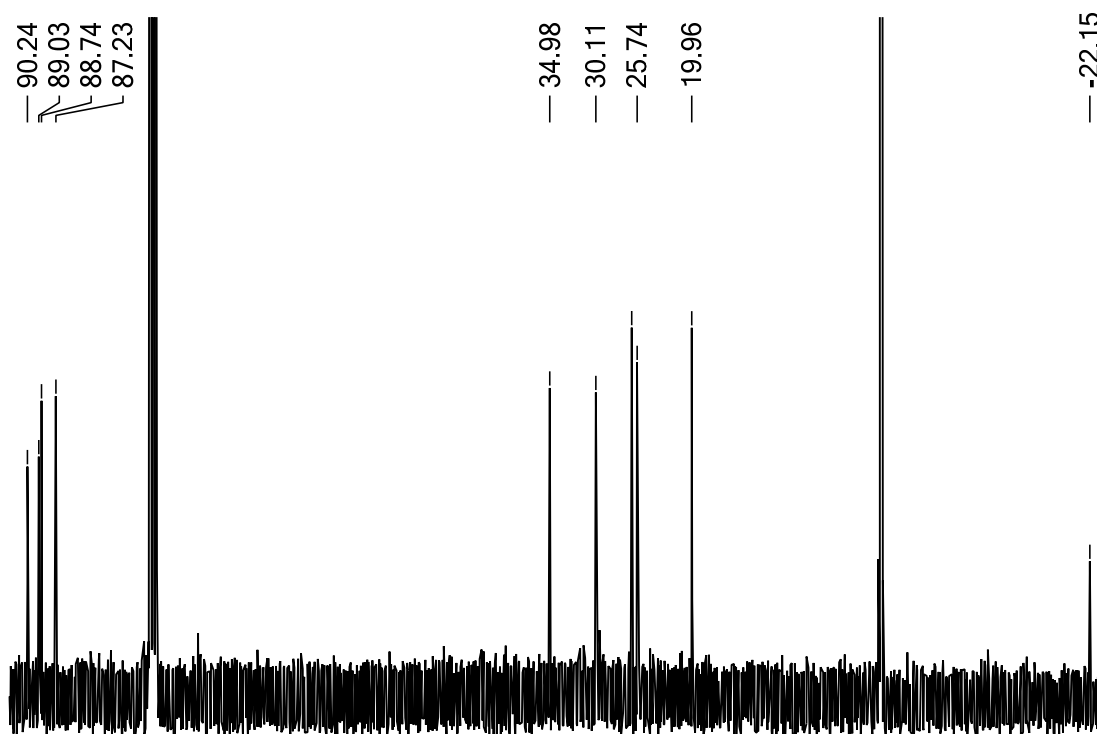


Figure B13 ¹³C NMR spectrum of compound 2b.

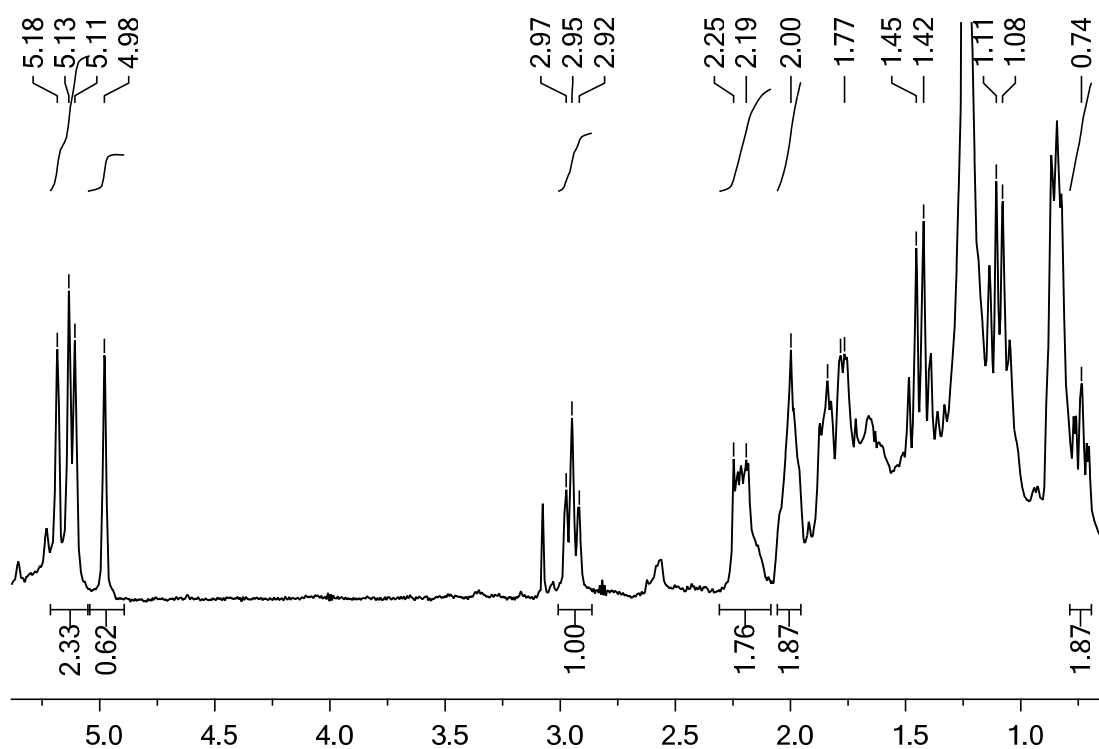


Figure B14 ¹H NMR spectrum of compound **2c**.

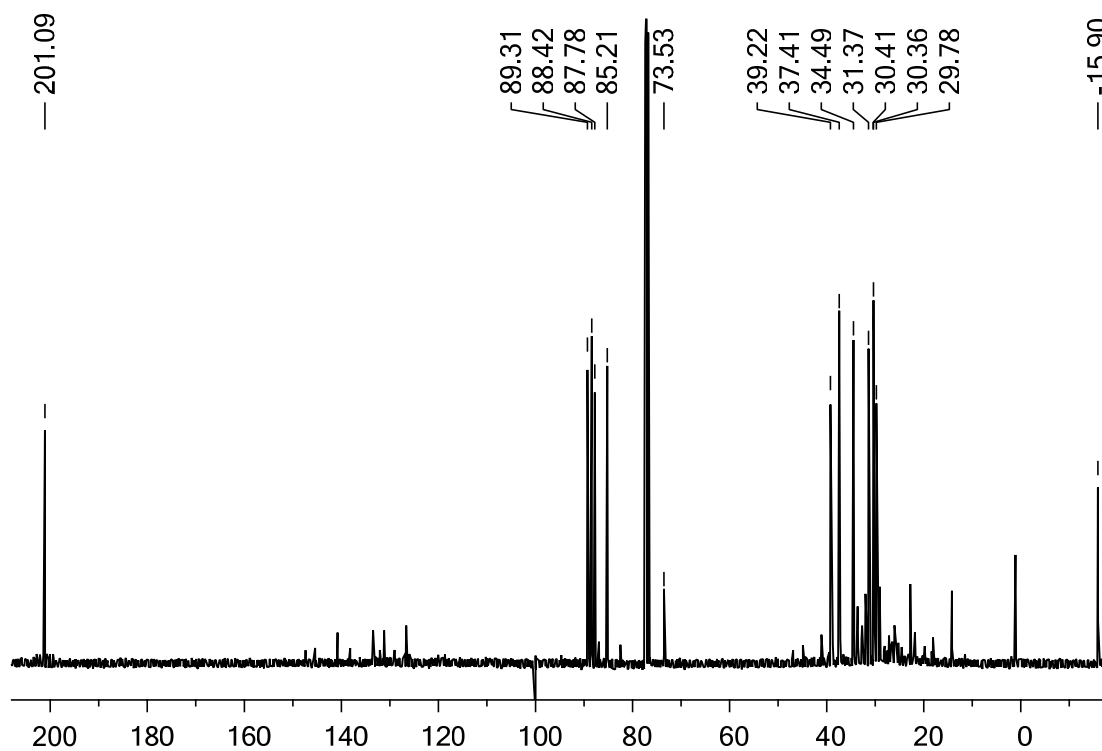


Figure B15 ¹³C NMR spectrum of compound **2c**.

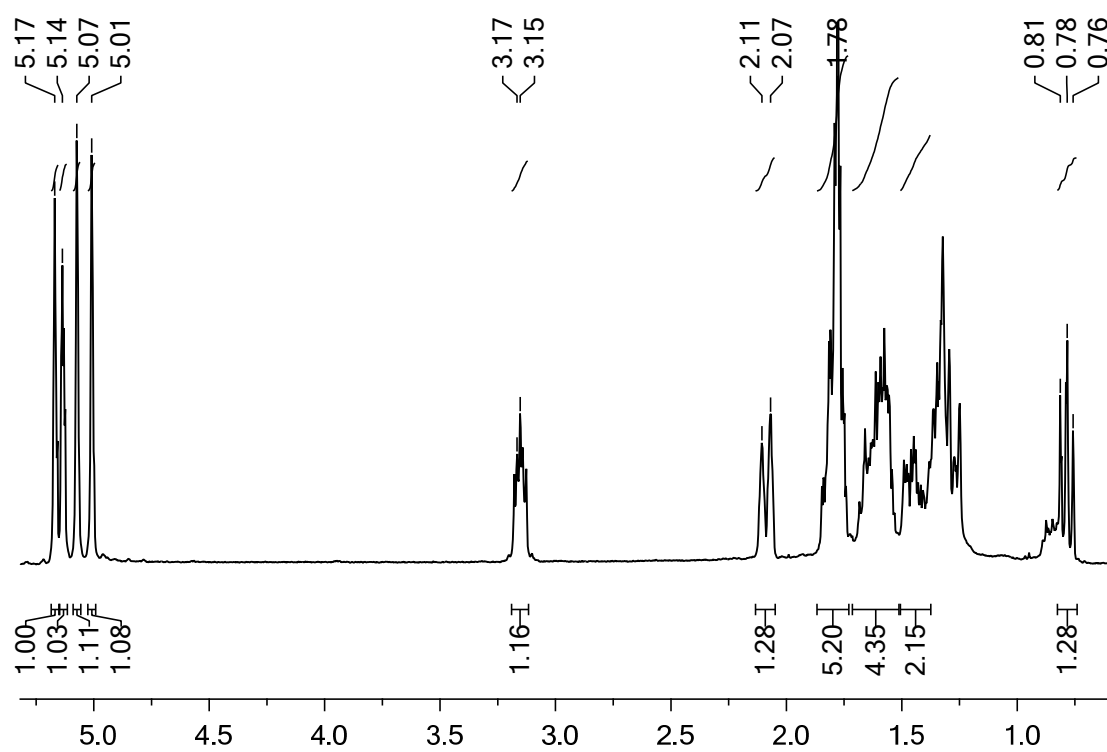


Figure B16 ^1H NMR spectrum of compound **2d**.

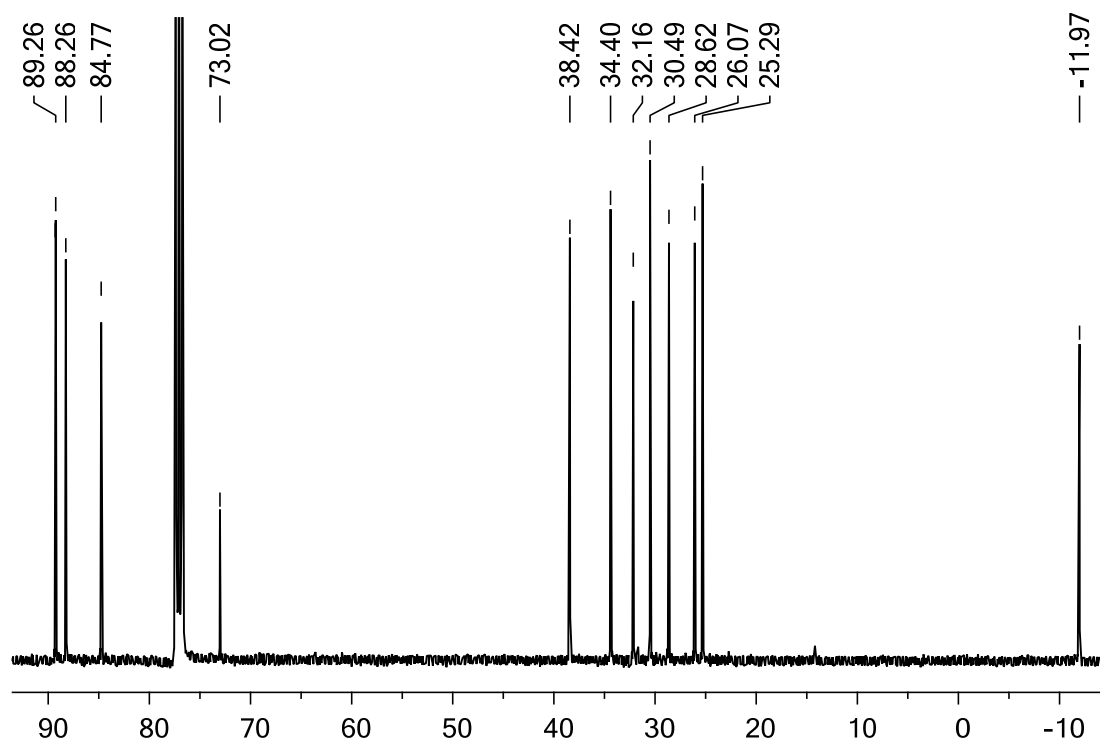


Figure B17 ^{13}C NMR spectrum of compound **2d**.

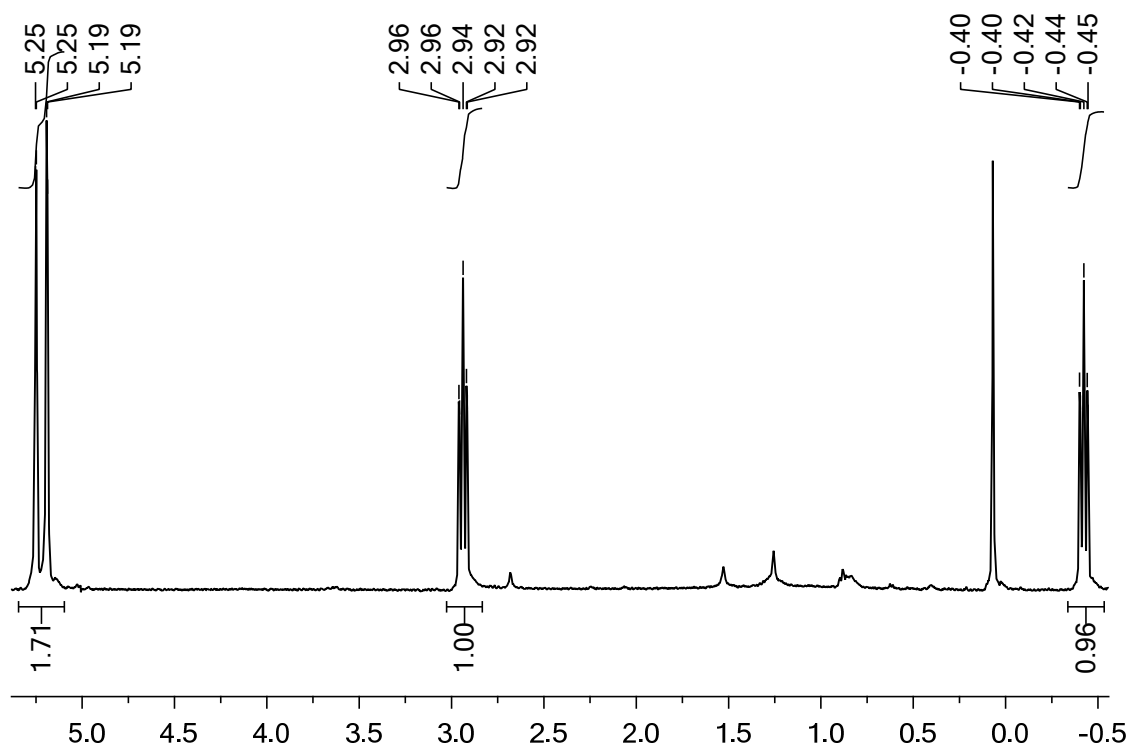


Figure B18 ¹H NMR spectra of compound **2e** (obtained with the Mo(CO)₃Me₃tach precursor).

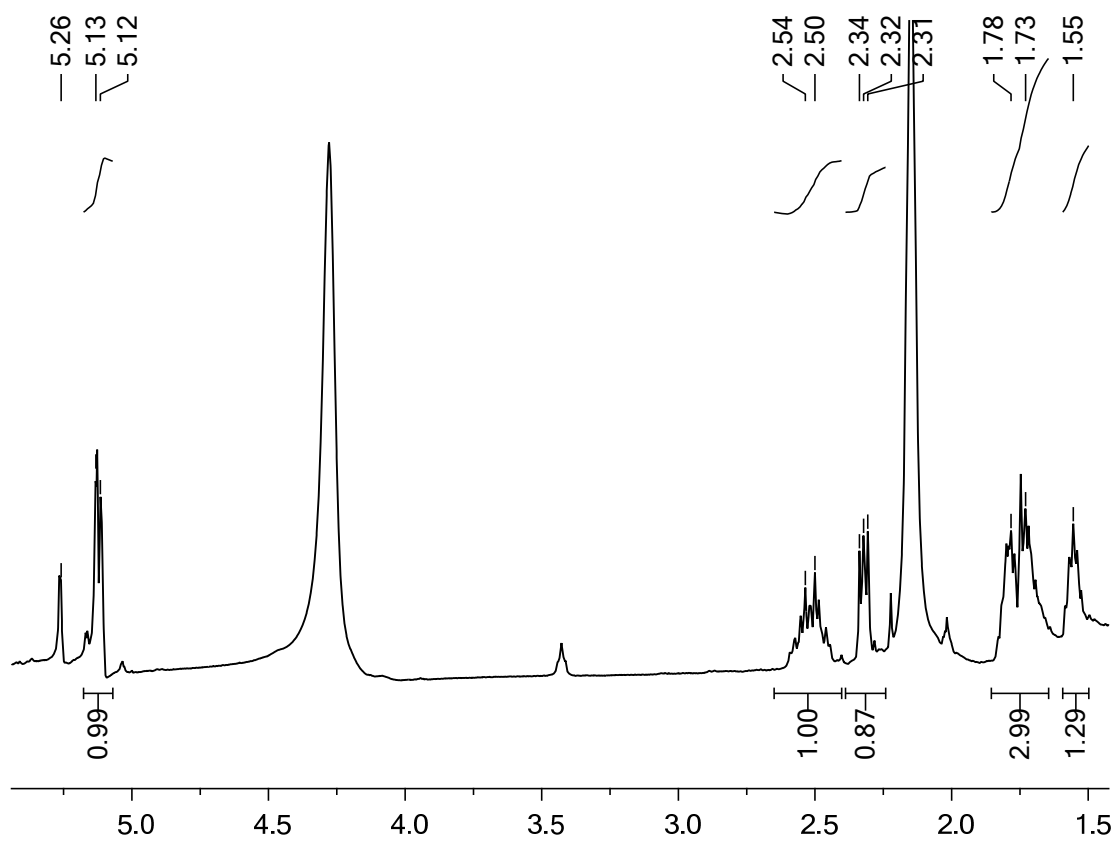


Figure B19 ¹H NMR spectra of compound **4a** (with traces of the dimeric species **5a**).

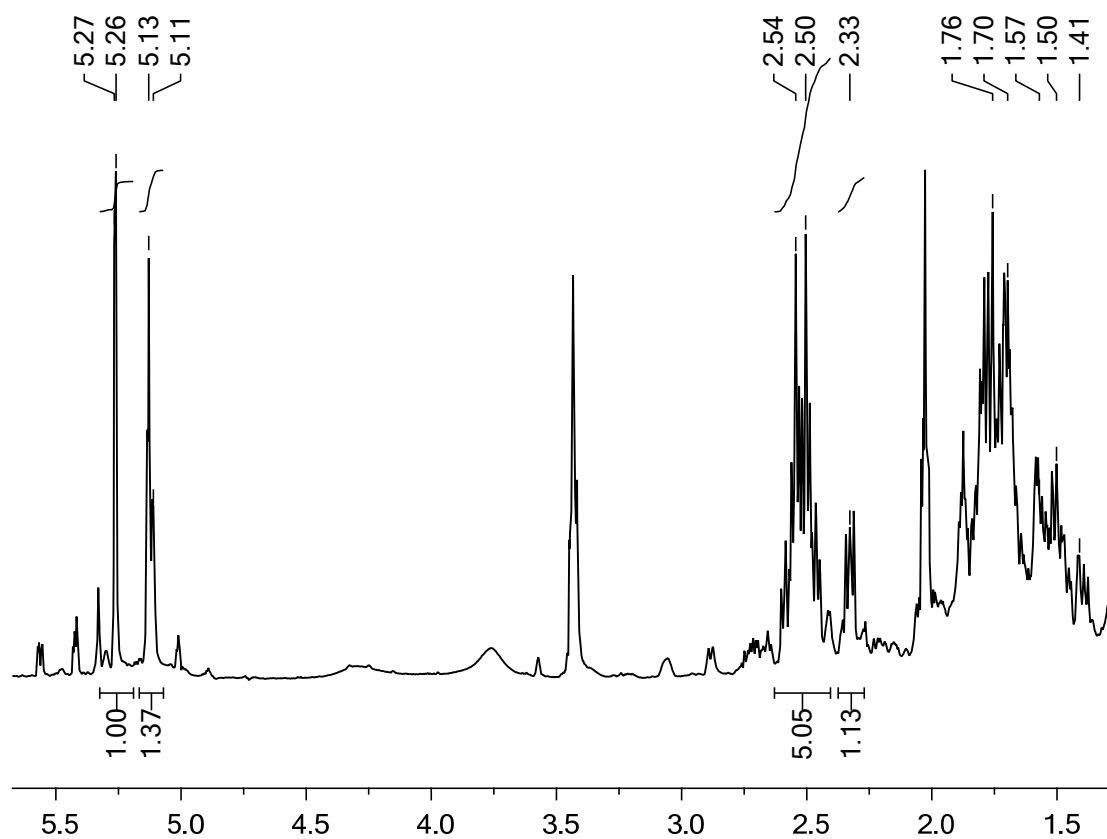


Figure B20 ^1H NMR spectra of the postulated dimeric compound **5a** (with traces of complex **4a**).

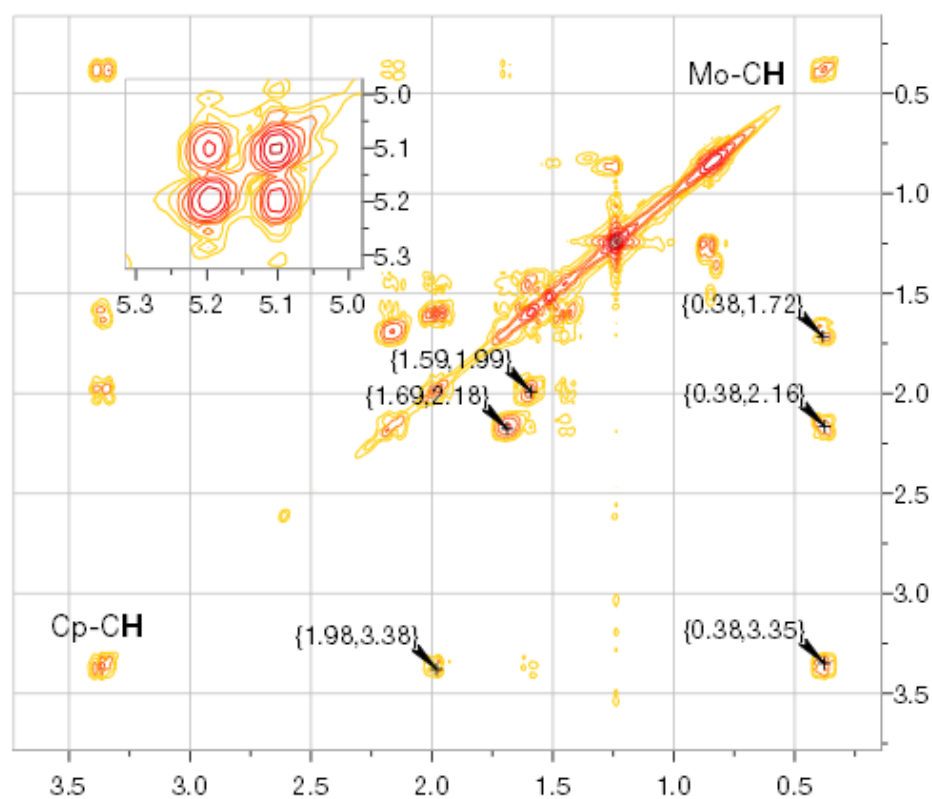


Figure B21 2D-COSY of **2a**, showing both the cyclopentadienyl (upper left corner) and the *ansa* cyclopentyl spin systems.

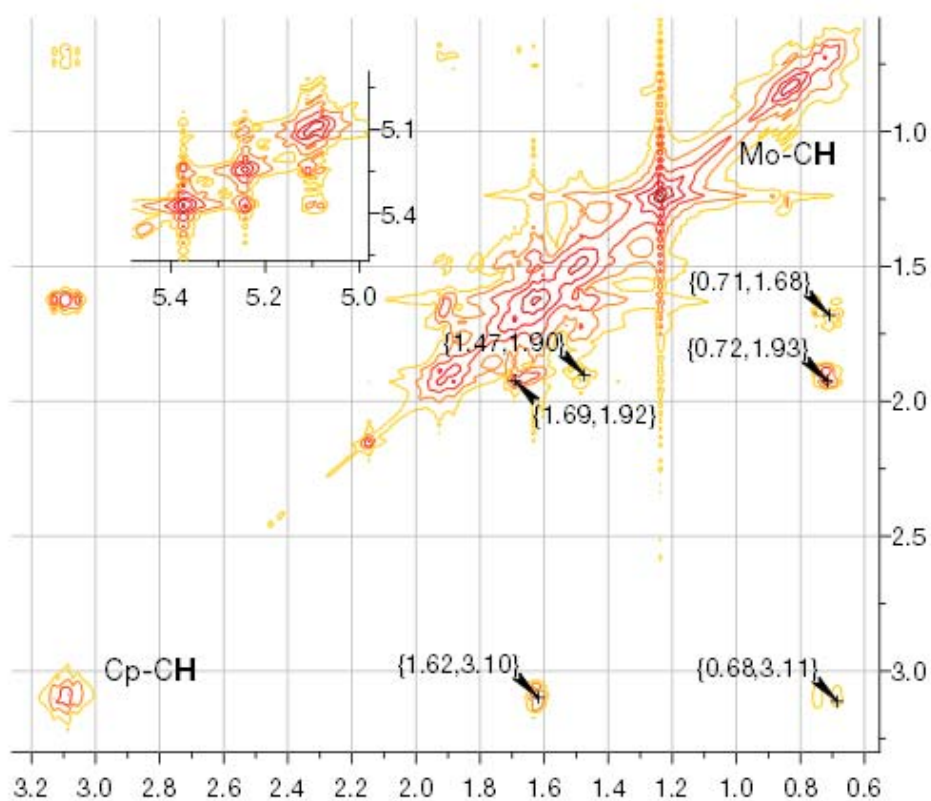


Figure B22 2D-COSY of **2b**, showing both the cyclopentadienyl (upper left corner) and the *ansa* cyclopentyl spin systems.

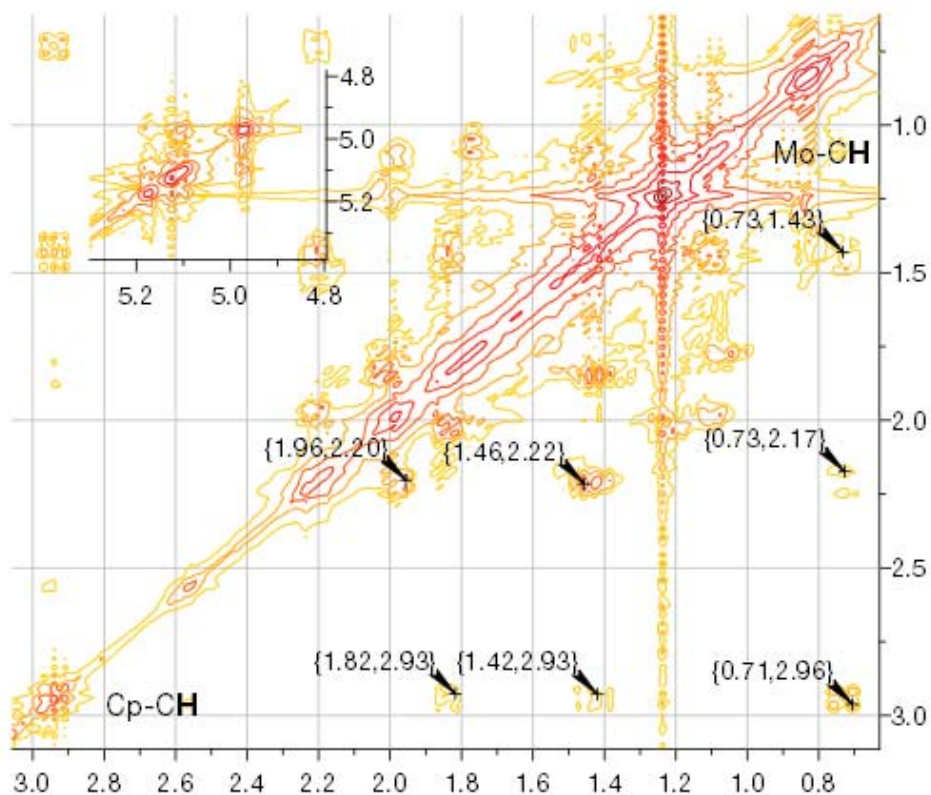


Figure B23 2D-COSY of **2c**, showing both the cyclopentadienyl (upper left corner) and the *ansa* cyclopentyl spin systems.

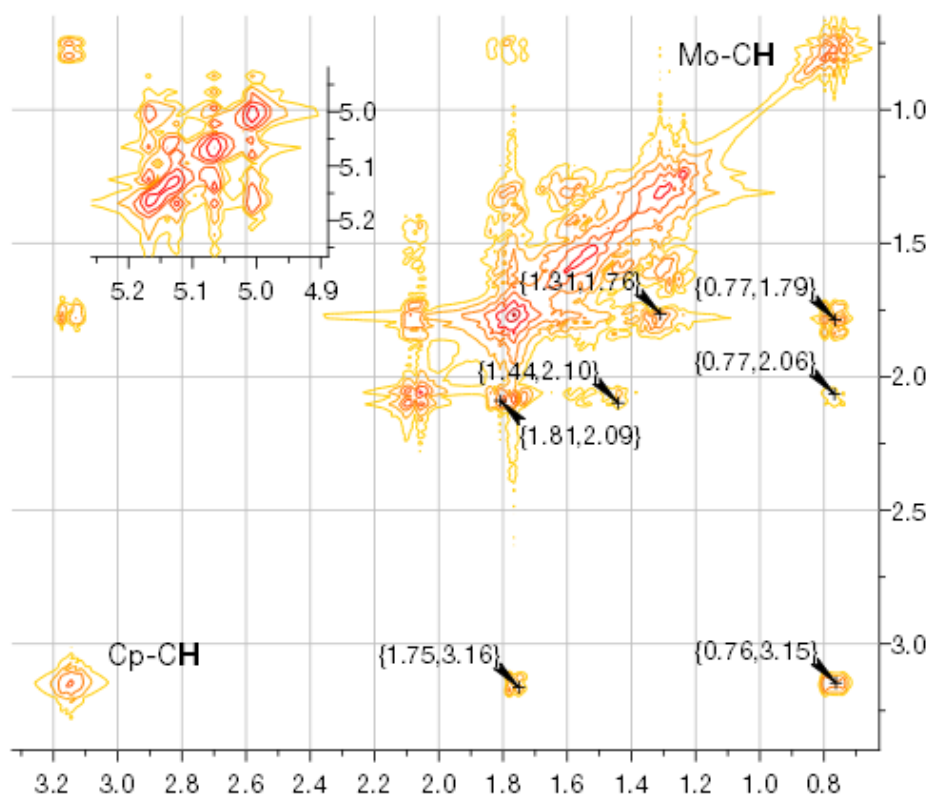
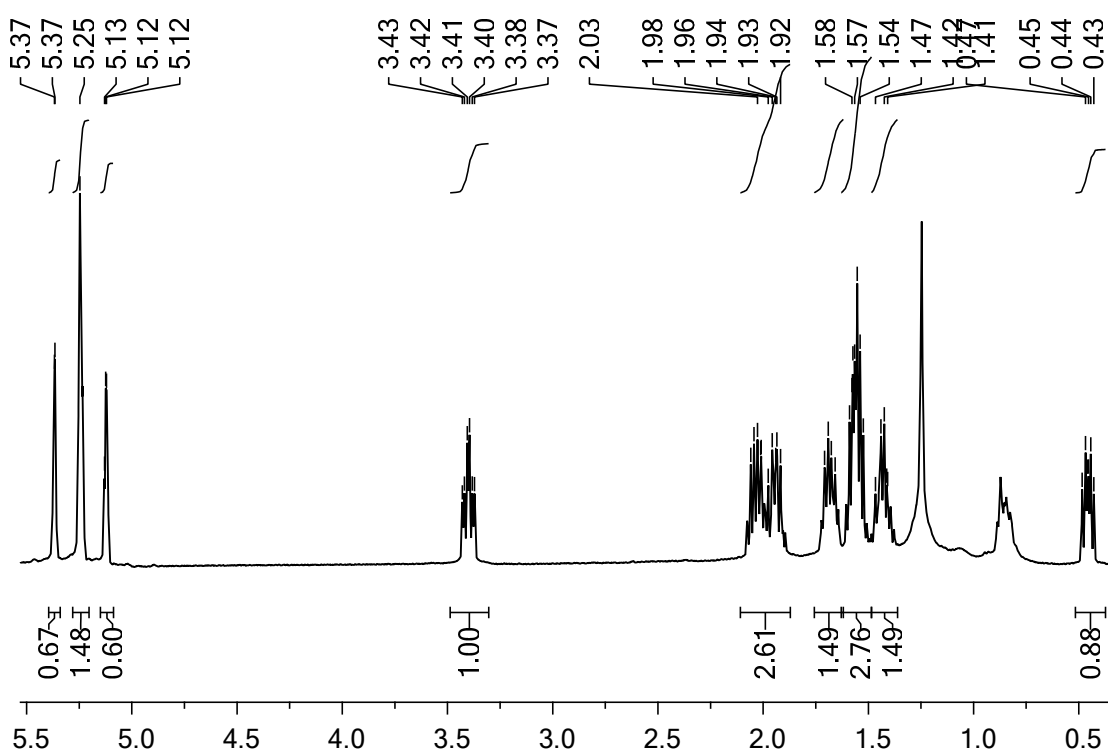
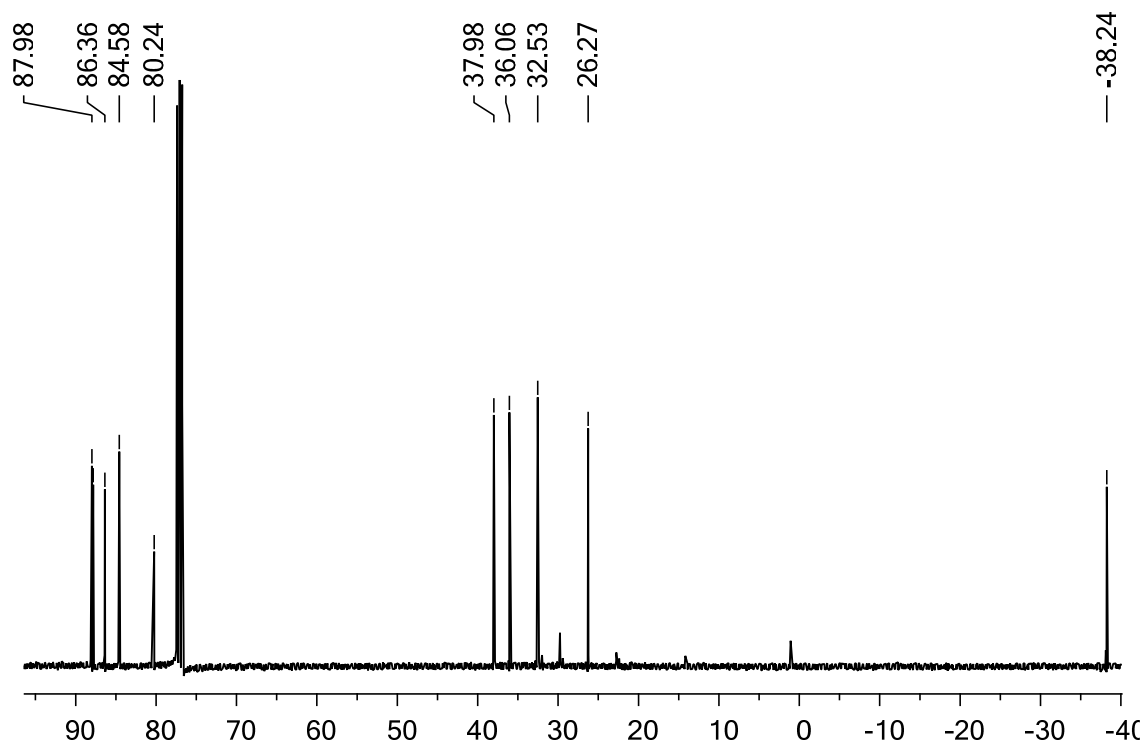


Figure B24 2D-COSY of **2d**, showing both the cyclopentadienyl (upper left corner) and the *ansa* cyclopentyl spin systems.

B.3 Compounds 3a-3e

Figure B25 ¹H NMR spectra of compound 3a.Figure B26 ¹³C NMR spectra of compound 3a.

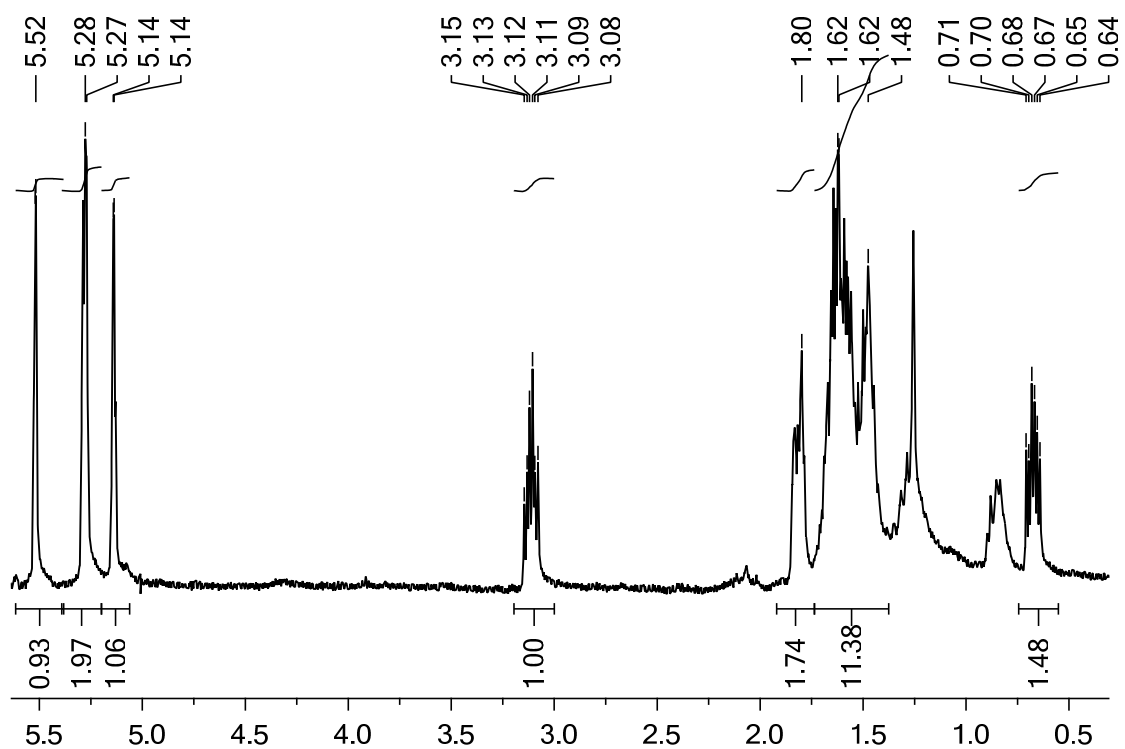


Figure B27 ¹H NMR spectra of compound **3b**.

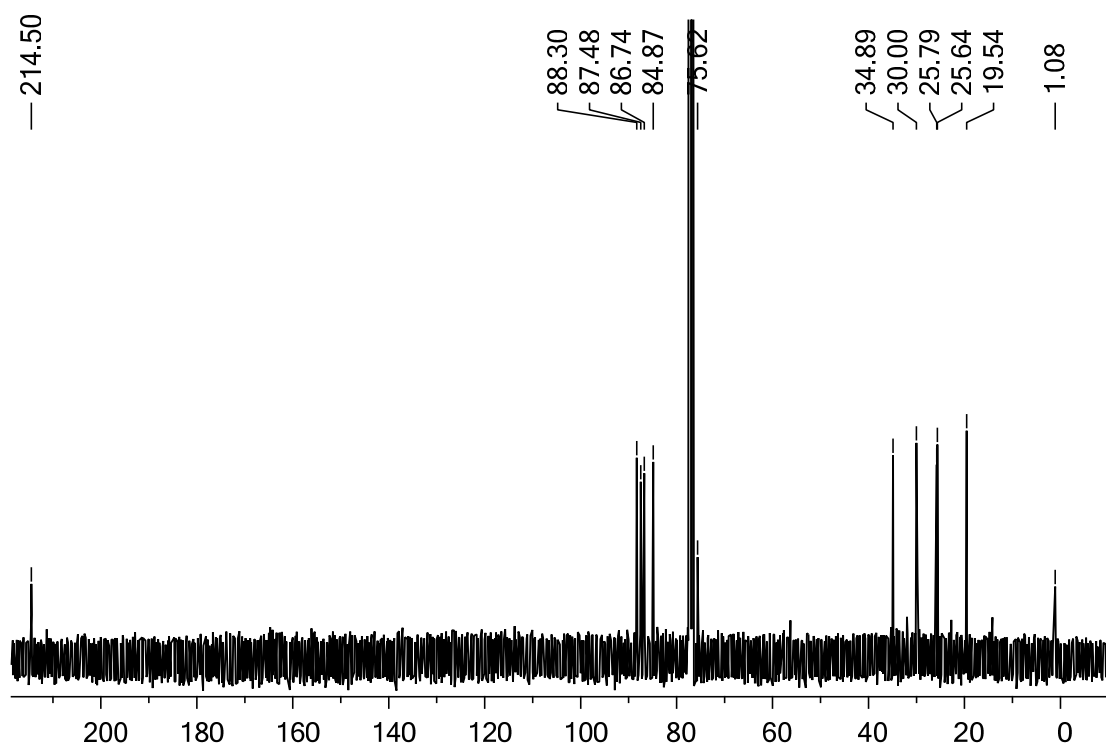
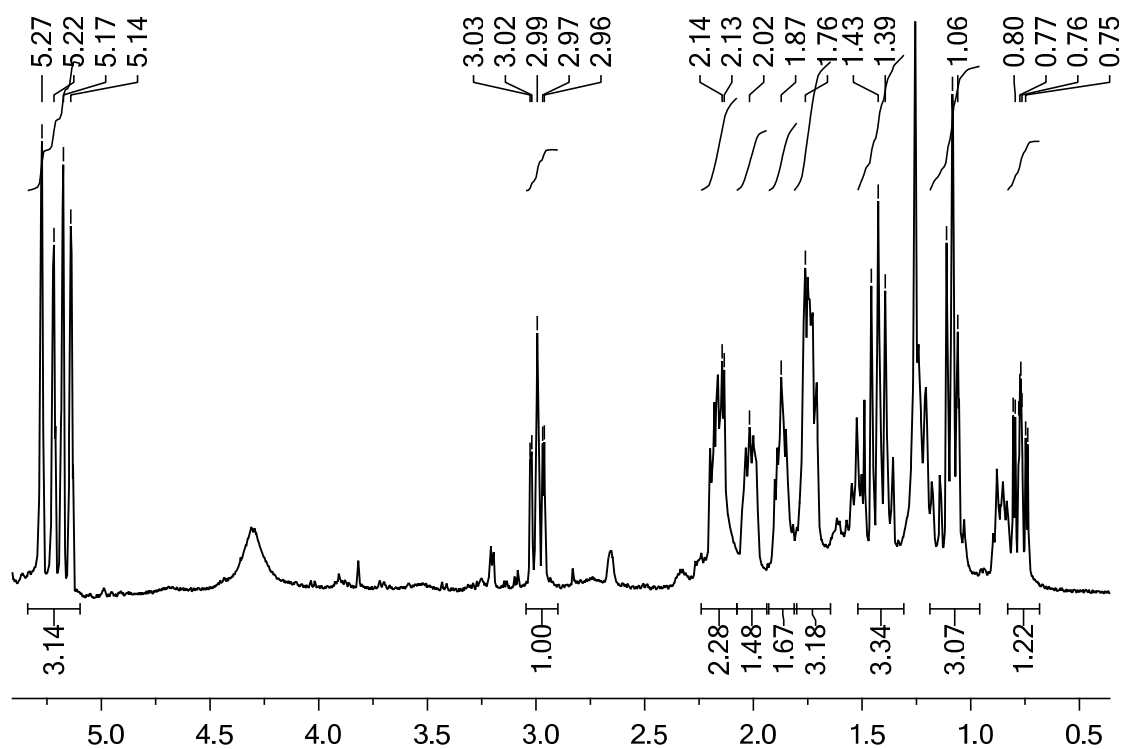
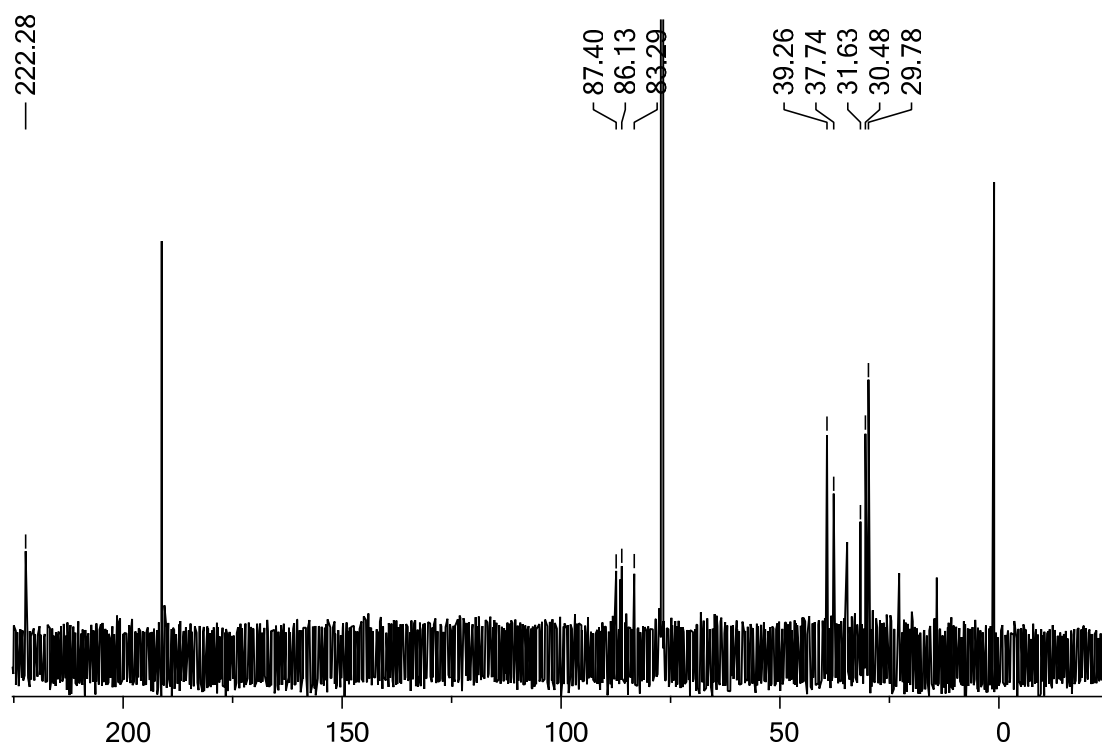


Figure B28 ¹³C NMR spectra of compound **3b**.

Figure B29 ¹H NMR spectra of compound 3c.Figure B30 ¹³C NMR spectra of compound 3c.

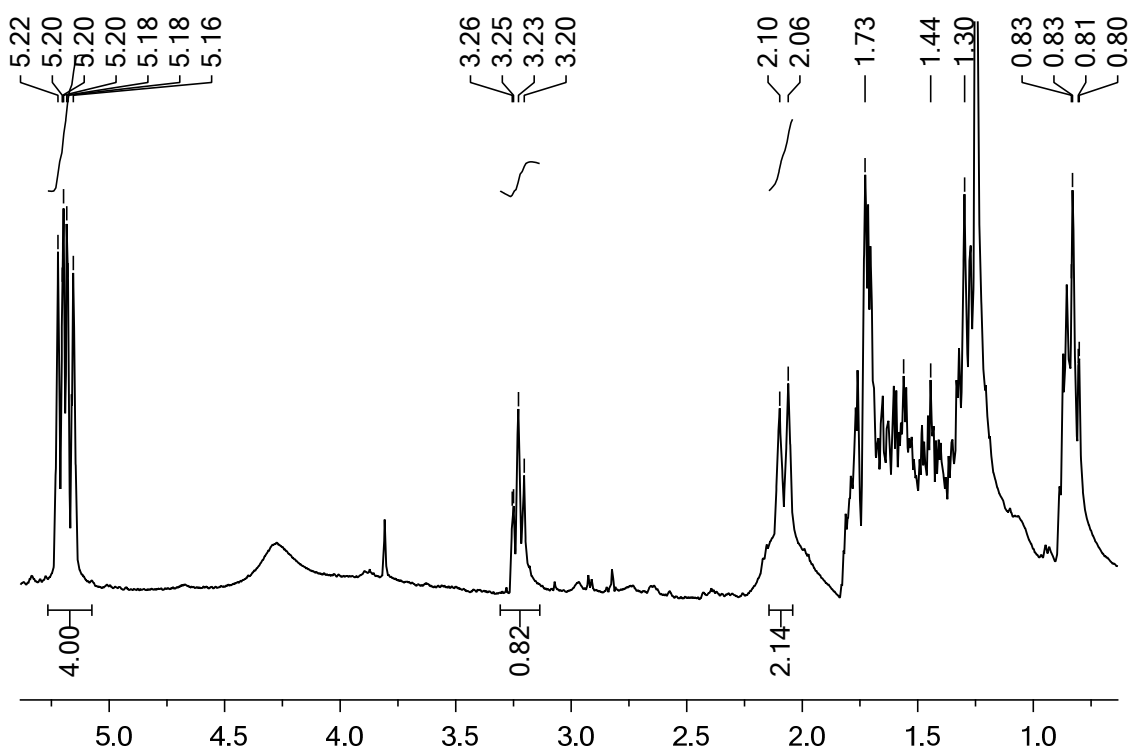


Figure B31 ^1H NMR spectra of compound **3d**.

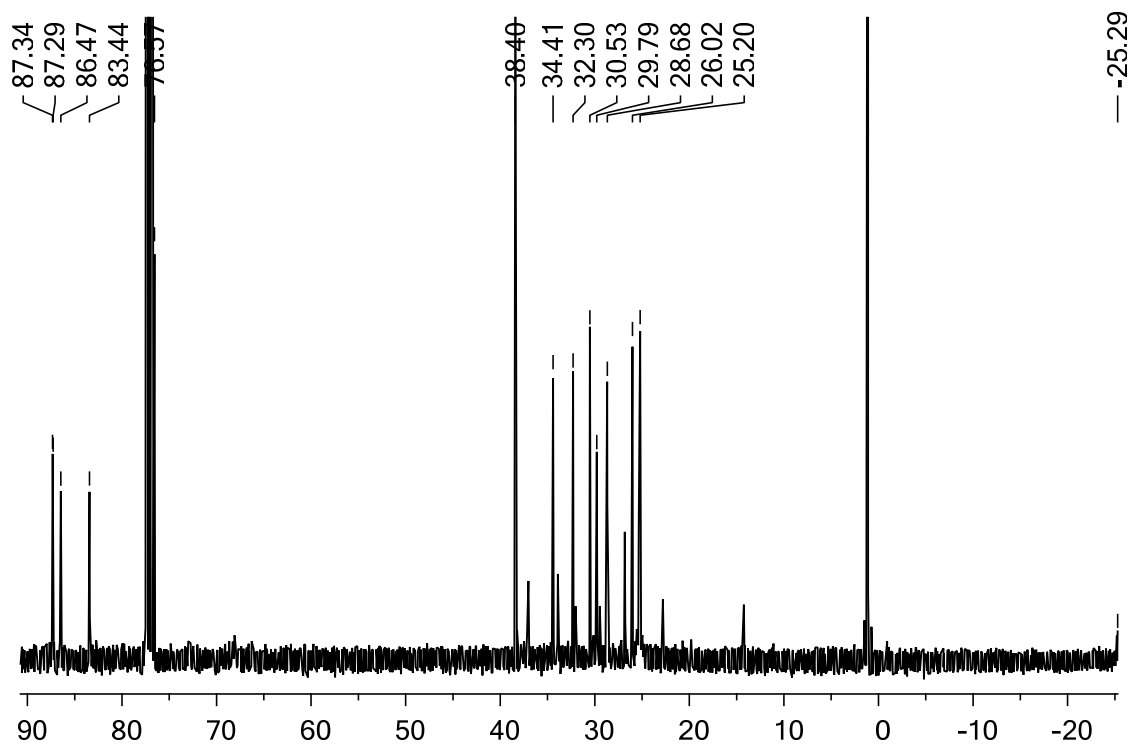


Figure B32 ^{13}C NMR spectra of compound **3d**.

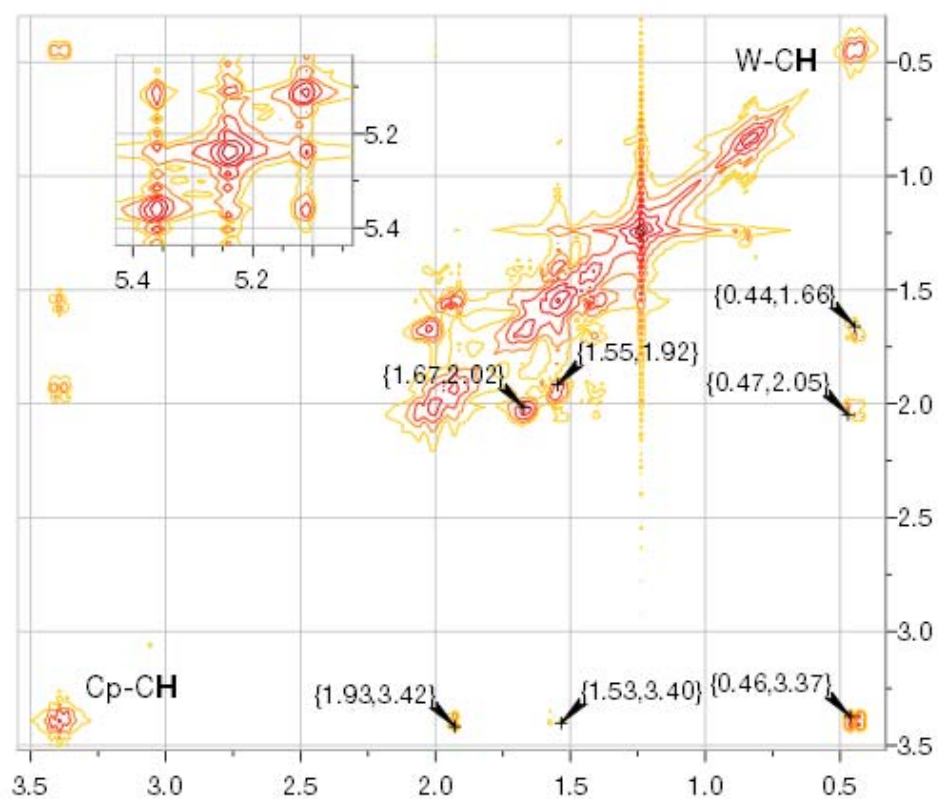


Figure B33 2D-COSY of **3a**, showing both the cyclopentadienyl (upper left corner) and the *ansa* cyclopentyl spin systems.

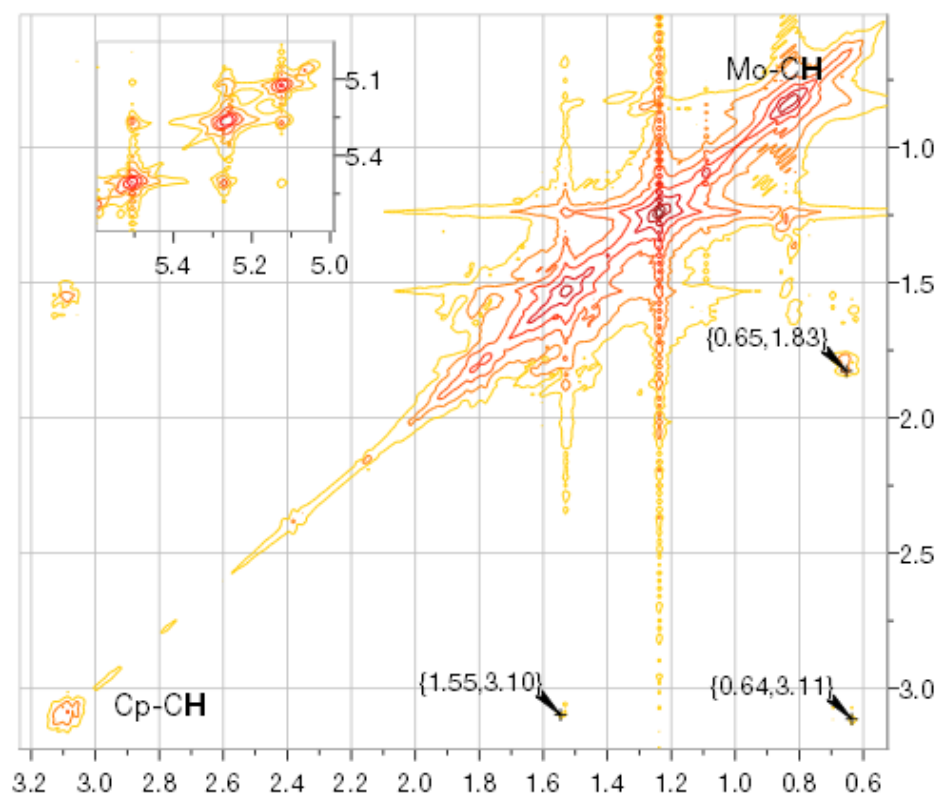


Figure B34 2D-COSY of **3b**, showing both the cyclopentadienyl (upper left corner) and the *ansa* cyclopentyl spin systems.

Appendix C: Publications resulted from this work

C.1: Publications as first author

- **Capapé, A.**; Zhou, M-D.; Zang, S-L.; Kühn, F. E.: “((2-Hydroxynaphthalen-1-yl)methylene)aniline derived Schiff base adducts of MTO: Synthesis and catalytic application”. *J. Organomet. Chem.* **2008**, 693, 3240-3244.
- **Capapé, A.**; Raith, A.; Kühn, F. E.: “Stable and Catalytically Highly Active ansa Compounds with Cycloalkyl Moieties as Bridging Units”. *Adv. Synth. Cat.* **2009**, 351, 1-2, 66-70.
- **Capapé, A.**; Raith, A.; Kühn, F. E.: “Synthesis and Catalytic Applications of ansa Compounds with Cycloalkyl Moieties as Bridging Units: A Comparative Study”. *Adv. Synth. Cat.* **2009**. (Submitted)
- Bruce, M.; **Capapé, A.**; Edlinger, C.; Raith, A.; Herdtweck, E.; Kühn, F. E.: “Terdentate amine Molybdenum and Tungsten carbonyl complexes as precursors for the synthesis of ansa Compounds”. *Eur. J. Inorg. Chem.* **2009** (In preparation)

C.2: Contributions to other publications

- Al-Ajlouni, A.; Veljanovski, D.; **Capapé, A.**; Zhao, J.; Herdtweck, E.; Calhorda, M. J.; Kühn, F. E.: “Kinetic Studies on the Oxidation of η^5 -Cyclopentadienyl Methyl Tricarbonyl Molybdenum(II) and the Use of Its Oxidation Products as Olefin Epoxidation Catalysts”. *Organometallics* **2009**, 28, 2, 639-645.
- Zhou, M-D.; Yu, Y.; **Capapé, A.**; Jain, K. R.; Herdtweck, E.; Li, X-R.; Li, J.; Zang, S-L.; Kühn, F. E.: “(N-Salicylidene)aniline Derived Schiff Base Complexes of Methyltrioxorhenium(VII): Ligand Influence and Catalytic Performance”. *Chem. As. J.* **2009**, 4, 411-418.

C.3: Communications

- Veljanovski, D.; **Capapé, A.**; Kühn, F. E.; Herrmann, W. A.: “*Kinetic and DFT Studies on the Oxidation of the Methyl Derivative of η^5 -Cyclopentadienyl Carbonyl Molybdenum*”. Communication (Poster), shown at the 2nd IDECAT Conference on Catalysis: Concepts, Complexity and Diversity in Catalysis (May **2008**, Porquerolles, France) and the 23rd ICOMC (International Conference on Organometallic Chemistry (July **2008**, Rennes, France)

Curriculum Vitae

Name Alejandro Capapé Miralles
Date of birth 27th August 1979
Place of birth Barcelona, Catalonia (Spain)
Civil Status Single

Education

1985 - 1996 School and High School, Escola Immaculada Concepció (Barcelona)
1996 - 1997 High School, Escola Pia de Nostra Senyora „Jaume Bofill“ (Barcelona)
1997 - 2003 B. of Sc. in Chemistry, Universitat de Barcelona
2003 - 2004 Working student in the Inorganic Chemistry Department, Universitat de Barcelona
2004 - 2005 M. of Sc. in Inorganic Chemistry, Inorganic Chemistry Department, Universitat de Barcelona
March-October 2006 Scientific assistant in the Inorganic Chemistry Department, TU München, under the supervision of Prof. Dr. Fritz Kühn
November 2006-February 2007 BASF-scholar in the Inorganic Chemistry Department, Molecular Catalysis group, TU München, under the supervision of Prof. Dr. Fritz Kühn
March 2007-presently Scientific co-worker in the Inorganic Chemistry Department, Molecular Catalysis group, TU München, under the supervision of Prof. Dr. Fritz Kühn

Languages

Catalan Native language
Spanish Native language
English Fluent (School and High School), 3-week language course (England) in 1994 and 1995
German Fluent, *Mittelstufe II* (Grade: B) in the Escola d'Idiomes Moderns, Universitat de Barcelona